2024

Investigating Hiv-1 Transmission To Human Cervix Using Reporter Virus Technologies

Dana Frances Indihar
University of Alabama at Birmingham

INVESTIGATING HIV-1 TRANSMISSION TO HUMAN CERVIX USING REPORTER VIRUS TECHNOLOGIES

by

DANA FRANCES INDIHAR

KEVIN HARROD, COMMITTEE CHAIR
CARRIE COLEMAN
PAUL GOEPFERT
ZDENEK HEL
JOHN C. KAPPES
CHRISTINA OCHSENBAUER

A DISSERTATION

Submitted to the graduate faculty of The University of Alabama at Birmingham,
in partial fulfillment of the requirements for the degree of
Doctor of Philosophy

BIRMINGHAM, ALABAMA

2024

INVESTIGATING HIV-1 TRANSMISSION TO HUMAN CERVIX USING REPORTER VIRUS TECHNOLOGIES

DANA FRANCES INDIHAR

MICROBIOLOGY

ABSTRACT

Around 39 million people globally are currently infected with Human immunodeficiency virus 1 (HIV-1), more than half of whom are women. HIV-1 is a retrovirus that infects and depletes an individual's immune cells, culminating in the development of acquired immunodeficiency syndrome (AIDS) if not managed with anti-retroviral therapies (ART). Most women acquire HIV-1 through heterosexual intercourse. However, the early mechanisms and virologic determinants of HIV-1 transmission to women remain unclear.

Herein, we demonstrate transmitted/founder (TF) HIV-1 representing two genetically and pathogenically distinct subtypes (A and D) *in vivo* have distinct replication phenotypes in an *ex vivo* cervical explant tissue (CET) model of mucosal HIV-1 transmission. We identified significant differences in the replication of biologically relevant infectious molecular clones (IMCs) representing subtype A and D TF HIV-1 in the CET model. This finding was enabled by our development and application of innovative HIV-1 reporter virus approaches, which underpin exceptional sensitivity and reproducibility in the quantification of HIV-1 replication *ex vivo* and *in cellulo*.

We conceptualized a novel reporter IMC in which a luminescent peptide, HiBiT, was appended to C-terminally truncated HIV-1 Vif. Previous research suggested that the

19 C-terminal residues of Vif were dispensable for Vif function. The Vif C-terminus was hypothesized to be interchangeable with HiBiT. The resulting Vif-HiBiT IMC was sensitively detected and replication-competent in HIV-1 target cells and retained the ability of Vif to mediate APOBEC3G degradation.

Our *ex vivo* studies of HIV-1 transmission were based on the hypothesis that properties mapping to Env affect the efficiency of mucosal HIV-1 transmission. Human cervical explant tissues were inoculated with IMCs engineered with an isogenic proviral backbone, a reporter gene, and encoded the Env ectodomains of pathogenically distinct HIV-1 subtypes. We determined that Env-based properties, CD4 binding and subtype of Env, affected viral transmission and replication *ex vivo*.

Our application of reporter virus technologies for studies of HIV-1 biology provides a powerful approach for the elucidation of HIV-1 mucosal transmission mechanisms, which is urgently needed for guiding the development of targeted HIV prevention strategies to improve the health outcomes of women at high risk of HIV infection worldwide.

Keywords: HIV-1, reporter virus, cervix, luciferase, *ex vivo*

DEDICATION

I dedicate this work to my husband, Ian, who was instrumental in supporting and helping me throughout my PhD journey. Without him, my accomplishments would be far fewer. I also dedicate this work to my parents, Gary and Janet Indihar, for pushing me to be the best version of myself and for their unwavering love, support, and encouragement. Thank you all for standing by me in both the peaks and the valleys of my graduate studies.

ACKNOWLEDGMENTS

To my husband, Ian, who, was unwavering in his patience, support, loyalty, and kindness. Your willingness to help me with anything and everything without question or complaint made the completion of my graduate studies possible. Thank you for your love.

To my parents, Gary and Janet. For my entire existence, you have educated me and supported me to become the ambitious, curious, focused, and independent woman I am today. You will forever have my love and my gratitude. Thank you for everything.

To my brother, Alex (a.k.a. “Dinklemuffin”), for offering support during my most stressful moments and for spoiling me absolutely rotten. Thank you for taking care of me.

To my best friend, Melody, who, for 20 years, has stood by my side. Our times together were a great comfort during my graduate studies. Thank you for your friendship.

To my undergraduate mentor, Dr. Michael, for introducing me to the exciting world of viruses and for inspiring me to pursue this journey. Thank you for my path.

To my beloved cat, Gertie, for providing me with unconditional love, comfort, and cuddles. Thank you for your companionship and for watching over me every day.

To Dr. Ochsenbauer, for helping bring this dissertation together, and to Dr. Kappes, for facilitating my publications. Thank you for your contributions to my future career.

To Gene Roddenberry, Masashi Kishimoto, and Eiichiro Oda, whose characters and stories reminded me to never give up on my goals. Thank you for the inspiration.

Finally, to the staff of the UAB Tissue Biorepository and to those who generously donated their cervical tissues for this work. Thank you for making my project possible.

TABLE OF CONTENTS

Page

ABSTRACT iii

DEDICATION v

ACKNOWLEDGMENTS vi

LIST OF TABLES ix

LIST OF FIGURES x

LIST OF ABBREVIATIONS xii

INTRODUCTION 1

Overview of HIV-1 Molecular Biology 1
HIV-1 Classification and Genome Organization 1
HIV-1 Virion Structure 2
HIV-1 Replication Cycle 3
Transmission, Attachment, and Binding 3
Fusion/Entry 5
Reverse Transcription 5
Integration 7
Transcription and Translation 8
Assembly 11
Budding and Maturation 12
Acute and Chronic HIV-1 Infection 13
Approaches for Inhibiting HIV-1 14
HIV-1 Subtype Diversity 19
Origins of HIV-1 19
Discovery and Classification of Subtypes 20
Distribution of Subtypes 21
Transmission and Pathogenesis of HIV-1 Subtypes 24
HIV-1 Today 28
Reporter Viruses as a Tool to Study HIV-1 29
Discovery and Types of Commonly Used Reporter Genes 29
HIV-1 Reporter Virus Design 34
Applications of Reporter Viruses in Studies of HIV-1 38
Thesis Overview and Rationale 41

1. C-TERMINALLY TRUNCATED HIV-1 VIF RETAINS BIOLOGIC FUNCTION, AND TAGGED WITH HIBIT PEPTIDE SERVES AS A NOVEL BIMOLECULAR LUMINESCENCE ASSAY REPORTER.....62

2. HIV-1 AND WOMEN.....114

3. *EX VIVO* MUCOSAL TISSUE MODELS TO INVETIGATE HIV-1 TRANSMISSION IN WOMEN.....132

4. HIGHLY SENSITIVE ANALYSIS OF CERVICAL MUCOSAL HIV-1 INFECTION USING REPORTER VIRUSES EXPRESSING SECRETED NANOLUCIFERASE..... 150

5. THE HIV-1 ENVELOPE GLYCOPROTEIN OF SUBTYPE A AND D VIRUSES MEDIATE DISTINCT PROPERTIES OF REPLICATION *EX VIVO* IN A CERVICAL MUCOSAL MODEL OF TRANSMISSION.....186

CONCLUSION.....250

GENERAL LIST OF REFERENCES.....256

LIST OF TABLES

Tables *Page*

C-TERMINALLY TRUNCATED HIV-1 VIF RETAINS BIOLOGIC FUNCTION, AND TAGGED WITH HIBIT PEPTIDE SERVES AS A NOVEL BIMOLECULAR LUMINESCENCE ASSAY REPORTER

1 Table 1. *Summary of Primers* 71

2 Table 2. *Summary of Plasmids*.....72

THE HIV-1 ENVELOPE GLYCOPROTEIN OF SUBTYPE A AND D VIRUSES MEDIATE DISTINCT PROPERTIES OF REPLICATION EX VIVO IN A CERVICAL MUCOSAL MODEL OF TRANSMISSION

3 Table 1. *Master Panel of IMCs*.....194

4 Table 2. *Flow Cytometry Antibody Panel*.....199

5 Table 3. *Demographic Information of the 46 CET Donors* 200

LIST OF FIGURES

Figure *Page*

C-TERMINALLY TRUNCATED HIV-1 VIF RETAINS BIOLOGIC FUNCTION, AND TAGGED WITH HIBIT PEPTIDE SERVES AS A NOVEL BIMOLECULAR LUMINESCENCE ASSAY REPORTER

1 Figure 1. Structure models of wild-type and C-terminally modified Vif from HIV-1 NL4-3 85

2 Figure 2. HiBiT activity in provirally transfected 293T cells and in HIV-1 IMC infected TZM-bl cells 87

3 Figure 3. Detection of Vif.HB in virions 89

3 Figure 4. Replication kinetics of IMC encoding WT and modified Vif are similar in non-permissive cells 91

5 Figure 5. Monitoring viral spread via the Vif-HiBiT reporter readout 93

6 Figure 6. Efficient passage of cell-associated Vif-HiBiT virus in non-permissive H9 and primary CD4+ T cells 95

7 Figure 7. Retention of Nef expression and function 97

8 Figure 8. Efficient APOBEC3G protein degradation indicates retention of Vif function in Vif.TR and Vif.HB 100

HIGHLY SENSITIVE ANALYSIS OF CERVICAL MUCOSAL HIV-1 INFECTION USING REPORTER VIRUSES EXPRESSING SECRETED NANOLUCIFERASE

9 Figure 1. Schematic of HIV-1 reporter virus construct 156

10 Figure 2. Anatomical origin, features, and dissection of CET specimens 165

11 Figure 3. Workflow for virus inoculation and preparation for culture 168

12 Figure 4. Productive HIV-1 infection of CET and intra-donor reproducibility 172

13 Figure 5. Inter-donor reproducibility of HIV-1 infection and replication profiles in CET....173

14 Figure 6. Examples of remnant cervical tissue specimens 179

THE HIV-1 ENVELOPE GLYCOPROTEIN OF SUBTYPE A AND D VIRUSES MEDIATE DISTINCT PROPERTIES OF REPLICATION *EX VIVO* IN A CERVICAL MUCOSAL MODEL OF TRANSMISSION

15 Figure 1. Subtype A and D Env-IMC reporter constructs infect and replicate similarly *in vitro*....202

16 Figure 2. Subtype A and D Env-IMCs have distinct replication kinetics in CETs....206

17 Figure 3. Subtype D Env-IMCs replicate more efficiently *ex vivo* than subtype A Env-IMCs. 209

18 Figure 4. Subtype A and D sNLuc TF-IMCs infect and replicate similarly to their Env-IMC counterparts....214

19 Figure 5. Subtype A Env-IMCs replicate differently in ectocervix compared to endocervix 217

20 Figure 6. Subtype A and D Env-IMCs similarly infect CD4 T cells derived from CETs at early timepoints 220

21 Figure 7. Mutations to HIV Env at residues 429 and 432 affect subtype-specific replication kinetics 222

22 Figure 8. Mutations to subtype D Env at residues 429 and 432 induce a replication phenotype similar to wildtype subtype A virus. 226

23 Figure 9. Mutations to HIV Env at residues 429 and 432 affect Env sensitivity to soluble CD4....228

LIST OF ABBREVIATIONS

β-gal	β-galactosidase
6HB	Six-Helix Bundle
-sssDNA	Minus-Strand Strong-Stop DNA
+sssDNA	Plus-Strand Strong-Stop DNA
ADCC	Antibody-Dependent Cellular Cytotoxicity
AIDS	Acquired Immunodeficiency Syndrome
APOBEC	Apolipoprotein B mRNA-editing enzyme, catalytic polypeptide
ART	Anti-retroviral therapy
bp	Base pairs
bnAbs	Broadly Neutralizing Antibodies
C1-C5	Conserved Domains of GP120
CA	Capsid
CAT	Chloramphenicol Acetyltransferase
CD4bs	CD4 binding site
CDC	Centers for Disease Control and Prevention
CET	Cervical explant tissue
CRF	Circulating Recombinant Form
CTD	Cytoplasmic Domain
CTL	Cytotoxic T Lymphocyte

D1-D4	CD4 Extracellular Domains
DMPA	Depot-Medroxyprogesterone Acetate
DRC	Democratic Republic of the Congo
EMCV	Encephalomyocarditis Virus
Env	Envelope protein
ER	Endoplasmic Reticulum
FLuc	Firefly Luciferase
FRT	Female reproductive tract
FSS	Frameshifting Stimulatory Signal
Gag	Group-Specific Antigen
GFP	Green fluorescent protein
GLuc	*Gaussia* Luciferase
gp	Glycoprotein
GUS	β-glucuronidase gene
HIV	Human immunodeficiency virus
HM	Humanized mice
HSA	Heat Stable Antigen
IDU	Injection Drug User
IgG	Immunoglobin G
IMC	Infectious Molecular Clone
IN	Integrase
INSTI	Integrase Strand Transfer Inhibitors

IRES	Internal Ribosome Entry Site
kb	Kilobase
LTR	Long Terminal Repeat
LucR	*Renilla reniformis* Luciferase Protein
MA	Matrix
mCD24	Mouse CD24
MDM	Monocyte-derived macrophage
MHC I	Major Histocompatibility Complex I
MSM	Men who have Sex with Men
Mφ	Macrophage
NC	Nucleocapsid
Nef	Negative Regulating Factor
NHP	Non-Human Primate
NK	Natural Killer
NLuc	NanoLuc
NNRTI	Non-Nucleoside Reverse Transcriptase Inhibitors
NRTI	Nucleoside Analog Reverse Transcriptase Inhibitors
NtRTI	Nucleotide Analog Reverse Transcriptase Inhibitors
NVP	Nevirapine
ORF	Open Reading Frame
PBMC	Peripheral Blood Mononuclear Cell
PBS	Primer Binding Site

Pol	Polymerase
PPT	Polypurine Tract
PR	Protease
PrEP	Pre-exposure Prophylaxis
‘R’ Region	Repeat Region
R5	CCR5
Rev	RNA Splicing Regulator
RFP	Red Fluorescent Protein
RRE	Rev-Responsive Element
RT	Reverse transcriptase
SAMHD1	Sterile alpha motif histidine-aspartic domain-containing protein 1
SIV	Simian immunodeficiency virus
sNluc	Secreted Nanoluciferase
smFRET	Single-molecule fluorescence resonance energy transfer
SSA	Sub-Saharan Africa
SU	Subunit
TAR	Trans-acting Responsive Region
Tat	Transactivator of Transcription
TF	Transmitted/founder
TMD	Transmembrane Domain
U.S.	United States
U3	Unique Region at the 3’ Genome End

U5	Unique Region at the 5’ Genome End
V1-V5	Variable Regions of gp120
Vif	Viral Infectivity Factor
VIA	Virus Inhibition Assay
Vpr	Virus Protein R
Vpu	Viral Protein Unique
WHO	World Health Organization
WT	Wildtype
X4	CXCR4
X-Gal	5-bromo-4-chloro-3-indolyl-3-o-galactoside
X-Gluc	5-bromo-4-chloro-3-indoyl β-D-glucuronide

INTRODUCTION

Human immunodeficiency virus 1 (HIV-1) attacks and depletes an individual's immune cells, leaving that individual susceptible to opportunistic infections by other pathogens and to immune dysregulation maladies, a disease state clinically referred to as acquired immunodeficiency syndrome (AIDS). Although anti-retroviral strategies have been developed to prevent the acquisition and progression of clinical HIV-1 infection, they are not always available or accessible. Additional strategies are needed to prevent the transmission of HIV-1 following viral exposure. An improved understanding of the mechanisms of HIV-1 transmission– gained through optimized tools and models to study HIV transmission– is critical to the development of efficient prevention strategies.

Overview of HIV-1 Molecular Biology

In this overview, the classification, genomic organization, and structure of HIV-1 will be described, followed by a summary of each step of the viral replication cycle: (1) attachment/binding, (2) fusion/entry, (3) reverse transcription, (4) integration, (5) transcription and translation, (6) assembly, (7) budding and maturation. Furthermore, we will summarize key anti-HIV drugs and therapeutics targeting distinct stages of the replication cycle.

HIV-1 Classification and Genome Organization

HIV-1 is an enveloped single-stranded RNA virus containing 2 copies of its positive-sense RNA genome[1]. HIV-1 is a member of the *Retroviridae* family in the *Lentivirus* genus[2]. As a member of the *Retroviridae* family, HIV-1 encodes reverse transcriptase (RT), an RNA-dependent DNA polymerase that converts the viral single-stranded RNA genome into double-stranded DNA that is then integrated into the chromosomes of a host cell to establish infection[3]. The HIV-1 RNA genome is between 9200-9600 nucleotides in size. It is flanked on both sides with a repeated (R) region and a unique region at the 5' and 3' ends of the genome (referred to as U5 and U3, respectively). Following reverse transcription, U5 and U3 are duplicated, forming long terminal repeats (LTRs) comprised of identical U3/R/U5 regions at both ends of the DNA genome[4]. The 5' LTR serves as the promoter region for host RNA polymerase II to transcribe viral DNA into mRNA or viral genomic RNA, and the 3' LTR contains regulatory elements involved in the 3'-end processing and polyadenylation of RNA transcripts[4,5]. The HIV-1 genome encodes 9 partially overlapping HIV-1 genes consisting of: *gag* and *env* (encoding structural proteins), *pol* (encoding enzymatic proteins), and *tat*, *rev*, *nef*, *vif*, *vpr*, and *vpu* (encoding regulatory and accessory proteins). The mRNAs transcribed from these overlapping genes undergo alternative splicing to generate viral proteins[6-9].

HIV-1 Virion Structure

Structurally, the mature HIV-1 virion is comprised of a spherical lipid membrane derived from the plasma membrane of infected host cells[10] embedded with as few as 7-14 envelope (Env) glycoprotein complexes[11]. Beneath the membrane the matrix protein (MA, p17) forms a discontinuous layer that encloses the viral capsid. Around 1200-1500 capsid proteins (CA, p24) form a lattice of ~250 CA hexamers and 12 CA pentamers that arrange

into a fullerene cone[10]. CA encapsulates cellular tRNA (such as Lys3) and two copies of the genomic viral RNA, which are bound and stabilized by nucleocapsid protein (NC, p7). The RT and integrase (IN, p32) enzymatic proteins are also enclosed within CA[12]. The functions of each of these virion components in the HIV-1 replication cycle are described hereon.

HIV-1 Replication Cycle

Transmission, Attachment, and Binding

HIV-1 is most commonly transmitted through sexual intercourse (homosexual or heterosexual), but it is also transmissible from mother to child and through contaminated blood (i.e. through needle-sharing during intravenous drug use or blood transfusions)[13-15]. During sexual intercourse, HIV-1 virions present in seminal fluid or vaginal secretions penetrate genital mucosal surfaces and encounter permissive target cells[16-18]. CD4+ T cells are considered to be the primary targets of heterosexually transmitted HIV[19,20], but macrophages (Mφs) have also been implicated as early targets of infection[21-28]. The main receptor required for viral entry into a cell is surface-expressed CD4. CD4 is a type I integral membrane protein with 4 extracellular immunoglobin-like domains called D1, D2, D3, and D4. HIV also requires a co-receptor for entry. The two most common co-receptors are CCR5 and CXCR4, but HIV can use alternative co-receptors, including: CXCR6, CCR1, GPCR1, CCR3, CCR8, and several others[29]. HIV strains that utilize the CXCR4 co-receptor are referred to as X4-tropic, R5-tropic if they utilize CCR5, or dual tropic if they use both[30].

HIV Env glycoprotein (gp) facilitates binding and entry into a host cell. The *env* orf encodes the Env gp160 precursor protein, which is proteolytically cleaved by host furin into a heterodimer comprised of the glycoprotein surface subunit (SU, gp120) and the transmembrane protein (TM, gp41)[31]. Three gp120 and gp41 heterodimers form a homotrimeric glycoprotein complex that is critical for receptor binding and viral entry into a host cell. Gp120 is composed of 5 conserved domains (C1-C5) and 5 variable loops (V1-V5), which are named for their degrees of genetic heterogeneity[32]. V1-V5 comprise the outer domain of gp120, which is a key target for HIV vaccine design, and a bridging sheet connects the outer domain and inner domain of gp120[33]. Gp120 is non-covalently attached to gp41, which imparts structural flexibility to the heterodimer that allows conformational changes for facilitating viral entry[34]. Gp120 and the extracellular portion of gp41 constitute the ectodomain of Env. The ectodomain contains the CD4 binding site (CD4bs) and the co-receptor binding site, and it is a target for host neutralizing antibodies[35]. Gp41 is anchored in the virion membrane via its transmembrane domain (TMD) and a cytoplasmic domain (CTD). Gp41 is necessary for fusing virus and host cell membranes during entry[31].

Viral attachment to host cells can either be specific (through interactions between Env and host α4β7 integrin) or non-specific (through virion interactions with negatively charged host surface heparan sulfate proteoglycans)[31]. Attachment brings the virion into close proximity to host cell receptors, where HIV-1 canonically enters host cells through interactions with surface receptors. The mature, cleaved, membrane-associated Env trimer is metastable, and single-molecule fluorescence resonance energy transfer (smFRET) studies have shown that Env trimer spontaneously transitions to one of three distinct prefusion conformational states: State 1 or the “closed” state, State 2 or the intermediate

state, and State 3 or the "open" state. In State 1, gp120 variable loops V1 and V2 obscure V3[36], and this is the predominate Env conformation because high activation barriers limit the transition of Env to other conformations[37]. The D1 domain of CD4 interacts with and becomes bound by the CD4bs of HIV Env[38], resulting in the State 2 conformation[36]. When the CD4bs of gp120 binds the CD4 D1 domain, activation barriers are lowered and Env trimer is triggered into the State 3 conformation. This "open" conformation of trimer permits the binding of an HIV co-receptor by the V3 loop of gp120[32,36,37].

Fusion/Entry

Recent data suggests that V3 binding of the CCR5 co-receptor brings Env trimer close to the host membrane to induce membrane fusion[39]. Co-receptor binding by the V3 loop triggers the exposure of a hydrophobic fusion peptide in the gp41 portion of Env, which inserts into the cell membrane and tethers the viral and host cell membranes together. The N-terminal and C-terminal hinge regions of each of the three gp41 subunits join together to form a six-helix bundle (6HB), which brings host and virus membranes into close proximity to create a fusion pore[32]. The formation and stabilization of the fusion pore enables the viral core to be delivered into the cytoplasm of the host cell[32,40]. This process represents viral entry into a host cell via a classic receptor/co-receptor mechanism. Alternatively, HIV-1 can enter cells (including epithelial, astrocyte, and HeLa cells without CD4) through endocytosis. Though the viral particles are usually shuttled to endosomes or lysosomes in clathrin- or caeloin- coated vesicles and degraded, a small number of particles have been observed to escape the vesicles and establish infection[41].

Reverse Transcription

Reverse transcription is initiated after viral entry[40], with the viral capsid serving as a container for reverse transcription to occur[42]. The cone-shaped capsid, formed by CA hexamers and pentamers, encloses the NC-bound viral genomic RNA to protect it from degradation by cellular nucleases[43]. Reverse transcription is executed by viral RT, which is a heterodimeric enzyme that reverse transcribes RNA into DNA. RT is comprised of two subunits: p66 and p51. The p66 subunit has DNA polymerizing and RNase H activities while p51, which has an identical amino acid sequence to p66 but lacks the RNase H domain, serves to stabilize the viral RNA/DNA replication complex[3,44,45]. RT thus has two enzymatic functions to carry out reverse transcription: as an RNA-dependent DNA polymerase and as an RNase H for degrading viral genomic RNA within RNA-DNA duplexes[3,40,44,45].

For the first step of reverse transcription, host tRNA (HIV-1 usually uses Lys3) binds the primer binding site (PBS), which is located ~180 nucleotides from the 5' end of the positive-sense viral genomic RNA. The tRNA is used as a primer by RT to synthesize the minus-strand strong-stop DNA (-sssDNA), which is a minus-strand DNA copy of the 5' end of the genomic RNA comprising R and U5. As -sssDNA is synthesized, an RNA-DNA duplex forms, and RT degrades the 5' end of the viral RNA template through its RNase H activity to expose the -sssDNA. The tRNA/-sssDNA complex is then translocated to the 3' end of the viral genomic RNA. The -sssDNA anneals to the 3' end because the R sequence at the 3' end of the genome and the newly synthesized R region of the -sssDNA are complementary. Minus-strand DNA synthesis and RNase H degradation then resume; however, the entire RNA template is not degraded[40,46].

Plus-strand DNA synthesis is primed and initiated at a purine-rich sequence adjacent to the 3' U3 called the polypurine tract (PPT), and this site is initially resistant to RNase H degradation. RT generates plus-strand DNA from the minus-strand DNA and the first 18 nucleotides of the tRNA, which forms the plus-strand strong stop DNA (+sssDNA) that contains U3/R/U5/PBS regions. RT RNase H activity then degrades the tRNA and PPT, exposing the +sssDNA. The PBS sequence in the +sssDNA is complementary to the PBS sequence in the minus-strand DNA, and the sequences anneal. DNA synthesis continues until both the plus and minus DNA strands are completed, resulting in linear, double-stranded viral DNA with identical LTRs at both ends[40,46]. As reverse transcription proceeds, CA transports the viral genome from the cytoplasm into the nucleus through a nuclear pore and shields the viral genome and replication proteins against host innate immune factors. Once inside the nucleus, CA disassembles after the completion of reverse transcription, and the newly synthesized double-stranded viral DNA is released into the nucleus along with IN[43].

Integration

IN processes the blunt 3' ends of the viral DNA, removing a dinucleotide from each end to create "sticky" or chemically reactive 3'-hydroxyl groups. IN then binds the host chromosomal DNA, particularly in transcriptionally-active chromatin regions for HIV-1, and uses the 3'-hydroxyl groups to form staggered cuts in the host DNA. This process also joins the 3'-hydroxyl groups at the ends of the viral DNA strands to the 5'-phosphate groups at the ends of host DNA. Gaps between the recombined viral/host DNA are repaired by host ligase to complete the integration reaction[47]. HIV-1 infection is established when the proviral genome is integrated into the host genome.

Transcription and Translation

Following integration of the provirus, HIV-1 temporally controls its gene expression through early and late phases, a strategy which helps virally infected cells evade host immune responses. During the early phase, transcription from the 5' LTR by host RNA polymerase II is low and transcripts are fully spliced into (~2 kb) early mRNA transcripts that are exported to the cytoplasm and translated into essential viral regulatory proteins[4-6,9,48,49]. These proteins include Tat (transactivator of transcription, p14) and Rev (RNA splicing-regulator, p19), and the accessory protein Nef (negative regulating factor, p27)[6,8,50]. Tat enters the nucleus and binds the trans-acting responsive region (TAR), a stable stem-loop structure that forms on the nascent RNAs, located in the 5' LTR. As Tat levels increase, so does TAR binding, which enhances transcriptional initiation and elongation of late mRNA trancripts[6,9,51]. After Rev levels increase in the cytoplasm following translation, Rev is re-imported into the nucleus. Rev then binds the Rev-responsive element (RRE) intron present in full-length RNA transcripts with high affinity, preventing the complete splicing of the transcripts[9,50]. This results in unspliced (~9 kb in length) or partially spliced (~4 kb) late RNA transcripts, which Rev transports out of the nucleus and into the cytoplasm for translation of late gene products[6,9,51]. Nef downregulates cell surface-expressed CD4 and major histocompatibility complex I (MHC I) to subvert host immune responses and sequester host restriction factors, such as tetherin, that interfere with viral particle release[9,52]. The early expression of Nef is advantageous to the virus because the downmodulation of host MHC I and CD4 facilitates the evasion of host immune responses that would otherwise destroy the infected cell during viral replication[53], including cytotoxic T lymphocyte (CTL)-mediated lysis and antibody-dependent cellular

cytotoxicity (ADCC). Nef contribution to the downregulation of CD4 also helps prevent superinfection of a cell and premature CD4 interaction with Env[54].

During the late phase of HIV-1 gene expression, unspliced and partially spliced RNA transcripts are transported out of the nucleus by Rev. The unspliced, full-length RNA has two roles: as mRNA encoding Gag and Gag-Pol polyprotein and as genomic RNA that will be packaged into nascent viral particles[48,55]. Ribosomal translation of the full-length mRNA primarily results in the generation of Gag, the polyprotein precursor of CA, MA, NC, and a p6 domain. Gag is crucial for virion assembly and budding, and its cleaved protein products comprise the major structural components of the mature virion[56]. In 1 out of 20 translations of Gag, a -1 frameshift occurs at the "slippery sequence" 5'-U UUU UUA-3' located at the 5' end of the mRNA. The -1 frameshift results in translation of Gag-Pol wherein Pol is the polyprotein precursor of the RT, IN, and protease (PR, p12) viral enzymes[55,57].

Env and Vpu (viral protein unique, p16) are translated from the singly-spliced *env/vpu* bicistronic mRNA. The 43S pre-initiation complex passes through the *vpu* start codon to initiate ribosome binding for Vpu translation, and a six-nucleotide sequence overlapping the *vpu* start codon initiates Env translation[58]. Vpu localizes to the endoplasmic reticulum (ER) of the host cell, where it retains *de novo* CD4 and facilitates CD4 degradation through the ER-associated degradation pathway. Vpu also contributes to the release of progeny virions by counteracting the restriction factor tetherin[59], similarly to Nef. Importantly, Nef, Vif, Vpr, and Vpu are all classified as HIV accessory proteins[8,50]. Env is translated in the rough ER from the *env/vpu* bicistronic mRNA, resulting in a gp160 polyprotein precursor with an N-terminal signal peptide[36,58]. The signal peptide anchors

the N-terminus of Env to the ER lumen, where the glycosylation of Env begins[36]. Env has approximately 25-30 N-linked glycosylation sites that become glycosylated in the ER-Golgi system, forming a "glycan shield" that accounts for ~50% of the mass of Env[33,36]. Glycosylation of Env is essential for viral infectivity, as previous studies have demonstrated that mutation of Env glycosylation sites results in the loss of viral infectivty[33]. Glycosylation continues following the delivery of Env to the Golgi apparatus and the cleavage of the signal peptide[33,36]. In the Golgi apparatus, host furin cleaves the gp160 polyprotein precursor into gp120 and gp41[31,36]. Additional information regarding the cleavage of Env and its incorporation into virions is described in the *Assembly* section. The structure and function of Env are described in the *Transmission, Attachment, and Binding* section.

Vif (viral infectivity factor, p23) and Vpr (virus protein R, p15) are translated from partially spliced mRNAs. Vif plays a critical role in viral infection by directing host APOBEC proteins to the E3 ubiquitin ligase complex for ubiquitination and degradation. If not degraded, the APOBEC proteins, in particular A3G, are incorporated into virions and mutate the cytidines present on minus-strand viral DNA to uridines during reverse transcription, creating non-functional viral proteins after the hypermutated viral genome is transcribed and translated[60-65]. Vif and its properties that were exploited in the optimization of a new virologic tool for HIV-1 transmission research are described further in Chapter 1. Vpr interferes with the host cell-cycle by impeding the transition from G2 to mitosis and then mediates viral entry into the nuclei of the non-dividing cells through an importin-independent pathway[66,67]. Vpr also increases the rate of viral replication in T cells and is critical for viral replication in Mφs[67,68].

Assembly

Once the Gag/Gag-Pol polyproteins are translated, the nascent virion is assembled at the plasma membrane of the host cell. The localization of the Gag and Gag-Pol polyprotein precursors to the host plasma membrane is mediated by interactions between MA and phosphatidylinositol-4,5-bisphosphate [$PI(4,5)P_2$] lipid, located within the host plasma membrane. MA binding to $PI(4,5)P_2$ lipid triggers a conformational change in MA that exposes a myristoyl group, which promotes the targeting of Gag to lipid rafts within the plasma membrane[69]. Around 2,500 copies of Gag polyprotein (MA-CA-NC-p6) assemble into a spherical layer beneath the plasma membrane in a radial arrangement, where the N-terminus of Gag attaches to the membrane and the C-terminus of Gag projects towards the center of the budding virion[10,12,70]. The CA domain stabilizes lateral Gag-Gag interactions, forming an immature hexameric lattice[71]. The immature lattice is contiguous with a single gap comprising approximately one-third of the virion membrane surface area[12]. The NC domain binds the Ψ site on the viral genomic RNA to capture the RNA and tether it to Gag for incorporation into virions[12,70]. Two copies of host cellular tRNA anneal to the 5' PBS located upstream of the Ψ site on the viral genomic RNAs[12].

There are two pathways through which Env is processed and transported to the cell surface for assembly and incorporation into virions: "conventional trafficking" through the Golgi and "unconventional trafficking" that bypasses the Golgi[37]. During "conventional trafficking", Env is transported through the Golgi apparatus where it is glycosylated, assembled into trimer, and then cleaved from the gp160 precursor into gp120 and gp41 by host furin[31,36,37,72], as discussed above. This mature, cleaved Env is then transported to the plasma membrane surface through the cellular secretory pathway, and Env gets

incorporated into viral particles following interactions between the MA myristoyl group and the CTD of Env gp41 through a currently unknown mechanism[12,70,72]. Although cleaved Env is critical to mediate the fusion of virus and host membranes to complete entry and cleaved Env is preferentially incorporated into virions, not all Env is cleaved[36,37]. Zhang *et. al* reported that a small amount of Env escapes the Golgi prior to cleavage, and this uncleaved Env may be incorporated into virions either through direct interactions with MA or through endocytic machinery. Zhang *et. al* also described the "unconventional trafficking" of Env, where the Golgi is bypassed completely, resulting in uncleaved Env that is transported to the host cell surface but inefficiently incorporated into virions. This surface-expressed, unconventionally trafficked Env may be advantageous to the virus by acting as a decoy to misdirect host antibody responses against uncleaved Env instead of the cleaved Env present on the surface of infectious virions[37].

Budding and Maturation

While assembly proceeds, the p6 domain of Gag binds host cellular endosomal sorting complex required for transport (ESCRT) pathway proteins, such as TSG101 and ALIX, to mediate budding. TSG101 and ALIX recruit ESCRT-III complexes, which are necessary for fission and release of cell and virus membranes[12,56,73]. ALIX and TSG101 link the p6 domain of Gag to the ESCRT-III complex, which facilitates the assembly of an ESCRT-III spiraling tube structure within the "neck" of the budding virion. The ESCRT-III tube constricts and pinches the "neck" until fission of viral membrane from host membrane occurs spontaneously[12,74]. At this budding step, host tetherin can block HIV release. However, viral Vpu and Nef can counteract tetherin[9,12,52,59].

When two Gag-Pol polyproteins (MA-CA-NC-p6-PR-RT-IN) interface, the PR, IN, and RT domains transiently dimerize[75]. This dimerization is driven by p66-p66 interaction and is necessary for the activation of PR, which cleaves viral protein precursors to form a mature and infectious virion. PR becomes activated after forming a homodimer between the PR domains of two Gag-Pol polyproteins and then autoprocessing the dimer though an autocatalytic process[76,77]. PR then proteolytically cleaves IN and RT into fully processed proteins[12,78]. IN is cleaved by PR following IN dimerization[75]. RT initially forms a p66 precursor homodimer until PR cleaves the RNase H domain from one subunit, creating the mature p66/p51 heterodimer[75,79]. Gag polyprotein is also proteolytically cleaved by PR in a highly ordered manner, resulting in the formation of mature and fully-processed MA, NC, CA, and p6 structural proteins. Mature MA remains associated with the lipid membrane of the virion. Mature CA collapses or disassembles from MA to form the mature fullerene cone comprised of pentameric and hexameric protein rings that encloses the viral genomic RNA. NC remains bound to the genomic RNA, and PR proteolysis further triggers the condensing of the RNA viral genome and the stabilization of CA around the viral RNA-NC complex[12,71,78,80].

Acute and Chronic HIV-1 Infection

Following maturation, the virion is ready to infect and replicate in new target cells[12]. Initially, after transmission to a new host, viral spread to new target cells (particularly CD4+ T cells) is rapid, and this period of acute infection can last from a few weeks to a few months. During this time, CD4+ T cells are depleted and viral load increases. In response, host CD8+ T cells become activated and engage in anti-viral activities to slow the rate of viral replication and spread[81,82]. Early during acute infection,

HIV-1 establishes latent reservoirs in effector T cells, myeloid cells, and potentially other cell types such as dendritic cells. These latent reservoirs occur when the virus becomes transcriptionally dormant following integration of the provirus into the host cell genome. Latently-infected cells are undetectable by host immune surveillance factors, and these cells can persist for years. These latent reservoirs contribute to chronic infection[81,82]. If the latently-infected cell divides, daughter cells will carry the provirus[83]. Stimulation of latently-infected cells during the host immune response can re-activate the provirus. Cellular transcription factors such as NF-κB are upregulated during the immune response, and these transcription factors can drive the initiation of proviral transcription following their recruitment to the HIV-1 LTR[84,85]. Although the activation of latently-infected cells stimulates the host immune response, continuous replication provides opportunity for the virus to adapt and continue to deplete and exhaust host immune cells. If left untreated, the depletion of their immune cells makes a host vulnerable to AIDS[81,82].

Approaches for Inhibiting HIV-1

Due to the large number of new HIV cases arising from sexual intercourse, the Centers for Disease Control and Prevention (CDC) recommends condom (or other barrier method) use as an effective strategy to prevent HIV transmission[14]. However, high-risk HIV populations, such as sex workers, may be unable to negotiate safe-sex practices out of concern for violent repercussions[86-89]. Victims of sexual and physical violence are 50% more likely to acquire HIV than non-victims[88] due to a combination of the injuries sustained during the violence and the low likelihood of the perpetrator using protection[90]. Thus, condoms/barrier methods are an important anti-HIV strategy, but they are not always an option. They are also ineffective if improperly applied by the user. Vaccines and the

elicitation of effective immune responses against HIV-1 are important topics of prevention research, but a vaccine that safely and effectively protects individuals against the virus has yet to be developed. Access of individuals to immediate medical intervention following exposure to HIV-1 and/or infection by the virus varies greatly by geographic region and socioeconomic status. Effective anti-HIV drugs targeting distinct steps of the HIV-1 replication cycle are available and described below.

To counteract HIV co-receptor binding, R5 antagonists, such as maraviroc, have been developed to prevent gp120-R5 binding and inhibit cell entry following viral exposure. These antagonists have been shown to be effective against R5-tropic viruses, but viral resistance caused by the selective transmission of X4-tropic and dual-tropic viruses can occur[91]. To prevent HIV fusion after (co-)receptor binding, fusion inhibitors, such as enfuvirtide, can be used to prevent entry of the virus into the host cell[92]. Enfuvirtide binds the first heptad-repeat in gp41 and blocks the 6HB formation required for fusion of the host cell and viral membranes[93]. However, mutations to gp41 can arise as enfuvirtide exerts a selective pressure for resistant virus[93,94]. Recently, Matsumoto *et. al* developed the novel CD4 mimetic compound YIR-821, which competitively binds CD4 to prevent viral entry. YIR-821 may have clinical applications as it was reported to inhibit the entry of HIV-1 clinical isolates into target cells *in vitro* [95]. Past approaches have also investigated soluble CD4 (sCD4) as a potential clinical inhibitor against HIV binding, but low concentrations of sCD4 were found to enhance infection[96].

To counteract reverse transcription, RT is a common target for anti-HIV therapeutics. There are multiple classes of RT inhibitors: nucleoside analog reverse transcriptase inhibitors (NRTIs), nucleotide analog reverse transcriptase inhibitors

(NtRTIs), and non-nucleoside reverse transcriptase inhibitors (NNRTIs)[92]. Both NRTIs and NtRTIs are competitive substrate inhibitors, acting as analogues of nucleosides or nucleotides that are incorporated during viral DNA synthesis by RT[92,97]. Unlike natural nucleosides/nucleotides, these analogues lack a 3'-hydroxyl group, preventing the formation of 5'-3' phosphodiester bonds with subsequent nucleosides/nucleotides and thus terminating the synthesis and extension of the viral DNA chain by RT. However, the analogues can also terminate host DNA synthesis— resulting in mitochondrial, renal, and bone toxicity— and resistant viruses can emerge[97]. Zidovudine, emtricitabine, stavudine, and lamivudine are examples of NRTIs, and tenofovir is an example of an NtRTI[92]. Pre-exposure prophylaxis (PrEP) (taken orally as a pill or received through regular injections) is recommended for individuals in high-risk populations, such as men who have sex with men (MSM), to prevent HIV from establishing infection, and it contains both tenofovir and emtricitabine[98]. NNRTIs are allosteric inhibitors that bind a hydrophobic pocket in the p66 domain near the RT active site, causing a conformational change in RT that disrupts the RT DNA polymerization function. However, the hydrophobic pocket is not as conserved as the RT active site, and resistant viruses can emerge quickly if the NNRTI is not used in combination with other ART[99]. Nevirapine (NVP) and rilpivirine are two examples of NNRTIs[92]. NVP is a useful tool in *ex vivo* and *in vitro* models because it inhibits *de novo* infection in cell and tissue culture. The utility of this drug in these models is demonstrated in Chapters 1, 4, and 5.

The inhibition of integrase during the integration step is another approach to counteract HIV. Some of the most effective integrase inhibitors to date are integrase strand transfer inhibitors (INSTIs), such as raltegravir and dolutegravir[92]. INSTIs preferentially

bind to the active site of integrase, which displaces viral DNA from the active site. This inhibitor strategy thus blocks integration of the viral DNA into the host DNA. INSTIs are advantageous because they pose a significant barrier to the emergence of resistant viruses and are highly effective at suppressing *de novo* virus. However, some classes of INSTIs can cause dyslipidemia and weight gain, leading to cardiovascular complications[100].

Ribosomal frameshifting is required for HIV-1 translation of Gag-Pol and is thus an important potential target for ART[55,101]. One approach to affect HIV-1 frameshifting is to target ribosomes, with drugs such as sparsomycin or anisomycin, but this can have detrimental consequences on other host cellular processes. Another approach is to use antisense oligonucleotides, which can affect frameshifting by stalling ribosomes on the slippery sequence, but they may bind to host Toll-like receptors and negatively affect immune modulation[55]. More recently, drugs/compounds targeting the HIV-1 frameshifting stimulatory signal (FSS) RNA, such as doxorubicin, have been developed to reduce viral infectivity, the emergence of drug-resistant strains, and negative effects on immune outcomes. However, these drugs/compounds are still in the early stages of development are not currently included in standard ART regimens[102].

The inhibition of CA is an approach to counteract the assembly of nascent virions. Benzodiazepines and benzimidazoles series compounds were shown to inhibit CA assembly and the formation of mature CA by directly binding the CA N-terminal domain. However, these compounds were ineffective against CA derived from clinical isolates containing polymorphisms within the N-terminal domain[103]. A more potent capsid inhibitor, GS-CA1, was then developed. GS-CA1 also binds the N-terminal domain of CA and was shown to inhibit HIV replication by 95% in animal models, but drug-resistant

viruses still emerged[104]. A similar inhibitor called GS-6207 (lenacapavir) is currently being used in clinical trials. While this is the most successful, potent inhibitor of capsid to date, the emergence of drug-resistant viral strains remains a concern[105].

One final anti-HIV approach is to prevent the formation of the mature viral particle through the inhibition of PR. Some examples of PR inhibitors include saquinavir, indinavir, nelfinavir, and darunavir[92]. PR inhibitors competitively bind to the catalytic site of PR, which prevents the cleavage of Gag and Gag-Pol into mature proteins required for viral replication[106]. ART regimens with PR inhibitor-based therapy were reported to generate less viral resistance than NNRTI-based therapy[107]. However, these inhibitors can have limited potency, create significant drug-drug interactions, and be toxic to the liver[106,107]. When used in experimental approaches and applied at the time of viral infection, these drugs block the second round of viral infection *in vitro* and *ex vivo*. These drugs are therefore useful HIV replication inhibitors in experimental approaches, and examples of this can be found in Chapters 1 and 5.

Over time, if medical intervention in the form ART is not obtained, HIV-infected individuals progress to AIDS and die. Though there is currently no cure for HIV/AIDS, the anti-HIV drugs/therapeutics described in this section, when used in combination, offer a way to limit viral transmission, infection, and replication in both newly and chronically infected people. As discussed throughout this section, resistant viruses emerge with nearly every anti-HIV drug developed, which is why long-term combination and multi-drug therapies are the recommended approach to treat HIV-infected individuals. Drug-resistant viruses also arise when patients do not comply with long-term drug therapy. The long-term therapy may be too expensive or inaccessible for the individual to continue, have toxicity

side effects, or cause undesirable drug-drug interactions[92]. Anti-HIV drugs and therapeutics that impair or prevent the transmission of HIV-1 following initial exposure may be the most effective approach for limiting the continued spread of the virus.

HIV-1 Subtype Diversity

Since its zoonotic transmission to humans, HIV-1 has evolved into several distinct subtypes, HIV strains that are phylogenetically and/or geographically linked[108]. The diversity of these subtypes is discussed below, as well as how the diversity of these viruses has complicated HIV vaccine and prevention efforts.

Origins of HIV-1

HIV-1 is a zoonotic virus originating from simian immunodeficiency virus (SIV)-infected Central chimpanzees (*Pan troglodytes troglodytes*) found in the Democratic Republic of the Congo (DRC)[109-112]. Although the exact circumstances under which the first transmission event from chimpanzee to human occurred are not known, the "Cut Hunter" Hypothesis places that first transmission event within a relevant historical and environmental context[113]. Briefly, the hypothesis suggests that around 1920 in the Belgian-occupied Congo, a hunter in search of bush meat accidentally cut himself while killing an SIV-infected Central chimpanzee, and the virus penetrated his bloodstream[113-116]. The man's cells were permissive to infection by the virus, and the virus was able to replicate. The man or someone he infected then relocated to Kinshasa, the modern-day capital of DRC, where the virus that would later be known as HIV-1 began to spread[111,113,117-119].

From Kinshasa, HIV-1 spread to the nearby cities of Brazzaville, Lubumbashi, and Mbuji-Mayi and then to the rest of Africa by the 1950s, but its existence was not

recognized. Railways transported infected individuals from Kinshasa to neighboring cities, and the use of unsterilized needles in disease clinics and the expansion of commercial sex work in Kinshasa contributed to the exponential increase of HIV-infected individuals in this region[112,116]. Around 1966, HIV-1 arrived from Africa to Haiti and the Caribbean, either due to sex trafficking or the return of Haitian workers from Africa[116,120]. HIV-1 was then introduced from Haiti to the United States between 1966-1972, where it is hypothesized to have circulated slowly in heterosexual populations before exponentially expanding in MSM populations engaging in high-risk sexual behaviors around 1978. HIV-1 was first officially recognized in the United States in 1981, but not before international travel contributed to the global distribution of HIV-1 from the United States[120].

Discovery and Classification of Subtypes

By 1959 in Kinshasa, HIV-1 had diversified from one or few ancestral strains into distinct subtypes[112]. HIV-1 is derived from four distinct lineages— Major (M), New (N), Outlier (O), and P— each of which arose from a separate cross-species transmission event. Group M was discovered first in the 1980s, followed by group O in 1990, group N in 1998, and group P in 2009. Group M originated in Kinshasa and represents the majority of HIV-1 pandemic strains worldwide[112,121,122]. Group M subtypes are defined and distinguished by sequencing data, where either the full-length viral genome is sequenced or the *env*, *gag*, and/or *pol* genes are sequenced[123]. The sequencing data are then phylogenetically assessed to determine genetic relatedness, and viral strains with equidistant "star-like" phylogeny (instead of "tree-like" phylogeny) are classified together as an HIV-1 subtype[108].

Group M is divided into ten "pure" subtypes— A, B, C, D, F, G, H, J, K, and L— and circulating recombinant forms (CRFs), which are viral strains comprised of

recombined viral genomes from different subtypes[122,124,125]. CRFs arise from dually (or multiply) infected people, resulting in a mosaic viral genome composed of regions from each of the infecting subtypes. Subtypes E and I are omitted from Group M because they were originally identified with incomplete sequencing information and have yet to be found as "pure" subtypes. Thus, subtype E was renamed to CRF01_AE, and subtype I was renamed to CRF04_cpx (cpx refers to "complex" recombination of multiple subtypes)[122]. Within an individual subtype, genetic variation among viral strains is estimated to be only 8-17%. Between subtypes, genetic variation is estimated to be 17-35% depending on the subtypes or the specific genomic regions of those subtypes being compared[126].

Distribution of Subtypes

Subtype C is the most prevalent subtype of HIV-1 globally (comprising an estimated 23% of all HIV-1 cases as of 2023). It is also the most common HIV-1 subtype found in Eastern and Southern Africa, where a reported 40.6% of HIV-1 cases are subtype C infections[127]. Phylogenetic assessments suggest that subtype C emerged from Mbuji-Mayi in the DRC around the 1950s before being introduced to other African countries—including Ethiopia, Kenya, Tanzania, Uganda, and Zimbabwe— by migrating mineworkers in the 1970s. Between 1980-1990, the subtype spread to Zimbabwe, Zambia, Tanzania, Mozambique, Botswana, and Malawi before expanding beyond Africa to Asian and Middle Eastern countries[116,128]. Subtype B comprises only 8.5% of global HIV-1 cases but is the dominant subtype in Latin America and the Caribbean (60.5% of HIV-1 cases in those regions) and in Western and Central Europe and North America (56.4%)[127]. Subtype B was present in Kinshasa by 1944, and by around 1964, it had been exported to Haiti.

From there, it spread to the United States and then to Europe, making it the most geographically dispersed of all the HIV-1 subtypes[116].

Subtype A is the second most prevalent HIV-1 subtype globally (16.7% of all HIV-1 cases as of 2023) and primarily circulates in Eastern and Southern Africa (24.7% of all HIV-1 cases in those regions) as well as Eastern Europe and Central Asia (38.9%), where subtype A is the most common HIV-1 subtype[127,129]. Subtype A is sub-divided into seven sub-subtypes based on phylogenetic analyses, including A1-A4 and A6-A8[125]. The A5 sub-subtype has yet to be found as a "pure" sub-subtype but was identified as part of CRF26_A5U, a CRF of A5 and an unknown (U) subtype, which circulates in Equatorial Guinea and the DRC[130]. The A8 sub-subtype was the most recently discovered A sub-subtype and is found in the Republic of Cabo Verde, an island nation off the coast of West Africa[125]. The A1 sub-subtype is the largest of the A sub-subtypes (~80% of all described A sequences) and is found primarily in Kenya and Rwanda. A2 and A4 are found primarily in the DRC, while A3 and A7 are restricted to Senegal[130]. Interestingly, A6, though of African origin, is found mostly in the Russian Federation, where it is spread primarily through injection drug use[130,131].

Subtype D comprises only 7.7% of global HIV-1 cases. It is almost exclusively found in Eastern and Southern Africa (12.5% of HIV-1 cases for those regions), with only a small number of cases reported throughout the rest of Africa[127,129]. Subtypes A and C co-circulate in the same African countries as subtype D, although the prevalence of subtype D in those countries has decreased over the years[129,132,133]. Grant *et. al* compared the prevalence of subtype D from blood serum samples acquired from Ugandan patients across three different time points (1986, 1998 to 1999, and 2007 to 2016) and found a significant

decline in the prevalence of subtype D from 67% of samples (1986), to 57% (1998-1999), to just 17% (2007-2016)[132]. Although the pervasiveness of subtype D in its "pure" form may be declining, the prevalence of subtype D recombinants has increased[133]. Subtype D frequently recombines with subtype A even though the genetic distance between the two subtypes is among the largest of the group M HIV-1 subtypes[129,133,134]. Subtypes D and B have the smallest genetic distance of all the HIV-1 subtypes, which lead Désiré *et. al* to suggest that the two subtypes should be reclassified as two sub-subtypes of one subtype[134]. This is especially interesting when considering that subtype B is largely absent from Eastern and Southern Africa[127,129].

The prevalence of the six other "pure" subtypes worldwide is as follows: 3.4% for subtype F, 2.3% for subtype G, 1.6% for subtype H, 0.6% for subtype J, and 7.3% for all other or unknown subtypes, including subtypes K and L. Subtype F is most commonly found in Latin America and the Caribbean (5.8% of all HIV-1 cases for those regions), subtypes G and J are most commonly found in West and Central Africa (8.8% and 5.1%, respectively), and subtype H is primarily found in Eastern and Southern Africa (2%)[127]. Subtype F is divided into two sub-subtypes, F1 and F2. Sub-subtype F1 was identified in an MSM cohort from Spain, while F2 was found in Cameroon and South America, where it frequently recombines with subtype B[129,135]. Subtype G is also commonly found in Cameroon, but also Cuba and the Iberian Peninsula. Nearly 80% of the CRFs in Cameroon have subtype G as a recombination parent[136]. Both subtypes H and J are estimated to have emerged from Matadi, a remote city in the DRC. Due to the poor connection of this city to the rest of Africa, the distribution of these two subtypes is limited to the DRC, Angola, and parts of Southern Africa[137]. Subtype K was originally classified as a subtype F sub-subtype

(F3), but was reclassified as its own subtype following the phylogenetic analysis of strains from the DRC and Cameroon, where it primarily circulates[138]. Subtype L was the most recently discovered subtype back in 2019, and it has yet to be found outside of the DRC[139].

The prevalence of CRFs globally is increasing rapidly and is expected to continue to grow[129]. The two most common CRFs worldwide are CRF01_AE, formerly classified as subtype E but it is instead a recombinant of subtypes A and E, and CRF02_AG, a recombinant of subtypes A and G[127,129]. CRF01_AE comprises 9.5% of HIV-1 cases globally but is most commonly found in Asia and the Pacific (29.5% of HIV-1 cases in that region)[127]. Though CRF01_AE originated in Central Africa around the 1970s, it was transferred to Thailand in the 1980s by female commercial sex workers before expanding to the rest of Asia, where it continues to circulate today[140,141]. CRF02_AG comprises 7.2% of HIV-1 cases globally and is responsible for nearly half of the HIV-1 infections in West and Central Africa (46.9%)[127]. CRF02_AG first emerged in Central Africa, spread to Western Africa and then Cameroon in the 1970s, to regions of the former Soviet Union in the 1990s. From there, it spread throughout the rest of Europe, where it remains one of the most common CRFs in both Eastern and Western Europe today[142]. The prevalence of all other CRFs worldwide is around 9.2%. These other CRFs circulate widely throughout the Middle East and North Africa, with a prevalence of 49.9% of HIV-1 cases in that region[127]. The reason for the high percentage of CRFs in this region has been attributed to circulation among high-risk groups, including: injection drug users (IDU), MSM populations, and female sex workers[143].

Transmission and Pathogenesis of HIV-1 Subtypes

The most common route of HIV-1 transmission is heterosexual transmission, which is responsible for ~70% of new HIV-1 infections globally, followed by MSM, IDU, and maternal-infant transmissions[144]. Sexually transmitted HIV-1 infection arises from a viral population bottleneck, where only a single or few genetically similar variants establish clinical infection in the host. However, the molecular, cellular, immunological, or viral reason(s) for this bottleneck remain poorly understood[20,144-148]. These single variants that are "transmitted" and go on to "found" infection are referred to as transmitted/founder (TF) viruses[149]. A single TF variant is responsible for establishing infection in ~80% of heterosexual transmissions, ~75% of MSM transmissions, 40-80% of IDU transmissions, and ~70% of maternal-infant transmissions[145]. To gain entry into host cells to establish infection, HIV-1 binds host cell surface CD4 and a co-receptor, usually either CXCR4 or CCR5. Although some TF viruses can utilize both co-receptors (referred to as "dual tropic" or "R5X4-tropic"), R5-tropic viruses are preferentially transmitted in the majority of clinical cases. The reasons(s) for this remain also poorly understood[144,147-150]. Interestingly, some individuals possess a mutant CCR5 allele containing a 32 bp deletion in the second extracellular loop of the receptor, and consequently, these individuals fail to support replication of R5-tropic viruses even after repeated exposure[151,152]. However, these individuals remain vulnerable to infection by dual tropic viruses[152].

Epidemiological data has suggested that the presence or prevalence of some HIV-1 subtypes in different regions across the globe may be affected by mode of transmission. Subtype G is more common among IDU in Europe than MSM or heterosexual populations[153]. Subtype B is common in heterosexual populations in the United States, but it is also one of the most common subtypes among MSM populations in Europe, North

Africa, and the Americas[153-157]. Subtype F is likewise common among MSM populations in South America and Europe[158]. Meanwhile, subtypes A, C, D, and CRF01_AE are more common in heterosexual populations across sub-Saharan Africa and Asia, where subtype B infection in heterosexual populations is infrequent[137,140,141,155,156]. These data raise questions that may be relevant to the aforementioned transmission bottleneck, including whether mode of transmission (i.e. penile-rectal, penile-vaginal, intravenous) affects the transmission efficiencies of different viral subtypes. Interestingly, TF HIV-1 was found to be more virulent (greater reduction in early CD4 cell counts) in heterosexual populations than MSM populations[159] despite the finding that anal intercourse was significantly more likely to transmit HIV-1 than penile-vaginal intercourse[160]. Whether this means that there are tissue-based factors limiting viral dissemination in rectal tissues compared to penile or cervicovaginal tissues is unclear.

The pathogenesis of these subtypes varies widely, with subtype D considered to be one of the most pathogenic group M subtypes. Individuals infected with subtype D experience rapid CD4+ T cell decline, greater resistance to ART, faster progression to AIDS, and higher mortality rates than those infected with subtypes A, B, C, or even some CRFs[121,132,161-170]. Within the genomes of CRFs with subtype D as a recombination parent, the TMD and the CTD of Env gp41, the *gag-pol* coding region, and the *tat* and *rev* exons are predominantly derived from subtype D, while the Env ectodomain is derived from the recombining strains[133,171]. Interestingly, CRFs that are subtype D recombinants have been demonstrated to be less pathogenic than "pure" subtype D[172]. One proposed reason for the pathogenicity of subtype D is the difference in co-receptor tropism of subtype D, mediated by Env, compared to other subtypes. Subtype D TF strains are more likely to use both

CCR5 and CXCR4 co-receptors than any other subtype, and this dual co-receptor usage has been associated with faster CD4+ T cell decline *in vivo*[121,132,164,173]. However, the high degree of virulence, coupled with selective pressures against CXCR4 tropism, may reduce opportunity for viral transmission events[132]. In contrast, subtype C may be one of the least pathogenic subtypes despite its global dominance[128,156,170,174]. *In vitro*, subtype C was shown to be outcompeted by other group M subtypes because it had significantly reduced replication kinetics and poorer entry efficiency. The slower kinetics and poorer entry observed *in vitro* may be associated with slower disease progression of subtype C observed *in vivo*[128]. Yet, these characteristics may be advantageous for subtype C transmission and spread because slower disease progression may increase the opportunity for transmission events[128,133].

The heterogeneity and diversity of these different subtypes thus makes vaccine design a challenge. Ideally, there would be one universal vaccine developed to offer global protection against HIV-1. To be successful, this vaccine would have to match circulating viral sequences as closely as possible while also providing cross-reactivity among subtypes[126]. This is likely not feasible, however, especially with how genetically diverse these strains are even within a single subtype. Env is the primary target of HIV vaccine development because of its critical role in establishing infection, ability to induce host neutralizing antibodies, and its surface exposure, but it can differ up to ~35% among different HIV subtypes[175,176]. Gag, Pol, and Nef are more conserved (15%, 10%, and 20% variation among subtypes, respectively) than Env[176], but vaccines directed against those targets may not elicit immune responses (i.e. CD8+ T cell response) as potent as bnAbs [177,178]. As early as 1997, Van Harmelen *et. al* submitted that HIV-1 epidemics in distinct

risk populations may be independent of each other, suggesting that HIV-1 interventions and therapies should be tailored separately for distinct risk groups[155]. Today, it is recognized that a preferred approach for vaccine design would be to customize vaccines for the circulating HIV-1 strains in a given region (i.e. Europe or West Africa) and/or for a specific risk population (i.e. heterosexual or homosexual). Problems may arise with this strategy too though, as it is challenging to know how many vaccines are feasible to develop. Further, with the global increase in CRFs, it is difficult to predict how effective those vaccines would be against future HIV-1 strains that will emerge.

HIV-1 Today

HIV-1 has claimed the lives of between 32.9-51.3 million people to date[179]. As of 2022, an estimated 39 million people are currently living with HIV/AIDS worldwide, and around 1.5 million of them are children[179,180]. More than half of those infected are women and girls, a subject which is expanded on in Chapter 2[14,181]. In the United States, the Centers for Disease Control and Prevention (CDC) reported that Black and Hispanic/Latino communities were disproportionately affected by HIV, comprising 40% and 29% of the new HIV diagnoses in 2021, respectively. Further, MSM populations accounted for 70% of new HIV acquisitions in 2021, making them the largest group affected by HIV in the United States[182]. An estimated 56% of new HIV cases in the United States were diagnosed in people between the ages of 13 and 34[183]. More than half (52%) of all people newly diagnosed with HIV in 2021 lived in the South, and MSM accounted for around 70% of diagnoses in the South[183,184].

In 2022, approximately 1.3 million people across the globe became newly infected with HIV. The number of new annual HIV infections peaked in 1995, and there has been

a 59% decline in new infections since 1995, although that decline has since slowed[180]. Increased education, testing services, surveillance, and awareness of HIV-1, coupled with the development of ART to counteract HIV-1 infection and replication, have been key contributors to the decline. Modern ART, if adhered to as prescribed, can lead to an undetectable viral load in infected individuals, allowing them to live longer lives and preventing them from transmitting HIV to HIV-negative partners. The underlying mechanisms that establish mucosal HIV-1 transmission, however, remain unclear. Manipulation of the genetic framework of HIV-1 to generate tools for studies of HIV-1, particularly of mucosal transmission, are described in the next section.

Reporter Viruses as a Tool to Study HIV-1

As discussed above, the pursuit of a vaccine or other prevention methods for HIV-1 has been hindered by diversity of HIV-1 subtypes and the emergence of drug-resistant strains. Having effective tools and models for HIV studies are critical for advancing the field. One approach that has proven useful for studying HIV-1 transmission, infection, and replication is the use of HIV-1 reporter viruses, in which an HIV proviral backbone is engineered to express a reporter gene. Reporter viruses enable the observation and quantification of viral infection/replication upon expression of the reporter gene as part of the viral genome. Described below are the most common types of reporter genes used in reporter viruses, how reporter viruses incorporating these genes were developed, and how reporter viruses have been used for studies pertaining to HIV prevention and vaccine research.

Discovery and Types of Commonly Used Reporter Genes

In 1962, Dr. Shimomura and colleagues isolated a 26.9 kDa protein from the *Aequorea victoria* jellyfish species that fluoresced green upon exposure to blue-ultraviolet light[185]. The gene (*gfp*) that generated this green fluorescent protein (GFP) was later cloned, sequenced, and demonstrated to be functional in both prokaryotes and eukaryotes in the 1990s by Dr. Tsien. He was eventually awarded the Nobel Prize in Chemistry in 2008 for his contribution[186]. The discovery of *gfp* revolutionized the field of cellular and molecular biology as scientists were able to introduce this gene into cells, viruses, or even mice to monitor fluorescent protein expression, trafficking, and localization in real-time[185,186]. Variants of the gene were later developed— including genes coding for enhanced yellow (*eyfp*), enhanced cyan (*ecfp*), and enhanced green (*egfp*) fluorescent proteins— but the emission spectra of GFP compared to its variants was difficult to distinguish for some applications such as flow cytometry. The red fluorescent protein gene (*rfp*), isolated from *Discosoma sp.* (a type of sea anemone) in the late 1990s, provided additional colors that were spectrally distinct from GFP[185,187], as did those encoded by various red and orange RFPs isolated from other coral species. *Gfp*, *rfp*, and their variants (including several engineered variants such as monomeric GFP, inducible GFP, StayGold, etc.) continue to be widely used today and have application in confocal microscopy, flow cytometry, detecting localized protein expression in transgenic reporter mouse models, and more. Fluorescent protein genes have also been engineered into proviral backbones to create HIV-1 reporter viruses that can be used to visualize and enumerate viral infection and spread *in vitro*, *in vivo*, and *ex vivo*.

Before *gfp*, one of the first non-fluorescent reporter gene systems to be applied in retroviruses was developed around 1982 by Drs. Gorman and Howard. They engineered a

recombinant plasmid in which *Escherichia coli* transposon chloramphenicol acetyltransferase (CAT) transcriptional activity was controlled by the Rous sarcoma virus LTR. This reporter plasmid was transfected into a variety of immortalized cell lines, and the LTR served as a transcriptional promoter for CAT mRNA synthesis. They determined that CAT enzymatic activity (the conversion of ^{14}C-chloramphenicol to monoacetate or diacetate forms) correlated with CAT mRNA synthesis[188]. Their approach became known as the CAT assay, which used autoradiography following thin-layer chromatography to separate acetylated products from cell lysates[189]. In 1986, Dr. Martin and colleagues sought to understand whether the co-infection of cells with HIV and DNA viruses increased the transcriptional activity of HIV[190]. They cloned the CAT gene downstream of the HIV-1 5' LTR in a recombinant plasmid (pBenn7; derived from HIV-1 lymphadenopathy-associated virus DNA, described in detail in[191]) that also contained the HIV-1 3' LTR and *tat*. Immortalized cell lines were then co-transfected with the recombinant plasmid and another plasmid containing DNA from DNA viruses such as bovine papilloma virus and varicella-zoster virus. Through modeling the co-infection of cells by HIV and other DNA viruses, they found that DNA viruses may stimulate HIV expression and that there was a correlation between CAT activity and mRNA expression[190]. This CAT reporter gene system was one of the first to use enzymatic activity of the translation product as a surrogate measure of transcriptional activity driven by a retroviral promoter (reviewed in[192]). The CAT assay and its molecular concepts were foundational to the development of the reporter gene systems used to create modern HIV-1 reporter viruses. However, this assay has limited application today as it reportedly has low sensitivity and does not allow for the visualization of CAT-expressing cells[185,192].

To improve the visualization of reporter activity, Dr. Jefferson developed another *E. coli*-based reporter system in the mid-1980s[192]. This system used the cauliflower mosaic virus 35S promoter to drive expression of the *E. coli* β-glucuronidase gene (GUS) to study gene expression in transformed plant tissues. Reporter activity was visualized when GUS-expressing stem sections were stained with 5-bromo-4-chloro-3-indoyl β-D-glucuronide (X-Gluc), resulting in a blue-green color produced from the hydrolysis of X-Gluc by GUS[193]. This reporter system continues to be used by plant and agriculture scientists today[192]. Around the same time GUS was in development, Lis *et. al* fused a different *E. coli* gene, *lacZ*, to the *Drosophila* heat shock gene with a promoter, hsp70, to study the response to heat shock in *Drosophila* [194]. The *lacZ* gene encoded β-galactosidase (β-gal) protein, which hydrolyzes lactose into galactose and glucose. It can also hydrolyze 5-bromo-4-chloro-3-indolyl-3-o-galactoside (X-Gal), which produces blue-colored products as a result[186,194]. In Lis *et. al*, β-gal activity was inducible by heat, and *Drosophila* abdomens turned blue when heated and exposed to X-Gal[194].

In the early 2000s, Drs. Kappes and Wu developed the TZM-bl cell line, which used the *lacZ* gene and the gene encoding Firefly luciferase as reporters for HIV infection[195]. The TZM-bl cell line was derived from a modified HeLa cell line, JC53[193], and engineered to express high levels of CD4 and CCR5, resulting in a cell line that was highly permissive to HIV infection[195,196]. Genes coding for β-gal and luciferase were introduced into the cells through an HIV-based vector, and reporter gene transcription was controlled by the HXB2 HIV LTR. Both β-gal and luciferase were expressed following HIV infection[195]. The TZM-bl cell line introduced a paradigm shift in the methodology for studies of HIV biology and vaccine development. It has been adapted for use in a variety

of assays and applications, including the TZM-bl assay, which is a standardized method for measuring antibody-mediated neutralization of HIV-1[197]. TZM-bl cells are also useful for normalizing the infectious titers of (transfection-derived) viral stocks through the β-gal assay[185]. The β-gal assay is described in greater detail in Chapter 4.

A third class of reporters utilized in the design of HIV reporter viruses are known as the luminescent or luciferase reporters. In 1885, Raphael Dubois, a French pharmacologist, used the abdomens of *Elateridae* click beetles to produce lab-generated bioluminescence. He referred to the molecule consumed in the reaction as "luciferin" and the enzyme catalyzing the reaction as "luciferase". In the 1940s, Drs. McElroy and Green extracted and purified the first luciferase proteins from a variety of firefly species. By 1947, McElroy and colleagues determined that ATP was required for bioluminescence with these luciferase proteins. However, in 1977 when Dr. Cormier purified the luciferase protein from *Renilla reniformis* (LucR), the sea pansy, he discovered that the LucR enzyme was ATP-independent. Instead of ATP and luciferin, the 36 kDa LucR enzyme uses coelenterazine and oxygen as cofactors to generate a "long-flash emission", a 480 nm wavelength of light emitted in a ~30 second burst[198]. A gene encoding Firefly Luciferase (FLuc) was first cloned in 1985 from *Photinus pyralis*, the North American firefly, by Dr. DeLuca. It was noted that this 61 kDa luciferase produced bioluminescence in the presence of oxidized luciferin and ATP[186,199]. *Gaussia* luciferase (GLuc)— isolated from the *Gaussia princeps* copepod marine organism in 2005[200]— is 19.9 kDa, uses coelenterazine as a cofactor, and is 2000-fold more sensitive than FLuc and LucR[200-202]. However, the luminescent signal declines rapidly after 10 seconds following coelenterazine addition, which limits the usability of GLuc for high-throughput assays[200,202]. In 2012, NanoLuc

(NLuc) was isolated from *Oplophorus gracilirostris*, the deep-sea shrimp[203]. It is 19 kDa and is another ATP-independent luciferase. When combined with furimazine, NLuc generates luminescent activity that is both 150-fold more sensitive and more stable than FLuc and LucR activity[198]. The utility of NLuc (and its derivatives) as an HIV-1 reporter virus gene is described in greater detail in Chapters 1, 4, and 5.

HIV-1 Reporter Virus Design

One of the earliest iterations of the HIV-1 reporter system was created in 1986, when the CAT gene was cloned downstream of the HIV-1 5' LTR into the pBenn7 recombinant plasmid, which also contained the HIV-1 3' LTR and *tat*. CAT enzymatic activity correlated with mRNA expression[190]. This HIV-1 reporter system only used a fraction of the HIV genome, and scientists eventually sought to go beyond studies of HIV LTR promoter activity to investigate viral entry, replication, and pathogenesis. In 1989, Drs. Terwilliger, Godin, Sodroski, and Haseltine inserted the CAT gene into the HIV proviral backbone of HXB2. They removed the region between the *Xba*I and *Kpn*I restriction sites (located near the 3' end of *env* and the 5' end of *nef*, respectively) by deleting the last 280 nucleotides of the 3' end of *env* and 220 nucleotides of *nef* (including the initiation codon) and inserted the CAT gene with a translational promoter derived from pU3R-I between the two restriction sites to replace the deleted region. They demonstrated for the first time that a foreign gene could be introduced into the HIV provirus without destroying viral replication (in Jurkat cells), that the foreign gene remained functional, and that the virus with the foreign gene was susceptible to anti-viral drugs *in vitro*. They also noted the importance of reporter gene size and that insertion of a foreign gene larger than 700 bp may prevent viral RNA from being packaged efficiently during assembly[204].

Since *nef* could be altered without inhibiting viral replication *in vitro*, it became a common location to modify for insertion of reporter genes. In 1994, Dr. Baltimore and colleagues introduced one of the first HIV-1 reporter viruses to incorporate luciferase. With this construct, the 34 amino acids coding region of HXB2 Nef between the *Not*I and *Xho*I restriction sites were deleted and FLuc was inserted in its place, preserving the Nef translation start site. Luciferase activity was observed to be a sensitive and quantifiable marker for HIV expression *in vitro*[205]. In 1997, Dr. Feinberg created a GFP-expressing HIV-1 reporter virus using the NL4-3 proviral backbone by truncating *env* and almost completely excising *nef* (from restriction sites *Bam*HI to *Xba*I) and inserting *gfp* (with modifications to its 5' end to initiate translation) in its place. This construct was replication-competent in H9 T cells and permitted quantification of viral infection[206]. By 1998, however, it was determined that the full or partial replacement of *nef* with a reporter gene could result in attenuated viral replication *in vitro* and impeded viral replication in animal models *in vivo*[207]. To overcome this limitation, Drs. Jamieson and Zack deleted 119 bp of HIV-1 NL4-3 *vpr* between *Xba*I and *Eco*RI and inserted mouse heat-stable antigen (HSA) between the two restriction sites. SCID-hu mice were then inoculated with the HSA reporter virus to model HIV-1 infection of human thymocytes. This became the first HIV-1 reporter virus that was replication-competent *in vivo*, but its replication kinetics remained significantly attenuated[207], and no further modifications in the central region of the HIV-1 genome for reporter virus design were described for decades.

In 2004, Levy *et. al* sought to use reporter virus technology to measure HIV-1 recombination in target cells. They inserted either *eyfp* or *ecfp* reporter genes between the *env* and *nef* orfs of NL4-3. An encephalomyocarditis virus (EMCV) internal ribosome entry

site (IRES)— around 200 amino acids in size— was included between the reporter gene and *nef* to direct downstream Nef expression[208]. The result was an *in vitro* replication-competent reporter virus that proved useful for its intended application but overexpressed Nef, had delayed replication kinetics in primary cells, and the reporter gene was not stably retained over multiple rounds of replication[208-210]. In addition to the 3' end (*nef*) and center (*vpr*) of the proviral genome, the 5' end of the HIV-1 genome was also considered as a potential location to insert reporter genes. In 2004 for example, Müller *et. al* inserted *gfp* into *gag* between the MA and CA domains. However, this reporter construct was significantly less infectious than wildtype virus and MA expression was reduced[211]. Reporter constructs with reporter genes inserted in or around *gag* continue to be used today for specific purposes[212,213], but issues regarding infectivity and viral protein expression persist and limit their broader applications.

In Edmonds *et. al* (2010), Drs. Kappes and Ochsenbauer devised a reporter virus design informed by the work of Levy *et. al* that preserved the orfs of all the viral genes and the stable expression of the reporter gene. The IRES element described in Levy *et. al* was replaced with the "self-cleaving" T2A peptide, a short peptide 18 amino acids in length[209]. The T2A peptide was derived from the aphthovirus foot-and-mouth disease virus polyprotein, and it modifies ribosomal activity to "skip" from an upstream codon to a downstream codon without forming a peptide bond during translation[214]. The LucR gene was fused in-frame to the T2A peptide, which was then inserted between NL4-3 *env* and *nef*, preserving the Nef start codon. The T2A peptide was included to drive Nef translation downstream of LucR, and the LucR-T2A reporter virus was demonstrated to be infectious and replication-competent in primary cells[209]. However, the design of this reporter was

expected to interfere with the N-terminal myristoylation of Nef and thus Nef function[209], and it also unexpectedly resulted in reduced Nef expression in infected T cells[215,216]. Recognizing the application limitation stemming from the reduced Nef expression, Drs. Kappes and Ochsenbauer improved on the reporter design by replacing T2A with an optimized, truncated EMCV IRES element (145 amino acids in size) referred to as "6ATRi" in Alberti *et. al* (2015). This IRES element was selected after screening 11 IRES elements ranging in size from around 63-200 amino acids. Though a slight delay in replication kinetics was observed with the 6ATRi element in proviral backbones from some HIV-1 strains, Nef expression and function were similar between the LucR-6ATRi reporter viruses and parental non-reporter virus[215,216].

Drs. Kappes and Ochsenbauer also pioneered the use of TF virus Envs in reporter virus design, which was done initially to study HIV-1 Env in the context of replication-competent virus. In Edmonds *et. al*, they had first replaced the Env ectodomain coding region of NL4-3 from the start of the C1 domain through the membrane spanning domain with two heterologous strain Env ectodomain coding sequences[209] followed by Env ectodomain coding sequences from the first, recently identified subtype B TF strains and reference panel *envs*[23,217]. The Env ectodomain region (encompassing gp120 and the extracellular portion of gp41) is a functionally favored, natural site of recombination in CRFs[146,171,218]. It has been demonstrated that the neutralization phenotypes[209,219] and the cellular tropism phenotypes[23] of TF viruses are transferable into proviral backbones through the introduction of their heterologous Env ectodomains. These HIV reporter viruses that incorporate the Env ectodomains of TF viruses from infectious molecular clones (IMCs) are referred to as reporter Env-IMCs. IMCs incorporating the genome of

entire TF HIV-1 strains[23,220] have also been engineered to express reporter genes, where the reporter gene cassettes were inserted between *env* and *nef* essentially as described in Edmonds *et. al* and Alberti *et. al*. The Env-IMC and TF-IMC reporter strategy has been expanded to include reporter genes coding for proteins aside from LucR, including those encoding: GFP, HSA (mCD24), NLuc, and derivatives of NLuc[23,216,221-238]. The diverse applications of these reporter Env-IMCs and reporter TF-IMCs in HIV-1 studies involving immortalized cell lines, primary cells, tissue explants, and animal models are described below.

Applications of Reporter Viruses in Studies of HIV-1

The applications of the reporter Env-IMCs and reporter TF-IMCs in studies of HIV-1 can be broadly summarized into 4 categories: elucidation of HIV-1 biology, *in vivo* modeling of HIV-1 acquisition and dissemination, investigation of host immune responses to HIV-1, and evaluation of the efficacy of anti-HIV therapeutics and vaccine research. In regards to the elucidation of HIV-1 biology, the reporter Env-IMCs have been employed to interrogate key steps of the HIV-1 replication cycle, study the functions of viral proteins, characterize viral-based components affecting transmission efficiency, and numerous other properties as expanded upon below. Cavrois *et. al* employed an HSA Env-IMC to study viral entry into primary CD4+ T cells and identified a subset of memory CD4+ T cells that were permissive to viral entry but did not support viral gene expression[221]. Alberti *et. al* used LucR Env-IMCs to analyze Nef function following the infection of T cell lines and primary cells[215]. Drs. Ochsenbauer and Astronomo have collaborated on multiple publications detailing the *ex vivo* infection of rectal and cervicovaginal explant tissues by

NLuc Env-IMCs, with an emphasis on the role of broadly neutralizing antibodies (bnAbs) in protecting against mucosal transmission[226,227].

Aside from *ex vivo* models, the biology of HIV-1 has also been studied *in vivo* using the reporter Env-IMCs and reporter TF-IMCs to inoculate humanized mice (HM) and hu-transgenic mice. HM are immunodeficient mice that have been engrafted with functional cells or tissues from humans[239]. Hu-transgenic mice are mice with genomes containing human DNA; these mice are created by injecting human DNA coding for a protein of interest into the nucleus of fertilized mouse eggs, and the offspring mice express the human protein[240]. Application of reporter IMCs in studies incorporating HM or hu-transgenic mice inform HIV-1 transmission and treatment efficacy in a biologically relevant system[222,229-232]. For studies using HM to study HIV-1, HM are engrafted with human hematopoietic stem cells or peripheral blood mononuclear cells (PBMCs), which are permissive to HIV-1 (including reporter Env-IMC) infection and replication and affected by anti-viral therapies *in vivo*. Ventura *et. al* observed that GFP TF-IMC and NLuc TF-IMC infection and spread were responsive to combination ART in HM *in vivo*[222]. Dr. Goldstein has used reporter Env-IMCs extensively in hu-transgenic mouse models[241-243]. The mice are transgenic for human CD4, CCR5, and cyclin T1, which are expressed by the mouse CD4+ T cells, dendritic cells, and monocytes[241], rendering them permissive to HIV-1 infection. Utilizing LucR Env-IMCs encoding subtype A/E or C TF Env ectodomains, the authors demonstrated that *in vivo* infection by LucR Env-IMCs in hu-transgenic mice is inhibited by bnAbs[242].

Reporter IMCs have also been used to study host immune responses elicited by vaccines, including bnAbs[217,237,244,245] and CD8+ T cell response[223,235,236,246-248]. The

presence of bnAbs in a vaccinated individual is one of the best correlates for vaccine efficacy[249-251]. BnAbs are one host immune response that has been interrogated *in vitro, in vivo,* and *ex vivo* using reporter Env-IMCs to understand their role in protecting against the acquisition and dissemination of HIV-1[226,227,237,241,242]. With regards to HIV-1, bnAbs are broad and potent host antibodies that inhibit viral entry into host cells by targeting conserved epitopes within HIV Env[249]. However, bnAbs are rarely induced in the presence of HIV infection because Env glycoprotein epitopes are shielded from the host immune system[249,250]. Non-HIV vaccines that induce neutralizing antibodies provide the strongest protection against non-HIV viruses in clinical settings, which is why the induction of broad and potent bnAbs against heterologous HIV-1 strains is a principal goal of HIV-1 vaccine design[250].

Another host immune response that has been investigated using reporter Env-IMCs is antibody-dependent cellular cytotoxicity (ADCC) responses to HIV-1 infection [216,237,244,252,253]. ADCC is an immune mechanism through which an effector cell, such as natural killer (NK) cells, recognizes IgG bound to epitopes on the surface of infected target cells and releases cytotoxic factors to destroy the infected cells[254]. Drs. Finzi and Ochsenbauer employed LucR Env-IMCs in a study that demonstrated that surface CD4 downregulation by Nef in HIV-infected cells was inversely correlated to ADCC activity, suggesting that Nef downregulation of CD4 protected HIV-infected cells against ADCC *in vitro*[216]. Mielke *et. al* used a panel of LucR Env-IMCs to investigate the neutralizing and ADCC activity of antibodies *in vitro* to inform strategies for improving HIV vaccine efficacy[244].

Induction of HIV-1 specific CD8+ T cell responses is also critical for effective control of HIV-1 infection and the goal for the development of efficacious vaccines. CD8+ T cell responses have been evaluated *in vitro* using reporter Env- and TF-IMCs [223,235,236,247,248]. In one example, Fernandez *et. al* isolated primary CD8+ T and CD4+ T cells from ART-naïve individuals living with HIV-1, then infected the CD4+ T cells with a panel of 35 LucR TF-IMCs to characterize autologous CD8+ T cell inhibition of viral replication and establish a standard virus inhibition assay (VIA)[235]. In addition to infection- and vaccine-elicited host immune responses, reporter Env-IMCs have been used to evaluate effectiveness of anti-HIV therapeutics in *ex vivo, in vitro* and *in vivo* humanized mouse models[222,226,227,233]. For example, George *et. al* determined that female genital fibroblasts reduced the efficacy of PrEP in protecting PBMCs from HSA Env-IMC infection *in vitro*[233]. In summary, reporter Env-IMCs and TF-IMC have demonstrated utility in a broad range of applications pertaining to studies of HIV-1 biology, virus-host interactions, and vaccine research.

Thesis Overview and Rationale

The HIV-1 field is over 40 years old, but a vaccine or cure for the virus has yet to be discovered. The rise of CRFs and the emergence of drug-resistant viral strains have impeded HIV-1 vaccine/cure discovery efforts. Gaps in knowledge in the most fundamental aspects of HIV-1 biology have also impeded these efforts. Foremost, despite the finding that heterosexual intercourse is the most common route for HIV-1 acquisition[144], viral factors contributing to the mucosal transmission of HIV-1 to the female reproductive tract (FRT) are poorly understood. Previous work has shown that viral replicative fitness, co-receptor usage, and early virus-host cell interactions can affect

mucosal transmission and subsequent disease progression[20,156,166,170,174,255-258]. However, many of the tools and model systems used in these studies are limited in their abilities to sensitively distinguish the earliest viral infection and replication events following transmission. Herein, we report on our findings from our investigation of viral properties affecting HIV-1 transmission using an innovative virologic approach and highly sensitive model system.

Reporter viruses are one tool used to study HIV-1 transmission. However, the design of many of these existing reporter viruses interferes with aspects of viral gene expression, reducing their usability for studies of mucosal transmission as described above. The reporter IMC utilizing the 6ATRi element to drive Nef expression was originally designed to overcome issues of viral gene expression observed with the T2A peptide-based design, but a slight delay in LucR Env-IMC replication kinetics was observed[215]. Prévost *et. al* also later demonstrated that with some viral strains, LucR.6ATRi Env-IMC Nef incompletely downregulated host surface CD4, causing infected cells to be more susceptible to ADCC compared to non-reporter virus *in vitro*[216]. These 6ATRi reporter IMCs have broad utility *in vitro, in vivo,* and *ex vivo,* as discussed above, but we further sought a new reporter virus design that avoided *nef* entirely. A newly optimized HIV reporter virus designed by our lab that incorporates a small NLuc derivative, the luminescent HiBiT peptide, attached to truncated Vif was demonstrated to overcome many of the aforementioned limitations of previous reporter viruses. Its potential usefulness for studies of HIV transmission is described in Chapter 1.

To study HIV-1 transmission in three-dimensional biological systems, reporter viruses have been employed in both *in vivo* and *ex vivo* models[222,226,227,229-232,234,242]. *In vivo*

models of mucosal HIV-1 transmission usually incorporate either genetically modified mice or non-human primates (NHP). These models have been useful for informing mechanisms of mucosal HIV-1 transmission and evaluating the efficacy of anti-HIV interventions[207,239,259-262]. However, differences in the anatomy/physiology, pH, cell trafficking, and microflora in the reproductive tissues of these animals suggest that the animal tissues may not fully recapitulate the human tissue environment[263-265]. *Ex vivo* models using human explant tissues may thus complement the findings of *in vivo* models by providing translationally-relevant insights into mucosal HIV-1 transmission. Explant tissues from the FRT are infectible *ex vivo* without the need for outside activation/stimulation[266-268]. Additionally, they support productive TF viral replication and even mimic the natural R5-tropic virus transmission bottleneck observed clinically[174,267]. Explant FRT tissues have been used to model HIV-1 infection and replication, test anti-HIV drugs, examine host immune responses to HIV, and investigate numerous other HIV-related mechanisms *ex vivo*[20,226,227,267,269-286]. The multiple applications of *ex vivo* FRT models to study HIV-1 are expanded on in Chapter 3.

The ability to elucidate the earliest viral infection and replication events, however, is limited in current *ex vivo* models of mucosal HIV-1 transmission. Thus, to address our main question of which viral properties affect mucosal transmission, we developed a reporter virus technology approach to interrogate mucosal HIV-1 transmission with unprecedented sensitivity in an *ex vivo* cervical explant model. The methodology detailing how to apply this reporter virus technology *ex vivo* for studies pertaining to HIV-1 transmission is described in Chapter 4. In Chapter 5, we investigate viral properties affecting HIV-1 transmission that map to HIV-1 Env by applying the methodology detailed

in Chapter 4. We determine that the subtype of HIV-1 Env and CD4 binding proficiency affect the efficiency of viral transmission and replication *ex vivo*.

REFERENCES

1. Lu, K., Heng, X. & Summers, M.F. Structural determinants and mechanism of HIV-1 genome packaging. *J Mol Biol* **410**, 609-33 (2011).
2. International Committee on Taxonomy of Viruses: ICTV. (2022).
3. Coffin JM, H.S., Varmus HE. The Place of Retroviruses in Biology. in *Retroviruses* (Cold Spring Harbor Laboratory Press, Cold Spring Harbor, NY, 1997).
4. Zhang, J. & Crumpacker, C. HIV UTR, LTR, and Epigenetic Immunity. *Viruses* **14**(2022).
5. Nilson, K.A. & Price, D.H. The Role of RNA Polymerase II Elongation Control in HIV-1 Gene Expression, Replication, and Latency. *Genet Res Int* **2011**, 726901 (2011).
6. van Heuvel, Y., Schatz, S., Rosengarten, J.F. & Stitz, J. Infectious RNA: Human Immunodeficiency Virus (HIV) Biology, Therapeutic Intervention, and the Quest for a Vaccine. *Toxins (Basel)* **14**(2022).
7. Emery, A. & Swanstrom, R. HIV-1: To Splice or Not to Splice, That Is the Question. *Viruses* **13**(2021).
8. Tazi, J. et al. Alternative splicing: regulation of HIV-1 multiplication as a target for therapeutic action. *The FEBS Journal* **277**, 867-876 (2010).
9. Sertznig, H., Hillebrand, F., Erkelenz, S., Schaal, H. & Widera, M. Behind the scenes of HIV-1 replication: Alternative splicing as the dependency factor on the quiet. *Virology* **516**, 176-188 (2018).
10. Ganser-Pornillos, B.K., Yeager, M. & Pornillos, O. Assembly and architecture of HIV. *Adv Exp Med Biol* **726**, 441-65 (2012).
11. Stano, A. et al. Dense Array of Spikes on HIV-1 Virion Particles. *J Virol* **91**(2017).
12. Sundquist, W.I. & Kräusslich, H.G. HIV-1 assembly, budding, and maturation. *Cold Spring Harb Perspect Med* **2**, a006924 (2012).
13. Jiao, Y. et al. Profile of HIV-1 infected patients from an AIDS clinic in Beijing from 2007-2008. *Current HIV research* **8**, 515-20 (2010).
14. HIV Basics. Vol. 2020 (Centers for Disease Control and Prevention, 2020).
15. Wawer, M.J. et al. Rates of HIV-1 transmission per coital act, by stage of HIV-1 infection, in Rakai, Uganda. *J Infect Dis* **191**, 1403-9 (2005).
16. Gonzalez, S.M., Aguilar-Jimenez, W., Su, R.-C. & Rugeles, M.T. Mucosa: Key Interactions Determining Sexual Transmission of the HIV Infection. *Frontiers in Immunology* **10**(2019).
17. Pudney, J., Quayle, A.J. & Anderson, D.J. Immunological Microenvironments in the Human Vagina and Cervix: Mediators of Cellular Immunity Are Concentrated in the Cervical Transformation Zone. *Biology of Reproduction* **73**, 1253-1263 (2005).
18. Cohen, M.S., Shaw, G.M., McMichael, A.J. & Haynes, B.F. Acute HIV-1 Infection. *N Engl J Med* **364**, 1943-54 (2011).
19. Peters, P.J. et al. Infection of ectocervical tissue and universal targeting of T-cells mediated by primary non-macrophage-tropic and highly macrophage-tropic HIV-1 R5 envelopes. *Retrovirology* **12**, 48 (2015).

20. Klein, K. et al. Deep Gene Sequence Cluster Analyses of Multi-Virus-Infected Mucosal Tissue Reveal Enhanced Transmission of Acute HIV-1. *J Virol* **95**(2021).
21. Baxter, A. et al. Macrophage Infection via Selective Capture of HIV-1-Infected CD4+ T Cells. *Cell Host & Microbe* **16**, 711-721 (2014).
22. Cassol, E., Cassetta, L., Alfano, M. & Poli, G. Macrophage polarization and HIV-1 infection. *J Leukoc Biol* **87**, 599-608 (2010).
23. Ochsenbauer, C. et al. Generation of Transmitted/Founder HIV-1 Infectious Molecular Clones and Characterization of Their Replication Capacity in CD4 T Lymphocytes and Monocyte-Derived Macrophages. **86**, 2715-2728 (2012).
24. Rodriguez-Garcia, M. et al. Estradiol reduces susceptibility of CD4+ T cells and macrophages to HIV-infection. *PLoS One* **8**, e62069 (2013).
25. Shen, R. et al. Macrophages in Vaginal but Not Intestinal Mucosa Are Monocyte-Like and Permissive to Human Immunodeficiency Virus Type 1 Infection. *Journal of Virology* **83**, 3258-3267 (2009).
26. Tuttle, D.L., Harrison, J.K., Anders, C., Sleasman, J.W. & Goodenow, M.M. Expression of CCR5 increases during monocyte differentiation and directly mediates macrophage susceptibility to infection by human immunodeficiency virus type 1. *J Virol* **72**, 4962-9 (1998).
27. Kruize, Z. & Kootstra, N.A. The Role of Macrophages in HIV-1 Persistence and Pathogenesis. *Frontiers in Microbiology* **10**(2019).
28. Stieh, D. et al. Th17 Cells Are Preferentially Infected Very Early after Vaginal Transmission of SIV in Macaques. *Cell Host & Microbe* **19**, 529-540 (2016).
29. Woodham, A.W. et al. Human Immunodeficiency Virus Immune Cell Receptors, Coreceptors, and Cofactors: Implications for Prevention and Treatment. *AIDS Patient Care STDS* **30**, 291-306 (2016).
30. Yi, Y. et al. Role of CXCR4 in cell-cell fusion and infection of monocyte-derived macrophages by primary human immunodeficiency virus type 1 (HIV-1) strains: two distinct mechanisms of HIV-1 dual tropism. *J Virol* **73**, 7117-25 (1999).
31. Ward, A.B. & Wilson, I.A. Insights into the trimeric HIV-1 envelope glycoprotein structure. *Trends Biochem Sci* **40**, 101-7 (2015).
32. Wilen, C.B., Tilton, J.C. & Doms, R.W. HIV: cell binding and entry. *Cold Spring Harb Perspect Med* **2**(2012).
33. Rathore, U. et al. Glycosylation of the core of the HIV-1 envelope subunit protein gp120 is not required for native trimer formation or viral infectivity. *J Biol Chem* **292**, 10197-10219 (2017).
34. Pancera, M. et al. Structure of HIV-1 gp120 with gp41-interactive region reveals layered envelope architecture and basis of conformational mobility. *Proc Natl Acad Sci U S A* **107**, 1166-71 (2010).
35. Prabakaran, P., Dimitrov, A.S., Fouts, T.R. & Dimitrov, D.S. Structure and function of the HIV envelope glycoprotein as entry mediator, vaccine immunogen, and target for inhibitors. *Adv Pharmacol* **55**, 33-97 (2007).
36. Zhao, C., Li, H., Swartz, T.H. & Chen, B.K. The HIV Env Glycoprotein Conformational States on Cells and Viruses. *mBio* **13**, e01825-21 (2022).
37. Zhang, S. et al. Dual Pathways of Human Immunodeficiency Virus Type 1 Envelope Glycoprotein Trafficking Modulate the Selective Exclusion of

Uncleaved Oligomers from Virions. *Journal of Virology* **95**, 10.1128/jvi.01369-20 (2021).
38. Claeys, E. & Vermeire, K. The CD4 Receptor: An Indispensable Protein in T Cell Activation and A Promising Target for Immunosuppression. *Archives of Microbiology & Immunology* **3**, 133-150 (2019).
39. Shaik, M.M. et al. Structural basis of coreceptor recognition by HIV-1 envelope spike. *Nature* **565**, 318-323 (2019).
40. Hu, W.S. & Hughes, S.H. HIV-1 reverse transcription. *Cold Spring Harb Perspect Med* **2**(2012).
41. Chauhan, A. & Khandkar, M. Endocytosis of human immunodeficiency virus 1 (HIV-1) in astrocytes: a fiery path to its destination. *Microb Pathog* **78**, 1-6 (2015).
42. Aiken, C. & Rousso, I. The HIV-1 capsid and reverse transcription. *Retrovirology* **18**, 29 (2021).
43. Müller, T.G., Zila, V., Müller, B. & Kräusslich, H.-G. Nuclear Capsid Uncoating and Reverse Transcription of HIV-1. *Annual Review of Virology* **9**, 261-284 (2022).
44. Hill, M., Tachedjian, G. & Mak, J. The packaging and maturation of the HIV-1 Pol proteins. *Curr HIV Res* **3**, 73-85 (2005).
45. Corona, A. et al. Ribonuclease H/DNA Polymerase HIV-1 Reverse Transcriptase Dual Inhibitor: Mechanistic Studies on the Allosteric Mode of Action of Isatin-Based Compound RMNC6. *PLOS ONE* **11**, e0147225 (2016).
46. Overview of Reverse Transcription. in *Retroviruses* (ed. Coffin JM, H.S., Varmus HE) (Cold Spring Harbor Laboratory Press, Cold Spring Harbor, NY, 1997).
47. Engelman, A.N. & Singh, P.K. Cellular and molecular mechanisms of HIV-1 integration targeting. *Cell Mol Life Sci* **75**, 2491-2507 (2018).
48. Ohlmann, T., Mengardi, C. & López-Lastra, M. Translation initiation of the HIV-1 mRNA. *Translation (Austin)* **2**, e960242 (2014).
49. Karn, J. & Stoltzfus, C.M. Transcriptional and posttranscriptional regulation of HIV-1 gene expression. *Cold Spring Harb Perspect Med* **2**, a006916 (2012).
50. Richter, S.N., Frasson, I. & Palù, G. Strategies for inhibiting function of HIV-1 accessory proteins: a necessary route to AIDS therapy? *Curr Med Chem* **16**, 267-86 (2009).
51. Das, A.T., Klaver, B. & Berkhout, B. The 5' and 3' TAR elements of human immunodeficiency virus exert effects at several points in the virus life cycle. *J Virol* **72**, 9217-23 (1998).
52. Buffalo, C.Z., Iwamoto, Y., Hurley, J.H. & Ren, X. How HIV Nef Proteins Hijack Membrane Traffic To Promote Infection. *J Virol* **93**(2019).
53. Foster, J.L. & Garcia, J.V. HIV-1 Nef: at the crossroads. *Retrovirology* **5**, 84 (2008).
54. Magadán, J.G. et al. Multilayered Mechanism of CD4 Downregulation by HIV-1 Vpu Involving Distinct ER Retention and ERAD Targeting Steps. *PLOS Pathogens* **6**, e1000869 (2010).
55. Brakier-Gingras, L., Charbonneau, J. & Butcher, S.E. Targeting frameshifting in the human immunodeficiency virus. *Expert Opin Ther Targets* **16**, 249-58 (2012).

56. Freed, E.O. HIV-1 assembly, release and maturation. *Nature Reviews Microbiology* **13**, 484-496 (2015).
57. Mouzakis, K.D., Lang, A.L., Vander Meulen, K.A., Easterday, P.D. & Butcher, S.E. HIV-1 frameshift efficiency is primarily determined by the stability of base pairs positioned at the mRNA entrance channel of the ribosome. *Nucleic Acids Res* **41**, 1901-13 (2013).
58. Guerrero, S. et al. HIV-1 replication and the cellular eukaryotic translation apparatus. *Viruses* **7**, 199-218 (2015).
59. Khan, N. & Geiger, J.D. Role of Viral Protein U (Vpu) in HIV-1 Infection and Pathogenesis. *Viruses* **13**(2021).
60. Sheehy, A.M., Gaddis, N.C., Choi, J.D. & Malim, M.H. Isolation of a human gene that inhibits HIV-1 infection and is suppressed by the viral Vif protein. *Nature* **418**, 646-650 (2002).
61. Sheehy, A.M., Gaddis, N.C. & Malim, M.H. The antiretroviral enzyme APOBEC3G is degraded by the proteasome in response to HIV-1 Vif. *Nature medicine* **9**, 1404-1407 (2003).
62. Marin, M., Rose, K.M., Kozak, S.L. & Kabat, D. HIV-1 Vif protein binds the editing enzyme APOBEC3G and induces its degradation. *Nature medicine* **9**, 1398-1403 (2003).
63. Stopak, K., de Noronha, C., Yonemoto, W. & Greene, W.C. HIV-1 Vif blocks the antiviral activity of APOBEC3G by impairing both its translation and intracellular stability. *Mol Cell* **12**, 591-601 (2003).
64. Wiegand, H.L., Doehle, B.P., Bogerd, H.P. & Cullen, B.R. A second human antiretroviral factor, APOBEC3F, is suppressed by the HIV-1 and HIV-2 Vif proteins. *EMBO J* **23**, 2451-8 (2004).
65. Hu, Y. et al. Structural basis of antagonism of human APOBEC3F by HIV-1 Vif. *Nature Structural & Molecular Biology* **26**, 1176-1183 (2019).
66. Emerman, M. HIV-1, Vpr and the cell cycle. *Current Biology* **6**, 1096-1103 (1996).
67. González, M.E. The HIV-1 Vpr Protein: A Multifaceted Target for Therapeutic Intervention. *International Journal of Molecular Sciences* **18**, 126 (2017).
68. Nodder, S.B. & Gummuluru, S. Illuminating the Role of Vpr in HIV Infection of Myeloid Cells. *Frontiers in Immunology* **10**(2019).
69. Yandrapalli, N. et al. Self assembly of HIV-1 Gag protein on lipid membranes generates PI(4,5)P(2)/Cholesterol nanoclusters. *Sci Rep* **6**, 39332 (2016).
70. Waheed, A.A., Ono, A. & Freed, E.O. Methods for the study of HIV-1 assembly. *Methods Mol Biol* **485**, 163-84 (2009).
71. Rossi, E., Meuser, M.E., Cunanan, C.J. & Cocklin, S. Structure, Function, and Interactions of the HIV-1 Capsid Protein. *Life (Basel)* **11**(2021).
72. Samal, A.B., Green, T.J. & Saad, J.S. Atomic view of the HIV-1 matrix lattice; implications on virus assembly and envelope incorporation. *Proceedings of the National Academy of Sciences* **119**, e2200794119 (2022).
73. Ghanam, R.H., Samal, A.B., Fernandez, T.F. & Saad, J.S. Role of the HIV-1 Matrix Protein in Gag Intracellular Trafficking and Targeting to the Plasma Membrane for Virus Assembly. *Front Microbiol* **3**, 55 (2012).

74. Weiss, E.R. & Göttlinger, H. The role of cellular factors in promoting HIV budding. *J Mol Biol* **410**, 525-33 (2011).
75. London, R.E. Structural Maturation of HIV-1 Reverse Transcriptase-A Metamorphic Solution to Genomic Instability. *Viruses* **8**(2016).
76. Agniswamy, J., Sayer, J.M., Weber, I.T. & Louis, J.M. Terminal interface conformations modulate dimer stability prior to amino terminal autoprocessing of HIV-1 protease. *Biochemistry* **51**, 1041-50 (2012).
77. Harrison, J. et al. Cryo-EM structure of the HIV-1 Pol polyprotein provides insights into virion maturation. *Sci Adv* **8**, eabn9874 (2022).
78. Weber, I.T., Wang, Y.F. & Harrison, R.W. HIV Protease: Historical Perspective and Current Research. *Viruses* **13**(2021).
79. Schmidt, T., Schwieters, C.D. & Clore, G.M. Spatial domain organization in the HIV-1 reverse transcriptase p66 homodimer precursor probed by double electron-electron resonance EPR. *Proceedings of the National Academy of Sciences* **116**, 17809-17816 (2019).
80. Kleinpeter, A.B. & Freed, E.O. HIV-1 Maturation: Lessons Learned from Inhibitors. *Viruses* **12**, 940 (2020).
81. Doitsh, G. & Greene, W.C. Dissecting How CD4 T Cells Are Lost During HIV Infection. *Cell Host Microbe* **19**, 280-91 (2016).
82. Chen, Q. et al. HIV associated cell death: Peptide-induced apoptosis restricts viral transmission. *Front Immunol* **14**, 1096759 (2023).
83. Coffin, J.M. & Hughes, S.H. Clonal Expansion of Infected CD4+ T Cells in People Living with HIV. *Viruses* **13**(2021).
84. Siliciano, R.F. & Greene, W.C. HIV latency. *Cold Spring Harb Perspect Med* **1**, a007096 (2011).
85. Vanhamel, J., Bruggemans, A. & Debyser, Z. Establishment of latent HIV-1 reservoirs: what do we really know? *J Virus Erad* **5**, 3-9 (2019).
86. UNAIDS. In Danger: UNAIDS Global AIDS Update 2022. (Geneva: Joint United Nations Programme on HIV/AIDS, 2022).
87. Baral, S. et al. Burden of HIV among female sex workers in low-income and middle-income countries: a systematic review and meta-analysis. *Lancet Infect Dis* **12**, 538-49 (2012).
88. Jewkes, R.K., Dunkle, K., Nduna, M. & Shai, N. Intimate partner violence, relationship power inequity, and incidence of HIV infection in young women in South Africa: a cohort study. *Lancet* **376**, 41-8 (2010).
89. Violence against women prevalence estimates, 2018: global, regional and national prevalence estimates for intimate partner violence against women, and global and regional prevalence estimates for non-partner sexual violence against women. (Geneva, 2021).
90. Lincoln, C., Perera, R., Jacobs, I. & Ward, A. Macroscopically detected female genital injury after consensual and non-consensual vaginal penetration: A prospective comparison study. *Journal of Forensic and Legal Medicine* **20**, 884-901 (2013).
91. Gilliam, B.L., Riedel, D.J. & Redfield, R.R. Clinical use of CCR5 inhibitors in HIV and beyond. *Journal of Translational Medicine* **9**, S9 (2011).

92. Ramana, L.N., Anand, A.R., Sethuraman, S. & Krishnan, U.M. Targeting strategies for delivery of anti-HIV drugs. *J Control Release* **192**, 271-83 (2014).
93. Lalezari, J.P. et al. A phase II clinical study of the long-term safety and antiviral activity of enfuvirtide-based antiretroviral therapy. *AIDS* **17**, 691-698 (2003).
94. Jamjian, M.C. & McNicholl, I.R. Enfuvirtide: first fusion inhibitor for treatment of HIV infection. *American Journal of Health-System Pharmacy* **61**, 1242-1247 (2004).
95. Matsumoto, K. et al. Characterization of a Novel CD4 Mimetic Compound YIR-821 against HIV-1 Clinical Isolates. *J Virol* **97**, e0163822 (2023).
96. Umotoy, J.C. & de Taeye, S.W. Antibody Conjugates for Targeted Therapy Against HIV-1 as an Emerging Tool for HIV-1 Cure. *Front Immunol* **12**, 708806 (2021).
97. Holec, A.D., Mandal, S., Prathipati, P.K. & Destache, C.J. Nucleotide Reverse Transcriptase Inhibitors: A Thorough Review, Present Status and Future Perspective as HIV Therapeutics. *Curr HIV Res* **15**, 411-421 (2017).
98. Jayne, J. Drug Resistance and Pre-exposure Prophylaxis (PrEP) Breakthrough Infections Threaten Goals to End the HIV/AIDS Epidemic. (American Society for Microbiology, Online, 2020).
99. Namasivayam, V. et al. The Journey of HIV-1 Non-Nucleoside Reverse Transcriptase Inhibitors (NNRTIs) from Lab to Clinic. *Journal of Medicinal Chemistry* **62**, 4851-4883 (2019).
100. Zhao, A.V. et al. A clinical review of HIV integrase strand transfer inhibitors (INSTIs) for the prevention and treatment of HIV-1 infection. *Retrovirology* **19**, 22 (2022).
101. Biswas, P., Jiang, X., Pacchia, A.L., Dougherty, J.P. & Peltz, S.W. The human immunodeficiency virus type 1 ribosomal frameshifting site is an invariant sequence determinant and an important target for antiviral therapy. *J Virol* **78**, 2082-7 (2004).
102. Anokhina, V.S. & Miller, B.L. Targeting Ribosomal Frameshifting as an Antiviral Strategy: From HIV-1 to SARS-CoV-2. *Accounts of Chemical Research* **54**, 3349-3361 (2021).
103. Thenin-Houssier, S. & Valente, S.T. HIV-1 Capsid Inhibitors as Antiretroviral Agents. *Curr HIV Res* **14**, 270-82 (2016).
104. Carnes, S.K., Sheehan, J.H. & Aiken, C. Inhibitors of the HIV-1 capsid, a target of opportunity. *Curr Opin HIV AIDS* **13**, 359-365 (2018).
105. McFadden, W.M. et al. Rotten to the core: antivirals targeting the HIV-1 capsid core. *Retrovirology* **18**, 41 (2021).
106. Diseases, N.I.o.D.a.D.a.K. LiverTox: Clinical and Research Information on Drug-Induced Liver Injury. in *Protease Inhibitors (HIV)* (Bethesda, MD, 2012).
107. Lv, Z., Chu, Y. & Wang, Y. HIV protease inhibitors: a review of molecular selectivity and toxicity. *HIV AIDS (Auckl)* **7**, 95-104 (2015).
108. Taylor, B.S., Sobieszczyk, M.E., McCutchan, F.E. & Hammer, S.M. The challenge of HIV-1 subtype diversity. *N Engl J Med* **358**, 1590-602 (2008).
109. Sharp, P.M. et al. The origins of acquired immune deficiency syndrome viruses: where and when? *Philos Trans R Soc Lond B Biol Sci* **356**, 867-76 (2001).

110. Hahn, B.H., Shaw, G.M., De Cock, K.M. & Sharp, P.M. AIDS as a zoonosis: scientific and public health implications. *Science* **287**, 607-14 (2000).
111. Sharp, P.M. & Hahn, B.H. The evolution of HIV-1 and the origin of AIDS. *Philos Trans R Soc Lond B Biol Sci* **365**, 2487-94 (2010).
112. Sharp, P.M. & Hahn, B.H. Origins of HIV and the AIDS pandemic. *Cold Spring Harb Perspect Med* **1**, a006841 (2011).
113. Rupp, S., Ambata, P., Narat, V. & Giles-Vernick, T. Beyond the Cut Hunter: A Historical Epidemiology of HIV Beginnings in Central Africa. *Ecohealth* **13**, 661-671 (2016).
114. Wertheim, J.O. & Worobey, M. Dating the age of the SIV lineages that gave rise to HIV-1 and HIV-2. *PLoS Comput Biol* **5**, e1000377 (2009).
115. Salemi, M. et al. Dating the common ancestor of SIVcpz and HIV-1 group M and the origin of HIV-1 subtypes using a new method to uncover clock-like molecular evolution. *Faseb j* **15**, 276-8 (2001).
116. Faria, N.R. et al. HIV epidemiology. The early spread and epidemic ignition of HIV-1 in human populations. *Science* **346**, 56-61 (2014).
117. Chitnis, A., Rawls, D. & Moore, J. Origin of HIV type 1 in colonial French Equatorial Africa? *AIDS Res Hum Retroviruses* **16**, 5-8 (2000).
118. Vidal, N. et al. Unprecedented degree of human immunodeficiency virus type 1 (HIV-1) group M genetic diversity in the Democratic Republic of Congo suggests that the HIV-1 pandemic originated in Central Africa. *J Virol* **74**, 10498-507 (2000).
119. Worobey, M. et al. Direct evidence of extensive diversity of HIV-1 in Kinshasa by 1960. *Nature* **455**, 661-664 (2008).
120. Gilbert, M.T. et al. The emergence of HIV/AIDS in the Americas and beyond. *Proc Natl Acad Sci U S A* **104**, 18566-70 (2007).
121. Kaleebu, P. et al. Relation between chemokine receptor use, disease stage, and HIV-1 subtypes A and D: results from a rural Ugandan cohort. *J Acquir Immune Defic Syndr* **45**, 28-33 (2007).
122. Robertson, D.L. et al. HIV-1 nomenclature proposal. *Science* **288**, 55-6 (2000).
123. Kessler, H.H. et al. Determination of human immunodeficiency virus type 1 subtypes by a rapid method useful for the routine diagnostic laboratory. *Clin Diagn Lab Immunol* **8**, 1018-20 (2001).
124. Fonjungo, P.N. et al. Human immunodeficiency virus type 1 group m protease in cameroon: genetic diversity and protease inhibitor mutational features. *J Clin Microbiol* **40**, 837-45 (2002).
125. Mendes Da Silva, R.K., Monteiro de Pina, A., II, Venegas Maciera, K., Gonçalves Morgado, M. & Lindenmeyer Guimarães, M. Genetic Characterization of a New HIV-1 Sub-Subtype A in Cabo Verde, Denominated A8. *Viruses* **13**(2021).
126. Hemelaar, J., Gouws, E., Ghys, P.D. & Osmanov, S. Global trends in molecular epidemiology of HIV-1 during 2000-2007. *Aids* **25**, 679-89 (2011).
127. Williams, A. et al. Geographic and Population Distributions of Human Immunodeficiency Virus (HIV)–1 and HIV-2 Circulating Subtypes: A Systematic Literature Review and Meta-analysis (2010–2021). *The Journal of Infectious Diseases* **228**, 1583-1591 (2023).

128. Gartner, M.J., Roche, M., Churchill, M.J., Gorry, P.R. & Flynn, J.K. Understanding the mechanisms driving the spread of subtype C HIV-1. *eBioMedicine* **53**(2020).
129. Bbosa, N., Kaleebu, P. & Ssemwanga, D. HIV subtype diversity worldwide. *Current Opinion in HIV and AIDS* **14**, 153-160 (2019).
130. Vidal, N., Bazepeo, S.E., Mulanga, C., Delaporte, E. & Peeters, M. Genetic characterization of eight full-length HIV type 1 genomes from the Democratic Republic of Congo (DRC) reveal a new subsubtype, A5, in the A radiation that predominates in the recombinant structure of CRF26_A5U. *AIDS Res Hum Retroviruses* **25**, 823-32 (2009).
131. Abidi, S.H. et al. Origin and evolution of HIV-1 subtype A6. *PLoS One* **16**, e0260604 (2021).
132. Grant, H.E. et al. A large population sample of African HIV genomes from the 1980s reveals a reduction in subtype D over time associated with propensity for CXCR4 tropism. *Retrovirology* **19**, 28 (2022).
133. Gounder, K. et al. Complex Subtype Diversity of HIV-1 Among Drug Users in Major Kenyan Cities. *AIDS Res Hum Retroviruses* **33**, 500-510 (2017).
134. Désiré, N. et al. Characterization update of HIV-1 M subtypes diversity and proposal for subtypes A and D sub-subtypes reclassification. *Retrovirology* **15**, 80 (2018).
135. Avila, M.M. et al. Two HIV-1 epidemics in Argentina: different genetic subtypes associated with different risk groups. *J Acquir Immune Defic Syndr* **29**, 422-6 (2002).
136. Tongo, M. et al. Phylogenetics of HIV-1 subtype G env: Greater complexity and older origins than previously reported. *Infection, Genetics and Evolution* **35**, 9-18 (2015).
137. Faria, N.R. et al. Distinct rates and patterns of spread of the major HIV-1 subtypes in Central and East Africa. *PLOS Pathogens* **15**, e1007976 (2019).
138. Triques, K. et al. Near-full-length genome sequencing of divergent African HIV type 1 subtype F viruses leads to the identification of a new HIV type 1 subtype designated K. *AIDS Res Hum Retroviruses* **16**, 139-51 (2000).
139. Yamaguchi, J. et al. Brief Report: Complete Genome Sequence of CG-0018a-01 Establishes HIV-1 Subtype L. *J Acquir Immune Defic Syndr* **83**, 319-322 (2020).
140. Li, X. et al. Tracing the epidemic history of HIV-1 CRF01_AE clusters using near-complete genome sequences. *Scientific Reports* **7**, 4024 (2017).
141. Alexiev, I. et al. Molecular Epidemiological Analysis of the Origin and Transmission Dynamics of the HIV-1 CRF01_AE Sub-Epidemic in Bulgaria. *Viruses* **13**(2021).
142. Kostaki, E.-G. et al. Spatiotemporal Characteristics of the Largest HIV-1 CRF02_AG Outbreak in Spain: Evidence for Onward Transmissions. *Frontiers in Microbiology* **10**(2019).
143. Rolland, M. & Modjarrad, K. Multiple co-circulating HIV-1 subtypes in the Middle East and North Africa. *Aids* **29**, 1417-9 (2015).
144. Shaw, G.M. & Hunter, E. HIV transmission. *Cold Spring Harb Perspect Med* **2**(2012).

145. Kariuki, S.M., Selhorst, P., Ariën, K.K. & Dorfman, J.R. The HIV-1 transmission bottleneck. *Retrovirology* **14**, 22 (2017).
146. Bagaya, B.S. et al. Functional bottlenecks for generation of HIV-1 intersubtype Env recombinants. *Retrovirology* **12**, 44 (2015).
147. Grivel, J.-C., Shattock, R.J. & Margolis, L.B. Selective transmission of R5 HIV-1 variants: where is the gatekeeper? *Journal of Translational Medicine* **9**, S6 (2010).
148. Margolis, L. & Shattock, R. Selective transmission of CCR5-utilizing HIV-1: the 'gatekeeper' problem resolved? *Nature Reviews Microbiology* **4**, 312-317 (2006).
149. Keele, B.F. et al. Identification and characterization of transmitted and early founder virus envelopes in primary HIV-1 infection. *Proc Natl Acad Sci U S A* **105**, 7552-7 (2008).
150. Parrish, N.F. et al. Phenotypic properties of transmitted founder HIV-1. *Proceedings of the National Academy of Sciences* **110**, 6626-6633 (2013).
151. Samson, M. et al. Resistance to HIV-1 infection in caucasian individuals bearing mutant alleles of the CCR-5 chemokine receptor gene. *Nature* **382**, 722-5 (1996).
152. Lopalco, L. CCR5: From Natural Resistance to a New Anti-HIV Strategy. *Viruses* **2**, 574-600 (2010).
153. Abecasis, A.B. et al. HIV-1 subtype distribution and its demographic determinants in newly diagnosed patients in Europe suggest highly compartmentalized epidemics. *Retrovirology* **10**, 7 (2013).
154. Buonaguro, L., Tornesello, M.L. & Buonaguro, F.M. Human immunodeficiency virus type 1 subtype distribution in the worldwide epidemic: pathogenetic and therapeutic implications. *J Virol* **81**, 10209-19 (2007).
155. van Harmelen, J. et al. An association between HIV-1 subtypes and mode of transmission in Cape Town, South Africa. *Aids* **11**, 81-7 (1997).
156. Ball, S.C. et al. Comparing the ex vivo fitness of CCR5-tropic human immunodeficiency virus type 1 isolates of subtypes B and C. *J Virol* **77**, 1021-38 (2003).
157. Junqueira, D.M. & Almeida, S.E.d.M. HIV-1 subtype B: Traces of a pandemic. *Virology* **495**, 173-184 (2016).
158. Pernas, B. et al. High prevalence of subtype F in newly diagnosed HIV-1 persons in northwest Spain and evidence for impaired treatment response. *Aids* **28**, 1837-40 (2014).
159. James, A. & Dixit, N.M. Transmitted HIV-1 is more virulent in heterosexual individuals than men-who-have-sex-with-men. *PLOS Pathogens* **18**, e1010319 (2022).
160. Patel, P. et al. Estimating per-act HIV transmission risk: a systematic review. *AIDS* **28**, 1509-1519 (2014).
161. Baeten, J.M. et al. HIV-1 Subtype D Infection Is Associated with Faster Disease Progression than Subtype A in Spite of Similar Plasma HIV-1 Loads. *The Journal of Infectious Diseases* **195**, 1177-1180 (2007).
162. Easterbrook, P.J. et al. Impact of HIV-1 viral subtype on disease progression and response to antiretroviral therapy. *J Int AIDS Soc* **13**, 4 (2010).

163. Eshleman, S.H. et al. Characterization of nevirapine resistance mutations in women with subtype A vs. D HIV-1 6-8 weeks after single-dose nevirapine (HIVNET 012). *J Acquir Immune Defic Syndr* **35**, 126-30 (2004).
164. Huang, W. et al. Coreceptor Tropism in Human Immunodeficiency Virus Type 1 Subtype D: High Prevalence of CXCR4 Tropism and Heterogeneous Composition of Viral Populations. *Journal of Virology* **81**, 7885-7893 (2007).
165. Kaleebu, P. et al. Effect of human immunodeficiency virus (HIV) type 1 envelope subtypes A and D on disease progression in a large cohort of HIV-1-positive persons in Uganda. *J Infect Dis* **185**, 1244-50 (2002).
166. Kapaata, A. et al. Infection with HIV-1 subtype D among acutely infected Ugandans is associated with higher median concentration of cytokines compared to subtype A. *IJID Regions* **3**, 89-95 (2022).
167. Kiwanuka, N. et al. HIV-1 viral subtype differences in the rate of CD4+ T-cell decline among HIV seroincident antiretroviral naive persons in Rakai district, Uganda. *J Acquir Immune Defic Syndr* **54**, 180-4 (2010).
168. Kyeyune, F. et al. Treatment failure and drug resistance is more frequent in HIV-1 subtype D versus subtype A-infected Ugandans over a 10-year study period. *AIDS* **27**, 1899-1909 (2013).
169. Parczewski, M. et al. Infection with HIV-1 subtype D adversely affects the live expectancy independently of antiretroviral drug use. *Infection, Genetics and Evolution* **90**, 104754 (2021).
170. Venner, C.M. et al. Infecting HIV-1 Subtype Predicts Disease Progression in Women of Sub-Saharan Africa. *EBioMedicine* **13**, 305-314 (2016).
171. Balinda, S.N. et al. Characterization of Near Full-Length Transmitted/Founder HIV-1 Subtype D and A/D Recombinant Genomes in a Heterosexual Ugandan Population (2006-2011). *Viruses* **14**(2022).
172. Ssemwanga, D. et al. Effect of HIV-1 Subtypes on Disease Progression in Rural Uganda: A Prospective Clinical Cohort Study. *PLOS ONE* **8**, e71768 (2013).
173. Panos, G. & Nelson, M. HIV-1 tropism. *Biomarkers in Medicine* **1**, 473-481 (2007).
174. Abraha, A. et al. CCR5- and CXCR4-tropic subtype C human immunodeficiency virus type 1 isolates have a lower level of pathogenic fitness than other dominant group M subtypes: implications for the epidemic. *J Virol* **83**, 5592-605 (2009).
175. Ringel, O. et al. The Hard Way towards an Antibody-Based HIV-1 Env Vaccine: Lessons from Other Viruses. *Viruses* **10**(2018).
176. Kim, D., Elizaga, M. & Duerr, A. HIV vaccine efficacy trials: towards the future of HIV prevention. *Infect Dis Clin North Am* **21**, 201-17, x (2007).
177. Ng'uni, T., Chasara, C. & Ndhlovu, Z.M. Major Scientific Hurdles in HIV Vaccine Development: Historical Perspective and Future Directions. *Front Immunol* **11**, 590780 (2020).
178. Borgo, G.M. & Rutishauser, R.L. Generating and measuring effective vaccine-elicited HIV-specific CD8 + T cell responses. *Curr Opin HIV AIDS* **18**, 331-341 (2023).
179. Global HIV & AIDS statistics — Fact sheet. (UNAIDS, 2023).
180. HIV.gov. The Global HIV and AIDS Epidemic. in *Data & Trends* Vol. 2024 (ed. HIV.gov) (HIV.gov, 2023).

181. UNAIDS. UNAIDS 2017. (2017).
182. HIV.gov. Impact on Racial and Ethnic Minorities. in *Data & Trends* Vol. 2024 (ed. HIV.gov) (HIV.gov, 2023).
183. HIV.gov. US Statistics. in *Data and Trends* Vol. 2024 (HIV.gov, Online, 2021).
184. HIV in the Southern United States. (Centers for Disease Control, 2019).
185. Li, S. et al. Overview of the reporter genes and reporter mouse models. *Animal Model Exp Med* **1**, 29-35 (2018).
186. Ghim, C.M., Lee, S.K., Takayama, S. & Mitchell, R.J. The art of reporter proteins in science: past, present and future applications. *BMB Rep* **43**, 451-60 (2010).
187. Consortium, U. Q9U6Y8 · RFP_DISSP. (ed. UniProt) (UniProt, 2024).
188. Gorman, C.M., Merlino, G.T., Willingham, M.C., Pastan, I. & Howard, B.H. The Rous sarcoma virus long terminal repeat is a strong promoter when introduced into a variety of eukaryotic cells by DNA-mediated transfection. *Proceedings of the National Academy of Sciences* **79**, 6777-6781 (1982).
189. Smale, S.T. Chloramphenicol acetyltransferase assay. *Cold Spring Harb Protoc* **2010**, pdb.prot5422 (2010).
190. Gendelman, H.E. et al. Trans-activation of the human immunodeficiency virus long terminal repeat sequence by DNA viruses. *Proc Natl Acad Sci U S A* **83**, 9759-63 (1986).
191. Ben-Artzi, H., Zeelon, E., Gorecki, M. & Panet, A. Double-stranded RNA-dependent RNase activity associated with human immunodeficiency virus type 1 reverse transcriptase. *Proc Natl Acad Sci U S A* **89**, 927-31 (1992).
192. Serganova, I. & Blasberg, R.G. Molecular Imaging with Reporter Genes: Has Its Promise Been Delivered? *Journal of Nuclear Medicine* **60**, 1665-1681 (2019).
193. Jefferson, R.A., Kavanagh, T.A. & Bevan, M.W. GUS fusions: beta-glucuronidase as a sensitive and versatile gene fusion marker in higher plants. *Embo j* **6**, 3901-7 (1987).
194. Lis, J.T., Simon, J.A. & Sutton, C.A. New heat shock puffs and beta-galactosidase activity resulting from transformation of Drosophila with an hsp70-lacZ hybrid gene. *Cell* **35**, 403-10 (1983).
195. Wei, X. et al. Emergence of resistant human immunodeficiency virus type 1 in patients receiving fusion inhibitor (T-20) monotherapy. *Antimicrob Agents Chemother* **46**, 1896-905 (2002).
196. Platt, E.J., Wehrly, K., Kuhmann, S.E., Chesebro, B. & Kabat, D. Effects of CCR5 and CD4 cell surface concentrations on infections by macrophagetropic isolates of human immunodeficiency virus type 1. *J Virol* **72**, 2855-64 (1998).
197. Sarzotti-Kelsoe, M. et al. Optimization and validation of the TZM-bl assay for standardized assessments of neutralizing antibodies against HIV-1. *J Immunol Methods* **409**, 131-46 (2014).
198. England, C.G., Ehlerding, E.B. & Cai, W. NanoLuc: A Small Luciferase Is Brightening Up the Field of Bioluminescence. *Bioconjug Chem* **27**, 1175-1187 (2016).
199. de Wet, J.R., Wood, K.V., Helinski, D.R. & DeLuca, M. Cloning of firefly luciferase cDNA and the expression of active luciferase in Escherichia coli. *Proc Natl Acad Sci U S A* **82**, 7870-3 (1985).

200. Tannous, B.A., Kim, D.E., Fernandez, J.L., Weissleder, R. & Breakefield, X.O. Codon-optimized Gaussia luciferase cDNA for mammalian gene expression in culture and in vivo. *Mol Ther* **11**, 435-43 (2005).
201. Suree, N., Koizumi, N., Sahakyan, A., Shimizu, S. & An, D.S. A novel HIV-1 reporter virus with a membrane-bound Gaussia princeps luciferase. *J Virol Methods* **183**, 49-56 (2012).
202. Maguire, C.A. et al. Gaussia luciferase variant for high-throughput functional screening applications. *Anal Chem* **81**, 7102-6 (2009).
203. Hall, M.P. et al. Engineered luciferase reporter from a deep sea shrimp utilizing a novel imidazopyrazinone substrate. *ACS Chem Biol* **7**, 1848-57 (2012).
204. Terwilliger, E.F., Godin, B., Sodroski, J.G. & Haseltine, W.A. Construction and use of a replication-competent human immunodeficiency virus (HIV-1) that expresses the chloramphenicol acetyltransferase enzyme. *Proc Natl Acad Sci U S A* **86**, 3857-61 (1989).
205. Chen, B.K., Saksela, K., Andino, R. & Baltimore, D. Distinct modes of human immunodeficiency virus type 1 proviral latency revealed by superinfection of nonproductively infected cell lines with recombinant luciferase-encoding viruses. *J Virol* **68**, 654-60 (1994).
206. KATHLEEN A. PAGE, T.L., and MARK B. FEINBERG. Use of a Green Fluorescent Protein as a Marker for Human Immunodeficiency Virus Type 1 Infection. *AIDS Research and Human Retroviruses* **13**, 1077-1081 (1997).
207. Jamieson, B.D. & Zack, J.A. In Vivo Pathogenesis of a Human Immunodeficiency Virus Type 1 Reporter Virus. *Journal of Virology* **72**, 6520-6526 (1998).
208. Levy, D.N., Aldrovandi, G.M., Kutsch, O. & Shaw, G.M. Dynamics of HIV-1 recombination in its natural target cells. *Proc Natl Acad Sci U S A* **101**, 4204-9 (2004).
209. Edmonds, T.G. et al. Replication competent molecular clones of HIV-1 expressing Renilla luciferase facilitate the analysis of antibody inhibition in PBMC. *Virology* **408**, 1-13 (2010).
210. Brown, A., Gartner, S., Kawano, T., Benoit, N. & Cheng-Mayer, C. HLA-A2 down-regulation on primary human macrophages infected with an M-tropic EGFP-tagged HIV-1 reporter virus. *J Leukoc Biol* **78**, 675-85 (2005).
211. Müller, B. et al. Construction and characterization of a fluorescently labeled infectious human immunodeficiency virus type 1 derivative. *J Virol* **78**, 10803-13 (2004).
212. Kirui, J. & Freed, E.O. Generation and validation of a highly sensitive bioluminescent HIV-1 reporter vector that simplifies measurement of virus release. *Retrovirology* **17**(2020).
213. Hübner, W. et al. Sequence of Human Immunodeficiency Virus Type 1 (HIV-1) Gag Localization and Oligomerization Monitored with Live Confocal Imaging of a Replication-Competent, Fluorescently Tagged HIV-1. *Journal of Virology* **81**, 12596-12607 (2007).
214. Donnelly, M.L.L. et al. Analysis of the aphthovirus 2A/2B polyprotein 'cleavage' mechanism indicates not a proteolytic reaction, but a novel translational effect: a putative ribosomal 'skip'. *J Gen Virol* **82**, 1013-1025 (2001).

215. Alberti, M.O. et al. Optimized Replicating Renilla Luciferase Reporter HIV-1 Utilizing Novel Internal Ribosome Entry Site Elements for Native Nef Expression and Function. *AIDS Res Hum Retroviruses* **31**, 1278-96 (2015).
216. Prévost, J. et al. Incomplete Downregulation of CD4 Expression Affects HIV-1 Env Conformation and Antibody-Dependent Cellular Cytotoxicity Responses. *J Virol* **92**(2018).
217. deCamp, A. et al. Global panel of HIV-1 Env reference strains for standardized assessments of vaccine-elicited neutralizing antibodies. *J Virol* **88**, 2489-507 (2014).
218. Simon-Loriere, E. et al. Molecular mechanisms of recombination restriction in the envelope gene of the human immunodeficiency virus. *PLoS Pathog* **5**, e1000418 (2009).
219. Binley, J.M. et al. Comprehensive cross-clade neutralization analysis of a panel of anti-human immunodeficiency virus type 1 monoclonal antibodies. *J Virol* **78**, 13232-52 (2004).
220. Salazar-Gonzalez, J.F. et al. Genetic identity, biological phenotype, and evolutionary pathways of transmitted/founder viruses in acute and early HIV-1 infection. *Journal of Experimental Medicine* **206**, 1273-1289 (2009).
221. Cavrois, M. et al. Mass Cytometric Analysis of HIV Entry, Replication, and Remodeling in Tissue CD4+ T Cells. *Cell Rep* **20**, 984-998 (2017).
222. Ventura, J.D. et al. Longitudinal bioluminescent imaging of HIV-1 infection during antiretroviral therapy and treatment interruption in humanized mice. *PLOS Pathogens* **15**, e1008161 (2019).
223. Freel, S.A. et al. Phenotypic and functional profile of HIV-inhibitory CD8 T cells elicited by natural infection and heterologous prime/boost vaccination. *J Virol* **84**, 4998-5006 (2010).
224. Pollara, J. et al. Association of HIV-1 Envelope-Specific Breast Milk IgA Responses with Reduced Risk of Postnatal Mother-to-Child Transmission of HIV-1. *J Virol* **89**, 9952-61 (2015).
225. Sung, J.A. et al. Dual-Affinity Re-Targeting proteins direct T cell-mediated cytolysis of latently HIV-infected cells. *J Clin Invest* **125**, 4077-90 (2015).
226. Astronomo, R.D. et al. Neutralization Takes Precedence Over IgG or IgA Isotype-related Functions in Mucosal HIV-1 Antibody-mediated Protection. *EBioMedicine* **14**, 97-111 (2016).
227. Astronomo, R.D. et al. Rectal tissue and vaginal tissue from intravenous VRC01 recipients show protection against ex vivo HIV-1 challenge. *J Clin Invest* **131**(2021).
228. Gornalusse, G.G. et al. Buprenorphine Increases HIV-1 Infection In Vitro but Does Not Reactivate HIV-1 from Latency. *Viruses* **13**(2021).
229. Seay, K. et al. In Vivo Activation of Human NK Cells by Treatment with an Interleukin-15 Superagonist Potently Inhibits Acute In Vivo HIV-1 Infection in Humanized Mice. *J Virol* **89**, 6264-74 (2015).
230. Seay, K. et al. The Vaginal Acquisition and Dissemination of HIV-1 Infection in a Novel Transgenic Mouse Model Is Facilitated by Coinfection with Herpes Simplex Virus 2 and Is Inhibited by Microbicide Treatment. *J Virol* **89**, 9559-70 (2015).

231. Bardhi, A. et al. Potent In Vivo NK Cell-Mediated Elimination of HIV-1-Infected Cells Mobilized by a gp120-Bispecific and Hexavalent Broadly Neutralizing Fusion Protein. *J Virol* **91**(2017).
232. Anthony-Gonda, K. et al. Multispecific anti-HIV duoCAR-T cells display broad in vitro antiviral activity and potent in vivo elimination of HIV-infected cells in a humanized mouse model. *Sci Transl Med* **11**(2019).
233. George, A.F. et al. Female Genital Fibroblasts Diminish the In Vitro Efficacy of PrEP against HIV. *Viruses* **14**, 1723 (2022).
234. Ma, T. et al. HIV efficiently infects T cells from the endometrium and remodels them to promote systemic viral spread. *Elife* **9**(2020).
235. Fernandez, N. et al. Assessment of a diverse panel of transmitted/founder HIV-1 infectious molecular clones in a luciferase based CD8 T-cell mediated viral inhibition assay. *Frontiers in Immunology* **13**(2022).
236. Hayes, P. et al. Breadth of CD8 T-cell mediated inhibition of replication of diverse HIV-1 transmitted-founder isolates correlates with the breadth of recognition within a comprehensive HIV-1 Gag, Nef, Env and Pol potential T-cell epitope (PTE) peptide set. *PLOS ONE* **16**, e0260118 (2021).
237. Richardson, S.I. et al. HIV Broadly Neutralizing Antibodies Expressed as IgG3 Preserve Neutralization Potency and Show Improved Fc Effector Function. *Frontiers in Immunology* **12**(2021).
238. Xie, G. et al. Characterization of HIV-induced remodeling reveals differences in infection susceptibility of memory CD4(+) T cell subsets in vivo. *Cell Rep* **35**, 109038 (2021).
239. Fujiwara, S. Humanized mice: A brief overview on their diverse applications in biomedical research. *J Cell Physiol* **233**, 2889-2901 (2018).
240. Council, N.R. Genetically Altered Mice: A Revolutionary Research Resource. in *Sharing Laboratory Resources: Genetically Altered Mice: Summary of a Workshop Held at the National Academy of Sciences, March 23-24, 1993* (National Academies Press, Washington DC, 1994).
241. Seay, K. et al. The Vaginal Acquisition and Dissemination of HIV-1 Infection in a Novel Transgenic Mouse Model Is Facilitated by Coinfection with Herpes Simplex Virus 2 and Is Inhibited by Microbicide Treatment. *Journal of Virology* **89**, 9559-9570 (2015).
242. Seay, K. et al. Mice transgenic for CD4-specific human CD4, CCR5 and cyclin T1 expression: a new model for investigating HIV-1 transmission and treatment efficacy. *PLoS One* **8**, e63537 (2013).
243. Anthony-Gonda, K. et al. In vivo killing of primary HIV-infected cells by peripheral-injected early memory-enriched anti-HIV duoCAR T cells. *JCI Insight* **7**(2022).
244. Mielke, D. et al. ADCC-mediating non-neutralizing antibodies can exert immune pressure in early HIV-1 infection. *PLOS Pathogens* **17**, e1010046 (2021).
245. Fouda, G.G. et al. Postnatally-transmitted HIV-1 Envelope variants have similar neutralization-sensitivity and function to that of nontransmitted breast milk variants. *Retrovirology* **10**, 3 (2013).
246. Grenningloh, R. et al. Ets-1 Maintains IL-7 Receptor Expression in Peripheral T Cells. *The Journal of Immunology* **186**, 969-976 (2011).

247. Freel, S.A. et al. Initial HIV-1 Antigen-Specific CD8⁺ T Cells in Acute HIV-1 Infection Inhibit Transmitted/Founder Virus Replication. *Journal of Virology* **86**, 6835-6846 (2012).
248. Naarding, M.A. et al. Development of a luciferase based viral inhibition assay to evaluate vaccine induced CD8 T-cell responses. *J Immunol Methods* **409**, 161-73 (2014).
249. Sok, D., Moldt, B. & Burton, D.R. SnapShot: broadly neutralizing antibodies. *Cell* **155**, 728-728.e1 (2013).
250. Haynes, B.F. et al. Strategies for HIV-1 vaccines that induce broadly neutralizing antibodies. *Nat Rev Immunol* **23**, 142-158 (2023).
251. Gilbert, P.B. et al. Neutralization titer biomarker for antibody-mediated prevention of HIV-1 acquisition. *Nature Medicine* **28**, 1924-1932 (2022).
252. Pollara, J. et al. High-throughput quantitative analysis of HIV-1 and SIV-specific ADCC-mediating antibody responses. *Cytometry Part A* **79A**, 603-612 (2011).
253. Mielke, D. et al. Selection of HIV Envelope Strains for Standardized Assessments of Vaccine-Elicited Antibody-Dependent Cellular Cytotoxicity-Mediating Antibodies. *Journal of Virology* **96**, e01643-21 (2022).
254. Deniskin, R. & Satter, L.F. Natural Kills Cells. in *Encyclopedia of Infection and Immunity* (ed. Rezaei, N.) 118-129 (Elsevier, Oxford, 2022).
255. Ganesan, A. et al. Immunologic and virologic events in early HIV infection predict subsequent rate of progression. *J Infect Dis* **201**, 272-84 (2010).
256. Claiborne, D.T. et al. Replicative fitness of transmitted HIV-1 drives acute immune activation, proviral load in memory CD4+ T cells, and disease progression. *Proceedings of the National Academy of Sciences* **112**, E1480-E1489 (2015).
257. Quiñones-Mateu, M.E. et al. A dual infection/competition assay shows a correlation between ex vivo human immunodeficiency virus type 1 fitness and disease progression. *J Virol* **74**, 9222-33 (2000).
258. Ariën, K.K. et al. The replicative fitness of primary human immunodeficiency virus type 1 (HIV-1) group M, HIV-1 group O, and HIV-2 isolates. *J Virol* **79**, 8979-90 (2005).
259. Calantone, N. et al. Tissue myeloid cells in SIV-infected primates acquire viral DNA through phagocytosis of infected T cells. *Immunity* **41**, 493-502 (2014).
260. Carias, A.M. et al. Defining the Interaction of HIV-1 with the Mucosal Barriers of the Female Reproductive Tract. *Journal of Virology* **87**, 11388-11400 (2013).
261. Hsu, M. et al. Increased Mucosal Transmission but Not Enhanced Pathogenicity of the CCR5-Tropic, Simian AIDS-Inducing Simian/Human Immunodeficiency Virus SHIV_{SF162P3} Maps to Envelope gp120. *Journal of Virology* **77**, 989-998 (2003).
262. Wessels, J.M. et al. Depot medroxyprogesterone acetate (DMPA) enhances susceptibility and increases the window of vulnerability to HIV-1 in humanized mice. *Scientific Reports* **11**, 3894 (2021).
263. Trifonova, R.T., Lieberman, J. & Van Baarle, D. Distribution of Immune Cells in the Human Cervix and Implications for HIV Transmission. *American Journal of Reproductive Immunology* **71**, 252-264 (2014).

264. Saba, I. et al. Immunocompetent Human 3D Organ-Specific Hormone-Responding Vaginal Mucosa Model of HIV-1 Infection. *Tissue Eng Part C Methods* **27**, 152-166 (2021).
265. Garcia-Tellez, T. et al. Non-human primates in HIV research: Achievements, limits and alternatives. *Infect Genet Evol* **46**, 324-332 (2016).
266. Grivel, J.-C. & Margolis, L. Use of human tissue explants to study human infectious agents. *Nature Protocols* **4**, 256-269 (2009).
267. Saba, E. et al. HIV-1 sexual transmission: early events of HIV-1 infection of human cervico-vaginal tissue in an optimized ex vivo model. *Mucosal Immunology* **3**, 280-290 (2010).
268. Estes, J.D., Legrand, R. & Petrovas, C. Visualizing the Immune System: Providing Key Insights into HIV/SIV Infections. *Frontiers in Immunology* **9**(2018).
269. Asin, S.N., Eszterhas, S.K., Rollenhagen, C., Heimberg, A.M. & Howell, A.L. HIV Type 1 Infection in Women: Increased Transcription of HIV Type 1 in Ectocervical Tissue Explants. *The Journal of Infectious Diseases* **200**, 965-972 (2009).
270. Buffa, V. et al. Cyanovirin-N potently inhibits human immunodeficiency virus type 1 infection in cellular and cervical explant models. *J Gen Virol* **90**, 234-43 (2009).
271. Rohan, L.C. et al. In vitro and ex vivo testing of tenofovir shows it is effective as an HIV-1 microbicide. *PLoS One* **5**, e9310 (2010).
272. Merbah, M. et al. Cervico-vaginal tissue ex vivo as a model to study early events in HIV-1 infection. *Am J Reprod Immunol* **65**, 268-78 (2011).
273. Rollenhagen, C. & Asin, S.N. Enhanced HIV-1 replication in ex vivo ectocervical tissues from post-menopausal women correlates with increased inflammatory responses. *Mucosal Immunology* **4**, 671-681 (2011).
274. Introini, A., Vanpouille, C., Lisco, A., Grivel, J.-C. & Margolis, L. Interleukin-7 Facilitates HIV-1 Transmission to Cervico-Vaginal Tissue ex vivo. *PLOS Pathogens* **9**, e1003148 (2013).
275. Scott, Y.M., Park, S.Y. & Dezzutti, C.S. Broadly Neutralizing Anti-HIV Antibodies Prevent HIV Infection of Mucosal Tissue Ex Vivo. *Antimicrobial Agents and Chemotherapy* **60**, 904-912 (2016).
276. Introini, A., Vanpouille, C., Fitzgerald, W., Broliden, K. & Margolis, L. Ex Vivo Infection of Human Lymphoid Tissue and Female Genital Mucosa with Human Immunodeficiency Virus 1 and Histoculture. *Journal of Visualized Experiments* (2018).
277. Perez-Zsolt, D. et al. Dendritic Cells From the Cervical Mucosa Capture and Transfer HIV-1 via Siglec-1. *Frontiers in Immunology* **10**(2019).
278. Nijmeijer, B.M. et al. HIV-1 subverts the complement system in semen to enhance viral transmission. *Mucosal Immunology* **14**, 743-750 (2021).
279. Fletcher, P. et al. The nonnucleoside reverse transcriptase inhibitor UC-781 inhibits human immunodeficiency virus type 1 infection of human cervical tissue and dissemination by migratory cells. *J Virol* **79**, 11179-86 (2005).

280. Maher, D., Wu, X., Schacker, T., Horbul, J. & Southern, P. HIV binding, penetration, and primary infection in human cervicovaginal tissue. *Proceedings of the National Academy of Sciences* **102**, 11504-11509 (2005).
281. Cummins, J.E., Jr. et al. Preclinical testing of candidate topical microbicides for anti-human immunodeficiency virus type 1 activity and tissue toxicity in a human cervical explant culture. *Antimicrob Agents Chemother* **51**, 1770-9 (2007).
282. Wheeler, L.A. et al. Inhibition of HIV transmission in human cervicovaginal explants and humanized mice using CD4 aptamer-siRNA chimeras. *J Clin Invest* **121**, 2401-12 (2011).
283. Palacio, J. et al. In vitro HIV1 infection of human cervical tissue. *Res Virol* **145**, 155-61 (1994).
284. Gupta, P. et al. Memory CD4(+) T cells are the earliest detectable human immunodeficiency virus type 1 (HIV-1)-infected cells in the female genital mucosal tissue during HIV-1 transmission in an organ culture system. *J Virol* **76**, 9868-76 (2002).
285. Patterson, B.K. et al. Susceptibility to human immunodeficiency virus-1 infection of human foreskin and cervical tissue grown in explant culture. *Am J Pathol* **161**, 867-73 (2002).
286. Zussman, A., Lara, L., Lara, H.H., Bentwich, Z. & Borkow, G. Blocking of cell-free and cell-associated HIV-1 transmission through human cervix organ culture with UC781. *AIDS* **17**, 653-661 (2003).

1. C-TERMINALLY TRUNCATED HIV-1 VIF RETAINS BIOLOGIC FUNCTION, AND TAGGED WITH HIBIT PEPTIDE SERVES AS A NOVEL BIMOLECULAR LUMINESCENCE ASSAY REPORTER

by

DANA F. INDIHAR, ANJA I. SCHOLLMEIER, JENNIFER J. JONES, JIE ZENG, ISABELLE CLERC, CHISU SONG, JOHN C. KAPPES, CHRISTINA OCHSENBAUER

Submitted to *Journal of Virology*

Format adapted for dissertation

ABSTRACT

HIV-1 infectious molecular clones (IMC) engineered with reporter genes are important tools in cell-based, *ex vivo*, and *in vivo* studies of HIV-1 infection, prevention, and cure. Different IMC designs offer sensitive, quantitative readouts via luminescent, fluorescent or other markers for many applications, but pose limitations for some experimental uses. Here, we report a novel approach utilizing a small luminescent peptide, HiBiT, appended to HIV-1 Vif truncated by 19 C-terminal residues (174-192), and informed by reports of non-hypermutated HIV-1 isolates encoding such Vif variants, one of which we described retained function in supporting HIV-1 replication in *vif-minus* non-permissive cells.

Prior Vif structure/function studies defined the SOCS-box domain, essential for Vif thwarting APOBEC3G restriction, to encompass residues 144-173, and predicted the C-terminus (residues 174-192) to be unstructured. We hypothesized that replacing the Vif C-terminus with a similarly unstructured, charged and sized linker-HiBiT peptide would minimally affect overall Vif folding and functionality. A premature stop at codon 174 removes the *vif/vpr* orfs overlap, facilitating insertion of the HiBiT sequence. HIV-1 NL4-3, and transmitted/founder viruses CH077.t and CH0505s remained replication competent in *vif-minus* non-permissive immortalized and primary cells when encoding truncated Vif-HiBiT. Infection was sensitively detected via HiBiT in bimolecular NanoBiT assays, and HiBiT was stably retained in viral genomes over multiple rounds of replication. Wild-type levels of Nef were preserved, unlike in some prior IMC reporter designs. Moreover, we

provide direct evidence that Vif retains the ability to reduce APOBEC3G levels when C-terminally truncated by 19 residues, even after the addition of HiBiT.

IMPORTANCE

This study describes a novel reporter virus strategy that preserves full functionality of all HIV-1 genes and thus promises to augment application of reporter viruses in cell-based and *in vivo* models of HIV-1 pathogenesis and prevention research. Moreover, our findings further the mechanistic understanding of Vif function and provide evidence that the C-terminal 19 amino acids of Vif are dispensable for its major known function of directing the A3G restriction factor for degradation.

Specifically, in an innovative molecular approach, we appended the sensitively quantifiable luminescent peptide, HiBiT, to the HIV-1 protein, Vif. We demonstrate that virologic properties of wild-type viruses are recapitulated by Vif-HiBiT HIV-1, and Vif that is C-terminally truncated by 19 residue and modified with HiBiT affords replication-competence in target cells non-permissive for *vif*-defective HIV-1. Moreover, truncated and HiBiT- modified Vif proteins from four different HIV-1 strains mediate wild-type levels of APOBEC3G degradation, an essential function, in cell-based assays.

INTRODUCTION

Around 38 million people globally are infected with HIV-1, and progress in the fight against AIDS has been slowing since 2020[1,2]. Efforts to develop urgently needed preventative or therapeutic vaccines that elicit efficacious antibody or T cell responses remain ongoing [discussed in 3-5]. Assessment of immune responses elicited by experimental vaccines requires a range of immune-monitoring assays, many of which are cell-based and utilize virologic approaches, including those that measure broadly neutralizing antibody (bNAb), antibody-dependent cell-mediated cytotoxicity (ADCC), and cytotoxic T lymphocytes (CTL) responses. Our laboratory has contributed HIV-1 reporter virus approaches that have found application in various immune-monitoring assays, and in other transmission and pathogenesis-related studies[6-27].

The specific molecular design of an HIV-1 reporter virus will determine its utility for any given application. Most commonly, the reporter genes are positioned within the 3' end of the HIV genome, including insertion into or adjacent to the *nef* or *env* open reading frames (orfs). We previously reported on an HIV-1 infectious molecular clone (IMC) approach originally intended to assess neutralization in primary cells[6] with insertion of *Renilla reniformis* luciferase (LucR) fused in-frame to an 18 aa-long "ribosome skipping" T2A peptide (LucR.T2A) between the *env* and *nef* genes. We later found that Nef expression was unexpectedly abrogated in CD4+ T cells infected with this IMC-LucR.T2A design[7,11]. We overcame this limitation by placing a truncated encephalomyocarditis virus (EMCV) internal ribosome entry site (IRES) element ("6ATRi") downstream of the LucR or other reporter orfs. Overall, we found that this design allowed Nef protein expression in CD4+ T cells at physiological levels[7]. However, among reporter gene-6ATRi cassette-

encoding IMC derived from a subset of parental proviruses, Nef expression and function was restored to levels only similar but not identical to that of the parental (wild-type) IMC[28]. While HIV-1 reporter IMC that use the 6ATRi design offer many advantages, the overall length of the exogenous reporter cassettes (i.e. modified IRES element of 435 nt in combination with the respective bioluminescent or fluorescent reporter gene) may represent a vulnerability to being selected against over multiple rounds of virus replication[7]. In addition, the proportionally higher presence of CG dinucleotides in heterologous reporter sequences *versus* the parental retroviral genome can exert selection pressure [29]. Thus, minimizing the reporter size, irrespective of position within the genome, is desirable.

Placement of reporter genes in the 5' half of the genome has also been pursued. The *c-myc* epitope and EGFP have been fused to Gag between the matrix (MA) and capsid (CA) domains[30,31]. Kirui and Freed inserted the Nano-luciferase (NanoLuc) reporter, chosen for its small size of ~19kDa, between the MA and CA and demonstrated minimal influence on either Gag expression or the release of viral particles[32]. However, like other Gag-fusion reporters[30,31], this construct resulted in virions with significantly reduced infectivity in TZM-bl and CD4+ T cells, and required trans-complementation with the wild-type (WT) molecular clone for full infectivity to be restored. More recently, Ozono *et. al* reported on appending a small luminescent reporter sequence (HiBiT [33]) to the C-terminus of HIV integrase (IN)[34], an approach that allowed them to sensitively quantify production of infectious virions.

We are unaware of any reports that describe placement of reporter genes in the accessory gene-encoding central region of the HIV genome without significant impairment

of viral replication or rapid deletion of the exogenous sequence. The overlapping orfs of the accessory genes make this region of the genome a challenging location for insertion of reporter genes, and we contend that the size of commonly used reporters genes like LucR, GFP, or even NanoLuc are especially disruptive in this area of the genome. However, based on reports of naturally occurring *vif* stop codons at amino acid 174[35-37] found in non-hypermutated HIV-1 genomes[35-37], we hypothesized that insertion of the short HiBiT luminescent reporter sequence[33] after residue 173 would be tolerated, and not disrupt essential Vif function. Since the premature stop is just prior to the *vpr* orf we sought to exploit the resulting "gap" between the two orfs for insertion of the HiBiT coding sequence. Importantly, we previously reported that the patient-derived Vif variant, A45-2, truncated by 19 C-terminal aa after residue 173 ("TR173") supported viral replication in cells that are non-permissive for *vif*-deficient HIV-1, including primary CD4+ T cells and the non-permissive H9 T cell line[36,38].

Recent insights into Vif structure and functional domains offer some explanation for this phenotype and help underpin the rationale for the approach presented herein. Vif is an essential HIV-1 protein required for viral replication[39-41 and reviewed in 42,43]. *In vivo*, defective *vif* is strongly associated with HIV-1 G-to-A hypermutation [37]. The main function of Vif is to counteract cellular restriction factors of the APOBEC3 (A3) family, which in the absence of Vif are incorporated into virions and block replication through deaminase activity with resulting viral genomic hypermutation as well as cytidine deaminase independent mechanisms [reviewed in 42,43]. A3G has been described as exerting the strongest restriction among the family of A3 proteins[44]. Vif hijacks cellular E3 ubiquitin ligase complexes, facilitated by CBFβ[45-48], to bind A3G and other A3 family proteins, thereby

blocking and directing them for proteasomal degradation[49-57]. One structural domain of Vif involved in E3 ligase hijacking is the SOCS-box domain[58]. This domain, which stretches from residues 144 to 173 near the C-terminus, contains the BC-box and Cullin-box regions, which interact with ElonginC and Cullin5 of E3 ligase, respectively[45,56-61]. Early work on Vif function found that changes to what is now known to be the SOCS-box domain, i.e. basic amino acid substitutions[62], or truncation of the C-terminus of Vif by 22 aa[63] resulted in significant reduction of productive HIV-1 infection and/or loss of Vif function. However, the above mentioned naturally occurring, non-hypermutated *vif* variants with a premature stop codon at codon 174[35-37] encode Vif proteins that maintain the entire SOCS-box. In WT Vif structure models, residues 174-192 represent an unstructured region[58,59], and appear to not be required for Vif-CBFβ complex binding to A3G [reviewed in 64,65]. This interpretation is in line with the finding that an HIV-1 IMC encoding the truncated Vif variant A45-2 described above maintained near WT levels of infectivity[36,38].

Here we report our findings from studies that fused the nt sequence encoding the 11 amino acid luminescent peptide, HiBiT[33], and a 10 amino acid linker sequence, in frame with the truncated *vif-TR173* sequence – taking advantage of the aforementioned "gap" between *vif-TR173* and *vpr,* and the predicted tolerance of Vif function to this truncation. Our approach minimizes the size of exogenous sequences in the viral genome and is intended to retain the full functionality of all of the HIV-1 genes. We demonstrate that this novel reporter virus strategy recapitulates virologic properties of WT viruses by demonstrating that the function of C-terminally truncated and modified Vif is retained: Firstly, Vif-HiBiT IMC remain replication competent in non-permissive CD4+ T cells. Secondly, truncated as well as HiBiT- modified Vif proteins from four different HIV-1

strains mediate wild-type levels of A3G degradation in a cell-based assay. The latter finding, in particular, contributes to furthering the mechanistic understanding of Vif function and provides direct evidence that the C-terminal 19 amino acids of Vif are dispensable for its major known function of directing the A3G restriction factor for degradation.

MATERIALS AND METHODS

Modelling of predicted protein structure of Vif-TR173 and Vif-TR173-HiBiT

Predicted protein structure models were generated from the aa sequences of Vif proteins of interest using Phyre2, which predicts models based on previously published structures[66]. We worked with the Vif protein from HIV NL4-3 (GenBank ID: M19921.2), for which a whole-protein structure derived from crystallography data at 3.30 Å resolution has been previously published (PDB: 4N9F)[59]. For our prediction analysis, we altered the NL4-3 Vif aa sequence to either reflect the 19 C-terminal aa truncation (TR173), or TR173 plus the addition of a linker sequence (GGSGG)2) and HiBiT[33,67] to the carboxyl end of truncated Vif. The more rigorous "intensive" setting of Phyre2 was used to predict structure models according to each aa sequence[66]. The predicted structures were then aligned to the PDB:4N9F structure in PyMOL to visualize any regions containing significant structural variation[68]. The TM-score of each predicted model relative to the published structure was calculated using the RaptorX Structure Alignment Server[69,70]. The TM-score is a calculation of folding similarity independent of protein length and is a measure of how similar the topology of any two proteins is based on a scale of 0 to 1, where a score of 1 indicates identical folding[71]. A TM-score above 0.6 indicates a 90% probability that the structures of the altered proteins relative to the published structure had similar folding[69-71].

Generation of Vif-HiBiT encoding HIV-1 proviral plasmid clones

To construct HIV-1 IMC that encode for either Vif.TR173 or Vif.TR173.HiBiT proteins, we used In-Fusion© cloning (Takara Bio USA) methods as outlined below. Derivatives of the pNL4-3[72] and pNL-BaL.ecto[6] plasmids were generated to encode for 19 aa C-terminally truncated Vif protein by introduction of a stop codon after *vif* codon 173 (pNL-Vif-TR173; pNL-Vif-TR173-BaL.ecto), followed in-frame by the existing *vpr* ATG, using two-fragment In-Fusion© ligation with overlapping primers in the *vif-vpr* junction and in the ampicillin resistance (AmpR) gene of the plasmid backbone. Using the same overall strategy, truncation of the *vif* orf after codon 173, was introduced in the transmitted/founder (T/F) IMCs, CH077.t ([73]Genbank JN944941) and CH0505s ([74], participant ID 703010505), respectively. Forward and reverse primers used for the two-fragment In-Fusion© ligation are shown in **Table 1**.

Vif-TR173 encoding plasmids were further modified by appending the HiBiT reporter sequence, via 10 aa linker sequence $((GGSGG)_2)$, onto Vif-TR173 (resulting IMCs named pNL-Vif.TR173.HiBiT; pNL-BaL.ecto-Vif.TR173.HiBiT; CH077.t-Vif.TR173.HiBiT; CH0505s-Vif.TR173.HiBiT). IMC specific primers for the HiBiT insertion are as follows (with: *vif* sequence capitalized and underlined; linker sequence lower case italicized; HiBiT sequence capitalized; *vpr* (lower case) start codon bolded and underlined): We have previously detailed the construction of Env-IMC-LucR.6ATRi and Env-IMC-LucR.T2A viruses[6,7]. Names and unique identifiers of proviral plasmids utilized, and corresponding abbreviations used throughout the text are shown in **Table 2.**

Table 1. *Summary of Primers*

Primer Name	**Forward or Reverse Primer**	**Primer Sequence**
NL-VifTR173-vpr-fwd	FWD	5’-gaacaagccccagaagaccaagggccaca-3’
NL-VifTR173 Vpr-rev	REV	5’-ttctggggcttgttccat**TTA**tctgtcctctgtcagtt-3’
AmpR.PvuI.fwd	FWD	5’-cgatcgttgtcagaagtaagttggccgcagtgtt-3’
AmpR.PvuI.rev	REV	5’- ttctgacaacgatcggaggaccgaaggagctaaccgctt -3’
NL-VifTR173-HiBit-fwd	FWD	5’-gcggatcaggggc-GTGAGCGGCTGGCGGCTGTTCAAGAAGATTAGCTAAatggaacaagccccagaagaccaagggcca-3’
NL-VifTR173-HiBiT-rev	REV	5’-C*gccccctgatccgcccccgcctgagcctcc*TCTGTCCTCTGTCAGTTTCCTAACACT-3’
CH077-VifTR173-HiBit-fwd	FWD	5’-*gggggc*GTGAGCGGCTGGCGGCTGTTCAAGAAGATTAGCTAA**atg**gaacaagccccagaa-3’
CH077-VifTR173-HiBit-rev	REV	5’-GCCGCTCAC*gccccctgatccgcccccgcctgagcctcc*TCTATCCTCTGTCAATTTCGC-3’
CH0505-VifTR173-HiBit-fwd	FWD	5’-*gggggc*GTGAGCGGCTGGCGGCTGTTCAAGAAGATTAGCTAA**atg**gaacaacccccagaa-3’
CH0505-VifTR173-HiBit-rev	REV	5’-GCCGCTCAC*gccccctgatccgcccccgcctgagcctcc*TCTATCCTCTACTAATTTCTT-3’

Table 2. *Summary of Plasmids*

proviral plamid name [1]	**unique lab ID**	**virus abbreviation in Figures**	**Env**	**T / F**	**Reporter**
pNL4-3	K629[1]	NL	NL4-3	N	-
pNL-Vif.TR173	K5327	NL-Vif.TR	NL4-3	N	-
pNL-Vif.TR173.HiBit	K5384	NL-Vif.HB	NL4-3	N	HiBiT
pNL-B.Bal.ecto	K2258	NL-Bal	BaL	N	-
pNL-B.Bal.ecto-Vif.TR173	K5050	NL-Bal-Vif.TR	BaL	N	-
pNL-B.Bal.ecto-Vif.TR173.HiBiT	K5383	NL-Bal-Vif.HB	BaL	N	HiBiT
pB.CH077.t	K2627[1]	CH077	CH077.t	Y	-
pB.CH077.t-Vif.TR173	K5566	CH077-Vif.TR	CH077.t	Y	-
pB.CH077.t-Vif.TR173.HiBiT	K5567	CH077-Vif.HB	CH077.t	Y	HiBiT
pC.CH0505s	K4374[1]	CH0505	CH0505s	Y	-
pC.CH0505s-Vif.TR173	K5568	CH0505-Vif.TR	CH0505s	Y	-
pC.CH0505s-Vif.TR173.HiBiT	K5569	CH0505-Vif.HB	CH0505s	Y	HiBiT
pNL- LucR.T2A-Nef^{STOP}	K4480	NL-Nef^{STOP}	NL4-3	N	LucR
pNL- NL-BaL-LucR.T2A.STOP	K4479	NL-BaL-LucR.T2A.Nef^{STOP}	BaL	N	LucR

1 - for references and GenBank No., see Materials and Methods section

T/F = transmitted/founder strain

Cells

Cells were grown at 37° C and at 5% CO_2. The H9 T lymphocyte cell line was obtained from NIH ARP (catalog no. 87, lot no. 140315). It is non-permissive to replication of HIV-1 lacking functional Vif [75,76]. H9 cells were cultured in RPMI 1640 growth medium supplemented with 10% FBS, HEPES (25 mM), L-glutamine (2 mM), streptomycin (100 µg/ml), and penicillin (100 U/ml). Cryopreserved human primary PBMC from 4 donors (obtained under IRB approval) were cultured for 24 hours after thawing in PBMC culture medium consisting of RPMI 1640 growth medium, 20% FBS, HEPES (25 mM), L-glutamine (2mM), streptomycin (100 µg/ml), penicillin (100 U/ml), and interleukin-2 (IL-2; 30 U/ml; Roche, Indianapolis, IN). CD4+ T cells were obtained by negative selection with a LS column using the Miltenyi MACS CD4+ T cell isolation kit (lot no. 5180810073), or by CD8 depletion using Dynal CD8 beads (cat. No. 11147D). The CD4+ T cells were cultured in PBMC medium supplemented with a CD3-CD28 bispecific antibody (2.6 µg/ml; generous gift from Drs. Xiaoyun Wu and Yang Zang, Immunowake LLC, Birmingham, AL, USA). After 4 days of stimulation, the cells from 4 donors were pooled by suspending in fresh PBMC culture medium and used immediately. The TZM-bl dual-reporter cell line was generated previously by us and is available through the NIH AIDS Reagent Program, Division of AIDS NIAID, NIH (catalog no. 8129)[77]. The Lenti-X 293T cell line was acquired from TaKaRa (cat no. 632180, lot no. 1610068A). Both the 293T and TZM-bl cell lines were maintained in Dulbecco's modified Eagle's medium (DMEM) supplemented with 10% FBS, HEPES (25 mM), L-glutamine (2mM), streptomycin (100 µg/ml), and penicillin (100 U/ml).

Generation of transfection-derived virus stocks and Vif-HiBiT expression in 293T cells

Viral stocks were derived from 293T-LentiX cells (3E+05 cells/6-well) transfected with proviral DNA using FuGENE HD in accordance with the manufacturer's protocol (catalog no. PRE2311; Promega) and as described previously[6,73]. Supernatants were harvested 66 hours post-transfection and clarified at 300 x g for 10 minutes before -80° C storage until use. Viral stocks were titered on TZM-bl cells via the quantification of beta-galactosidase-stained colonies as previously described[77].

Transfected cells were resuspended in 1 ml PBS/6-well and analyzed for NanoGlo activity using the Nano-Glo® HiBiT Lytic Detection System (Promega; catalog no. N3030) kit. Briefly, 100µl of resuspended cells (1E+04) were transferred into a white 96-well luminometer plate. In each well, 100 µl of the Nano-Glo® Reaction buffer (containing lytic buffer, substrate and LgBiT protein) were added in accordance with the manufacturer's protocol, and mixed for 10 min at room temperature on a microplate shaker. The NanoBiT luminescence was then read on a GloMax Microplate Luminometer (Promega) programmed with an integration time of 1s/well. Measured values were denoted as relative light units (RLU) of NanoBiT activity.

Western blot analysis of Gag, Vif and Nef in provirally-transfected and infected cells, and of pelleted virions

Samples for Western blot analysis were prepared from 293T cells, which were transfected with proviral plasmids as described above, as well as from infected primary CD4+ T cells. Proviral plasmid transfected 293T cells seeded in 6-well plates were washed at 60-72 h post transfection (p.t.) with PBS and lysed with equal volumes of Laemmli 2x sample buffer (Sigma Aldrich).

For Western blot analysis following infection of primary CD4+ T cells, cells were derived from CD8-depleted, CD3/CD28 stimulated PBMC from 4 donors, as described above, and pooled. To ensure sufficient infection levels, high-titer virus stocks were prepared in 293T cells essentially as described above by transfection with the respective IMC, but also including VSV-G expression plasmid for pseudotyping. Enhanced safety protocols were observed when handling these virus stocks. CD8-depleted, pooled PBMC (6E+06 cells) were infected at Multiplicity of Infection (MOI) of 1 with 200 µl 293T cell-derived virus supernatants on 24-well plates coated with RetroNectin (TakaraBio, Cat. No. T100B) as per manufacturer's instructions. After 72 hr culture, cell numbers per condition were counted, % p24+ cells were determined by flow cytometry, and pelleted cells were lysed in Laemmli buffer, normalized to 2E+05 total p24/Gag+ cells per 20 µl**.**

To analyse virions released into the supernatant from provirally-transfected 293T cells, 9 ml of supernatants from 3 replica wells per IMC were combined. Supernatants were pelleted in an SW41 rotor through 1.8 ml of 20% sucrose cushion at 25,000 rpm (~107,000 g) for 2 hours. Pellets were resuspended in 100 µl of PBS; an aliquot was serially diluted in PBS and directly analysed for HiBiT using the NanoGlo lytic detection system (Promega); NanoBiT activity was expressed as relative light units (RLU). Additional virion pellet aliquots were lysed with 2X Laemmli buffer for SDS-PAGE.

All lysates were sonicated and boiled for 10 min at 95° C. Proteins from either equivalent numbers of transfected 293T cells, or associated pelleted virions, or equivalent numbers of HIV-1 p24 positive primary CD4+ T cell (determined by p24 flow cytometry), respectively, were separated on a denaturing SDS-polyacrylamide gel and transferred onto a nitrocellulose membrane using a wet electroblotting system. After blocking with 10%

non-fat dried milk in Tris-buffered saline, HiBiT-tagged proteins were visualized by using the Nano-Glo® HiBiT Blotting System (Promega; catalog no. N2410) according to the manufacturer's protocol. Replica membranes were probed with the primary mouse-anti-Gag antibody (clone 183-H12-5C; NIH AIDS Reagent Program, Division of AIDS NIAID, NIH; catalog no. ARP-1513), polyclonal rabbit anti-Vif serum (catalog no. ARP-809; detects full-length Vif), polyclonal rabbit anti- Nef (catalog no. ARP-2949), and appropriate horseradish peroxidase (HRP) conjugated goat secondary antibodies (SouthernBiotech; Birmingham, AL). PageRuler Prestained Protein Ladder (Thermo Fisher, USA) was used to estimate the molecular weight of protein bands. NanoBiT luminescence and HRP activity detected by chemiluminescence were imaged with a LAS-4000 Imager and software (Fujitsu America) or a UVP ChemStudio gel imager (Analytick Jena US).

Determination of virus infectivity and NanoBiT activity in TZM-bl cells

Virus infectivity and HiBiT gene expression were further analyzed in the TZM-bl cell line. Briefly, 1E+04 cells were seeded one day prior to infection into a 96-well plate and infected with 293T-derived virus stocks. The virus was serially diluted to a Multiplicity of Infection (MOI) range between 3 and 0.037 then added to the cells in the presence of DEAE-dextran (10 µg/ml). After incubation for 4 hours at 37° C, the virus was removed and replaced by fresh medium. Then, 48 hours post infection (p.i.), cells were washed twice with PBS and lysed by adding 50 µl of 5x PLB. To measure the viral infectivity through cell-encoded firefly luciferase (LucF), 20 µl of each sample was analyzed by Luciferase Assay System (Promega; catalog no. E4530) using a Victor X Light Luminometer (Perkin Elmer) with 100 µl Luciferase Assay Reagent injection and an exposure time of 10 seconds

per well. To analyze functionality of proviral encoded HiBiT, 100 µl of each sample was used for Nano-Glo HiBiT Lytic Detection System (Promega; catalog no. N3030). NanoGlo activity was determined using GloMax 96 Microplate Luminometer (Promega) programmed with an integration time of 1 second/well. Both results were reported in RLU.

Infection of and replication kinetics in vif ^{minus} non-permissive H9 cells

H9 cells were resuspended at 5E+05 cells per ml in complete RPMI medium (prepared as described above) with 5 µg/ml DEAE-dextran, and 1 ml of cell suspensions was aliquoted into microtubes. Transfection-derived viruses produced in 293T-cells as described above (NL, NL-Vif.TR, and NL-Vif.HB) were added at TZM-bl MOIs between 0.1 and 0.3. The tubes were rotated at 37° C for 3 hours. Cells were then pelleted at 300 g for 5 minutes, the virus inoculum supernatant was removed, and the cell pellet was resuspended in 1 ml of fresh, pre-warmed media before being transferred to a 24-well plate. To limit viral replication to one round, the HIV protease inhibitor Indinavir (IDV) was added to replica samples at 10 µg/ml. Cells were cultured at 37° C for up to two weeks in a Celltron incubator-shaker (INFORS HT) at low speed (96 rpm). Separate (unpublished) studies of cell-to-cell virus spread reliant on cell-contact from our lab revealed that these conditions were optimal for cell growth and cell-mediated spread of HIV-1 in T cell cultures. Every two days, cells were gently resuspended, and a 150 µl sample was taken from each well to be stained with the KC57 anti-p24 FITC antibody. The percentage of cells positive for p24 (i.e. HIV infected) was determined by flow cytometric analysis.

Additionally, to measure HiBiT-LgBiT trans-complementation via NanoGlo RLU readout, a 50 µl sample (~2.5E+04 cells) was extracted from each well of the 24-well plate and transferred to a white 96-well luminometer plate. Next, 50 µl of the Nano-Glo® HiBiT

Lytic Detection System kit (catalog no. N3030) was added to each well in accordance with the manufacturer's protocol (Promgea). The plate was then read on the GloMax Microplate Luminometer (Promega), and the data was recorded and plotted. This process was repeated every other day for up to two weeks. After cell samples were extracted, each well was replenished with 200 µl of fresh media. Under the given conditions, the cell density was ~1.5E+06 cells/well every two days

Infection and replication kinetics in CD4+ T cells isolated from primary PBMCs

Primary CD4+ T cells were derived from PBMC as described above and stimulated for 4 days with CD3-CD28 antibody. The purity and quantity of the CD4+ T cells were confirmed by flow cytometry. Cells were infected in parallel with a panel of HIV IMCs including NL-Vif.HB, NL-Bal-Vif.HB, CH077-Vif.HB, and CH0505-Vif.HB alongside their WT counterparts. CD4+ T cells in PBMC medium were rotated with virus at a range of TZM-bl-based MOIs (2E+06 cells per condition at MOI 0.05; or 5E+05 cells at MOI between 0.8 and 1.2) in 2 ml microtubes at 37° C for 4 hours. Cells were pelleted at 300 g for 5 minutes, the virus inoculum supernatant was discarded, and cell pellets were resuspended in 1 ml of fresh medium in the absence or presence of 10 µg/ml IDV. Cell suspensions were transferred to 24-well plates and cultured at 37°C on the Celltron incubator-shaker for 9 days post infection (p.i.). Infection of cells infected at MOI of 0.05 was monitored by removing 1E+05 cells on indicated days (1/20 of total), and measuring NanoBiT activity. For cells infected at MOI of ~1, on odd numbered days, cells were gently resuspended and 200 µl of cell suspension (1/5 of total) were removed. A 150 µl sample (~7.5E+04 cells) from each well was stained with the KC57 anti-p24 FITC antibody. The percentage of cells positive for p24 (i.e. HIV infected) was determined by flow cytometric

analysis. Vif-HiBiT IMC infection of primary cells was also assessed via RLU readout with the Nano-Glo® HiBiT Lytic Detection System, as described above. The remaining 50 µl cell suspension sample (~2.5E+04 cells) taken from each well containing cells inoculated with the Vif-HiBiT IMCs was analyzed for NanoBiT activity. Cultures were replenished with 250 µl of fresh PBMC media following extraction of p24 and NanoBiT samples. On even numbered days, only a 50 µl (~2.5E+04 cells) sample for RLU analysis was taken from each well with Vif-HiBiT IMCs. NanoBit RLU determined via a GloMax luminometer are normalized to 1.0E+05 or 2.5E+04 cells for experiments performed with a MOI of 0.05 and MOI of ~1, respectively.

Cell-mediated passaging of Vif.HB IMC infection

Infection of H9 cells (at MOI 0.1-0.3) and PBMC derived CD4+ T cells (MOI 0.8-1.2) with Vif.HB IMCs, and consecutive culture, in the absence of IDV, are described above. At day 10 p.i. for H9 cells, and at day 6 p.i. for PBMCs, 5,000 cells were collected from these infected cultures, washed to remove virus present in supernatant, and added to 45,000 fresh, uninfected cells suspended in 1ml of medium in 24-wells in duplicate with or without IDV (10 µg/ml). The 24-well plates were kept at 37° C on the Celltron Shaker for 8 to 9 days at 96 rpm. Almost daily, a 50 µl cell suspension sample from each well was taken (i.e. 1/20 of total cells, or 2,500 cells on day 1), combined with the Lytic Detection System kit as per the manufacturer's protocol, and analyzed for NanoGlo readout on the GloMax machine. Infected H9 cells cultures were split 1:2 at days 3 and 5 p.i., and infected PBMC cultures were split 1:2 on day 3 p.i., in each case by removing 500 µl of 1 ml resuspended cells and replenishing with the respective fresh culture medium with or without IDV.

Determination of Vif.HB expression stability over time

Following infection of 5E+05 H9 or primary CD4+ T cells/well in 24 well plates with Vif.HB IMC as described above, 300 µl of supernatant was removed every two days p.i. to be used to determine the stability of HiBiT reporter expression over several replication cycles, essentially as previously described [6,7]. Following supernatant removal, wells were replenished with 300 µl of fresh media. The supernatant was clarified and then stored at -80° C in 150 µl aliquots until use. In flat-bottom 96-well plates, 1E+04 TZM-bl cells were infected with 50 µl of supernatant from each time point as well as transfection-derived (TD) virus from 293T cells, in a total of 200µl medium with 10 µg/ml DEAE-dextran. The plates were left at 37°C for 48 hours, after which 50µl of 5x PLB (Promega) was added to each well (1x final concentration), and plates stored at -80°C until use. Infected TZM-bl cell lysates were analyzed for both cell-encoded LucF activity – to measure overall infectivity; and Vif.HB bimolecular trans-complementation for NanoBiT activity, essentially as above – to determine virus-encoded HiBiT activity to assess the relative viral reporter gene expression.

LucF activity was measured on a Victor X Light Luminometer with a single-channel injector (PerkinElmer) using the Luciferase Assay System (Promega; catalog no. E4530). NanoBiT activity was determined using the Nano-Glo® HiBiT Lytic Detection System (providing both LgBiT and NanoGlo substrate), on a GloMax luminometer (Promega). The level of NanoBiT expression relative to infectivity at each time point was calculated as the ratio of virus-encoded NanoBiT RLU to cell-encoded LucF RLU essentially as described [6,7], normalized to NanoBiT-to-LucF ratio attained from TD supernatants, and plotted over time.

Determination of Nef function as measured by regulations of CD4 and MHC-1 cell surface expression

H9 cells (2E+06) in 1 ml of medium with 5 µg DEAE-dextran/ml were added directly to vials containing 250 µl of virus stock (NL, NL-Vif.TR, NL-Vif.HB, and NL-LucR.T2A.Nef^{STOP}) and were rotated at 37° C for 4 hours. The contents of the vials were then transferred to a 24-well plate, and fresh medium was added, bringing the final volume of each well up to 2 ml. The plate was incubated at 37° C overnight atop the Celltron incubator-shaker at 96 rpm. After 22 hours p.i., a 500 µl sample was taken from each well and cells were stained for p24, CD4, and MHC-1 expression and analyzed via flow cytometry.

For analysis in primary cells, 2E+06 of PBMC-derived CD4+ cells were resuspended in 1 ml of media and combined with 200 µl of each virus (NL, NL-Vif.TR, NL-Vif.TR-HB, NL-LucR.T2A.Nef^{STOP}, NL-Bal, NL-Bal-Vif.TR, NL-Bal-Vif.HB, and NL-Bal-LucR.T2A.Nef^{STOP}) in separate vials as before. Vials were rotated at 37° C for 4 hours, after which the vial contents were transferred to a 24-well plate. At 24 hours p.i., 1 ml of fresh media was added to each well. The plate was incubated on the Celltron Shaker at 37° C for 96 hours at 96 rpm. At 96 hours p.i., a 500 µl sample was taken from each well and in the cells were stained for p24, CD4, and MHC-1 expression for analysis by flow cytometry.

Determination of Vif function through APOBEC3 degradation

293T cells were plated in 6-well plates at a density of 800,000 cells per well one day prior to transfection. Cells were co-transfected with 250 ng of HA-tagged A3G[78], A3F

[79], or A3B [80,81] and 750 ng of a Vif expression plasmid using PEI transfection method [82]. Vif expression plasmids were created via In-Fusion ligation methods to fuse *vif* coding regions (WT, as well as TR173 or TR173-HiBiT derivatives) from HIV-1 reference strain NL4-3, the patient isolate A45 [35,36], and the T/F IMC B.CH077.t, and C.CH0505s into a pFM-1 backbone [83]. Resulting Vif expression plasmids are referred to by "name (unique lab ID)": pFM-1-Vif_NL4.3 (K5792), pFM-1-Vif-TR173_NL4.3 (K5793), pFM-1-Vif-TR173-HiBiT_NL4.3 (K5794), pFM-1-Vif45-FL (K5795), pFM-1-Vif45-2 (K5796), pFM-1-Vif45-2-HiBiT (K5797), pFM-1-Vif_CH0505s (K5804), pFM-1-Vif-TR173_CH077.t (K5805), pFM-1-Vif-TR173_CH0505s (K5806), pFM-1-Vif_CH077.t (K5803), and expressed Vif proteins are referred to using abbreviation consistent with those for their parental IMC.

Two days post transfection, cells were lysed in a 1% NP-40 based lysis buffer with the addition of a protease inhibitor cocktail (Millipore Sigma) and subsequently sonicated to release nuclear-localized proteins followed by centrifugation at 10,000 × g for 10 minutes at 4° C. Total protein concentrations of the cell lysates were quantified using a BCA protein assay (Thermo Fisher Scientific) and normalized, and 20 ug of proteins were denatured using a 10% DTT and 4× LDS sample buffer (Thermo Fisher Scientific), boiled for 7 minutes at 92° C, and analyzed by electrophoresis through a 4%–12% Bolt bis–tris electrophoresis gel (Thermo Fisher Scientific). After electrophoresis, separated proteins were transferred to a PVDF membrane (Thermo Fisher Scientific), followed by immunoblotting. A3 proteins were visualized using anti-HA antibody (Sigma #H9658); Vif protein was detected using a mouse monoclonal anti-Vif antibody[84] raised against and recognizing full-length Vif, and obtained through the NIH HIV Reagent Program, Division

of AIDS, NIAID, NIH: Anti-Human Immunodeficiency Virus (HIV)-1 Vif monoclonal Antibody (#319), ARP-6459, contributed by Dr. Michael Malim. Lamin B antibody (Genetex #103292) was used for a control. Fluorescent-labeled secondary antibodies were used in conjunction with the Odyssey CLx imaging system (Li-Cor) to detect protein signal as described in Scholtes 2021[80].

RESULTS

The Vif C-terminus minimally influences Vif protein folding modelled in silico

Using *in silico* modeling, we assessed the predicted structural impact from addition of the 11 amino acid luminescent peptide, HiBiT[33], via an 10 amino acid linker sequence [(GGSGG)2] in frame at residue position 174 of Vif. We chose the HiBiT peptide (~1.3 kDa), derived from NanoLuc, as a much smaller alternative to reporter proteins like GFP or LucR. Tagged onto a protein of interest, HiBiT constitutes one part of the NanoBiT bipartite-luciferase reporter system[33,67]. HiBiT binds with high affinity to (exogenously added or co-expressed) LgBiT (~18 kDa), thereby reconstituting functional NanoBiT enzyme, which, in the presence of substrate[67], produces a highly sensitive and quantitative luminescence signal. For *in silico* modelling, we modified a previously published HIV NL4-3 Vif structure model[59] by removing the 19 C-terminal aa of Vif (Vif.TR173, or Vif.TR) or by additionally appending HiBiT via the 10 aa linker sequence to ascertain that the Vif.TR173.HiBiT (or Vif.HB) C-terminus remained flexible and solvent-exposed. We then generated hypothetical protein structures of these modified Vif-HiBiT fusion proteins using *Phyre2*[66], and compared them to the published NL4-3 Vif model (PDB:4N9F) in PyMOL[59,68]. The 5 alpha helices and 6 beta sheets of Vif encompassing known functional

domains appeared unchanged by the C-terminal modifications (**Fig. 1A-C**). Neither the 19 C-terminal aa truncation alone nor the addition of HiBiT with linker sequence affected the formation or orientation of secondary structures. To further assess whether protein folding may be affected, we calculated the TM-scores of the protein pairs, where a score >0.6 indicates at least a 90% chance that a pair of proteins have a similar fold[69,70]. This analysis was conducted to quantify the degree to which truncation or truncation with HiBiT would affect the protein folding of Vif compared to WT. TM scores for Vif.TR and Vif.HB compared to WT were 0.99 and 0.89, respectively (**Fig. 1D**), indicating that modifications to the C-terminus of Vif after residue 173 did not appear to significantly impact Vif protein folding. Based on these *in silico* findings we predicted that fusing HiBiT to truncated Vif would have minimal influence on overall Vif function (i.e. would not significantly impair viral infectivity and replication in non-permissive cells, or A3G degradation).

Similar conclusions were drawn when the WT and modified Vif proteins from HIV-1 transmitted/founder virus strains CH077.t[73], and CH0505s[74], and patient-derived Vif A45-2[35,36] were modelled (data not shown).

Vif.HB IMC are infectious in TZM-bl cells and infection is sensitively and specifically detectable by NanoBiT luciferase luminescence.

We next generated derivatives of the pNL4.3 proviral clone[72] encoding Vif.TR truncated after aa residue 173, and Vif.HB, in which we appended the HiBiT peptide with a linker to Vif.TR, using the molecular design shown in **Fig. 1E**. We furthermore created derivatives of plasmids of CCR5-utilizing IMCs: pNL-BaL.ecto[6], and the transmitted/founder (T/F) IMCs p.CH077.t[73] and p.CH0505s[74]. HiBiT expression from the Vif.HB IMCs was confirmed in lysates from 293T cells transfected with the respective

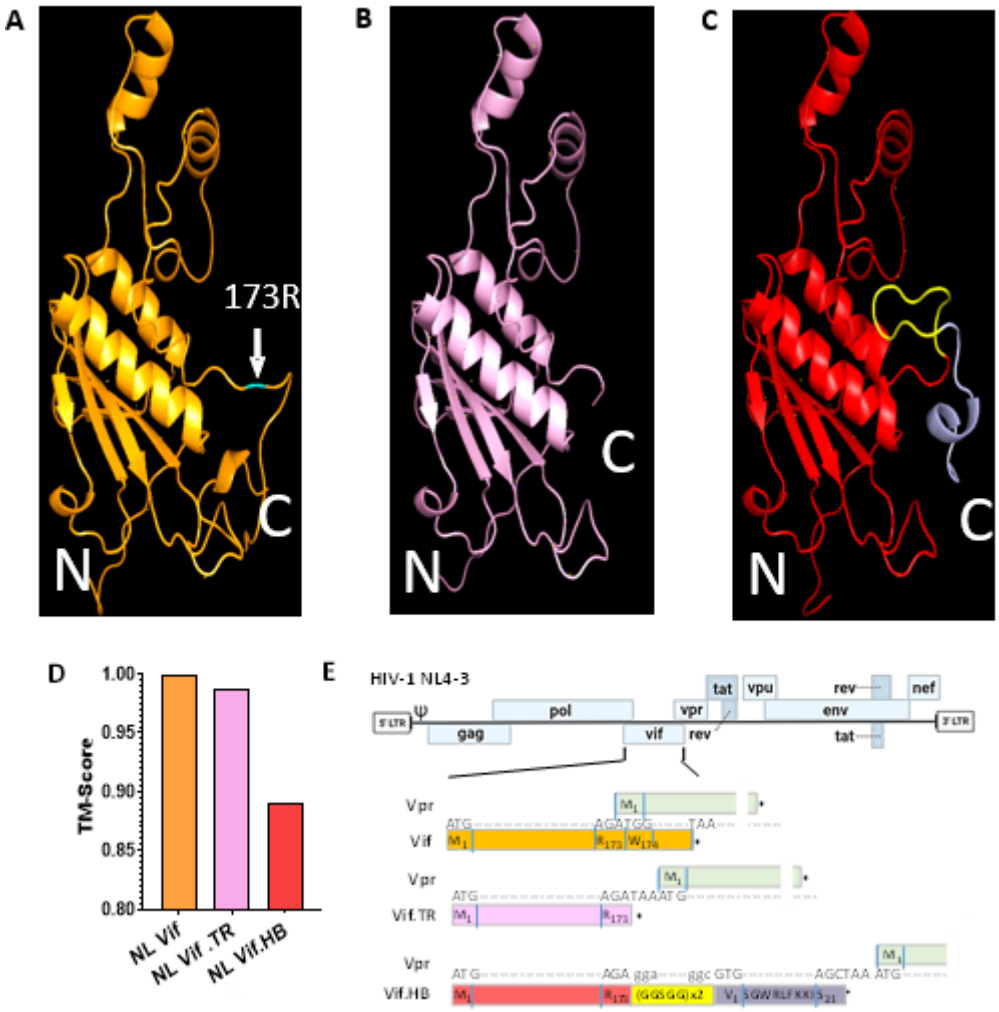

Figure 1. Structure models of wild-type and C-terminally modified Vif from HIV-1 NL4-3.

Structure model PDB files of all Vif proteins were generated from Phyre2 with ≥ 88% of the protein residues modelled at >90% confidence (10). **A)** Structure model of HIV-1 NL4-3 Vif (orange) derived from PDB:4N9F. Residue 173 (highlighted in blue and identified with a white arrow) is the point of truncation for other Vif variants. **(B)** NL4-3 Vif truncated after residue 173 (pink). **(C)** NL4-3 Vif truncated after residue 173 with linker sequence (GGSGG)x2 (yellow) followed by HiBiT (purple). **(D)** Comparison of TM-scores, determined by the RaptorX Structure Alignment Server, of NL4-3 WT Vif (NL Vif), NL Vif.TR and NL Vif.HB. **(E)** Schematic of the introduction of the truncation after codon 173, as well as the addition of the linker-HiBiT sequence in the HIV-1 proviral genome. Relevant amino acid residues are indicated in the color-coded bars; the corresponding codons are shown above to illustrate the respective nucleotide sequence.

proviral plasmids (**Fig. 2A**). Western blot analysis of transfected 293T cells lysates (**Fig. 2B**) show the expression levels of HIV-1 NL4-3 Gag and Nef proteins, respectively for WT, Vif.TR and Vif.HB IMCs. Only the full-length Vif protein was detected with anti-Vif antibodies available to us, as has been previously reported[36,38]; detection of Vif.TR requires antiserum raised against the truncated Vif variant[38]. Expression of Vif.HB protein was demonstrated using the Nano-Glo® HiBiT Blotting System (Promega).

Importantly, 293T cell-derived virus supernatants of WT Vif, Vif.TR and Vif.HB IMC were infectious on TZM-bl cells with similar titers (enumerated following β-galactosidase staining; data not shown). Furthermore, we demonstrated dose-dependent, sensitive, and specific detection of HiBiT reporter activity in TZM-bl cells infected with Vif.HB IMCs, with a linear dynamic range spanning two orders of magnitude, paralleling the 100-fold serial dilution rage of the input MOI (**Fig. 2C**). As expected, all non-reporter and Vif.HB IMC resulted in essentially identical levels of TZM-bl cell-encoded Firefly luciferase at the range of tested MOI, respectively (**Fig. 2D**).

Vif.HB is incorporated into virions and detectable via NanoBiT luciferase activity

We found NanoBiT activity is detectable in virus stocks (data not shown). This may, in part, be derived from Vif.HB released from damaged 293T cells. However, it has been previously demonstrated that Vif protein is incorporated into HIV-1 virions even though this does not appear to be required for virion infectivity; reportedly, levels of virion-associated Vif are low, and Vif in virions is generally only insensitively detected (e.g. by Western blot), and difficult to quantify[84-89]. Here, we investigated whether the addition of HiBiT to Vif.TR would result in detection of virion-associated HiBiT from virus stocks.

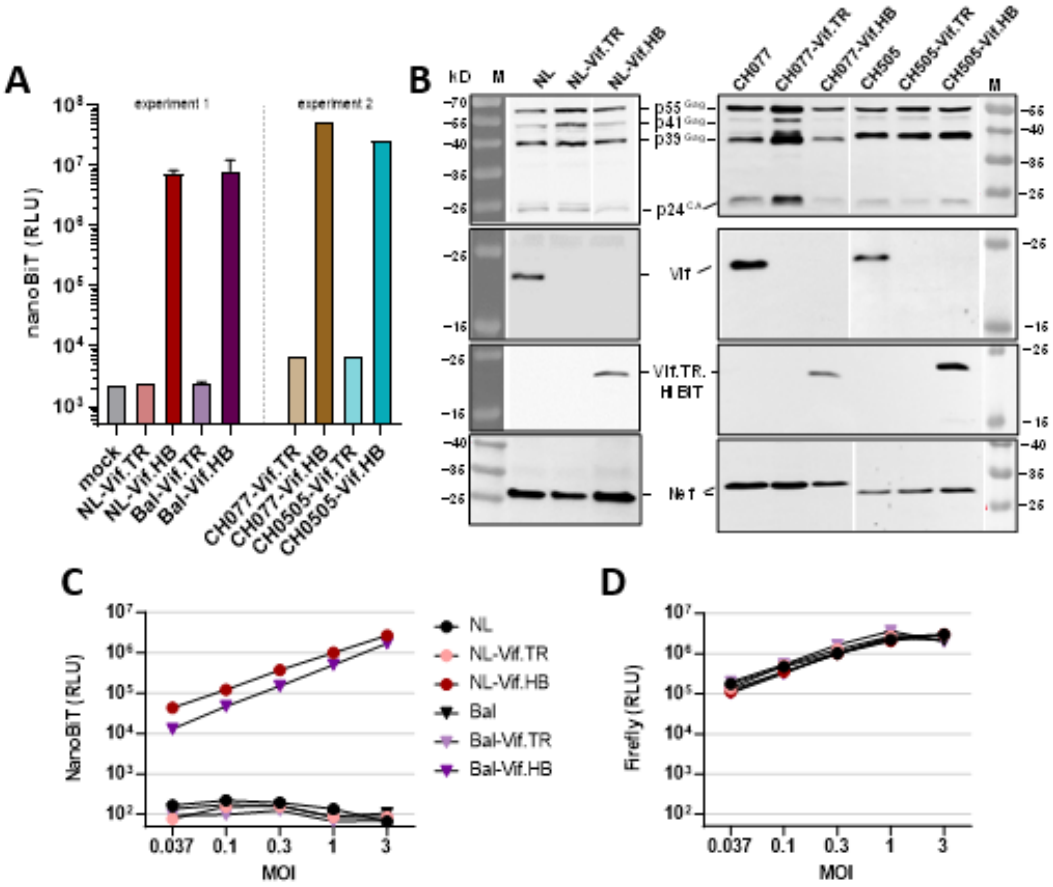

Figure 2. HiBiT activity in provirally transfected 293T cells (A-B) and in HIV-1 IMC infected TZM-bl cells (C-D).

(A) 293T cells transfected (in two separate experiments) with mock control, Vif.TR173 and Vif.TR173.HiBiT proviral clones were lysed after three days and analyzed for nanoBiT activity. **(B)** Transfected cells from (A) and matched wild-type IMC-transfected controls were analyzed by Western blotting for Gag, Nef, and full-length Vif. Expression of Vif.HB was analyzed using the HB Blotting System (Promega). **(C)** We assessed detection of virus encoded HiBiT following infection with NL-Vif.HB and NL-BaL-Vif.HB, and non-reporter parental IMC by the nanoBiT trans-complementation luciferase assay. All RLU values are blank corrected. **(D)** In parallel, TZM-bl cells were infected with 293T cell transfection-derived viruses, including NL4-3- and NL-BaL.ecto based IMC each comprising full-length Vif, Vif.TR, and Vif.HB, respectively, at the indicated MOIs (determined by β-galactosidase staining and enumeration following titration on TZM-bl). The dose-dependent levels of cell-encoded firefly luciferase activity at 48 h p.i. are plotted.

Virions from culture supernatants of 293T cells transfected with Vif WT, Vif-TR173, and Vif-HiBiT IMCs were pelleted through 20% sucrose by ultracentrifugation. By Western blotting $p24^{CA}$ and its precursors were detectable in both virions and corresponding cell lysates, with a higher degree of processing to $p24^{CA}$ in virions, as expected. (**Figure 3A**). WT Vif from HIV-1 NL4-3 was detected by anti-$Vif_{(full\text{-}length)}$ antibody in Western blot of cells but not virions despite transfection with identical amounts of IMC (**Figure 3B**). Vif.TR from HIV-1 strains NL43, CH077.t, and CH505s was not detectable with the antibody available to us, as noted above (**Figure 2B**). Importantly, however, Vif-HiBiT from all three tested HIV-1 strains was detected in both cell lysates and virions via the Nano-Glo® HiBiT Blotting System (Promega) (**Figure 3C**). This observation is consistent with virion incorporation of Vif, including in this case, truncated, C-terminally modified Vif. Furthermore, we sensitively detected NanoBit activity (**Figure 3G)** in serially diluted aliquots of the pelleted NL-Vif.HB virions, down to an unconcentrated virus stock equivalent of 0.75 µl and 0.075 µl (RLU 10-fold and 1.5-fold above background). Thus, in all following experiments involving T cell infection, cells were washed after the indicated virus stock incubation periods to remove virus inoculum and reduce Vif.HB background activity.

Vif.HB IMC are replication-competent in cells non-permissive for Vif-deficient HIV-1

When HIV-1 that lacks functional Vif is produced in permissive cells, including 293T, the virions are fully infectious. However, if the infected cells are non-permissive cells, like H9 or primary CD4+ T cells, secondary infection and replication of Vif-defective virus is abrogated [39-41,90-94]. Thus, demonstrating replication of Vif-HB IMC in non-permissive cells would indicate that the modification of, and HiBiT addition to, the C-

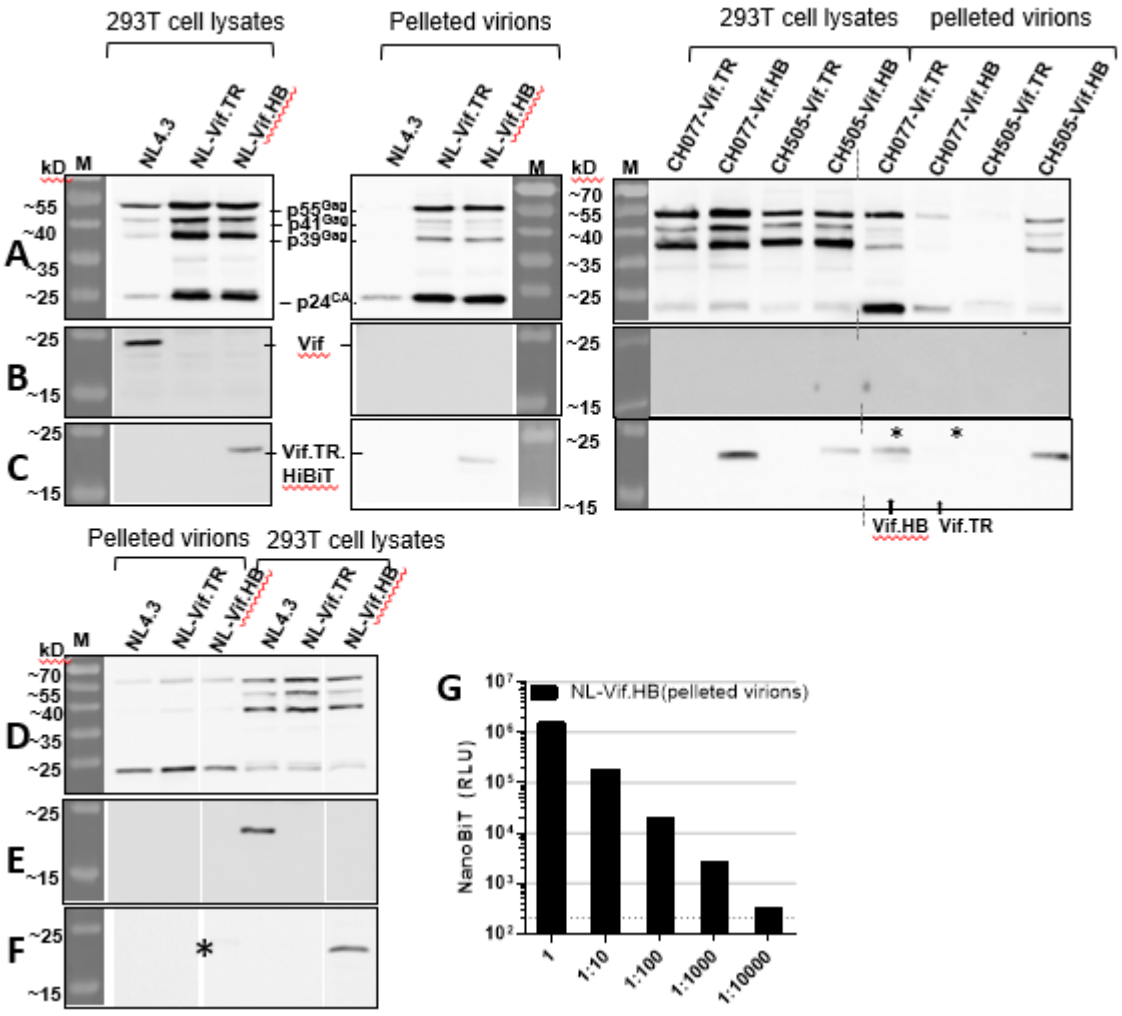

Figure 3. Detection of Vif.HB in virions.
293T cells were transfected with Vif WT, Vif.TR, and Vif.HB IMC proviral plasmids, virion containing culture supernatants were collected, and pelleted through 20% sucrose by ultracentrifugation as described in Material and Methods. **(A-C** – experiment 1, **D-G** – experiment 2**).** Lysates from cells as well as pelleted virions were subjected to SDS-PAGE, followed by Western blot to visualize Gag/p24 **(A, D)**, or full-length Vif **(B, E)**, respectively, or by Vif-HiBiT detection via the Nano-Glo® HiBiT Blotting System (Promega) (**C, F**); In (C) * and ↑ indicate that the samples for CH077-Vif.TR and CH077-Vif.HB were loaded on the gel in reverse order. In (F) * marks the position of the weak but positive Vif.HB band in virions. In (D,E, F) gaps in the image indicate where one lane with an irrelevant sample was digitally removed from the contiguous blot membrane. **(G)** An aliquot of pelleted virions from NL-Vif.HB (experiment 2) was 10-fold serially diluted in PBS, and samples corresponding to unconcentrated virus stock volumes from 750 µl to 0.075 µl were analysed for Vif-HiBiT trans-complemented NanoBiT activity.

terminus of Vif did not abrogate Vif function. We infected H9 cells with NL4-3, NL-Vif.TR, and NL-Vif.HB and over the course of 2 weeks enumerated the percentage of p24+ cells every 2 days by flow cytometry. We found that the NL-Vif.TR, and NL-Vif.HB IMCs were replication-competent in H9 cells, with replication kinetics paralleling that of WT virus (**Fig. 4A**).

Importantly, Vif.HB viruses were replication-competent and exhibited similar replication kinetics as the matched WT viruses in stringently non-permissive primary CD4+ T cells derived from human PBMC (**Figure 4B-E**). Infection with four Vif.HB viruses (NL-Vif.HB, NL-Bal-Vif.HB, CH077-Vif.HB, and CH0505-Vif.HB) resulted in kinetics of % p24+ cells detected by flow cytometry that were almost indistinguishable from those of WT viruses tested in parallel. These findings imply that the addition of HiBiT to Vif.TR173 had a negligible impact on overall Vif function, and viral replication. In the presence of the control, IDV, a low percentage of p24+ cells resulted from the initial round of infection with all viruses, without evidence for further virus spread.

Monitoring of virus infection and spread via Vif.HB/LgBiT bimolecular trans-complementation.

Given that the Vif.HB IMCs were replication competent in non-permissive cells, we next determined whether virus infection and spread over time in CD4+ T cells could be quantified using the bimolecular NanoBiT trans-complementation assay. In infected TZM-bl cells (**Figure 2D**), the HiBiT peptide fused to the C-terminus of Vif produces detectable luminescence after cell lysate was combined with exogenous LgBiT[67]. In H9 cells infected with NL-Vif.HB (**Figure 5A**) in the presence of IDV, we observed a steady decline in RLU signal after day 2, whereas the Vif.HB reporter activity in IDV untreated cells increased

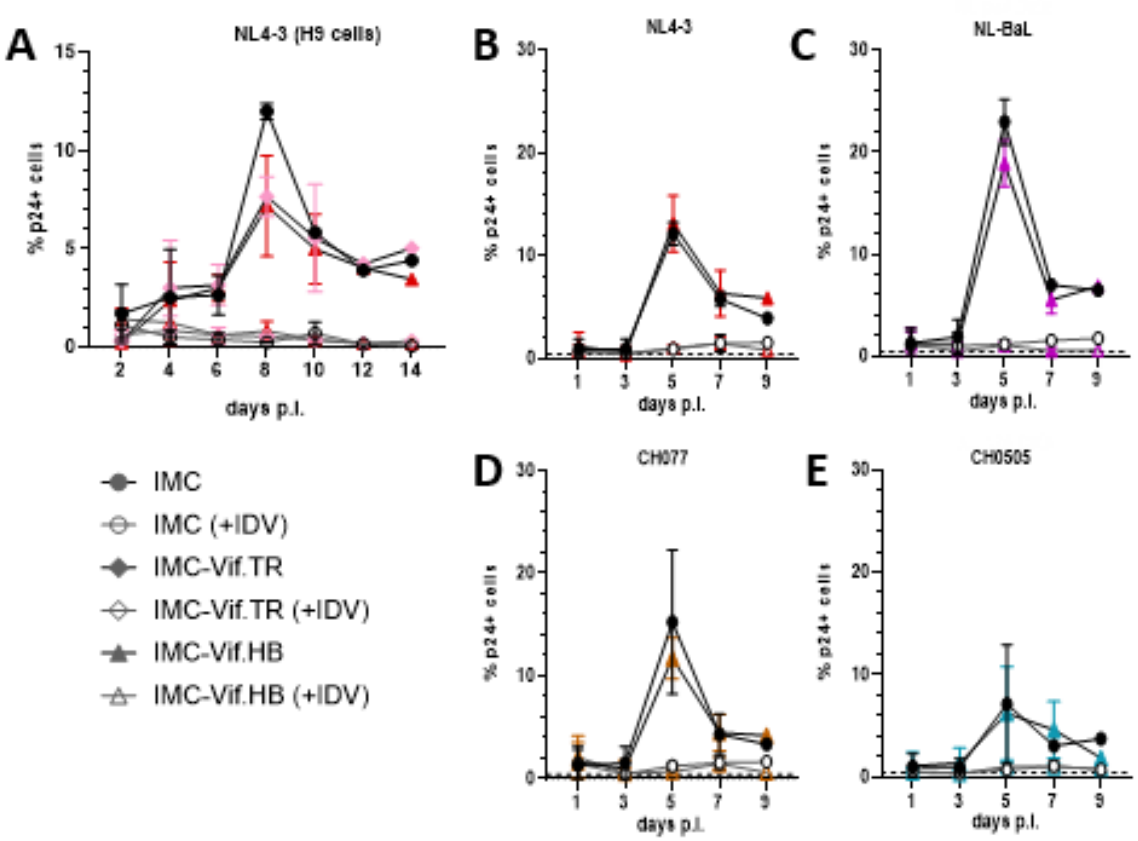

Figure 4. Replication kinetics of IMC encoding WT and modified Vif are similar in non-permissive cells.

(A) H9 cells were infected with NL4-3, NL-Vif.TR, and NL-Vif.HB in the absence or presence of the protease inhibitor, indinavir (IDV), and % p24+ cells were determined by flow cytometry over 14 days. **(B-E)** Primary CD4+ T cells isolated from PBMC were infected with parental and Vif-HiBiT virus of (B) NL4-3, (C) NL-Bal, (D) CH077.t, and (E) CH0505s, with or without IDV, and % p24+ cells were determined by flow cytometry over 7- 9 days; the mean values with range from two independent experiments are shown.

over the course of two weeks, suggesting that the Vif.HB reporter enabled quantification of ongoing virus infection and spread over multiple rounds of replication.

Similarly, we monitored virus replication in primary CD4+ T cells of four Vif.HB IMCs. At a MOI of 0.05 (**Figure 5B**), by day 2 p.i. RLU for NL-Vif.HB and NL-BaL-Vif.HB were already 3- and 7-fold higher, respectively, in the absence of IDV than in its presence. By day 4 p.i. RLUs from untreated cultures exceeded RLUs from single round infection (+IDV) by 300- and800-fold, respectively, which is consistent with reinfection and viral spread. At a 20-fold higher virus inoculum (MOI 0.8 to 1.2), infection with the four viruses (NL-Vif.HB, NL-Bal-Vif.HB, CH077-Vif.HB, and CH0505-Vif.HB) resulted in RLU_{-IDV} / RLU_{+IDV} value ratios at day 1 p.i. of 0.9, 1.0, 1.0, and 1.1, respectively, indicating equal levels of first round infection (**Figure 5C-F**). By day 2 p.i., the relative increase of RLU values from NL-Vif.HB and NL-Bal-Vif.HB infection (**Figure 5C-D**) in the absence *versus* presence of IDV was 3.3- and 6.9-fold, respectively, and thus, similar to that observed at low MOI of 0.05. For all four Vif.HB viruses at MOI ~1, (**Fig. 5C-F**) a high level of Vif.HB reporter activity was retained in IDV untreated cells over the next several days, while in the presence of IDV, Vif.HiBiT activity levels remained low and declined over time. Thus, the findings from H9 cell and primary CD4 T cell infection at low and high MOI suggest that the Vif.HB reporter did not interfere with and enabled quantification of ongoing virus infection and spread over multiple rounds of replication. These data further support the findings obtained by flow-cytometric quantification of p24+ HIV-infected cells, and indicate that IMC expressing the modified Vif-HiBiT fusion proteins are infectious as cell-free virus and replication competent in non-permissive cells.

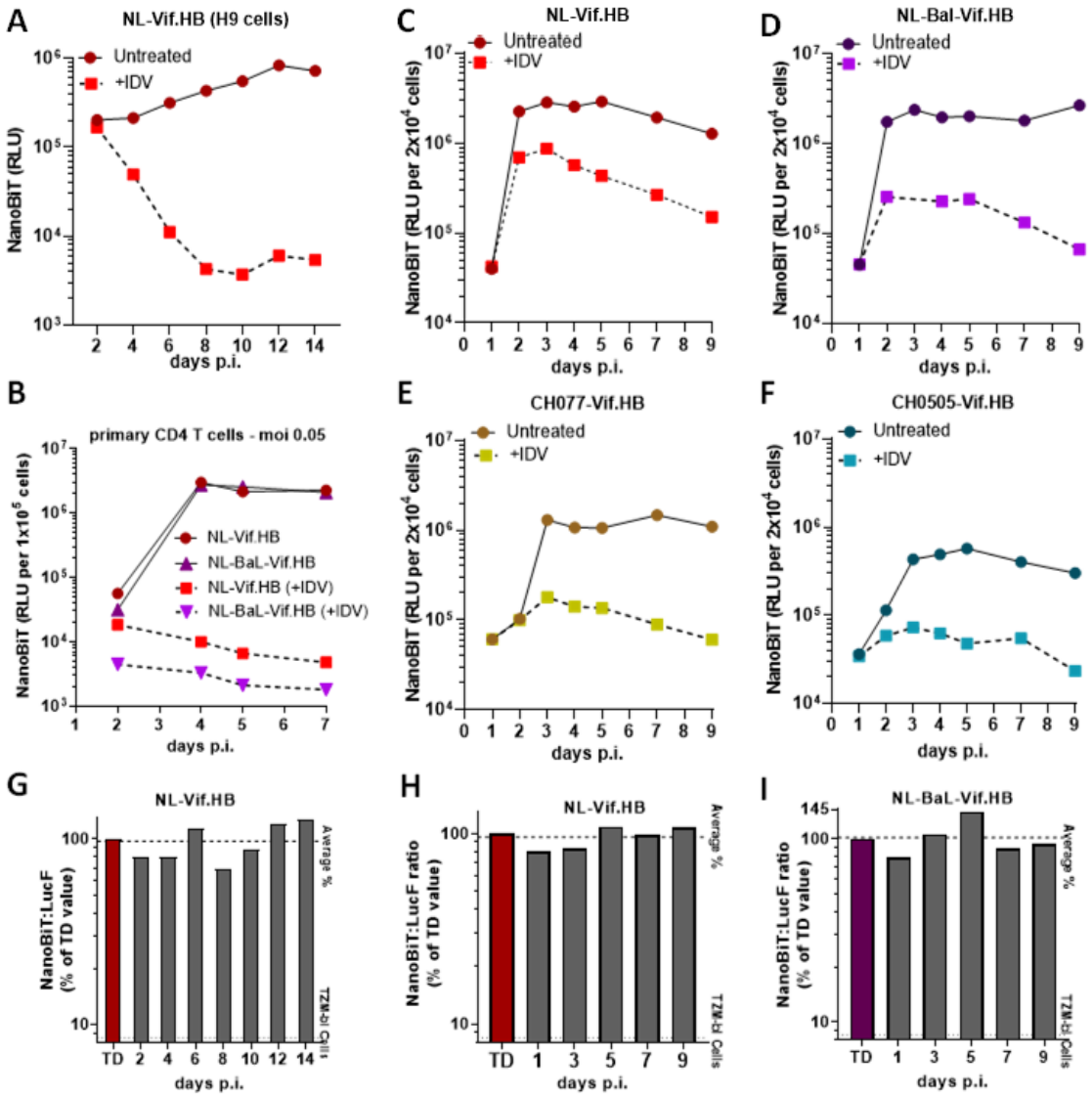

Figure 5. Monitoring viral spread via the Vif-HiBiT reporter readout.
(A) H9 cells were infected with NL-Vif.HB and cultured for 2 weeks with and without IDV, respectively. Every 2 days, a 50 uL cell suspension sample was taken from the infected H9 cell cultures (1/20 of total) and analyzed for NanoBiT luminescence (RLU) (n=2). **(B-E)** Primary CD4+ T cells isolated from PBMC were infected with one of four Vif-HiBiT viruses in either the absence or presence of IDV: **(B)** NL-Vif-HB – MOI 0.05 and NL-Bal-Vif.HB – MOI 0.05; **(C)** NL-Vif.HB – MOI ~1, (**D**) NL-Bal-Vif.HB – MOI ~1, **(E)** CH077-Vif.HB – MOI ~1 , and **(F)** CH0505-Vif.HB – MOI ~1. Samples collected over 9 days were analyzed for NanoBiT activity (RLU). Data in **(B-E)** are from single experiments, respectively, but representative of two replicas. TZM-bl cells were infected with: (**G**) supernatants taken from H9 cells (from A); and (**H, I**) supernatants from primary CD4+ T cells (from C and D) at the indicated days p.i., as well as with transfection-derived (TD) virus. The stability of Vif-HiBiT expression relative to infectivity was determined by calculating the ratio of RLU stemming from virus-encoded Vif-HiBiT and cell-encoded LucF. All infectivity ratio values are expressed relative to the ratio calculated for transfection-derived virus.

The retention of replication competency of Vif.HB-IMC is further supported by our observation that Vif.HB viruses could be passaged in a cell-associated manner in non-permissive H9 and primary CD4+ T cell cultures, respectively, (**Figure 6**) when "donor cells" from Vif.HB virus infected H9 cultures (from **Figure 5A**) and primary CD4+ T cell cultures (from **Figure 5C-F**) were added to a 9-fold excess of uninfected cells. This further supports the conclusion that the Vif.HB viruses are infectious and replication-competent in both permissive and non-permissive cells (**Figure 6**). In the absence of IDV, RLU values increased significantly in the first 2-3 days p.i., indicative of the spread of Vif.HB IMC produced in both types of non-permissive "donor cells" to uninfected target cells. RLU continued to increase even when cultures were split, indicative of ongoing replication. Importantly, IDV, which abrogates proteolytic maturation of *de novo* produced Gag and Gag-Pol, blocked virus spread, resulting in a steady decline of Vif.HB activity in the cultures.

Vif-HiBiT activity is stably maintained over multiple replication cycles

Adding exogenous sequences into the HIV-1 genome may exert selection pressure on viral infectivity and replication kinetics and may interfere with reporter gene retention and expression over multiple rounds of replication [6,7,29]. Hence, in parallel to assessing replication kinetics, we determined if the HiBiT reporter was stably expressed after multiple cycles of replication, using an approach essentially as we previously described [6,7] **(Figure 5G-I)**. 293T cell transfection-derived (TD) virus, and supernatants from Vif-HiBiT IMC infected cultures of H9 cells **(from Figure 5A**) and primary CD4+ T cells (**from Figures 5C-F**) collected at indicated time points were used to infect TZM-bl cells as described in Material and Methods. TZM-bl cells express cell-encoded firefly luciferase

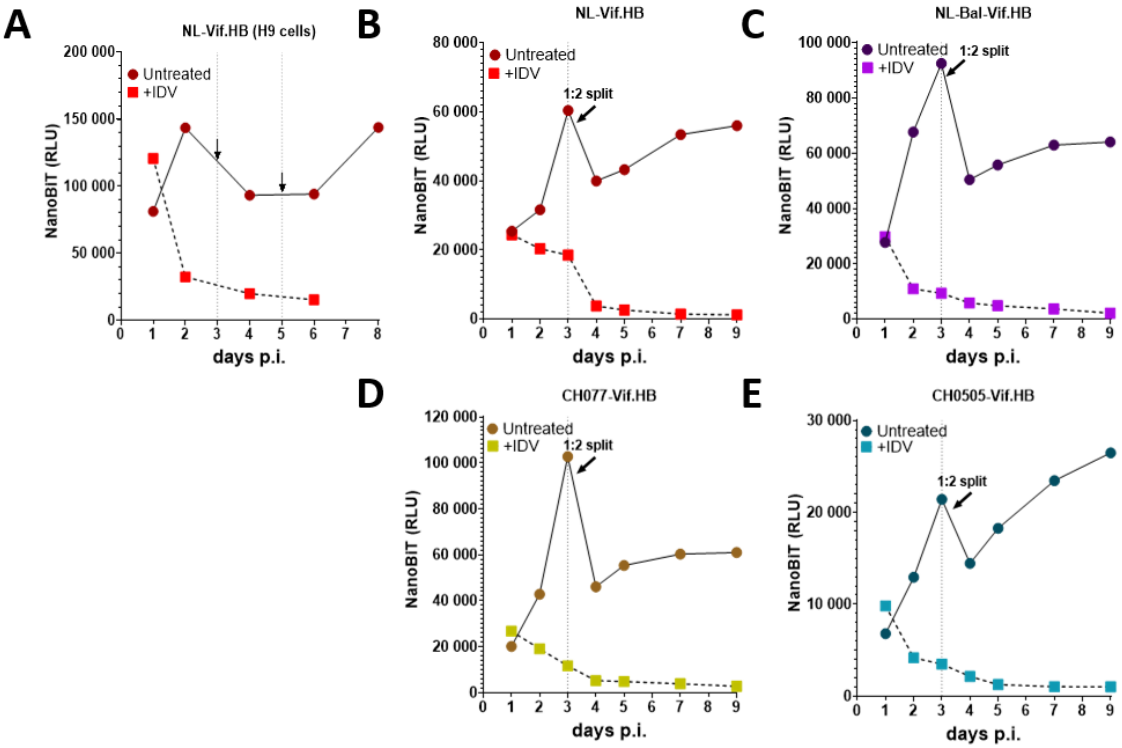

Figure 6. Efficient passage of cell-associated Vif-HiBiT virus in non-permissive H9 and primary CD4+ T cells.

(**A**) 45,000 H9 cells were inoculated with 5,000 washed NL-Vif.HB infected H9 cells derived at day 10 p.i. from the culture shown in **Fig. 5A**, and cultured either with or without IDV. (**B-E**) Similarly, 45,000 primary CD4+ T cells were inoculated with 5,000 washed CD4+ T cells derived at day 6 p.i. from cultures infected with NL-Vif.HB, NL-Bal-Vif.HB, CH077-Vif.HB, and CH0505-Vif.HB, shown in **Fig. 5C-F**, respectively, and cultured with or without IDV. Cells (1/20 of total cells, or 2,500 cells on day 1) were collected from the cultures daily for 9 days and analyzed for RLU as described in Methods. Arrows and dotted lines indicate days at which cultures were split 1:2 by removing half of the volume of resuspended cell cultures and replenishing with an equal volume of medium (-/+ IDV). Data shown are from single experiments, but representative of two replicas.

(LucF) upon HIV-1 infection, which means LucF activity represents a measure of overall infectivity of a given virus inoculum [77]. We determined both LucF activity and Vif-HiBiT trans-complemented NanoBiT activity in infected TZM-bl cells, calculated the ratio of NanoBiT RLU to the LucF RLU, and compared it to the normalized ratio obtained from TZM-bl infection with TD virus stocks. A reduction in the ratio would indicate a loss of NanoBiT activity relative to virion infectivity, possibly due to silencing or loss of the reporter gene. In H9 cells **(Figure 5G**), trans-complemented NanoBiT activity from NL-Vif.HB was retained over the course of two weeks, during which the average NanoBiT:LucF ratio was 97% of that obtained for TD virus. NanoBiT activity in Vif.HB IMC infected primary CD4+ T cells was also maintained over 9 days with the average NanoBiT:LucF ratio for NL-Vif.HB (**Figure 5H**) at 95%, and for NL-BaL-Vif.HB (**Figure 5I**) at 101% of the TD virus-derived value. Thus, we concluded that Vif.HB continues to be stably expressed over multiple replication cycles.

Wildtype Nef expression and function is retained with Vif-HiBiT reporter viruses

One premise for the new Vif.HB reporter approach was to retain wildtype Nef expression by avoiding an expression strategy that may compromise Nef function. Thus, we sought to demonstrate that our molecular strategy for HiBiT expression *via* fusion to Vif.TR did not interfere with Nef expression and function (**Figure 7**). We assessed Nef-dependent CD4 and MHC-1 downregulation at 48 and 72 h p.i, essentially as we previously described [7,95], in H9 cells infected with NL4-3 WT, Vif.TR, and Vif.HB IMCs, and a *nef*^{minus} control IMC, NL-Nef^{STOP} [7]. The degree of CD4 downregulation in Gag/p24+ H9 cells (**Figure 7A)** at both time points was essentially the same following infection with the WT, Vif.TR and Vif.HB IMC. As expected, a partial reduction of surface CD4 levels (due

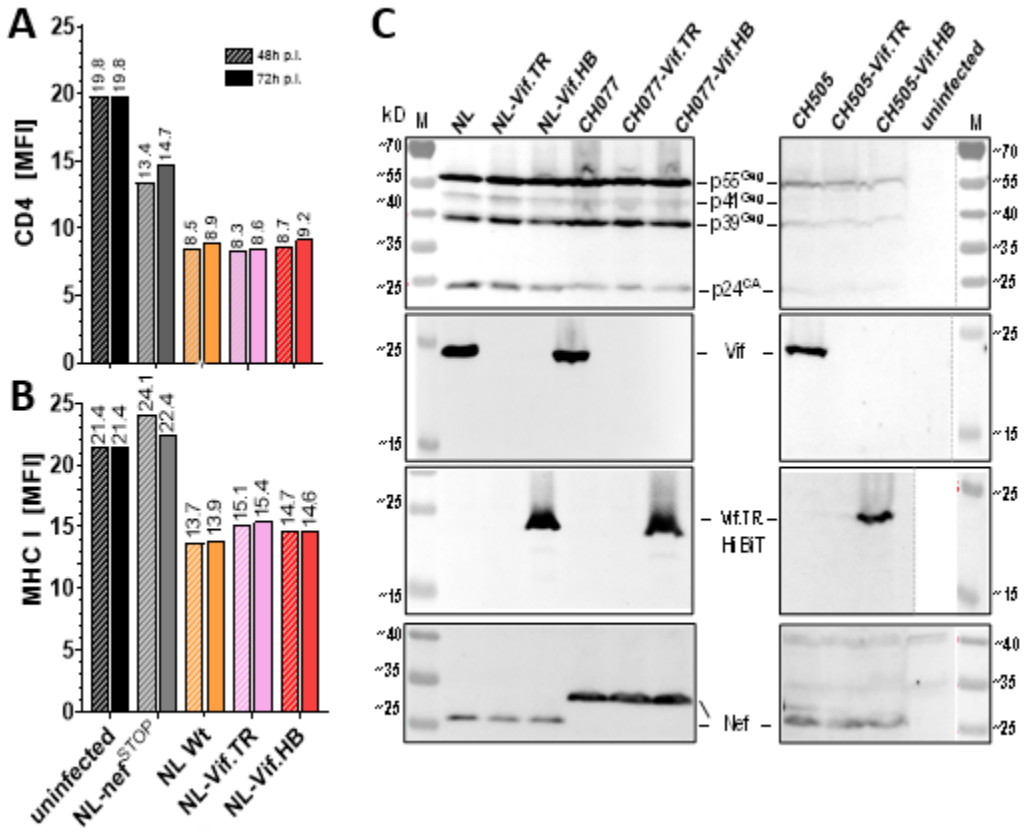

Figure 7. Retention of Nef expression and function. (A-B)
In H9 cells infected with the indicated IMC, Nef-dependent downregulation of CD4 and MHC I was assessed by flow cytometric analysis at 48h and 72h post infection (p.i.). **(A)** CD4 levels are expressed as geometric mean fluorescent intensity (MFI), in Gag/p24+ H9 cells, and compared to CD4 MFI in uninfected culture. **(B)** MHC I levels are expressed as MFI in Gag/p24+ H9 cells, and compared to MHC I MFI in p24– H9 cells in the same culture**. (C)** Primary CD4 T cells infected with NL4-3, CH077.t and CH0505s IMC encoding Vif WT, Vif.TR and Vif.HB, respectively, were enumerated by flow cytometry for Gag/p24+, lysed, and the equivalent of 150,000 p24+ cells each were analyzed in Western Blot for Gag, Nef, and full-length Vif with respective specific antibodies. Vif.TR.HB was visualized with HiBiT Blotting System (Promega).

to Vpu activity) was seen for NL-Nef^{STOP}. Furthermore, in Gag/p24+ H9 cells, infection with NL4-3 WT, Vif.TR and Vif.HB viruses resulted in similar levels of MHC-1 downregulation, while cells infected with *nef^{minus}* HIV-1 did not downregulate MHC I (**Figure 7B)**.

In primary CD4+ T cells infected with IMCs of HIV-1 NL4-3, or the T/F strains CH077.t and CH0505s, encoding either WT Vif, Vif.TR or Vif.HB, respectively, we observed essentially the same CD4 and MHC I downregulation phenotypes as in H9 cells (data not shown). For these three HIV-1 strains, Western blot analysis (**Figure 7C**) of primary CD4+ T cell lysates, normalized to equal numbers of Gag/p24+ infected cells, showed that Nef expression for Vif.TR and Vif.HB IMC relative to Gag/p24 was basically indistinguishable from that of their matched wildtype (Vif+) IMCs. This observation agrees with that previously seen in transfected 293T cells (**Figure 1B**). Only full-length Vif proteins, but not Vif.TR, were detected with anti-Vif antibodies available to us. Vif.HB protein was detected using the Nano-Glo® HiBiT Blotting System (Promega).

These data therefore indicate that neither truncating Vif after residue 173 nor fusing HiBiT to Vif-TR173 appears to interfere with Nef expression or function in infected continuous or primary CD4+ T cells. Thus, the potential utility of this reporter is expanded since Nef function is preserved.

Vif function of APOBEC3 protein degradation is retained for Vif-TR173 and Vif-HiBiT

An important function of Vif is to direct host A3 proteins for degradation by recruiting the E3 ubiquitin ligase complex[49-53]. It has been well established that A3G is more sensitive to Vif-mediated degradation than A3F[96,97], while A3B is mostly resistant to

this Vif-mediated degradation. Given that Vif-TR173 and Vif-HiBiT IMCs retained replication competency, we sought to directly demonstrate that Vif truncated after residue 173 preserved the ability to degrade A3G similarly to full-length Vif. We employed a 293T cell-based assay in which the steady-state expression of HA-tagged A3G, A3F, or A3B proteins co-expressed in the absence or presence of functional Vif can be monitored by anti-HA Western blot (**Figure 8)**. We observed that co-transfection of plasmid encoding HA-tagged A3G with expression vectors encoding Vif protein derived from four HIV-1 strains (NL4-3, the T/F IMCs CH077.t and CH505s, and patient isolate A45 [35,36]) resulted in similar reduction in A3G steady state levels for full-length (FL) and C-terminally modified forms of Vif. Please note that the mouse monoclonal anti-Vif antibody used here does not detect truncated forms of Vif, and fails to detect CH505 Vif. These findings agree with those by Nakashima *et. al* who could detect neither similarly truncated Vif nor certain alanine scanning mutants using the same reagent [56]. Importantly, the results from our co-transfection and expression study indicated efficient A3G degradation mediated by WT Vif, Vif.TR, and Vif.HB (**Fig. 8A**). Steady-state levels of A3F and A3B were not significantly affected by co-expression of any of the Vif proteins under these experimental conditions (**Fig. 8B, 8C**). Importantly, our findings are the first direct evidence that truncation of the 19 C-terminal aa of Vif (or addition of HiBiT) does not significantly affect efficient Vif-mediated A3G degradation, and thus, that the unstructured 19 C-terminal aa of Vif are dispensable for this critical Vif function.

DISCUSSION

In vivo, defective *vif* function is strongly associated with HIV-1 G-to-A hypermutation [37]. In the absence of Vif expression in HIV-1 infected non-permissive cells,

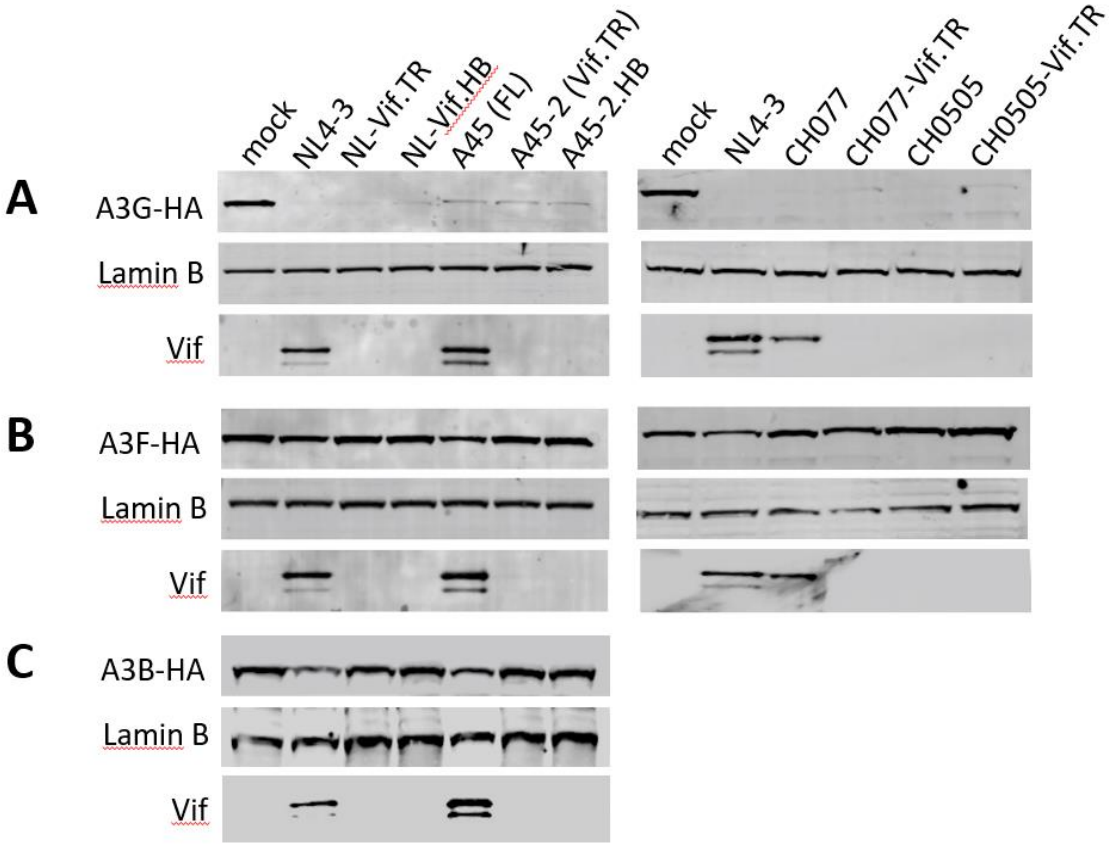

Figure 8. Efficient APOBEC3G protein degradation indicates retention of Vif function in Vif.TR and Vif.HB.

293T cells were co-transfected with the indicated HA-tagged A3, and Vif expression plasmid combinations. Two days post transfection, cells were lysed as described in Material and Methods, and normalized amounts of cellular proteins were separated on 4%-12 % gradient SDS-PAGE. To determine steady state levels of A3 protein in the presence of WT and modified Vif proteins, A3G **(A)**, A3F **(B)**, and A3B **(C)** proteins were visualized using anti-HA antibody; a mouse monoclonal anti-Vif antibody (recognizing full-length Vif) was used to probe for Vif protein; and Lamin B antibody served as a normalization control.

A3 family restriction factors are incorporated into nascent virions and block replication through deaminase activity with resulting viral genomic hypermutation, as well as through cytidine deaminase independent mechanisms [reviewed in 42,43,64]. Vif blocks this restriction by directing host A3 proteins to an E3 ubiquitin ligase complex for ubiquitination and degradation[49-53,57]. It has also been recognized that Vif can induce G2/M cell cycle arrest in infected cells[98,99]. More recently it was discovered that Vif recruits the same E3 ligase complex used to inhibit and degrade A3 proteins to degrade a family of PPP2R5 phospho-regulatory proteins [*reviewed in* 42]. Over the last decade, structural information on Vif in complex with Cullin-RING ubiquitin ligase (CRL) complex, transcription cofactor core-binding factor beta (CBFβ), Elongin B and C, and/or A3 family proteins has provided detailed mechanistic insights into Vif function. The BC-box and Cullin-box regions, contained within the SOCS-box domain that stretches from residues 144 to 173 near the C-terminus, interact with ElonginC and Cullin5 of E3 ligase, respectively[45,57-61,100,101], [reviewed in 56,65]. Of note, interaction sites of the Vif protein with A3G and A3F differ in key residues, indicating a functional dissociation between the A3F and A3G interaction motif[57] [reviewed in 56,65]. Most recently, Li *et. al* reported that ssRNA acts as molecular glue for the Vif–A3G interaction[100].

For the 19 C-terminal amino acid residues of Vif, spanning from residue 174 immediately adjacent to the SOCS box to residue 192, a clear functional and structural role has not yet been identified. The region is apparently not required for Vif-CBFβ complex binding to A3G [reviewed in 64,65]. So far, experimental structural data for Vif have been generated with Vif truncated at residue 176, including most recently by Li *et. al*[100]. Structural modelling suggests that the C-terminal region is unstructured, conformationally

dynamic[58,59,101], and possibly solvent exposed, making crystallization of full-length Vif protein difficult and impractical.

Findings suggesting that the Vif C-terminus may in fact be dispensable for Vif function underpin our molecular strategy for a new IMC design that aims to maintain wild-type Nef function in order to augment the application of HIV-1 reporter viruses. Prior to the discovery of the role of Vif in counteracting A3G restriction[49,50], we had described a naturally occurring, patient-derived *vif* variant (A45-2) with a premature stop at residue 174, which we found retained replication competence of virus in cells non-permissive to *vif*-defective HIV-1, including H9 T-lymphocytes, PBMC, and monocyte-derived macrophages[36,94]. Pace *et. al*[37] later also described *in vivo vif* variants with a premature stop at codon 174, from non-A3G-hypermutated provirus. Interestingly, the A45-2 truncated Vif protein contained several rare amino acid substitutions found in less than 5% of 77 contemporaneous Vif sequences[35,36]; whether the presence of rare substitutions in isolates with naturally truncated *vif* may be compensatory in nature has not been explored. Further, it was recently described that passaging of *vif*-negative HIV-1 in the presence of sub-lethal levels of A3G can result in compensatory mutations in *env*[102]. How mutations to Env and Vif may affect Vif function require further investigation but may inform important HIV host-adaptation mechanisms.

Given these findings and data from structure models, we tested the hypothesis that the 19 C-terminal amino acids of Vif could be replaced without loss of essential function by the HiBiT fluorescent peptide tag that is similar in length and charge, and similarly unstructured in *in silico* predictions based on published Vif structure data.

Our data demonstrate that HIV-1 IMC that encode Vif proteins truncated after aa 173, as well as Vif-Tr173 modified with the HiBiT peptide retain Vif function as it pertains to replication competence in non-permissive target cells. This was the case for the widely used reference strain NL4-3, as well as the two transmitted founder (TF) HIV-1 strains we tested, and applied to both cell-free and cell-mediated passage of virus. Furthermore, in an experimental approach that assessed Vif-dependent reduction of HA-tagged A3G steady state levels, we observed no differences in A3G degradation by full-length, truncated, or HiBiT-modified Vif proteins from NL4-3, TF IMCs CH077.t and CH505s, as well as the patient-derived *vif* variant A45. To our knowledge, this is the first experimental evidence of this nature. A3G has been described as exerting the strongest restriction among the family of A3 proteins[44]. Under the given experimental conditions degradation of A3F and A3B was minimal and indistinguishable between wildtype and modified Vif proteins. Of note, the mouse monoclonal anti-Vif antibody used in these experiments did not recognize C.CH050s Vif protein (**Figure 8**), unlike the polyclonal rb-anti-Vif antibody used to visualize Vif expressed from proviruses in transfected and infected cells (**Figures 2, 7**). Neither antibody detected truncated Vif variants on Western blots, as also observed by Nakashima *et. al* for the same mouse monoclonal antibody[56]. Bosch and colleagues had previously noted this for a different polyclonal rb-anti-Vif antibody, and generated antibody specifically against Vif truncated after residue 173[38]; however, this reagent was not accessible to us at the time this study was conducted.

In addition to providing insights into the non-essential role of the 19 C-terminal amino acids of Vif, we demonstrate utility of Vif.HB as a novel reporter gene. We find that not only does luminescence activity from HiBiT linked to Vif in the bimolecular nanoBiT

assay serve as a sensitive reporter to quantify HIV-1 single-round infection, but also that it is stably retained over multiple cycles of replication in CD4+ target cells, including primary human CD4+ lymphocytes. We conclude that this was achievable due to HiBiT's key advantages, including its small size and the large dynamic range of sensitive detection, in combination with the tolerance of HIV-1 for Vif-Tr173 fused to HiBiT. HiBiT has also proven advantageous in the generation of reporter viruses with unimpaired replication properties for the study of Influenza A/H3N2 and *Flaviviridae*[103,104], and for quantification of HIV-1 virion release[34].

Stable retention of reporter activity is critical for experimental applications that require multiple rounds of replication. These applications may include models of HIV-1 infection in primary cells and tissue explant culture, as well as *in vivo* in humanized mice or, with SIV, in non-human primates (NHP). We previously described retention of *Renilla* luciferase (LucR) activity in PBMC using two different NL4-3 based HIV-1 reporter IMCs in which the reporter gene was located immediately upstream of *nef*[6,7]. The value of improving reporter gene retention is also highlighted by work from Roy *et. al*[29] who described that the higher CG dinucleotide content in nanoLuc and iRFP reporter genes, engineered into the same HIV-1 IMC backbone we previously described[7], led to *in vivo* loss of reporter activity over time in humanized mice despite high viral load. They showed that removal of CG dinucleotides in the reporter coding regions improved replication *in vitro* and reporter expression *in vivo* and *ex vivo*. The short 33 bp coding sequence for the linker-HiBiT peptide that we appended to Vif contains five CG dinucleotides (i.e. 1 per 6.6 bp), while the entire 9.7 kbp-long NL4-3 proviral genome contains only 92 CG dinucleotides (i.e.1 per 105 bp). We have not yet explored if eliminating the five CG

dinucleotides in the linker-HiBiT sequence may further improve HIV-1 Vif.HB IMC performance, but this may be warranted to further optimize the utility of this Vif.HB molecular strategy.

Achieving stable reporter gene expression with the HIV-1 Vif.HB approach is notable also as a successful example of reporter gene insertion in the central, accessory-protein-encoding region of the proviral genome. While this work was ongoing, Ozono *et. al*[34] reported on an approach that allows for rapid quantification of virion production from NL4-3-based IMC and *env*-minus pseudoviruses via HiBiT activity. pNL-Luc2IN/HiBiT construct was derived from pNL-Luc-E-R+ (with Firefly luciferase (LucF) expressed in place of Nef)[105] and engineered with HiBiT appended to the C-terminus of integrase (IN), leading to virion incorporation. The NL-IN/HiBiT-Fin IMC was infectious and replication-competent in M8166 cells and PBMC. The authors did not address whether HiBiT reporter activity was retained over multiple rounds of virus replication. It is also notable that the dual HiBiT-LucF reporter viruses do not encode a functional *nef* gene.

One major goal for our Vif.HB reporter IMC design was to maintain unaltered Nef expression and function, which is challenging to achieve when the reporter gene is inserted in the 3' region of the genome. We previously addressed this challenge[6,7], and found that inserting the *Renilla* luciferase (LucR) reporter gene in frame with the *nef* start codon followed by a truncated EMCV IRES ("6ATRi", which dampens activity compared to wildtype EMCV IRES) allowed for Nef protein expression from the bicistronic mRNA at physiological levels of parental non-reporter provirus[7]. This approach had significant advantages for LucR, mCD24, GFP, and nanoLuc reporter IMC in several applications[7,10-12,106-108]. However, the level of Nef expression and function in IMCs comprising a

reporter-6ATRi cassette, as compared to their parental IMC, may be dependent on the virus strain used. By avoiding the *env/nef* region with the Vif.HB IMC design, we demonstrated that wild-type levels of Nef expression and function, as demonstrated by CD4 and MHC I downregulation, were retained in NL4-3 and primary TF HIV-1 derived Vif.HB reporter IMC.

In summary, our novel strategy for a HiBit-based HIV reporter virus that is replication competent and preserves the function of all HIV-1 encoded genes provide a uniquely useful virologic tool for experimental approaches that call for sensitive detection of HIV-1 infection, and inhibition thereof. The Vif.HB IMC approach promises to broaden the application of HIV-1 reporter virus approaches for interrogating important questions in a physiologically relevant context, including in cell-based immunoassays requiring fully functional Nef, in *ex vivo* models, or *in vivo* applications such as humanized mice or nun-human primates (NHP). Importantly, our findings shed light on Vif structure-function relationships and the underexplored role of the C-terminal domain of Vif that spans 19 residues adjacent to the functionally critical SOCS Box.

ACKNOWLEDGEMENTS

This work was supported, in whole or in part, by the Bill & Melinda Gates Foundation (OPP1146996 and INV-036842, CAVD/CAVIMC). Under the grant conditions of the Foundation, a Creative Commons Attribution 4.0 Generic License has already been assigned to the Author Accepted Manuscript version that might arise from this submission. Work by DI, AS, JJ, JZ, JK, and CO was supported by BMGF OPP1146996 and INV-036842. CS and IC were supported by NIH P01 AI 131346.

REFERENCES

1. UNAIDS. UNAIDS Fact Sheet 2022. (2022).
2. UNAIDS. Full Report - In Danger: UNAIDS Global AIDS Update 2022. (2022).
3. Haynes, B.F. et al. Strategies for HIV-1 vaccines that induce broadly neutralizing antibodies. *Nature Reviews Immunology* (2022).
4. Hannah, S., Chinyenze, K., Shattock, R., Yola, N. & Warren, M. HIV vaccines in 2022: where to from here? *J Int AIDS Soc* **25**, e25923 (2022).
5. Macatangay, B.J.C., Landay, A.L., Garcia, F. & Rinaldo, C.R. Editorial: Advances in T Cell Therapeutic Vaccines for HIV. *Frontiers in Immunology* **13**(2022).
6. Edmonds, T.G. et al. Replication competent molecular clones of HIV-1 expressing Renilla luciferase facilitate the analysis of antibody inhibition in PBMC. *Virology* **408**, 1-13 (2010).
7. Alberti, M.O. et al. Optimized Replicating Renilla Luciferase Reporter HIV-1 Utilizing Novel Internal Ribosome Entry Site Elements for Native Nef Expression and Function. *AIDS Res Hum Retroviruses* **31**, 1278-96 (2015).
8. Sarzotti-Kelsoe, M. et al. Optimization and validation of a neutralizing antibody assay for HIV-1 in A3R5 cells. *Journal of Immunological Methods* **409**, 147-160 (2014).
9. deCamp, A. et al. Global panel of HIV-1 Env reference strains for standardized assessments of vaccine-elicited neutralizing antibodies. *J Virol* **88**, 2489-507 (2014).
10. Cavrois, M. et al. Mass Cytometric Analysis of HIV Entry, Replication, and Remodeling in Tissue CD4+ T Cells. *Cell Rep* **20**, 984-998 (2017).
11. Prévost, J. et al. Incomplete Downregulation of CD4 Expression Affects HIV-1 Env Conformation and Antibody-Dependent Cellular Cytotoxicity Responses. *J Virol* **92**(2018).
12. Ventura, J.D. et al. Longitudinal bioluminescent imaging of HIV-1 infection during antiretroviral therapy and treatment interruption in humanized mice. *PLOS Pathogens* **15**, e1008161 (2019).
13. Freel, S.A. et al. Phenotypic and functional profile of HIV-inhibitory CD8 T cells elicited by natural infection and heterologous prime/boost vaccination. *J Virol* **84**, 4998-5006 (2010).
14. Naarding, M.A. et al. Development of a luciferase based viral inhibition assay to evaluate vaccine induced CD8 T-cell responses. *J Immunol Methods* **409**, 161-73 (2014).
15. Pollara, J. et al. High-throughput quantitative analysis of HIV-1 and SIV-specific ADCC-mediating antibody responses. *Cytometry A* **79**, 603-12 (2011).
16. Pollara, J. et al. Association of HIV-1 Envelope-Specific Breast Milk IgA Responses with Reduced Risk of Postnatal Mother-to-Child Transmission of HIV-1. *J Virol* **89**, 9952-61 (2015).
17. Sung, J.A. et al. Dual-Affinity Re-Targeting proteins direct T cell-mediated cytolysis of latently HIV-infected cells. *J Clin Invest* **125**, 4077-90 (2015).
18. Astronomo, R.D. et al. Neutralization Takes Precedence Over IgG or IgA Isotype-related Functions in Mucosal HIV-1 Antibody-mediated Protection. *EBioMedicine* **14**, 97-111 (2016).

19. Astronomo, R.D. et al. Rectal tissue and vaginal tissue from intravenous VRC01 recipients show protection against ex vivo HIV-1 challenge. *J Clin Invest* **131**(2021).
20. Gornalusse, G.G. et al. Buprenorphine Increases HIV-1 Infection In Vitro but Does Not Reactivate HIV-1 from Latency. *Viruses* **13**(2021).
21. Mielke, D. et al. ADCC-mediating non-neutralizing antibodies can exert immune pressure in early HIV-1 infection. *PLoS Pathog* **17**, e1010046 (2021).
22. Mielke, D. et al. Selection of HIV Envelope Strains for Standardized Assessments of Vaccine-Elicited Antibody-Dependent Cellular Cytotoxicity-Mediating Antibodies. *J Virol* **96**, e0164321 (2022).
23. Seay, K. et al. Mice transgenic for CD4-specific human CD4, CCR5 and cyclin T1 expression: a new model for investigating HIV-1 transmission and treatment efficacy. *PLoS One* **8**, e63537 (2013).
24. Seay, K. et al. In Vivo Activation of Human NK Cells by Treatment with an Interleukin-15 Superagonist Potently Inhibits Acute In Vivo HIV-1 Infection in Humanized Mice. *J Virol* **89**, 6264-74 (2015).
25. Seay, K. et al. The Vaginal Acquisition and Dissemination of HIV-1 Infection in a Novel Transgenic Mouse Model Is Facilitated by Coinfection with Herpes Simplex Virus 2 and Is Inhibited by Microbicide Treatment. *J Virol* **89**, 9559-70 (2015).
26. Bardhi, A. et al. Potent In Vivo NK Cell-Mediated Elimination of HIV-1-Infected Cells Mobilized by a gp120-Bispecific and Hexavalent Broadly Neutralizing Fusion Protein. *J Virol* **91**(2017).
27. Anthony-Gonda, K. et al. Multispecific anti-HIV duoCAR-T cells display broad in vitro antiviral activity and potent in vivo elimination of HIV-infected cells in a humanized mouse model. *Sci Transl Med* **11**(2019).
28. Prévost, J. et al. Influence of the Envelope gp120 Phe 43 Cavity on HIV-1 Sensitivity to Antibody-Dependent Cell-Mediated Cytotoxicity Responses. *Journal of Virology* **91**, JVI.02452-16 (2017).
29. Roy, C.N., Benitez Moreno, M.A., Kline, C. & Ambrose, Z. CG Dinucleotide Removal in Bioluminescent and Fluorescent Reporters Improves HIV-1 Replication and Reporter Gene Expression for Dual Imaging in Humanized Mice. *J Virol* **95**, e0044921 (2021).
30. Müller, B. et al. Construction and characterization of a fluorescently labeled infectious human immunodeficiency virus type 1 derivative. *J Virol* **78**, 10803-13 (2004).
31. Hübner, W. et al. Sequence of Human Immunodeficiency Virus Type 1 (HIV-1) Gag Localization and Oligomerization Monitored with Live Confocal Imaging of a Replication-Competent, Fluorescently Tagged HIV-1. *Journal of Virology* **81**, 12596-12607 (2007).
32. Kirui, J. & Freed, E.O. Generation and validation of a highly sensitive bioluminescent HIV-1 reporter vector that simplifies measurement of virus release. *Retrovirology* **17**(2020).
33. Schwinn, M.K. et al. CRISPR-Mediated Tagging of Endogenous Proteins with a Luminescent Peptide. *ACS Chemical Biology* **13**, 467-474 (2018).

34. Ozono, S., Zhang, Y., Tobiume, M., Kishigami, S. & Tokunaga, K. Super-rapid quantitation of the production of HIV-1 harboring a luminescent peptide tag. *J Biol Chem* **295**, 13023-13030 (2020).
35. Wieland, U. et al. In Vivo Genetic Variability of the HIV-1 vif Gene. *Virology* **203**, 43-51 (1994).
36. Ochsenbauer, C., Bosch, V., Oelze, I. & Wieland, U. Unimpaired function of a naturally occurring C terminally truncated vif gene product of human immunodeficiency virus type 1. *J Gen Virol* **77 (Pt 7)**, 1389-95 (1996).
37. Pace, C. et al. Population level analysis of human immunodeficiency virus type 1 hypermutation and its relationship with APOBEC3G and vif genetic variation. *J Virol* **80**, 9259-69 (2006).
38. Henzler, T. et al. Fully functional, naturally occurring and C-terminally truncated variant human immunodeficiency virus (HIV) Vif does not bind to HIV Gag but influences intermediate filament structure. *Journal of General Virology* **82**, 561-573 (2001).
39. Fisher, A.G. et al. The sor gene of HIV-1 is required for efficient virus transmission in vitro. *Science* **237**, 888-893 (1987).
40. Gabuzda, D.H. et al. Role of vif in replication of human immunodeficiency virus type 1 in CD4+ T lymphocytes. *Journal of virology* **66**, 6489-6495 (1992).
41. Strebel, K. et al. The HIV A (sor) gene product is essential for virus infectivity. *Nature* **328**, 728-730 (1987).
42. Salamango, D.J. & Harris, R.S. Dual Functionality of HIV-1 Vif in APOBEC3 Counteraction and Cell Cycle Arrest. *Frontiers in Microbiology* **11**(2021).
43. Goila-Gaur, R. & Strebel, K. HIV-1 Vif, APOBEC, and intrinsic immunity. *Retrovirology* **5**, 51 (2008).
44. Chaipan, C., Smith, J.L., Hu, W.-S. & Pathak, V.K. APOBEC3G Restricts HIV-1 to a Greater Extent than APOBEC3F and APOBEC3DE in Human Primary CD4⁺ T Cells and Macrophages. *Journal of Virology* **87**, 444-453 (2013).
45. Kim, Y.K. et al. Structural basis of intersubunit recognition in elongin BC-cullin 5-SOCS box ubiquitin-protein ligase complexes. *Acta Crystallogr D Biol Crystallogr* **69**, 1587-97 (2013).
46. Zhang, W., Du, J., Evans, S.L., Yu, Y. & Yu, X.-F. T-cell differentiation factor CBF-β regulates HIV-1 Vif-mediated evasion of host restriction. *Nature* **481**, 376-379 (2012).
47. Jäger, S. et al. Vif hijacks CBF-β to degrade APOBEC3G and promote HIV-1 infection. *Nature* **481**, 371-375 (2012).
48. Fribourgh, J.L. et al. Core Binding Factor Beta Plays a Critical Role by Facilitating the Assembly of the Vif-Cullin 5 E3 Ubiquitin Ligase. *Journal of Virology* **88**, 3309-3319 (2014).
49. Sheehy, A.M., Gaddis, N.C., Choi, J.D. & Malim, M.H. Isolation of a human gene that inhibits HIV-1 infection and is suppressed by the viral Vif protein. *Nature* **418**, 646-650 (2002).
50. Sheehy, A.M., Gaddis, N.C. & Malim, M.H. The antiretroviral enzyme APOBEC3G is degraded by the proteasome in response to HIV-1 Vif. *Nature medicine* **9**, 1404-1407 (2003).

51. Marin, M., Rose, K.M., Kozak, S.L. & Kabat, D. HIV-1 Vif protein binds the editing enzyme APOBEC3G and induces its degradation. *Nature medicine* **9**, 1398-1403 (2003).
52. Stopak, K., de Noronha, C., Yonemoto, W. & Greene, W.C. HIV-1 Vif blocks the antiviral activity of APOBEC3G by impairing both its translation and intracellular stability. *Mol Cell* **12**, 591-601 (2003).
53. Wiegand, H.L., Doehle, B.P., Bogerd, H.P. & Cullen, B.R. A second human antiretroviral factor, APOBEC3F, is suppressed by the HIV-1 and HIV-2 Vif proteins. *EMBO J* **23**, 2451-8 (2004).
54. Conticello, S.G., Harris, R.S. & Neuberger, M.S. The Vif Protein of HIV Triggers Degradation of the Human Antiretroviral DNA Deaminase APOBEC3G. *Current Biology* **13**, 2009-2013 (2003).
55. Yu, X. et al. Induction of APOBEC3G Ubiquitination and Degradation by an HIV-1 Vif-Cul5-SCF Complex. *Science* **302**, 1056-1060 (2003).
56. Nakashima, M. et al. Structural Insights into HIV-1 Vif-APOBEC3F Interaction. *Journal of Virology* **90**, 1034-1047 (2016).
57. Hu, Y. et al. Structural basis of antagonism of human APOBEC3F by HIV-1 Vif. *Nature Structural & Molecular Biology* **26**, 1176-1183 (2019).
58. Stanley, B.J. et al. Structural Insight into the Human Immunodeficiency Virus Vif SOCS Box and Its Role in Human E3 Ubiquitin Ligase Assembly. *Journal of Virology* **82**, 8656-8663 (2008).
59. Guo, Y. et al. Structural basis for hijacking CBF-β and CUL5 E3 ligase complex by HIV-1 Vif. *Nature* **505**, 229-233 (2014).
60. Chen, G., He, Z., Wang, T., Xu, R. & Yu, X.-F. A Patch of Positively Charged Amino Acids Surrounding the Human Immunodeficiency Virus Type 1 Vif SLVx4Yx9Y Motif Influences Its Interaction with APOBEC3G. *Journal of Virology* **83**, 8674-8682 (2009).
61. He, Z., Zhang, W., Chen, G., Xu, R. & Yu, X.F. Characterization of conserved motifs in HIV-1 Vif required for APOBEC3G and APOBEC3F interaction. *J Mol Biol* **381**, 1000-11 (2008).
62. Goncalves, J., Shi, B., Yang, X. & Gabuzda, D. Biological activity of human immunodeficiency virus type 1 Vif requires membrane targeting by C-terminal basic domains. *J Virol* **69**, 7196-204 (1995).
63. Goncalves, J., Jallepalli, P. & Gabuzda, D.H. Subcellular localization of the Vif protein of human immunodeficiency virus type 1. *J Virol* **68**, 704-12 (1994).
64. Hu, Y., Knecht, K.M., Shen, Q. & Xiong, Y. Multifaceted HIV-1 Vif interactions with human E3 ubiquitin ligase and APOBEC3s. *The FEBS Journal* **288**, 3407-3417 (2021).
65. Azimi, F.C. & Lee, J.E. Structural perspectives on HIV-1 Vif and APOBEC3 restriction factor interactions. *Protein Sci* **29**, 391-406 (2020).
66. Kelley, L.A., Mezulis, S., Yates, C.M., Wass, M.N. & Sternberg, M.J.E. The Phyre2 web portal for protein modeling, prediction and analysis. *Nature Protocols* **10**, 845-858 (2015).
67. Promega. Nano-Glo® HiBiT Lytic Detection System. (Promega, 2020).
68. PyMOL Molecular Graphics System, V.S., LLC.

69. Wang, S., Peng, J. & Xu, J. Alignment of distantly related protein structures: algorithm, bound and implications to homology modeling. *Bioinformatics* **27**, 2537-2545 (2011).
70. Wang, S., Ma, J., Peng, J. & Xu, J. Protein structure alignment beyond spatial proximity. *Scientific Reports* **3**(2013).
71. Xu, J. & Zhang, Y. How significant is a protein structure similarity with TM-score = 0.5? *Bioinformatics* **26**, 889-895 (2010).
72. Adachi, A. et al. Production of acquired immunodeficiency syndrome-associated retrovirus in human and nonhuman cells transfected with an infectious molecular clone. *J Virol* **59**, 284-91 (1986).
73. Ochsenbauer, C. et al. Generation of Transmitted/Founder HIV-1 Infectious Molecular Clones and Characterization of Their Replication Capacity in CD4 T Lymphocytes and Monocyte-Derived Macrophages. **86**, 2715-2728 (2012).
74. Gao, F. et al. Cooperation of B cell lineages in induction of HIV-1-broadly neutralizing antibodies. *Cell* **158**, 481-91 (2014).
75. ATCC. H9 [derivative of HuT 78] (ATCC® HTB-176™).
76. Madani, N. & Kabat, D. Cellular and Viral Specificities of Human Immunodeficiency Virus Type 1 Vif Protein. *Journal of Virology* **74**, 5982-5987 (2000).
77. Wei, X. et al. Emergence of Resistant Human Immunodeficiency Virus Type 1 in Patients Receiving Fusion Inhibitor (T-20) Monotherapy. *Antimicrobial Agents and Chemotherapy* **46**, 1896-1905 (2002).
78. Song, C., Sutton, L., Johnson, M.E., D'Aquila, R.T. & Donahue, J.P. Signals in APOBEC3F N-terminal and C-terminal deaminase domains each contribute to encapsidation in HIV-1 virions and are both required for HIV-1 restriction. *J Biol Chem* **287**, 16965-74 (2012).
79. Donahue, J.P. et al. Genetic analysis of the localization of APOBEC3F to human immunodeficiency virus type 1 virion cores. *J Virol* **89**, 2415-24 (2015).
80. Scholtes, G.K. et al. The von Hippel-Lindau Cullin-RING E3 ubiquitin ligase regulates APOBEC3 cytidine deaminases. *Transl Res* **237**, 1-15 (2021).
81. Doehle, B.P., Schafer, A. & Cullen, B.R. Human APOBEC3B is a potent inhibitor of HIV-1 infectivity and is resistant to HIV-1 Vif. *Virology* **339**, 281-8 (2005).
82. Durocher, Y., Perret, S. & Kamen, A. High-level and high-throughput recombinant protein production by transient transfection of suspension-growing human 293-EBNA1 cells. *Nucleic Acids Res* **30**, E9 (2002).
83. Lois, C., Hong, E.J., Pease, S., Brown, E.J. & Baltimore, D. Germline transmission and tissue-specific expression of transgenes delivered by lentiviral vectors. *Science* **295**, 868-72 (2002).
84. Simon, J.H., Miller, D.L., Fouchier, R.A. & Malim, M.H. Virion incorporation of human immunodeficiency virus type-1 Vif is determined by intracellular expression level and may not be necessary for function. *Virology* **248**, 182-7 (1998).
85. Simon, J.H., Sheehy, A.M., Carpenter, E.A., Fouchier, R.A. & Malim, M.H. Mutational analysis of the human immunodeficiency virus type 1 Vif protein. *J Virol* **73**, 2675-81 (1999).

86. Liu, H. et al. The Vif protein of human and simian immunodeficiency viruses is packaged into virions and associates with viral core structures. *J Virol* **69**, 7630-8 (1995).
87. Karczewski, M.K. & Strebel, K. Cytoskeleton association and virion incorporation of the human immunodeficiency virus type 1 Vif protein. *J Virol* **70**, 494-507 (1996).
88. Fouchier, R.A., Simon, J.H., Jaffe, A.B. & Malim, M.H. Human immunodeficiency virus type 1 Vif does not influence expression or virion incorporation of gag-, pol-, and env-encoded proteins. *J Virol* **70**, 8263-9 (1996).
89. Camaur, D. & Trono, D. Characterization of human immunodeficiency virus type 1 Vif particle incorporation. *J Virol* **70**, 6106-11 (1996).
90. Borman, A.M., Quillent, C., Charneau, P., Dauguet, C. & Clavel, F. Human immunodeficiency virus type 1 Vif- mutant particles from restrictive cells: role of Vif in correct particle assembly and infectivity. *J Virol* **69**, 2058-67 (1995).
91. Fan, L. & Peden, K. Cell-free transmission of Vif mutants of HIV-1. *Virology* **190**, 19-29 (1992).
92. Sakai, H. et al. Cell-dependent requirement of human immunodeficiency virus type 1 Vif protein for maturation of virus particles. *J Virol* **67**, 1663-6 (1993).
93. Schwedler, U.v., Song, J., Aiken, C. & Trono, D. Vif is crucial for human immunodeficiency virus type 1 proviral DNA synthesis in infected cells. *Journal of Virology* **67**, 4945-4955 (1993).
94. Ochsenbauer, C., Wilk, T. & Bosch, V. Analysis of vif-defective human immunodeficiency virus type 1 (HIV-1) virions synthesized in 'non-permissive' T lymphoid cells stably infected with selectable HIV-1. *J Gen Virol* **78 (Pt 3)**, 627-35 (1997).
95. Cavrois, M. et al. Mass Cytometric Analysis of HIV Entry, Replication, and Remodeling in Tissue CD4+ T Cells. *Cell Reports* **20**, 984-998 (2017).
96. Smith, J.L. & Pathak, V.K. Identification of specific determinants of human APOBEC3F, APOBEC3C, and APOBEC3DE and African green monkey APOBEC3F that interact with HIV-1 Vif. *J Virol* **84**, 12599-608 (2010).
97. Liddament, M.T., Brown, W.L., Schumacher, A.J. & Harris, R.S. APOBEC3F properties and hypermutation preferences indicate activity against HIV-1 in vivo. *Curr Biol* **14**, 1385-91 (2004).
98. Wang, J. et al. The Vif accessory protein alters the cell cycle of human immunodeficiency virus type 1 infected cells. *Virology* **359**, 243-52 (2007).
99. Sakai, K., Dimas, J. & Lenardo, M.J. The Vif and Vpr accessory proteins independently cause HIV-1-induced T cell cytopathicity and cell cycle arrest. *Proc Natl Acad Sci U S A* **103**, 3369-74 (2006).
100. Li, Y.-L. et al. The structural basis for HIV-1 Vif antagonism of human APOBEC3G. *Nature* **615**, 728-733 (2023).
101. Ball, K.A. et al. Conformational Dynamics of the HIV-Vif Protein Complex. *Biophysical Journal* **116**, 1432-1445 (2019).
102. Ikeda, T. et al. HIV-1 adaptation studies reveal a novel Env-mediated homeostasis mechanism for evading lethal hypermutation by APOBEC3G. *PLoS Pathog* **14**, e1007010 (2018).

103. Zhang, C. et al. Development of an HiBiT-tagged reporter H3N2 influenza A virus and its utility as an antiviral screening platform. *Journal of Medical Virology* **95**, e28345 (2023).
104. Tamura, T. et al. Characterization of Recombinant Flaviviridae Viruses Possessing a Small Reporter Tag. *Journal of Virology* **92**, 10.1128/jvi.01582-17 (2018).
105. Connor, R.I., Chen, B.K., Choe, S. & Landau, N.R. Vpr Is Required for Efficient Replication of Human Immunodeficiency Virus Type-1 in Mononuclear Phagocytes. *Virology* **206**, 935-944 (1995).
106. Neidleman, J.A. et al. Mucosal stromal fibroblasts markedly enhance HIV infection of CD4+ T cells. *PLoS Pathog* **13**, e1006163 (2017).
107. Fernandez, N. et al. Assessment of a diverse panel of transmitted/founder HIV-1 infectious molecular clones in a luciferase based CD8 T-cell mediated viral inhibition assay. *Front Immunol* **13**, 1029029 (2022).
108. Hayes, P. et al. Breadth of CD8 T-cell mediated inhibition of replication of diverse HIV-1 transmitted-founder isolates correlates with the breadth of recognition within a comprehensive HIV-1 Gag, Nef, Env and Pol potential T-cell epitope (PTE) peptide set. *PLoS One* **16**, e0260118 (2021).

2. HIV-1 AND WOMEN

In Chapter 1, we described the design and optimization of the Vif.HB IMC, which offers new opportunities for application in studies of HIV-1 transmission. HIV-1 is most commonly transmitted through heterosexual intercourse[1], but the mechanisms underlying how clinical HIV-1 infection gets established in the mucosal genital tissues of women are unclear. In the coming chapters, we will describe the results from published studies that interrogated mucosal HIV-1 transmission and replication mechanisms in female reproductive tract (FRT) tissues. In this chapter, Chapter 2, we will focus on HIV-1 transmission risk factors for women and their critical public health implications, which will underpin investigations in later sections of this dissertation that focus on addressing knowledge gaps in mucosal HIV-1 transmission mechanisms. Below, we expound the epidemiology of HIV in women, the unique HIV transmission risk factors women face, and obstacles to preventing or treating HIV infection in women.

Introduction

In the summer of 1981, the first reported cases of a disease that would later be known as AIDS began to emerge across the United States. The disease quickly gained a negative stigma, as the first people who were diagnosed with the disease were homosexual men[2-5]. The media and members of the public viewed these homosexual men with AIDS as "sexual deviants" and dubbed the disease they had been afflicted with as "gay cancer"[3,5]. This type of language not only intensified the negative stigma associated with AIDS, but also skewed public perception regarding the susceptibility of women to HIV/AIDS[5,6]. A famous example of this is the January 1988 *Cosmopolitan* article written by psychiatrist Dr. Robert E. Gould, where he conjectured that American women would not contract HIV from having unprotected intercourse with HIV-positive men as long as their vaginas were healthy or they had sex in the missionary position[7]. Misinformed perceptions such as these contributed to the exclusion of women from early HIV/AIDS treatment and prevention research in the United States.

Although the first case of a woman being diagnosed with (what would later be known as) AIDS also occurred in 1981[8], women were rarely included in early HIV drug trials or provided with HIV/AIDS-specific medical treatment for over a decade[9]. It took until 1993, with the passing of the NIH Revitalization Act, followed by a policy change in 1994, when the U.S. Department of Health and Human Services began to require those applying for NIH grant monies to incorporate "the appropriate inclusion of women and minorities in clinical research"[9], for women to be properly considered and included in HIV-related research. Today, although there has been a substantial increase in the participation of women in HIV-related research compared to the early days of the epidemic, women are still under-represented in clinical trials in the United States[10,11]. A review by Curno *et al.*

reported that only 19.2% of the participants in clinical studies of HIV antiretroviral drugs (n=387) and 11.1% of the participants in curative strategy studies (n=104) in the United States were women[11]. The inclusion of women in HIV research is highly relevant for the effective management and treatment of HIV/AIDS globally. Understanding the unique vulnerabilities to HIV/AIDS women face, including acquisition risk factors and barriers to treatment, is essential for developing effective prevention and treatment strategies. These vulnerabilities, and the current epidemiology of HIV/AIDS in women, are discussed in more detail in this chapter.

Epidemiology Overview of HIV in Women

Of the approximately 39 million people currently infected with HIV-1 globally, an estimated 52% are female (sex assigned at birth)[12,13]. The region containing the highest numbers of HIV-infected women and girls is sub-Saharan Africa (SSA), where between 14.5% to 39.5% of the female population are estimated to be currently infected[12,14-18]. Within SSA, women are disproportionately affected by HIV[12-18]. In 2021, women and girls accounted for 63% of new HIV diagnoses in the region, with those aged between 15 to 24 years receiving three times the number of diagnoses as their male counterparts[15,18]. Though the total number of new HIV diagnoses declined in SSA between 2010 and 2021, the decline was far greater among men (52%) than women (38%)[18]. Gender-based violence, limited access to reproductive health services, unequal prevention education, and oppressive consent laws perpetuate the HIV epidemic among women in this region[13-16,18].

Outside of SSA, Asia and the Pacific face the largest HIV/AIDS epidemic, with an estimated 6 million people living with HIV as of 2021[18]. Although only 32% of new HIV cases were diagnosed in women, most new cases were diagnosed in women between the

ages of 25-49. A similar statistic was found in Latin America, where a majority of women newly diagnosed with HIV were between the ages of 25-49[18]. Women in Latin American countries face high levels of wealth inequality compared to men in the same region and ~27% have experienced domestic violence[19,20], which have undermined HIV/AIDS prevention and treatment efforts in those countries[18]. In the Caribbean, nearly half (43%) of new HIV cases were diagnosed in women in 2021, and these women face similar wealth disparities compared to men as their Latin American counterparts[18]. The Middle East and North African region boasts the lowest HIV burden globally, but their low numbers may be due to limitations in data collection and HIV surveillance efforts[18,21]. The number of new HIV cases has risen in this region over the past decade and has been linked to the migration of refugees and the discontinuation of HIV prevention/treatment efforts in conflict-ridden countries[21]. Women accounted for 36% of new HIV diagnoses in this region in 2021[18]. The number of new HIV cases has also risen in Eastern Europe since 2010. Contributing factors to this rise include unsafe injection drug practices and poor distribution of HIV prevention/treatment resources[18,22]. Women comprised 31% of new HIV diagnoses in this region in 2021[18].

In the United States, women accounted for 18% of new HIV diagnoses in 2020, with Black women comprising the majority of those diagnoses (54%)[23,24]. Women between the ages of 25 to 34 had the greatest number of new diagnoses (27%) compared to all other age groups[23]. Among all the regions within the United States, the South experiences the highest number of new HIV cases annually (51%), and women in this region are disproportionately affected by HIV[23,24]. Heterosexual Southern women are infected with HIV at twice the rate as their heterosexual male counterparts, and Black Southern women

experience the greatest HIV burden, accounting for 67% of new HIV diagnoses among Southern women[24]. Socioeconomic circumstances in the South (such as limited access to health care services, the inability to afford expensive health insurance or medications, and higher levels of HIV-related stigma) create barriers that prevent Southern women from seeking and/or receiving HIV prevention treatments and care[12,24].

HIV Transmission and Acquisition Risk Factors in Women

There are biological, behavioral, and social factors that increase risk of HIV transmission to women. The majority of women become newly infected with HIV as a consequence of heterosexual transmission[12-14,16,18,24]. When engaging in sexual intercourse with an HIV-infected partner, women can be exposed to high volumes of cell-free viral particles and productively infected CD4+ T cells and Mϕs in semen[25,26]. Women have a greater risk of acquiring HIV-1 transmission during coitus if their partner is experiencing acute HIV infection[27,28]. During acute HIV-1 infection, there are an estimated 4.0×10^6 virions per ml of semen and around 5.0×10^3 virions per ml of semen during chronic infection[28]. Semen itself can also enhance risk of HIV acquisition. Interleukin-7 (IL-7), an abundant cytokine found in the semen of healthy males, was shown to significantly enhance viral replication in an *ex vivo* cervicovaginal system[29]. Semen also neutralizes cervicovaginal mucus by shifting its pH from ~4 to a pH between 6 and 7, thus reducing the "trapping" efficiency of the mucus and promoting rapid viral diffusion through the mucus[30].

Following sexual intercourse, HIV is hypothesized to infiltrate the submucosa of the FRT through either mucosal Langerhans cells[31], epithelial transmigration mechanisms (paracellular passage or transcytosis), through micro-lacerations[32,33], or a combination of

mechanisms. However, the exact mechanisms contributing to the acquisition of clinical HIV infection in the FRT are currently not understood. FRT mucosal tissues are highly susceptible to breaks and microtraumas, with a reported 61% of women experiencing vaginal epithelial tears following coitus[34]. Lacerations and tears in mucosal tissue from intercourse are a key biological risk factor of HIV transmission. Epithelial breaks provide HIV-1 with direct access to high concentrations of permissive cells (i.e. CD4+ T cells) that are present throughout the FRT shortly after virus exposure[35,36]. This process has been directly demonstrated in non-human primate (NHP) models, where the number of histologically identified tears in the FRT epithelium has been correlated with the detection of SIV DNA in genital tissues following vaginal inoculation with SIV[36]. Douching— the practice of intravaginal washing particularly after intercourse— also results in tearing through the desiccation or disruption of mucosal membranes and upregulation of inflammatory cytokines in the FRT, furthering HIV transmission risk[37-41]. HIV transmission risk following FRT tearing during intercourse can be reduced or prevented through condom usage and the application of lubricants[13,14,16,18,42].

Hormones are another key biological factor affecting HIV transmission risk to women. Women of reproductive age experience menstruation, which is a cyclical hormonal process in the FRT that fluctuates between the follicular phase (when estrogen levels peak) and the luteal phase (when progesterone levels peak)[43,44]. During the luteal phase, women may be more susceptible to HIV-1 infection due to heightened progesterone levels that increase uterine epithelial cell expression of HIV-1 target receptors[45], decrease epithelium thickness[43], and increase the number of HIV-permissive cells that migrate to the FRT[46]. In contrast, the presence of estrogen during the follicular phase may reduce HIV acquisition

risk through the stimulation of antimicrobial production (i.e. defensins and secretory leukocyte protease inhibitor) in the FRT[47] and the reduction of HIV-target cell migration to the FRT by inhibition of pro-inflammatory cytokine expression[46]. Estrogen has also been demonstrated to reduce viral entry into CD4+ T cells and macrophages *in vitro*[48].

As women progress beyond reproductive age, they undergo menopause, which occurs when the cyclic hormone fluctuations experienced during menstruation subside[47,49]. Menopausal women may be more susceptible to HIV transmission because of the decline in both their estrogen levels and in their innate immune response, including: the thinning of the vaginal epithelium, the reduction of vaginal microenvironment acidity, and the increase in pro-inflammatory cytokine (i.e. TNFα) levels[47,49,50]. Hormonal birth controls, such as depot medroxyprogesterone acetate (DMPA), have also been demonstrated to increase risk of HIV infection in women by 40-50%[51-53]. DMPA is a progesterone-based contraceptive widely used among women in SSA[51-54], and it may enhance HIV susceptibility through the expansion of HIV-target cells in the FRT and the impairment of the FRT epithelial barrier, as demonstrated *in vivo*[54].

Pregnancy may also affect a woman's risk of acquiring HIV-1. During pregnancy, progesterone levels increase significantly from the first trimester to the third[55]. A study by Sheffield *et. al* demonstrated that in lower genital tract biopsies from pregnant women, the rising progesterone levels with each trimester corresponded with an increase in the percentage of T cells and CD14+ cells expressing the CCR5 co-receptor. They suggested that the higher progesterone levels experienced by pregnant women may enhance their susceptibility to HIV acquisition due to the increased number of CCR5+ target cells[56]. Indeed, after monitoring 686 pregnancies from HIV-serodiscordant couples, Thomson *et.*

al reported that the probability of acquiring HIV while pregnant increased throughout each trimester of the pregnancy, but that women were most vulnerable to acquiring HIV postpartum[57]. Coupled with rising progesterone levels, the changes the cervicovaginal microbiome undergoes during and after pregnancy may also enhance HIV acquisition risk.

The cervicovaginal microbiome is colonized with a variety of *Lactobacilli* species, which have been demonstrated to be protective against HIV transmission by competitively excluding other bacterial species that promote mucosal inflammation[58]. Lai *et. al* found that human cervicovaginal mucus that had been acidified by *Lactobacilli* efficiently reduced the diffusion of HIV by over 1000-fold more than neutral mucosal environments, such as those exposed to semen[30]. During the third trimester and postpartum stages, however, *Lactobacilli* population numbers and diversities decline[59,60]. Women with low *Lactobacilli* are more likely to be diagnosed with STIs and HIV postpartum compared to those with greater *Lactobacilli* colonization[59], and the probability of *Lactobacilli* species recovering in postpartum women is only ~49% within the first year following childbirth[60]. Thus, semen, physical injury to mucosal tissues, hormones, and changes to the cervicovaginal microbiome are all biological factors that may affect HIV-1 transmission and acquisition risk in women.

In addition to biological factors, social and behavioral factors also impact HIV acquisition risk. Foremost, the World Health Organization (WHO) estimates that 1 in 3 women will become victims of physical or sexual violence during their lifetimes[61,62]. These victims are 50% more likely to acquire HIV than non-victims[63]. Non-consensual sexual intercourse in particular increases HIV transmission risk[64]. Lincoln *et. al* demonstrated that non-consensual intercourse was around 20 times as likely to cause vaginal injury (including

lacerations, abrasions, and bruises) than consensual intercourse, and that condoms (or other barrier protection methods) were not used by perpetrators in more than 90% of non-consensual acts[42]. The higher levels of injury and lack of protection usage experienced during non-consensual intercourse increase opportunity for HIV transmission. Female sex workers have the highest risk of becoming victims of non-consensual acts, as between 45-75% experience sexual and physical violence through their profession[65]. Fear of violence among sex workers also prevents them from negotiating condom use and other safe-sex practices or even seeking healthcare services[18,63,65,66]. Consequently, female sex workers are 30 times more likely to acquire HIV than other women[18].

Limitations to HIV-1 Treatment in Women

In early 2022, the International Maternal Pediatric Adolescent AIDS Clinical Trial Network (IMPAACT) P1107 reported on the first known case of a woman being cured of HIV following a novel transplant strategy involving dual stem cell therapy. Though an important and promising accomplishment for the HIV field and for women's health globally, it was noted that extending this approach to the millions of other women currently infected with HIV was not feasible due to the risk, complexity, and invasiveness associated with the transplant strategy[67]. It is recommended that women infected with HIV take ART as prescribed to maintain undetectable viral loads and to prevent the transmission of the virus to HIV-negative partners[68]. Effective ART concentrations differ between men and women[69-73], and ART half-life can be affected by hormone fluctuations, such as those experienced during menstruation[74]. Although ART is highly effective at controlling viral infections in women, it has limitations including negative drug-drug interactions and reliance on regular adherence to prevent ART-resistant viral mutants[75,76]. ART treatment

also becomes costly over an individual's lifetime[77], creating an economic burden for both the infected person and their caregiver(s). Cost can also be an obstacle that prevents some individuals from continuing long-term treatment[78-80].

The CDC describes multiple challenges preventing women from receiving sufficient HIV prevention and treatment therapies in the United States. These challenges can be summarized into 3 categories: knowledge barriers, social barriers, and health barriers. Knowledge barriers can include a lack of awareness of HIV status, understanding of transmission risk factors, or knowledge of HIV prevention medications, such as PrEP[81]. PrEP contains tenofovir and emtricitabine, RT inhibitors, and can be taken as a daily oral pill or administered through injections about every two months. There are also no known interactions between PrEP and hormonal birth control[82]. To reduce or prevent the risk of HIV acquisition, PrEP is available for women. Though effective in women, PrEP can cause negative side effects, including headaches and nausea, which may discourage use[83]. In the United States, where PrEP is widely available and covered by most insurance plans, only 10% of at-risk women seek PrEP due to limited awareness, distrust of health care providers, or concern of negative partner response[23,82]. However, for women and girls in SSA, availability of PrEP is low, the cost is high, and there is stigma associated with its use[13-16,18]. Some SSA countries, such as Botswana, require women to have spousal consent to receive PrEP (underaged girls must have parental consent), hindering them from accessing necessary HIV prevention treatment[18]. A lack of HIV-related knowledge is a problem for women globally, particularly those from low-income or low-education backgrounds, as it prevents them from advocating for safe-sex practices and seeking adequate prevention or treatment interventions[84-86].

The social barrier can include negative partner response, HIV-related stigma, or poor experiences with healthcare providers[81], impacting women in both the United States and worldwide. According to the WHO, nearly 30% of women globally have experienced intimate partner violence. An estimated 27% of women and girls aged 15-49 have been victims of intimate partner violence[62]. Thus, some women may be hesitant to disclose their HIV status to their partners out of fear of violent repercussions[61,65,87]. Additionally, women have reported experiencing stigma from healthcare providers following their HIV diagnoses, including maltreatment and neglection of privacy, which discouraged them from seeking out or adhering to HIV treatments[88-90].

The health barrier includes a broad range of challenges from mental health concerns to pre-existing infection with non-HIV STIs[81]. Waldron *et al.* reported that HIV-infected women experience higher rates of depression, anxiety, and trauma than women without HIV or even men infected with HIV. These mental health complications interfere with the ability of HIV-infected women to manage their conditions, including reduced adherence to ART treatments and continued participation in high-risk transmission behaviors[87]. Interventions that address and lessen the converging mental health and HIV infection stigmas these women face are crucial for improving their long-term quality of life and well-being[91]. In addition to psychological concerns, women who are already infected with an STI (i.e. herpes, gonorrhea, chlamydia, syphilis, etc.) are at high risk of HIV acquisition[92-97]. These STIs create a pro-inflammatory environment, which expands the migration and activation of HIV target cells to the cervicovaginal mucosa, and they can even outcompete the *Lactobacilli* species in human cervicovaginal tissues, resulting in favorable conditions for HIV acquisition and spread[96,97]. Interventions that mitigate inflammation and preserve

a healthy cervicovaginal microbiome are key to lowering HIV acquisition risk in women already infected with an STI[97].

Conclusion

Overall, women worldwide are impacted by HIV/AIDS and face unique vulnerabilities to HIV transmission. These vulnerabilities include biologically-based susceptibilities, treatment barriers, and sexual/physical violence. Greater efforts need to be made globally by government, medical, and scientific leadership to involve women in HIV clinical/curative studies. In addition, research efforts that focus on the elucidation of the biological mechanisms contributing to HIV transmission to the FRT need to be expanded.

REFERENCES

1. Shaw, G.M. & Hunter, E. HIV transmission. *Cold Spring Harb Perspect Med* **2**(2012).
2. *The Social Impact Of AIDS In The United States*, (National Academies Press (US), Washington, DC, 1993).
3. Wright, J. ALL THINGS CONSIDERED. in *Remembering the Early Days of 'Gay Cancer'* (ed. Block, M.) (NPR, 2006).
4. Altman, L.K. RARE CANCER SEEN IN 41 HOMOSEXUALS. in *The New York Times* (1981).
5. Sontag, S. AIDS and Its Metaphors. in *Illness as Metaphor and AIDS and Its Metaphors* (Anchor Books, Doubleday, New York, 1989).
6. Logie, C.H. & Gibson, M.F. A mark that is no mark? Queer women and violence in HIV discourse. *Culture, Health & Sexuality* **15**, 29-43 (2013).
7. Gould, R.E. Why Most Women are Safe From AIDS. in *Cosmopolitan* (1988).
8. Dean, H.D., Lee, L.M., Thompson, M. & Dannemiller, T. Impact of HIV on women in the United States. *Emerg Infect Dis* **10**, 2030-1 (2004).
9. A Timeline of HIV and AIDS. Vol. 2023 (ed. HIV.gov) (U.S. Department of Health & Human Services, 2023).
10. Namiba, A. et al. From presumptive exclusion towards fair inclusion: perspectives on the involvement of women living with HIV in clinical trials, including stakeholders' views. *Therapeutic Advances in Infectious Disease* **9**, 20499361221075454 (2022).
11. Curno, M.J. et al. A Systematic Review of the Inclusion (or Exclusion) of Women in HIV Research: From Clinical Studies of Antiretrovirals and Vaccines to Cure Strategies. *J Acquir Immune Defic Syndr* **71**, 181-8 (2016).
12. HIV Basics. Vol. 2020 (Centers for Disease Control and Prevention, 2020).
13. UNAIDS. UNAIDS 2017. (2017).
14. UNAIDS. Global AIDS Response Progress Reporting 2015. (World Health Organization and UNAIDS 2015, UNAIDS.org, 2015).
15. Avert. WOMEN AND GIRLS, HIV AND AIDS. in *Global information and education on HIV and AIDS* (Avert, 2020).
16. UNAIDS. UNAIDS 2020. 2 edn (2020).
17. Ramjee, G. & Daniels, B. Women and HIV in Sub-Saharan Africa. *AIDS Res Ther* **10**, 30 (2013).
18. UNAIDS. In Danger: UNAIDS Global AIDS Update 2022. (Geneva: Joint United Nations Programme on HIV/AIDS, 2022).
19. Top 10% ingreso nacional share. in *World Inequality Database* (ed. Database, W.I.) (World Inequality Database, 2023).
20. OECD. *SIGI 2020 Regional Report for Latin America and the Caribbean*, (2020).
21. Karbasi, A. et al. An Evolving HIV Epidemic in the Middle East and North Africa (MENA) Region: A Scoping Review. *Int J Environ Res Public Health* **20**(2023).
22. LaMonaca, K. et al. HIV, Drug Injection, and Harm Reduction Trends in Eastern Europe and Central Asia: Implications for International and Domestic Policy. *Current Psychiatry Reports* **21**, 47 (2019).
23. Diagnoses of HIV Infection in the United States and Dependent Areas 2020. in *HIV Surveillance Report* Vol. 33 (Centers for Disease Control and Prevention, 2020).

24. HIV in the Southern United States. (Centers for Disease Control, 2019).
25. Saba, I. et al. Immunocompetent Human 3D Organ-Specific Hormone-Responding Vaginal Mucosa Model of HIV-1 Infection. *Tissue Eng Part C Methods* **27**, 152-166 (2021).
26. Bernard-Stoecklin, S. et al. Semen CD4+ T Cells and Macrophages Are Productively Infected at All Stages of SIV infection in Macaques. *PLoS Pathogens* **9**, e1003810 (2013).
27. Wawer, M.J. et al. Rates of HIV-1 transmission per coital act, by stage of HIV-1 infection, in Rakai, Uganda. *J Infect Dis* **191**, 1403-9 (2005).
28. Carias, A.M. et al. Defining the Interaction of HIV-1 with the Mucosal Barriers of the Female Reproductive Tract. *Journal of Virology* **87**, 11388-11400 (2013).
29. Introini, A., Vanpouille, C., Lisco, A., Grivel, J.-C. & Margolis, L. Interleukin-7 Facilitates HIV-1 Transmission to Cervico-Vaginal Tissue ex vivo. *PLOS Pathogens* **9**, e1003148 (2013).
30. Lai, S.K. et al. Human immunodeficiency virus type 1 is trapped by acidic but not by neutralized human cervicovaginal mucus. *J Virol* **83**, 11196-200 (2009).
31. Nijmeijer, B.M. et al. HIV-1 subverts the complement system in semen to enhance viral transmission. *Mucosal Immunology* **14**, 743-750 (2021).
32. Gonzalez, S.M., Aguilar-Jimenez, W., Su, R.-C. & Rugeles, M.T. Mucosa: Key Interactions Determining Sexual Transmission of the HIV Infection. *Frontiers in Immunology* **10**(2019).
33. Shacklett, B.L. Mucosal Immunity in HIV/SIV Infection: T Cells, B Cells and Beyond. *Curr Immunol Rev* **15**, 63-75 (2019).
34. Norvell, M.K., Benrubi, G.I. & Thompson, R.J. Investigation of microtrauma after sexual intercourse. *J Reprod Med* **29**, 269-71 (1984).
35. Pudney, J., Quayle, A.J. & Anderson, D.J. Immunological Microenvironments in the Human Vagina and Cervix: Mediators of Cellular Immunity Are Concentrated in the Cervical Transformation Zone. *Biology of Reproduction* **73**, 1253-1263 (2005).
36. Miller, C.J. & Shattock, R.J. Target cells in vaginal HIV transmission. *Microbes Infect* **5**, 59-67 (2003).
37. Rodriguez, V.J. et al. Assessing Intravaginal Practices in HIV Prevention Research: Development and Validation of an Intravaginal Practices Questionnaire. *Archives of Sexual Behavior* (2022).
38. Cottrell, B.H. An Updated Review of of Evidence to Discourage Douching. *MCN: The American Journal of Maternal/Child Nursing* **35**, 102-107 (2010).
39. Maria L. Alcaide, V.J.R., Megan R. Brown, Suresh Pallikkuth, Kristopher Arheart, Octavio Martinez, Margaret Roach, Raina N. Fichorova, Deborah L. Jones, Savita Pahwa, and Margaret A. Fischl. High Levels of Inflammatory Cytokines in the Reproductive Tract of Women with BV and Engaging in Intravaginal Douching: A Cross-Sectional Study of Participants in the Women Interagency HIV Study. *AIDS Research and Human Retroviruses* **33**, 309-317 (2017).
40. Low, N. et al. Intravaginal Practices, Bacterial Vaginosis, and HIV Infection in Women: Individual Participant Data Meta-analysis. *PLOS Medicine* **8**, e1000416 (2011).

41. Atashili, J., Poole, C., Ndumbe, P.M., Adimora, A.A. & Smith, J.S. Bacterial vaginosis and HIV acquisition: a meta-analysis of published studies. *AIDS* **22**, 1493-1501 (2008).
42. Lincoln, C., Perera, R., Jacobs, I. & Ward, A. Macroscopically detected female genital injury after consensual and non-consensual vaginal penetration: A prospective comparison study. *Journal of Forensic and Legal Medicine* **20**, 884-901 (2013).
43. Poonia, B. et al. Cyclic changes in the vaginal epithelium of normal rhesus macaques. *J Endocrinol* **190**, 829-35 (2006).
44. Thiruchelvam, U., Dransfield, I., Saunders, P.T. & Critchley, H.O. The importance of the macrophage within the human endometrium. *J Leukoc Biol* **93**, 217-25 (2013).
45. Wira, C.R. & Fahey, J.V. A new strategy to understand how HIV infects women: identification of a window of vulnerability during the menstrual cycle. *Aids* **22**, 1909-17 (2008).
46. Wira, C.R., Rodriguez-Garcia, M. & Patel, M.V. The role of sex hormones in immune protection of the female reproductive tract. *Nat Rev Immunol* **15**, 217-30 (2015).
47. Wira, C.R., Patel, M.V., Ghosh, M., Mukura, L. & Fahey, J.V. Innate immunity in the human female reproductive tract: endocrine regulation of endogenous antimicrobial protection against HIV and other sexually transmitted infections. *Am J Reprod Immunol* **65**, 196-211 (2011).
48. Rodriguez-Garcia, M. et al. Estradiol reduces susceptibility of CD4+ T cells and macrophages to HIV-infection. *PLoS One* **8**, e62069 (2013).
49. Aging, N.I.o. What Is Menopause? in *NIH* (U.S. Department of Helath & Human Services, 2017).
50. Anderson, B.L. & Cu-Uvin, S. Clinical parameters essential to methodology and interpretation of mucosal responses. *Am J Reprod Immunol* **65**, 352-60 (2011).
51. Brind, J., Condly, S.J., Mosher, S.W., Morse, A.R. & Kimball, J. Risk of HIV Infection in Depot-Medroxyprogesterone Acetate (DMPA) Users: A Systematic Review and Meta-analysis. *Issues Law Med* **30**, 129-39 (2015).
52. Polis, C.B. et al. An updated systematic review of epidemiological evidence on hormonal contraceptive methods and HIV acquisition in women. *AIDS* **30**, 2665-2683 (2016).
53. Morrison, C.S. et al. Hormonal Contraception and the Risk of HIV Acquisition: An Individual Participant Data Meta-analysis. *PLOS Medicine* **12**, e1001778 (2015).
54. Wessels, J.M. et al. Depot medroxyprogesterone acetate (DMPA) enhances susceptibility and increases the window of vulnerability to HIV-1 in humanized mice. *Scientific Reports* **11**, 3894 (2021).
55. Kutteh, W.H. & Franklin, R.D. Quantification of immunoglobulins and cytokines in human cervical mucus during each trimester of pregnancy. *American Journal of Obstetrics and Gynecology* **184**, 865-874 (2001).
56. Sheffield, J.S., Wendel, G.D., Jr., McIntire, D.D. & Norgard, M.V. The effect of progesterone levels and pregnancy on HIV-1 coreceptor expression. *Reprod Sci* **16**, 20-31 (2009).

57. Thomson, K.A. et al. Increased Risk of HIV Acquisition Among Women Throughout Pregnancy and During the Postpartum Period: A Prospective Per-Coital-Act Analysis Among Women With HIV-Infected Partners. *J Infect Dis* **218**, 16-25 (2018).
58. Armstrong, E. & Kaul, R. Beyond bacterial vaginosis: vaginal lactobacilli and HIV risk. *Microbiome* **9**, 239 (2021).
59. Li, K.T. et al. Changes in the Vaginal Microbiome During Pregnancy and the Postpartum Period in South African Women: a Longitudinal Study. *Reprod Sci* (2023).
60. Costello, E.K. et al. Abrupt perturbation and delayed recovery of the vaginal ecosystem following childbirth. *Nat Commun* **14**, 4141 (2023).
61. Devastatingly pervasive: 1 in 3 women globally experience violence. (2021).
62. Organization, W.H. Violence against women. Vol. 2024 (World Health Organization, Online, 2021).
63. Jewkes, R.K., Dunkle, K., Nduna, M. & Shai, N. Intimate partner violence, relationship power inequity, and incidence of HIV infection in young women in South Africa: a cohort study. *Lancet* **376**, 41-8 (2010).
64. Kabapy, A.F., Shatat, H.Z. & Abd El-Wahab, E.W. Attributes of HIV infection over decades (1982–2018): A systematic review and meta-analysis. *Transboundary and Emerging Diseases* **67**, 2372-2388 (2020).
65. Violence against women prevalence estimates, 2018: global, regional and national prevalence estimates for intimate partner violence against women, and global and regional prevalence estimates for non-partner sexual violence against women. (Geneva, 2021).
66. Baral, S. et al. Burden of HIV among female sex workers in low-income and middle-income countries: a systematic review and meta-analysis. *Lancet Infect Dis* **12**, 538-49 (2012).
67. First case of HIV cure in a woman after stem cell transplantation reported at CROI-2022. (World Health Organization, 2022).
68. HIV and Women's Health Issues. (HIV.gov, 2022).
69. Hawkins, C. et al. Sex differences in antiretroviral treatment outcomes among HIV-infected adults in an urban Tanzanian setting. *AIDS* **25**, 1189-1197 (2011).
70. Differences between HIV-Infected men and women in antiretroviral therapy outcomes - six African countries, 2004-2012. *MMWR Morb Mortal Wkly Rep* **62**, 945-52 (2013).
71. Mosha, F. et al. Gender differences in HIV disease progression and treatment outcomes among HIV patients one year after starting antiretroviral treatment (ART) in Dar es Salaam, Tanzania. *BMC Public Health* **13**, 38 (2013).
72. Kipp, W. et al. Gender differences in antiretroviral treatment outcomes of HIV patients in rural Uganda. *AIDS Care* **22**, 271-278 (2010).
73. Cohn, J., Ake, J., Moorhouse, M. & Godfrey, C. Sex Differences in the Treatment of HIV. *Current HIV/AIDS Reports* **17**, 373-384 (2020).
74. Melanie R. Nicol, M.L.C., Amanda H. Corbett, Lameck Chinula, Gerald Tegha, Frank Z. Stanczyk, Stacey Hurst, Athena P. Kourtis, and Jennifer H. Tang. Endogenous Hormones and Antiretroviral Exposure in Plasma, Cervicovaginal

Fluid, and Upper-Layer Packed Cells of Malawian Women Living with HIV. *AIDS Research and Human Retroviruses* **36**, 641-646 (2020).
75. Potential Drug Interactions: Hormonal Contraceptives and Antiretroviral Drugs. (Centers for Disease Control and Prevention, Division of Reproductive Health, National Center for Chronic Disease Prevention and Health Promotion, 2010).
76. Solomon, D.A. & Sax, P.E. Current state and limitations of daily oral therapy for treatment. *Curr Opin HIV AIDS* **10**, 219-25 (2015).
77. Tran, H. et al. Global estimates for the lifetime cost of managing HIV. *Aids* **35**, 1273-1281 (2021).
78. Katana, P.V. et al. Economic burden and mental health of primary caregivers of perinatally HIV infected adolescents from Kilifi, Kenya. *BMC Public Health* **20**, 504 (2020).
79. Zamani-Hank, Y. The Affordable Care Act and the Burden of High Cost Sharing and Utilization Management Restrictions on Access to HIV Medications for People Living with HIV/AIDS. *Popul Health Manag* **19**, 272-8 (2016).
80. Cost Considerations and Antiretroviral Therapy. in *Limitations to Treatment Safety and Efficacy* (HIV.gov, 2022).
81. HIV and Women: Prevention Challenges. (ed. Division of HIV Prevention, N.C.f.H., Viral Hepatitis, STD, and TB Prevention, Centers for Disease Control and Prevention) (Centers for Disease Control and Prevention, 2022).
82. PrEP is for Women. (Centers for Disease Control and Prevention, 2022).
83. Koppe, U. et al. Barriers to using HIV pre-exposure prophylaxis (PrEP) and sexual behaviour after stopping PrEP: a cross-sectional study in Germany. *BMC Public Health* **21**, 159 (2021).
84. Kasymova, S. Awareness and knowledge about HIV/AIDS among women of reproductive age in Tajikistan. *AIDS Care* **32**, 518-521 (2020).
85. Abate, B.B., Kassie, A.M., Reta, M.A., Ice, G.H. & Haile, Z.T. Residence and young women's comprehensive HIV knowledge in Ethiopia. *BMC Public Health* **20**, 1603 (2020).
86. Yaya, S., Bishwajit, G., Danhoundo, G., Shah, V. & Ekholuenetale, M. Trends and determinants of HIV/AIDS knowledge among women in Bangladesh. *BMC Public Health* **16**, 812 (2016).
87. Waldron, E.M. et al. Mental Health in Women Living With HIV: The Unique and Unmet Needs. *J Int Assoc Provid AIDS Care* **20**, 2325958220985665 (2021).
88. Valencia-Garcia, D., Rao, D., Strick, L. & Simoni, J.M. Women's experiences with HIV-related stigma from health care providers in Lima, Peru: "I would rather die than go back for care". *Health Care Women Int* **38**, 144-158 (2017).
89. Whitney S. Rice, B.T., Faith E. Fletcher, Tessa M. Nápoles, Melonie Walcott, Abigail Batchelder, Mirjam-Colette Kempf, Deborah J. Konkle-Parker, Tracey E. Wilson, Phyllis C. Tien, Gina M. Wingood, Torsten B. Neilands, Mallory O. Johnson, Sheri D. Weiser, and Janet M. Turan. A Mixed Methods Study of Anticipated and Experienced Stigma in Health Care Settings Among Women Living with HIV in the United States. *AIDS Patient Care and STDs* **33**, 184-195 (2019).

90. Small, L.A., Godoy, S.M. & Lau, C. Perceptions of healthcare accessibility and medical mistrust among Black women living with HIV in the USA. *Culture, Health & Sexuality* **25**, 1295-1309 (2023).
91. Orza, L. et al. How does living with HIV impact on women's mental health? Voices from a global survey. *J Int AIDS Soc* **18**, 20289 (2015).
92. Hook, E.W., 3rd et al. Herpes simplex virus infection as a risk factor for human immunodeficiency virus infection in heterosexuals. *J Infect Dis* **165**, 251-5 (1992).
93. Freeman, E.E. et al. Herpes simplex virus 2 infection increases HIV acquisition in men and women: systematic review and meta-analysis of longitudinal studies. *Aids* **20**, 73-83 (2006).
94. Hayes, R., Watson-Jones, D., Celum, C., van de Wijgert, J. & Wasserheit, J. Treatment of sexually transmitted infections for HIV prevention: end of the road or new beginning? *Aids* **24 Suppl 4**, S15-26 (2010).
95. Cohen, M.S., Council, O.D. & Chen, J.S. Sexually transmitted infections and HIV in the era of antiretroviral treatment and prevention: the biologic basis for epidemiologic synergy. *J Int AIDS Soc* **22 Suppl 6**, e25355 (2019).
96. Mwatelah, R., McKinnon, L.R., Baxter, C., Abdool Karim, Q. & Abdool Karim, S.S. Mechanisms of sexually transmitted infection-induced inflammation in women: implications for HIV risk. *Journal of the International AIDS Society* **22**, e25346 (2019).
97. Mtshali, A., Ngcapu, S., Mindel, A., Garrett, N. & Liebenberg, L. HIV susceptibility in women: The roles of genital inflammation, sexually transmitted infections and the genital microbiome. *Journal of Reproductive Immunology* **145**, 103291 (2021).

3. *EX VIVO* MUCOSAL TISSUE MODELS TO INVESTIGATE HIV-1 TRANSMISSION IN WOMEN

In Chapter 2, the impact of HIV-1 on women worldwide and the many risk factors that contribute to HIV transmission in women were described. While these risk factors were shown to increase the likelihood of HIV acquisition, there remains a gap in knowledge in the cellular, immunological, and/or virologic mechanisms that establish HIV-1 infection in the female reproductive tract (FRT). *Ex vivo* mucosal tissue models offer biologically relevant insights into such mechanisms. In this chapter, the contributions of these *ex vivo* models to studies of mucosal HIV-1 transmission to the FRT will be discussed, including their advantages and limitations. We will also describe how these *ex vivo* models, used in combination with reporter virus technologies, are useful approaches for modeling HIV-1 transmission and dissemination mechanisms. In Chapters 4 and 5, we will describe the application of an improved, highly sensitive *ex vivo* FRT model that incorporates reporter virus technology. Using this model, we identified virologic properties mapping to HIV Env that affected the efficiency of mucosal transmission and replication *ex vivo.*

Introduction

In 1926, Drs. Strangeways and Fell from Cambridge discovered that undifferentiated limb-buds could be removed from the embryos of Gold or White Leghorns (breeds of chickens) and cultured using *in vitro* techniques. Remarkably, they observed that the cells within the limb-buds continued to undergo mitosis, and the limb-buds eventually differentiated into "normal" limb-bud structures[1]. Their methods were considered to be the first organ culture system. However, their system was limited to the culturing of undifferentiated embryonic tissues. In 1958, Dr. Trowell developed a new organ culture system that maintained the viability of fully-differentiated, mature tissues *in vitro*. The mature tissues he used were derived from adult rats and mice, and included: ureter tubes, exocrine glands, kidneys, lungs, endocrine glands, gonads, skin, adipose, haemopoietic organs, nervous system, and eyeballs. The tissues were dissected into 2 mm blocks, placed atop a stainless-steel mesh grid (~20 blocks per grid), and suspended in 5-6 ml of culture medium in a glass 48 mm shallow culture dish. He determined that muscle and epithelial tissues survived the best, maintaining their viability and histological structures for at least 9 days in culture[2].

In 1972, Drs. McMahon and Thomas sought to expand upon the method outlined by Trowell and optimize it for human organ culture. They and others had previously attempted to use Trowell's methods to culture intact human tissues, including: benign tumors, carcinomas, various epithelial tissues, and even prostate. However, they were largely unsuccessful, with reports of necrosis and loss of histological architecture shortly after the tissues were introduced to culture. To increase tissue viability, McMahon and Thomas, using the same stainless-steel mesh grids as Trowell, placed either a slab of agar

gelled medium or a piece of collagen raft between the grid and blocks of benign human prostatic hyperplasia tissue. They observed some necrosis, but the histological architecture of tissue that had been cultured for 10 days was similar to that of fresh tissue[3]. By 1973, Fink *et. al* adapted the techniques of McMahon and Thomas to create the first *ex vivo* FRT mucosal tissue model, the cervical explant tissue (CET) model. Using their methods, endocervical explants could be maintained in culture (placed on agar gelled medium atop a stainless-steel grid) up to 10 days, although shifts in culture pH were implicated as the cause of metaplasia that was observed in some of the CETs[4].

In 1976, Fink, Thomas, and colleagues demonstrated that the CET model, with pH balancing buffer added to media, could support the productive replication of herpes simplex virus type 2 (HSV-2)[5]. This was the first time replication of a virus was observed and quantified in a human CET model. In 1988, Pomerantz *et. al* discovered that HIV was detectable in cervical biopsy specimens of HIV-infected women and suggested that HIV-infected lymphocytes and Mφs within cervix may be involved in the lower FRT mucosal transmission of the virus[6]. Based on this observation, Palacio *et. al* sought to interrogate the primary cellular targets of heterosexual HIV transmission, and used human CETs to model HIV transmission/infection *ex vivo* for the first time in 1994. They dissected the CETs into 3x3x2 mm blocks, immersed the blocks in cell-free R5-tropic or X4-tropic virus stock, washed the excess virus from the surface of the blocks, then cultured the blocks up to 7 days at the air-liquid interface atop a stainless-steel mesh grid. Interestingly, HIV infection was detectable by immunohistochemistry for p24 antigen in CETs exposed to R5-tropic virus but not X4-tropic virus[7].

In 1995, Glushakova *et. al* demonstrated that collagen rafts could be used to culture HIV-infected explant tissues without the stainless-steel mesh grids[8], which could be difficult to manufacture and keep sterile. By 2000, other human FRT tissues, including vaginal tissue, were adapted for studies of mucosal HIV transmission *ex vivo* and to test HIV viricidal agents[9]. In 2009, Drs. Grivel and Margolis integrated the work of multiple labs with their own findings to outline more efficient *ex vivo* human tissue culture systems to study mucosal HIV transmission, including a cervicovaginal system[10]. Though other *ex vivo* cervicovaginal systems have been described and used over the decades, the one described by Drs. Grivel and Margolis was foundational for modern studies of mucosal HIV-1 transmission, infection, and replication in human tissues *ex vivo*.

Overview of Ex Vivo FRT Tissue Models for Studies of HIV-1 Transmission

Although the first human FRT tissue used for studies of *ex vivo* mucosal HIV-1 transmission was cervix[7], other FRT tissues have since been adapted for these studies, including: vaginal, endometrial, and fallopian tube. According to Drs. Grivel and Margolis, culturing human explant tissues *ex vivo* permits the study of HIV-1 within the cytoarchitectural context of tissue in a controlled laboratory environment[10]. To prepare human FRT explant tissue for HIV-1 studies using their methods, the FRT tissue must first be obtained from biopsy, hysterectomy, or through other surgical means. The mucosal surfaces are then removed from the remnant FRT tissue and dissected into uniform 2-3 mm^3 tissue blocks. For studies pertaining to HIV-1, the tissue blocks are incubated with cell-free virus, washed, and then placed atop a collagen raft inside one well of a flat-bottom 6-well, 12-well, or 24-well culture plate[10-12]. To improve detection of virus and reduce intra-donor variation (variation between tissue blocks from the same donor), Drs. Grivel

and Margolis recommend culturing between 4-8 tissue blocks on one raft in one well (this constitutes a single experimental replicate)[10]. Virus/viral proteins are then detected either from culture supernatant or by digesting the tissue to isolate infected cells. In this format, tissue blocks can be viably cultured for 2-3 weeks[10-12].

One major advantage of the approach outlined above is that the explant tissues do not need to be activated prior to viral exposure and culture[10], which increases the biological relevance of *ex vivo* FRT models. Originally, explant activation— through the addition of phytohemagglutinin (PHA) and interleukin (IL)-2 into tissue culture media— was considered necessary for HIV-1 replication *ex vivo* because early methods to detect infection in explant culture (i.e. p24 ELISA, immunohistochemistry, RT assay, etc.) were inefficient for detecting low concentrations of viral proteins. However, RPMI media supplemented with fetal bovine serum (FBS) was found to be sufficient for maintaining viral replication in the explant tissues without prior activation by PHA and IL-2[9,12]. Another important feature of the above approach is that the explant tissues preserve the susceptibility of mucosal tissues to R5-tropic HIV-1 variants but not X4-tropic variants[10-12], resembling *in vivo* observations where clinical HIV-1 infection is established primarily by TF viruses that are predominantly R5-tropic [13,14]. The observation that *ex vivo* FRT explants were susceptible to R5-tropic (and not X4-tropic) HIV was initially made in the first human CET model in 1994[7], but was demonstrated in other CET models as well throughout the 2000s[15,16].

Implementation of HIV-1 Reporter Technologies in Ex Vivo FRT Tissue Models

One of the earliest examples of applying reporter technology to *ex vivo* tissue models was in 1995, when Drs. Margolis, Glushakova, and colleagues implanted mouse

tumor cells labeled with a fluorescent dye onto mouse lung explant tissue cultured *ex vivo*. They observed that the fluorescent tumor cells were able to invade the explant tissue. However, the fluorescent label was diluted after multiple cell replication cycles because the label was not stably expressed in the cells[17]. To address this limitation, Chishima *et. al* (1997) cultured stable *gfp*-expressing tumor cells with lung explant tissue *ex vivo* and observed that the tumor cells invaded and replicated within the explant tissue. The daughter tumor cells contained functional *gfp*, indicating that fluorescence was stably expressed over multiple rounds of mitosis[18]. In 2002, Bounou *et. al* were among the first to apply an HIV-1 reporter virus approach to human explant tissue. They inoculated explant human lymphoid tissue with an HIV-1 reporter virus that encoded FLuc in place of *nef*, then digested the tissue after 72 hours to determine infection. The tissue had to be disrupted to detect FLuc activity, and the FLuc reporter virus was not replication-competent *ex vivo*[19].

In 2009, Shen *et. al* described the first use of an HIV-1 reporter pseudovirus to inoculate human FRT tissue. They digested human vaginal explant tissue to isolate lymphocytes and Mφs, then inoculated the cells with a pseudovirus derived from co-transfecting an *env*-minus HIV-1 NL4-3 proviral backbone encoding *gfp* between *env* and *nef* with HIV-1 Env expression plasmids. Shen *et. al* used immunohistochemistry to detect p24 antigen, and though the pseudovirus was not replication-competent, they demonstrated that vaginal Mφs were permissive to R5-tropic HIV-1 entry[20]. In 2016, Astronomo *et. al* were the first to report on the inoculation of human FRT tissues *ex vivo* with a replication-competent HIV-1 reporter virus[21]. Using the cloning strategy originally developed by Drs. Kappes and Ochsenbauer in Edmonds *et. al*[22], the gene encoding secreted nanoluciferase (sNLuc) was cloned in frame to the T2A peptide coding sequence followed by *nef*.

Astronomo *et. al* inoculated vaginal explants with the sNLuc Env-IMCs and cultured the explants for 21 days, using luciferase activity as a surrogate indicator for viral gene expression in vaginal tissues. Luciferase activity as a surrogate for viral gene expression was measured over time by sampling the explant culture supernatant and analyzing it on a luminometer for relative light units (RLU). They used this approach to investigate the inhibitory activity of neutralizing antibodies *ex vivo* and also demonstrated that infection by and replication of the sNLuc Env-IMCs in explant tissue could be inhibited by RT and PR inhibitors (used as controls), respectively[21].

The reporter virus method implemented by Astronomo *et. al* improved on earlier approaches due to the following: (i) the sNLuc Env-IMC is more translationally relevant than pseudotyped virus because it preserves the orfs of all the HIV genes and is replication-competent, (ii) sNLuc activity can be measured from culture supernatant without having to digest the tissues like with FLuc, extending the usability of the tissue beyond a single timepoint, (iii) detection of sNLuc is more sensitive than other methods such as immunohistochemistry, which can have limited sensitivity if concentrations of viral proteins are low, and (iv) increases in sNLuc activity over time reflect *de novo* viral gene expression. Though this method of applying replication-competent HIV-1 reporter technology to *ex vivo* human FRT tissue models has been published on for less than a decade, the method has been shown to have utility in the study of viral transmission, the identification of host responses to virus, and the development of anti-HIV drugs. Non-reporter viruses have been used in similar applications *ex vivo*, but replication-competent reporter viruses offer a highly sensitive approach to detect, observe, and quantify viral infection and replication in explant FRT tissues.

Current Applications of Ex Vivo FRT Tissue Models for Studies of HIV-1

Ex vivo human FRT tissue models have been used to assess anti-HIV drugs, antimicrobial peptides, and other viricides in a translationally-relevant model system. One of the earliest examples of an *ex vivo* FRT model being used to test a viricidal agent was reported in 2000. Greenhead *et. al* pretreated human CET explants cultured on stainless-steel mesh grids with one of three vaginal viricides— nonoxynol-9 (N-9; a non-ionic surfactant), gramicidin (GD; a viricidal peptide), and PRO 2000 (a naphthalene sulfonate polymer)— then inoculated the explants with R5-tropic HIV. All three viricides variably blocked HIV infection *ex vivo* (as measured by immunohistochemistry of p24), with the most effective being PRO 2000 (97% maximal inhibition of viral infection after 8 days)[9]. A topical gel form of tenofovir, an NtRTI used in PrEP, applied to human CETs was shown to inhibit HIV subtype A, B, and C infection *ex vivo* by p24 ELISA[23]. Additional anti-HIV drugs and microbicides— such as dextrin sulphate (DxS), D2A21 (an anti-microbial peptide), CD4 aptamer-siRNA chimeras (CD4-AsiCs), UC-781 (an NNRTI), and many others— have also been evaluated in FRT tissues for their efficacy in inhibiting HIV-1 infection, stimulation of host inflammatory responses to HIV-1, and their toxicity in tissues[24-29]. The introduction of replication-competent reporter virus technology allowed both viral infection and replication to be more sensitively and effectively/conveniently detected and quantified in the absence or presence of anti-HIV drugs or microbicides in *ex vivo* FRT tissue models. Zidovudine, an NRTI, and indinavir, a PR inhibitor, were both shown to prevent replication of sNLuc Env-IMC *ex vivo*[21]. The reporter approach was advantageous in this study because it permitted the direct comparison of viral replication

in inhibitor-treated and non-treated vaginal explants with great sensitivity over three weeks in culture, which could not have been achieved effectively by measuring p24.

Ex vivo human FRT tissue models also have utility in studies of HIV-1 transmission that interrogate host immune factors in the presence of viral infection. The role of lectins in limiting mucosal HIV-1 transmission is one host immune factor that has been modeled *ex vivo* using human FRT tissue explants. Klein *et. al* showed that C-type lectins— transmembrane receptors expressed primarily by myeloid cells shown to bind/capture virus[30]— "trap" HIV-1 in cervical explants, and suggested that this mechanism may help prevent systemic infection *in vivo* by impeding the dissemination of the virus from the mucosa to blood[31]. Sialic acid binding immunoglobulin-like lectin-1 (Siglec-1/CD169) is a myeloid lectin induced by type-1 interferon (IFN) that promotes the capture and storage of HIV-1 in virus containing-compartments (VCCs)[32]. VCCs are pre-existing compartments within myeloid cells with a neutral pH that have been shown to harbor mature HIV virions[33]. Perez-Zsolt *et. al* showed that myeloid cells from CETs expressing Siglec-1/CD169 mediate viral capture and *trans*-infection *ex vivo*[32]. Induction of inflammatory cytokines/chemokines and inhibitory response of bnAbs are additional host immune factors that have been modeled *ex vivo* in human FRT tissue explants. It has been demonstrated that mucosal HIV-1 replication modeled in FRT explants is enhanced in the presence of exogenously added pro-inflammatory cytokines/chemokines (i.e. IL-1β, IL-6, monocyte chemotactic protein-1 (MCP-1), IP-10, and more)[34-36] but inhibited in the presence of bnAbs[21,34,37,38]. Cheeseman *et. al* reported that in human cervicovaginal explants pre-incubated with exogenous VRC01— an IgG1 bNAb that targets the CD4bs of HIV-1 Env— HIV-1 infection was inhibited[38]. However, detection of the low

concentrations of p24 antigen from explant culture supernatant to determine infection levels was challenging. Astronomo *et. al* later confirmed the findings of Cheeseman *et. al* by demonstrating that sNLuc Env-IMC infection was inhibited in cervicovaginal explants from donors that had been intravenously infused with VRC01[37]. Their reporter virus approach allowed for more sensitive detection and quantification of VRC01 neutralization activity *ex vivo* compared to Cheeseman *et. al*.

The heterosexual transmission of HIV-1 has been modeled *ex vivo* through the exposure of human FRT explants to semen containing infectious virus[35,39-41]. In 2005, Maher *et. al* demonstrated that virion-spiked seminal plasma initiated *de novo* HIV infection of cervicovaginal tissue culture[40]. Their findings were supported by Introini *et. al* in 2013, who showed that seminal IL-7 significantly enhanced HIV-1 infection and replication in cervicovaginal explants, as demonstrated through the increase of p24 production detected in culture supernatant over 12 days[41]. Introini *et. al* (2017) later expanded on this work and determined HIV-1 replication was enhanced in CETs following exposure to seminal plasma due to an upregulation of inflammatory factors (i.e. IL-6, TNF, CCL20, CXCL1, CXCL8, and others) in the CETs. Their results suggested that an inflammatory response elicited by seminal plasma following heterosexual intercourse may promote HIV-1 transmission to the FRT mucosae[35]. The efficacy of bnAbs against HIV-1 in the presence of semen has also been investigated using *ex vivo* human FRT tissue models. Scott *et. al* demonstrated that bnAbs, including VRC01, topically applied to CETs reduced HIV-1 transmission even in the presence of semen[42].

Future Applications of HIV-1 Reporter Technologies in Ex Vivo FRT Tissue Models

Many open questions remain for the research described above. Two areas that have not been modeled and investigated with reporter technologies applied *ex vivo* are heterosexual transmission and the host microbiome. To date, replication-competent reporter viruses have not been used to model the sexual transmission of HIV-1 to human FRTs. Sexual transmission could be sensitively modeled in CET or vaginal tissues with reporter HIV, as could the influence of the host microflora on mucosal HIV-1 susceptibility. As described in Chapter 2, the FRT microbiome, especially *Lactobacilli* species, reduces HIV-1 transmission risk through the competitive restriction of pro-inflammatory bacteria and the acidification of the mucosal environment[43-47]. An improved understanding of the dynamics between the host FRT microflora and virus— interrogated sensitively through reporter virus technologies applied *ex vivo*— may explicate potential mechanisms operative during mucosal HIV-1 transmission. Investigating the impact of gender affirming hormone therapies (GAHT) on susceptibility of mucosal tissue to HIV-1 infection is another application that can be underpinned by the reporter virus/FRT explant approach. Characterizing mucosal infection and replication kinetics of HIV-1 in the presence of exogenously added hormones used in GAHT or employing cervicovaginal explant tissue obtained from biopsies or medically indicated hysterectomies from transgender men undergoing GAHT may elucidate unrecognized HIV-1 acquisition risk factors for transgender men. Such information is largely absent from the HIV field but is of critical importance to informing HIV prevention strategies for transgender men.

Limitations of Ex Vivo FRT Tissue Models for Studies of HIV-1

A major limitation of *ex vivo* FRT tissue models is low sensitivity for investigating early viral infection and replication events. Prior to the implementation of reporter virus

technology to infect these tissues, HIV infection and replication in the explant tissues were monitored through detection of RT activity or p24 antigen in culture supernatant. However, sufficiently sensitive, longitudinal detection of these viral products (especially before 4 days following viral inoculation of the explant tissues) is challenging. Thus, improving the sensitivity and reproducibility of current *ex vivo* FRT tissue models, especially for the longitudinal monitoring of individual tissue blocks will/would greatly facilitate and accelerate the interrogation of the earliest mucosal transmission mechanisms.

To bolster detection of virus in FRT tissues *ex vivo*, Drs. Grivel and Margolis recommended culturing multiple tissue blocks together, at least 4 cervicovaginal tissue blocks for a single technical replica[10]. This was also recommended to reduce intra-donor variability[11]. However, this approach limits the number of conditions that can be tested within a single donor explant tissue because of the large amount of tissue required for just one set of replicas. In addition, though the tissue pooling strategy may reduce intra-donor variation, inter-donor variation remains an issue, limiting the reproducibility of *ex vivo* FRT tissue models. To further improve detection of virus *ex vivo*, some labs digest the explant tissues first, isolate individual cell populations, and then infect the cells with either reporter or non-reporter HIV virus. Although this method facilitates detection of virus and infected cells and offers opportunity for phenotyping of target cells, it removes the cells from the three-dimensional context of the tissues and affects the cell-cell and cell-virus interactions that would otherwise occur in intact tissues. Preservation of the intact tissues is thus desirable to preserve more authentic and translationally-relevant host-virus dynamics.

These issues discussed above prompted us to explore ways to improve on current *ex vivo* FRT tissue model approaches. In Chapters 4 and 5, we describe the application of highly sensitive reporter technology, sNLuc Env-IMCs, in a CET model. Our improved approach allows for the sensitive detection of *de novo* viral replication by three days following inoculation of the CETs with the sNLuc Env-IMCs, wherein replication within productively infected CETs is distinguishable from inhibitor-treated CETs. The CET blocks are infected and cultured intact over 14 days, and we demonstrate that reporter activity can be detected from single CET blocks. The CET blocks are thus cultured individually, increasing the number of experimental conditions that can be tested with a single donor tissue.

One final limitation of the CET model is the uncertainty of whether the experimental results of these FRT explant models are generalizable to female populations worldwide. Miller and Shattock criticized work utilizing these models for using explants that were surgically obtained from women in developed countries. They argued that because around 30-70% of women in developing countries have underlying FRT inflammation, the results gained from non-inflamed "normal" tissue used in Western explant models may not be applicable for those women[48]. However, in Western countries, FRT explant tissues are often acquired from women undergoing medically-necessary hysterectomies. The most common reasons for hysterectomies include fibroids and endometriosis[49], which can both lead to inflammatory states in the FRT[50]. Therefore, one could hypothesize that a lower level inflammatory state in the FRT may be a "normal" state. Whether experimental findings acquired through explants obtained from women in developed countries are applicable to women globally is thus unclear.

Conclusion

The *ex vivo* FRT models discussed herein have been developed over a long lineage of work. Though they have some limitations, they remain a valuable and highly translational approach for modeling and investigating the complexities of mucosal HIV-1 transmission. The application of reporter virus technology to these *ex vivo* models has further transformed our ability to study mucosal HIV-1 transmission by permitting a more sensitive interrogation of the host cell and virus mechanisms. The work outlined in the next two chapters describe further advancement of reporter technology applied to FRT tissues *ex vivo*. Through this work, we identify Env-based properties that affect the efficiency of mucosal HIV-1 transmission *ex vivo*. Ultimately, the full scope of potential applications for reporter technology in FRT tissues for *ex vivo* studies of HIV-1 transmission, drug discovery, and virus-host interactions has yet to be realized.

REFERENCES

1. Strangeways, T.S.P. & Fell, H.B. Experimental Studies on the Differentiation of Embryonic Tissues Growing in vivo and in vitro.--I. The Development of the Undifferentiated Limb-Bud (a) when Subcutaneously Grafted into the Post-Embryonic Chick and (b) when Cultivated in vitro. *Proceedings of the Royal Society of London. Series B, Containing Papers of a Biological Character* **99**, 340-366 (1926).
2. Trowell, O.A. The culture of mature organs in a synthetic medium. *Experimental Cell Research* **16**, 118-147 (1959).
3. McMahon, M.J. & Thomas, G.H. Morphological changes of benign prostatic hyperplasia in culture. *Br J Cancer* **27**, 323-35 (1973).
4. Fink, C.G., Thomas, G.H., Allen, J.M. & Jordan, J.A. Metaplasia in endocervical tissue maintained in organ culture--an experimental model. *J Obstet Gynaecol Br Commonw* **80**, 169-75 (1973).
5. Birch, J., Fink, C.G., Skinner, G.R., Thomas, G.H. & Jordan, J.A. Replication of type 2 herpes simplex virus in human endocervical tissue in organ culture. *Br J Exp Pathol* **57**, 460-71 (1976).
6. Pomerantz, R.J. et al. Human immunodeficiency virus (HIV) infection of the uterine cervix. *Ann Intern Med* **108**, 321-7 (1988).
7. Palacio, J. et al. In vitro HIV1 infection of human cervical tissue. *Res Virol* **145**, 155-61 (1994).
8. Glushakova, S., Baibakov, B., Margolis, L.B. & Zimmerberg, J. Infection of human tonsil histocultures: a model for HIV pathogenesis. *Nat Med* **1**, 1320-2 (1995).
9. Greenhead, P. et al. Parameters of Human Immunodeficiency Virus Infection of Human Cervical Tissue and Inhibition by Vaginal Virucides. *Journal of Virology* **74**, 5577-5586 (2000).
10. Grivel, J.-C. & Margolis, L. Use of human tissue explants to study human infectious agents. *Nature Protocols* **4**, 256-269 (2009).
11. Introini, A., Vanpouille, C., Fitzgerald, W., Broliden, K. & Margolis, L. Ex Vivo Infection of Human Lymphoid Tissue and Female Genital Mucosa with Human Immunodeficiency Virus 1 and Histoculture. *Journal of Visualized Experiments* (2018).
12. Merbah, M. et al. Cervico-vaginal tissue ex vivo as a model to study early events in HIV-1 infection. *Am J Reprod Immunol* **65**, 268-78 (2011).
13. Grivel, J.-C., Shattock, R.J. & Margolis, L.B. Selective transmission of R5 HIV-1 variants: where is the gatekeeper? *Journal of Translational Medicine* **9**, S6 (2010).
14. Margolis, L. & Shattock, R. Selective transmission of CCR5-utilizing HIV-1: the 'gatekeeper' problem resolved? *Nature Reviews Microbiology* **4**, 312-317 (2006).
15. Abraha, A. et al. CCR5- and CXCR4-tropic subtype C human immunodeficiency virus type 1 isolates have a lower level of pathogenic fitness than other dominant group M subtypes: implications for the epidemic. *J Virol* **83**, 5592-605 (2009).

16. Saba, E. et al. HIV-1 sexual transmission: early events of HIV-1 infection of human cervico-vaginal tissue in an optimized ex vivo model. *Mucosal Immunology* **3**, 280-290 (2010).
17. Margolis, L.B., Glushakova, S.E., Baibakov, B.A., Collin, C. & Zimmerberg, J. Confocal microscopy of cells implanted into tissue blocks: Cell migration in long-term histocultures. *In Vitro Cellular & Developmental Biology - Animal* **31**, 221-226 (1995).
18. Chishima, T. et al. Use of histoculture and green fluorescent protein to visualize tumor cell host interaction. *In Vitro Cellular & Developmental Biology - Animal* **33**, 745-747 (1997).
19. Bounou, S., Leclerc, J.E. & Tremblay, M.J. Presence of Host ICAM-1 in Laboratory and Clinical Strains of Human Immunodeficiency Virus Type 1 Increases Virus Infectivity and CD4⁺-T-Cell Depletion in Human Lymphoid Tissue, a Major Site of Replication In Vivo. *Journal of Virology* **76**, 1004-1014 (2002).
20. Shen, R. et al. Macrophages in Vaginal but Not Intestinal Mucosa Are Monocyte-Like and Permissive to Human Immunodeficiency Virus Type 1 Infection. *Journal of Virology* **83**, 3258-3267 (2009).
21. Astronomo, R.D. et al. Neutralization Takes Precedence Over IgG or IgA Isotype-related Functions in Mucosal HIV-1 Antibody-mediated Protection. *EBioMedicine* **14**, 97-111 (2016).
22. Edmonds, T.G. et al. Replication competent molecular clones of HIV-1 expressing Renilla luciferase facilitate the analysis of antibody inhibition in PBMC. *Virology* **408**, 1-13 (2010).
23. Rohan, L.C. et al. In vitro and ex vivo testing of tenofovir shows it is effective as an HIV-1 microbicide. *PLoS One* **5**, e9310 (2010).
24. Fletcher, P.S., Wallace, G.S., Mesquita, P.M. & Shattock, R.J. Candidate polyanion microbicides inhibit HIV-1 infection and dissemination pathways in human cervical explants. *Retrovirology* **3**, 46 (2006).
25. Cummins, J.E., Jr. et al. Preclinical testing of candidate topical microbicides for anti-human immunodeficiency virus type 1 activity and tissue toxicity in a human cervical explant culture. *Antimicrob Agents Chemother* **51**, 1770-9 (2007).
26. Zussman, A., Lara, L., Lara, H.H., Bentwich, Z. & Borkow, G. Blocking of cell-free and cell-associated HIV-1 transmission through human cervix organ culture with UC781. *AIDS* **17**, 653-661 (2003).
27. Dezzutti, C.S. et al. Pharmacodynamic Activity of Dapivirine and Maraviroc Single Entity and Combination Topical Gels for HIV-1 Prevention. *Pharmaceutical Research* **32**, 3768-3781 (2015).
28. Fraietta, J.A. et al. Abasic Phosphorothioate Oligomers Inhibit HIV-1 Reverse Transcription and Block Virus Transmission across Polarized Ectocervical Organ Cultures. *Antimicrobial Agents and Chemotherapy* **58**, 7056-7071 (2014).
29. Wheeler, L.A. et al. Inhibition of HIV transmission in human cervicovaginal explants and humanized mice using CD4 aptamer-siRNA chimeras. *J Clin Invest* **121**, 2401-12 (2011).
30. Drouin, M., Saenz, J. & Chiffoleau, E. C-Type Lectin-Like Receptors: Head or Tail in Cell Death Immunity. *Frontiers in Immunology* **11**(2020).

31. Klein, K. et al. Deep Gene Sequence Cluster Analyses of Multi-Virus-Infected Mucosal Tissue Reveal Enhanced Transmission of Acute HIV-1. *J Virol* **95**(2021).
32. Perez-Zsolt, D. et al. Dendritic Cells From the Cervical Mucosa Capture and Transfer HIV-1 via Siglec-1. *Frontiers in Immunology* **10**(2019).
33. Graziano, F., Vicenzi, E. & Poli, G. Immuno-Pharmacological Targeting of Virus-Containing Compartments in HIV-1-Infected Macrophages. *Trends in Microbiology* **24**, 558-567 (2016).
34. Rollenhagen, C. & Asin, S.N. Enhanced HIV-1 replication in ex vivo ectocervical tissues from post-menopausal women correlates with increased inflammatory responses. *Mucosal Immunology* **4**, 671-681 (2011).
35. Introini, A. et al. Seminal plasma induces inflammation and enhances HIV-1 replication in human cervical tissue explants. *PLoS Pathog* **13**, e1006402 (2017).
36. Asin, S.N., Eszterhas, S.K., Rollenhagen, C., Heimberg, A.M. & Howell, A.L. HIV Type 1 Infection in Women: Increased Transcription of HIV Type 1 in Ectocervical Tissue Explants. *The Journal of Infectious Diseases* **200**, 965-972 (2009).
37. Astronomo, R.D. et al. Rectal tissue and vaginal tissue from intravenous VRC01 recipients show protection against ex vivo HIV-1 challenge. *J Clin Invest* **131**(2021).
38. Cheeseman, H.M. et al. Broadly Neutralizing Antibodies Display Potential for Prevention of HIV-1 Infection of Mucosal Tissue Superior to That of Nonneutralizing Antibodies. *J Virol* **91**(2017).
39. Shattock, R.J. & Moore, J.P. Inhibiting sexual transmission of HIV-1 infection. *Nature Reviews Microbiology* **1**, 25-34 (2003).
40. Maher, D., Wu, X., Schacker, T., Horbul, J. & Southern, P. HIV binding, penetration, and primary infection in human cervicovaginal tissue. *Proceedings of the National Academy of Sciences* **102**, 11504-11509 (2005).
41. Introini, A., Vanpouille, C., Lisco, A., Grivel, J.-C. & Margolis, L. Interleukin-7 Facilitates HIV-1 Transmission to Cervico-Vaginal Tissue ex vivo. *PLOS Pathogens* **9**, e1003148 (2013).
42. Scott, Y.M., Park, S.Y. & Dezzutti, C.S. Broadly Neutralizing Anti-HIV Antibodies Prevent HIV Infection of Mucosal Tissue Ex Vivo. *Antimicrobial Agents and Chemotherapy* **60**, 904-912 (2016).
43. Armstrong, E. & Kaul, R. Beyond bacterial vaginosis: vaginal lactobacilli and HIV risk. *Microbiome* **9**, 239 (2021).
44. Lai, S.K. et al. Human immunodeficiency virus type 1 is trapped by acidic but not by neutralized human cervicovaginal mucus. *J Virol* **83**, 11196-200 (2009).
45. Maria L. Alcaide, V.J.R., Megan R. Brown, Suresh Pallikkuth, Kristopher Arheart, Octavio Martinez, Margaret Roach, Raina N. Fichorova, Deborah L. Jones, Savita Pahwa, and Margaret A. Fischl. High Levels of Inflammatory Cytokines in the Reproductive Tract of Women with BV and Engaging in Intravaginal Douching: A Cross-Sectional Study of Participants in the Women Interagency HIV Study. *AIDS Research and Human Retroviruses* **33**, 309-317 (2017).

46. Mtshali, A., Ngcapu, S., Mindel, A., Garrett, N. & Liebenberg, L. HIV susceptibility in women: The roles of genital inflammation, sexually transmitted infections and the genital microbiome. *Journal of Reproductive Immunology* **145**, 103291 (2021).
47. Mwatelah, R., McKinnon, L.R., Baxter, C., Abdool Karim, Q. & Abdool Karim, S.S. Mechanisms of sexually transmitted infection-induced inflammation in women: implications for HIV risk. *Journal of the International AIDS Society* **22**, e25346 (2019).
48. Miller, C.J. & Shattock, R.J. Target cells in vaginal HIV transmission. *Microbes Infect* **5**, 59-67 (2003).
49. Vessey, M.P., Villard-Mackintosh, L., McPherson, K., Coulter, A. & Yeates, D. The epidemiology of hysterectomy: findings in a large cohort study. *Br J Obstet Gynaecol* **99**, 402-7 (1992).
50. Jessica L. Gleason, M.E.T., Naomi Zukerman Willinger, and Edmond D. Shenassa. Endometriosis and Uterine Fibroids and Their Associations with Elevated C-Reactive Protein and Leukocyte Telomere Length Among a Representative Sample of U.S. Women: Data from the National Health and Nutrition Examination Survey, 1999–2002. *Journal of Women's Health* **31**, 1020-1028 (2022).

4. HIGHLY SENSITIVE ANALYSIS OF CERVICAL MUCOSAL HIV-1 INFECTION USING REPORTER VIRUSES EXPRESSING SECRETED NANOLUCIFERASE

by

DANA F. INDIHAR, JENNIFER J. JONES, CHRISTINA OCHSENBAUER, AND JOHN C. KAPPES

HIV Protocols, 4th Edition

Format adapted for dissertation

ABSTRACT

Ex vivo cervical tissue explant models offer a physiologically relevant approach for studying virus-host interactions that underlie mucosal HIV-1 transmission to women. However, the utility of cervical explant tissue (CET) models has been limited for both practical and technical reasons. These include assay variation, inadequate sensitivity for assessing HIV-1 infection and replication in tissue, and constraints imposed by the requirement for using multiple replica samples of CET to test each experimental variable and assay parameter. Here, we describe an experimental approach that employs secreted nanoluciferase (sNLuc) and current HIV-1 reporter virus technologies to overcome certain limitations of earlier *ex vivo* CET models. This method augments application of the CET model for investigating important questions involving mucosal HIV-1 transmission.

INTRODUCTION

HIV-1 infection of the genital mucosa represents the principal route of all transmission events worldwide[1,2]. Tissue explant models may offer major advantages for studying disease and virus-host interactions in humans since they recapitulate the cytoarchitecture, and temporal-spatial dynamics and functional interactions that exist *in vivo*. Unique insights into key aspects of mucosal HIV-1 transmission have come from multi-parametric imaging studies of mucosal tissue following simian immunodeficiency virus (SIV) vaginal challenge of rhesus macaques, including the identification of early infected target cells *in vivo*, early virus-host dynamics, and patterns of viral acquisition and dissemination[3-6]. Virus challenge studies utilizing human mucosal tissue models have helped to understand early pathogen-host interactions[7,8].

Cervical explant tissue (CET) has been utilized to create *ex vivo* model systems of mucosal HIV-1 transmission. A standardized protocol using CET to study human pathogens that cause infection through mucosal routes was described in 2009 by Margolis and Grivel[9]. This *ex vivo* cervical tissue model has notable features pertinent to the assessment of early virus-host interactions in a physiologically relevant context, including that the tissue cytoarchitecture and spatial distribution of HIV-target cell populations is preserved during short-term culture, and exogenous activation is not required for infection of tissue resident CD4 T lymphocytes[9-14]. Notably, the CET model recapitulates infection by CCR5-tropic HIV-1, while it is refractory to infection by CXCR4-tropic virus[10,15,16]. In other studies utilizing the *ex vivo* CET model, transmitted-founder (TF) viruses were shown to productively infect cervical tissue and replicate in CD4 T cells[17]. As our understanding of HIV transmission biology improved, these models evolved to address more complex

questions. In 2018, Introini *et al.* described *ex vivo* CET culture methods using gelatin sponges for non-polarized CET infection that facilitate access of the cultured tissue to medium nutrients and improve viability[16]. These and other *ex vivo* cervical tissue culture systems have been successfully used to investigate early disease pathogenesis, cell targets of acute mucosal HIV infection[18,19], infection and replication efficiencies of mucosally-transmitted HIV[15,17,19], and efficacy of anti-HIV therapeutics[20-23].

Intact virus-infected CET can be analyzed by various methods to assess HIV-1 infection and virus-host interactions. The temporal-spatial dynamics of virus replication and spread among target cells within the tissue can be evaluated using techniques such as multi-parametric imaging analysis of virus antigen (e.g., p24 antigen) and cell-specific differentiation markers. Using cells isolated from the tissue, multi-color flow cytometric analyses have helped inform the identity and dynamics of target cell infection. While these *ex vivo* CET models offer certain advantages over monotypic bi-dimensional cell cultures, the models are technologically demanding. Obtaining meaningful research results is further complicated by intra- and inter- donor variation, and the progressive loss of tissue integrity and functional architecture during *ex vivo* culture. Established CET models analyze multiple replica tissue samples for assessment of each experimental condition to augment sensitivity and minimize assay variation[9,10,16,24]. Practical constraints imposed by requiring multiple replica samples of dissected tissue for the assessment of each experimental variable and assay parameter have further limited usefulness of the CET model.

Here, we describe a method that employs HIV-1 reporter virus technologies using physiologically relevant HIV-1 strains engineered to encode secreted nanoluciferase (sNLuc) to overcome certain limitations of the *ex vivo* CET transmission model of HIV-1

infection. The method offers unprecedented sensitivity for detecting and quantifying *de novo* HIV-1 infection and replication *in situ* within the first few days after virus challenge. Notably, using the highly sensitive sNLuc readout, quantitative assessment of infection and replication kinetics of HIV-1 reporter viruses in individual 2-mm^2 mucosal explant tissue blocks is highly reproducible, and minimizes the intra- and inter- donor variation that has been reported with previous CET models[9,10,16,24]. Thus, this method, which expresses sNLuc from replication-competent HIV-1 reporter viruses engineered in a manner intended to retain wild-type-like expression and function of all viral proteins with physiologically relevant HIV-1 virus strains, augments the utility of the CET model. In this chapter, we describe experimental methods that utilize sNLuc reporter viruses to analyze HIV-1 infection and replication in human CET. We describe applicable HIV-1 reporter virus technologies, the generation and titration of viral stocks, the acquisition and dissection of CET for *ex vivo* culture, an efficient non-polarized approach for virus inoculation, and the sampling and analysis of CET culture supernatants for sNLuc activity as a surrogate of productive HIV-1 infection. Finally, we show representative results to demonstrate performance in terms of assay sensitivity and reproducibility. The methodology can be adapted to augment research on correlates of mucosal HIV-1 transmission, and to help understand early virus-host interactions that underlie that acquisition of mucosal HIV-1 infection.

MATERIALS

2.1 Human Tissue Acquisition

The use of human tissues must adhere to all Institutional Review Board (IRB) protocols and guidelines, including those for informed patient consent. Remnant cervical tissue may

be obtained from individuals undergoing medically necessary hysterectomies in hospitals associated with the research institution or sourced from a tissue bank. Standard clinical protocol requires assessment of the resected tissue by the surgical pathology laboratory for abnormalities and disease. Clear and precise communication with individuals directly involved with tissue procurement from the surgical pathology lab is vital for obtaining useful remnant tissue (*see* **Note 1**).

2.2 HIV-1 Reporter Infectious Molecular Clones

The methods described herein utilize replication-competent HIV-1 reporter viruses engineered to express secreted nanoluciferase (sNLuc) in a manner intended to retain wild-type-like expression and function of all viral proteins, including Nef. HIV-1 infectious molecular clones (IMCs) modified to express sNLuc can comprise either full-length proviral genomes of primary viruses (e.g. T/F HIV-1 IMC), or an isogenic NL4-3 proviral backbone modified to encode the Env ectodomain of heterologous *env* genes of interest (Env-IMC). Notably, the latter strategy facilitates studies involving the virologic and biological properties of different Env strains of HIV-1 while retaining the entire NL4-3 *vpu*, *tat* and *rev* open reading frames, thus avoiding inter-strain chimerisms[25]. **Figure 1** depicts the molecular genetic structure of the two complementary strategies: sNLuc-IMCs and sNLuc-Env-IMCs. We have extensively reported on the rationale, molecular design, and virologic properties of different reporter virus approaches (*see* **Note 2**).

1. sNLuc-Env-IMC and sNLuc-IMC proviral plasmids. These plasmid DNA are prepared using appropriate midi- or maxi-prep methods to ensure high quality, endotoxin-free, and sufficiently concentrated (ideally >0.5 μg/μl) DNA master stocks (*see* **Note 3**). For consideration of virus strains to utilize *see* **Note 4**.

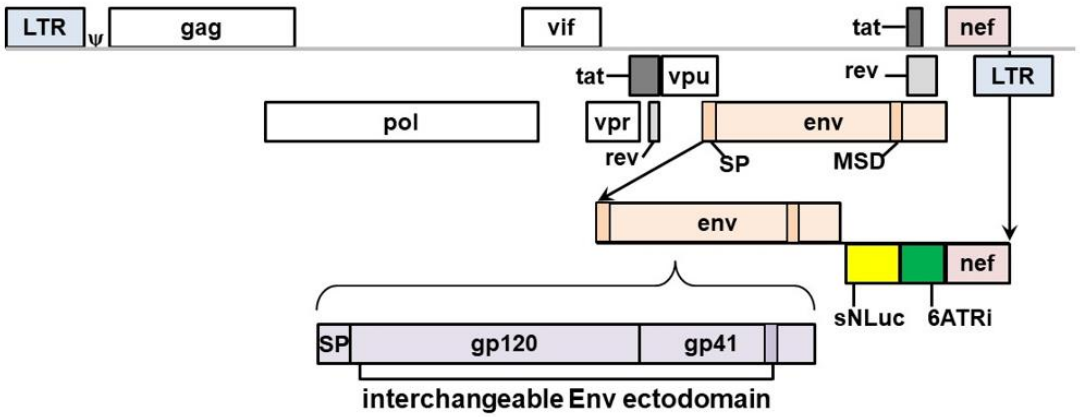

Fig 1. Schematic of HIV-1 reporter virus construct.
Schematic representation of the insertion of the coding sequence for a reporter gene (shown in yellow), followed by a modified, truncated ECMV internal ribosome entry site (IRES) sequence (6ATRi, shown in green), into an HIV-1 proviral genome between the *env* and *nef* orfs. First described in Alberti *et al* [31] for the *Renilla* (LucR) reporter 6ATRi cassette, this approach has been adapted to express sNLuc [44], used herein, as well as other reporter genes (*see* **Note 2**). The modified 6ATRi IRES has been shown to maintain native-like levels of Nef expression [31,32,37,39]. The reporter cassette can be inserted into T/F-IMC or HIV-1 references strains like NL4-3. The schematic also depicts how the coding sequence for the NL4-3 Env ectodomain, encompassing essentially all of gp120 and the external and membrane-spanning domain (MSD) of gp41, can be exchanged for heterologous *env* sequences. As illustrated, this avoids any overlap with *vpu*, *tat* and *rev* orfs, and mimics preferential *in vivo* recombination sites in the C1 and membrane spanning domain coding regions of *env* [56,57]. SP: signal peptide; MSD: membrane spanning domain.

2.3 Generation of Virus Stocks

1. HIV proviral DNA plasmid clones to generate infectious virus by transfection.
2. 293T cells. These human embryonic kidney cells contain the simian virus 40 (SV40) large tumor antigen (T-antigen), which enhances expression from transfected plasmid DNA containing the SV40 origin of replication sequence[26,27].
3. Dulbecco's Modified Eagle's Medium (DMEM) (*see* **Note 5**).
4. D10++ Medium: DMEM comprising 10% heat-inactivated fetal bovine serum (FBS), 25 mM HEPES, 2 mM L-glutamine, 100 µg/ml streptomycin, 100 U/ml of penicillin.
5. FuGENE™ HD Transfection Reagent, or equivalent.
6. 2 ml screw-cap microtubes.
7. Standard 6-well mammalian cell culture plates: clear, flat-bottom, sterile, polystyrene.

2.4 Virus Stock Titration

1. TZM-bl reporter cells[28], available from the NIH HIV Reagent Program (managed by the ATCC), and contributed by Drs. John C. Kappes and Xiaoyun Wu. In response to HIV-1 infection and Tat expression, TZM-bl cells express both firefly luciferase and β-galactosidase (β-gal). In this chapter, we us the β-gal reporter to determine virus titers: TZM-bl infectious units per ml (IU/ml).
2. D10++ Medium: As described above.
3. D1++ Medium: DMEM comprising 1% heat-inactivated fetal bovine serum (FBS), 25 mM HEPES, 2 mM L-glutamine, 100 µg/ml streptomycin, 100 U/ml of penicillin.
4. DEAE-Dextran stock solution: Sterile deionized water containing 10 mg/ml diethylaminoethyl-dextran hydrochloride. Aliquot 500-1000 µl into microtubes and store at -20°C.

5. Standard 24-well mammalian cell culture plates: Clear, flat-bottom, sterile, polystyrene, treated for cell culture.
6. Cell fixation buffer: Combine 500 ml of 1x PBS with 4 ml glutaraldehyde solution (Grade I; 25% in H_2O) and 11 ml formaldehyde solution (37 wt. % in H_2O; contains 10-15% methanol as stabilizer). Store in the dark at 4°C.
7. X-gal (5-Bromo-4-Chloro-3-Indolyl-AY-D-galactopyranoside) stock solution: 100 ml Dimethyl Sulfoxide (DMSO) containing 40 mg/ml X-gal.
8. TZM-bl cell β-gal staining solution: For 100 ml of staining solution, combine 94.8 ml of 1x PBS, 2 ml 0.2M Potassium Ferricyanide, 2 ml 0.2M Potassium Ferrocyanide, 200 µl $MgCl_2$, and 1 ml of 40 mg/ml X-gal stock solution. Store the individual components in the dark at 4°C and combine to make the X-gal staining solution fresh when needed.
9. Brightfield or phase-contrast microscope.
10. Manual tally counter for enumerating β-gal+ cells.

2.5 Cervical Explant Medium (CEM)

1. Cervical explant medium (CEM): RPMI 1640 medium comprising 1X Modified Eagle's medium (MEM) non-essential amino acids solution, 1 mM sodium-pyruvate, 50 µg/ml gentamicin, 15% fetal bovine serum (FBS), 2 mM L-glutamine, 100 U/ml penicillin, 100 ug/ml streptomycin. Store at 4°C. Just prior to use for cervical explant culture, supplement CEM with 30 U/ml IL-2.

2.6 Tissue Dissection

1. The materials and reagents described in this section should be readily available to ensure that tissue can be processed without delay after it is received.
2. Class II biological safety cabinet.

3. CEM: Described in 2.5.
4. The surgical instruments listed below are recommended for tissue dissection. These instruments (a-e) should be autoclaved before dissection in order to reduce risk of microbial contamination.
   (a) #4 stainless-steel scalpel blade handle.
   (b) Standard stainless-steel dissecting scissors.
   (c) General-purpose extra-long stainless-steel tweezers/forceps.
   (d) Precision tweezers/forceps with curved tips and fine serrated points.
   (e) Precision straight and tapered tweezers/forceps.
   (f) Disposable, sterile surgical blades fitting the #4 stainless-steel scalpel blade handle.
   (g) Mopec BladeFLASK Blade Remover (or equivalent) to safely remove scalpel blades from the handle.
5. Sterile WypAll™ L40 Wipers, or equivalent. These are thick wipes/pads that help delineate a sterile workspace during the dissection process. Prepare and store in a reusealable vessel that will withstand steam sterilization.
6. Laminated 2-mm x 2-mm dissection guide. This is a reusable template made to facilitate the tissue dissection into uniform 2 mm^3 blocks. Go to https://gridzzly.com and in the white box with the text “Make your own grid paper with Gridzzly”, click on the “□” and then type “2” into the first space. This will generate a 2-mm x 2-mm grid pattern. Print on 8.5x11” paper, cut into four quadrants, and laminate.
7. Standard tissue culture dish: sterile, 10 cm diameter.

8. Vinyl ruler: ~15 cm in length with 1 mm demarcations. Choose one that is flat, with low profile that can be positioned under a cell culture dish for measuring dimensions of remnant tissue samples.
9. Surgical face masks.
10. Powder-free nitrile gloves.
11. Optional tools that may facilitate tissue dissection: A focused-beam light source, a dissection microscope, surgical/dental loupes.

2.7 CET Infection and Culture

1. 2 ml screw-cap microtubes.
2. Tube revolver/rotator with 2 ml microtube paddle attachments, or equivalent device.
3. Humidified CO_2 incubator with CO_2 levels at 5% and temperature at 37°C.
4. Standard 48-well tissue culture plates, clear, flat-bottom, sterile, polystyrene, treated for cell culture.
5. Standard tissue culture dishes: sterile, 10 cm diameter.
6. SURGIFOAM Absorbable Gelatin Sponge purchased in sterile pieces measuring 2 cm x 6 cm x 0.7 cm, referred to as "gelatin sponge" throughout the text.
7. 12-channel reagent reservoirs with lids: sterile, contains up to 5 ml per channel.

2.8 Secreted nano-luciferase analysis

1. Promega Nano-Glo™ Luciferase Assay System. This assay kit includes Nano-Glo™ Luciferase assay Substrate, and Nano-Glo™ Luciferase Assay Buffer (*see* **Note 6**). This Nano-Glo™ System generates a continuous glow-type luminescence with a half-life of approximately 120 minutes.
2. Luminometer (Promega GloMax 96 Microplate Luminometer or equivalent).

3. 96-well white plates: Non-sterile, flat-bottom.
4. Computer based data analysis and graphing software.

METHODS

3.1 Generation of infectious HIV-1 stocks

The generation of HIV-1 stocks involves replication competent HIV-1 molecular clones and recombinant DNA. Therefore, appropriate biosafety practices must be followed, including the necessary biocontainment infrastructure. This includes consulting applicable Occupational Safety and Health Administration (OSHA) regulations and implementing proper biosafety level (BSL) containment procedures and practices, and review of the NIH Guidelines for research involving recombinant or synthetic nucleic acid molecules[29], and the CDC report on Biosafety in Microbiological and Biomedical Laboratories (BMBL)[30]. Herein, we describe how stocks (master banks) of HIV-1 reporter viruses are generated, aliquoted into multiple vials, stored at -80°C and titered for TZM-bl infectious units. Working from master banks of characterized virus augments the reproducibility of results between experiments, and ensures that the viruses are ready for immediate use when tissue becomes available.

1. Seed $4x10^5$ 293T cells in 3 ml of D10++ medium per well in 6-well plates. The next day, the cells should be adherent and evenly distributed on the bottom of each well. Suboptimal virus titers will be obtained if the wells contain cell aggregates or regions of high cell density around the perimeter or the center of the wells.
2. Between 18-24 hours after seeding, transfect the 293T cells with proviral DNA to generate infectious virus (*see* **Note 7**).

3. Collect the culture supernatant 60-72 hours after transfection, and centrifuge it at 200 g for 10 minutes to precipitate cells. Transfer the supernatant into a new tube. A second centrifugation step at higher speed can be performed to remove subcellular debris.
4. Aliquot the clarified supernatant into pre-labeled 2 ml screw-cap microtubes and store at -80°C. We generally recommend aliquots of 250 µl. Each well of transfected cells will yield ~3 ml of supernatant, which represents 12 vials containing 250 µl each. Depending on the scope of the research, it may be beneficial to transfect additional cells/wells to procure greater amounts of virus, both in terms of volume per vial and number of vials.

3.2 Titration of HIV-1 stocks

Viruses should be titered using TZM-bl cells[28] by β-gal staining to quantify infectious units (IU) per milliliter. The efficiency of proviral DNA transfection, condition of the TZM-bl cell culture, and the viral strain are all factors that will influence the virus titer.

1. Seed $7x10^4$ TZM-bl cells in each well of a 24-well plate with 500 µl of D10++ medium per well, and incubate at 37°C with 5% CO_2. The titration of each virus will require 10 wells.
2. The next day, prepare serial dilutions of the virus for titration. Using a 96-well plate, mix 20 µl of the virus stock with 180 µl of D1++ medium supplemented with 40 µg/ml DEAE-dextran. Then prepare five 5-fold serial dilutions by transferring 40 µl into 160 µl of D1++ medium containing 40 µg/ml DEAE-dextran.
3. Gently remove the cell culture supernatant from the 24-well plate and replace it with 200 µl per well of D1++ medium containing 40 µg/ml of DEAE-dextran. Add 50 µl of each of the 5-fold virus dilutions to two replica wells (50 µl each) of the 24-well plate,

and mix by gentle horizontal rotation and side-to-side movement. Incubate at 37°C for 4 hours, and then add 500 µl per well of pre-warmed D10++ medium per well. Continue to incubate at 37°C for 48 hours.

4. Remove the supernatant from each well and add 250 µl of TZM-bl cell fixation buffer being careful to not dislodge the cells in these and subsequent steps, and incubate for 5-8 minutes at room temperature. Gently remove the cell fixation buffer, and wash each well 3 times with 500 µl of PBS. After the final wash, add 250 µl of TZM-bl β-gal staining solution per well and incubate at 37°C for 2 hours.
5. Remove the β-gal staining solution and add 250 µl PBS per well. The β-gal+ blue-stained cells can be enumerated immediately or the 24-well plate can be stored in a sealed plastic bag at 4°C for counting at a later time.
6. To calculate the TZM-bl IU-titer from the β-gal+ blue-stained cells, use a microscope to visually inspect each well at each dilution. Identify two replica-dilution wells with 50-200 blue-stained cells each. With a grid marked on the underside of the wells to aid counting, use a manual tally counter and enumerate the number of blue-stained cells in each of the replica wells. Calculate the average and divide it by the dilution factor to determine IU per ml. (*see* equation below).
7. Equation to calculate IU/ml: $\left(\frac{(\#\text{ of well 1 blue cells} + \#\text{ of well 2 blue cells})\div 2}{\text{virus stock input per well [µl]}}\right) \times 1000 = IU/ml$
8. Example calculation: $\left(\frac{(58\text{ cells} + 62\text{ cells})\div 2}{0.0016\ \mu\text{l}}\right) \times 1000 = 3.75E+07\ IU/ml$

3.3 Preparation of CETs for dissection

The laboratory location for CET dissection and HIV infection should be considered prior to receiving tissue. We recommend both procedures be performed in a Class II biosafety cabinet. Once tissue is received, it should be immediately dissected and used for HIV infection (*see* **Note 8**).

1. Take 1-2 autoclaved WypAll™ wipes, unfold them, and lay them flat inside of the biosafety cabinet. This area is the "sterile working space", and all preparation and dissection steps should occur within this area.
2. Place one sterile tissue culture dish (10 cm) and its lid atop the WypAll™ wipes. Add 4-5 ml of fresh CEM into the lid and set it aside. Add 10-15 ml of CEM to the base of the culture dish.
3. Use the curved tip tweezers to place the explant tissue into the CEM-containing culture dish base. Gently swirl the media over the tissue. Carefully use the tweezers to manipulate and evaluate the general condition of the tissue (*see* **Note 9**)
4. Visually identify the anatomical features of the tissue, in particular the mucosal surfaces comprising the ectocervix and endocervix (**Fig. 2**).
5. Slide a vinyl ruler under the tissue culture dish to measure the length of the ectocervix and endocervix. These measurements allow for an estimation of the total number of tissue blocks that can be obtained by dissection. Document the appearance of the tissue specimen by photographing it.

3.4 Dissection of the CET

1. With the CET in the base of the tissue culture dish, use sterile curved tip tweezers to grip the tissue, then use a sterile surgical blade attached to a #4 scalpel blade handle to excise the endocervix and ectocervix surfaces from the remaining part of the tissue.

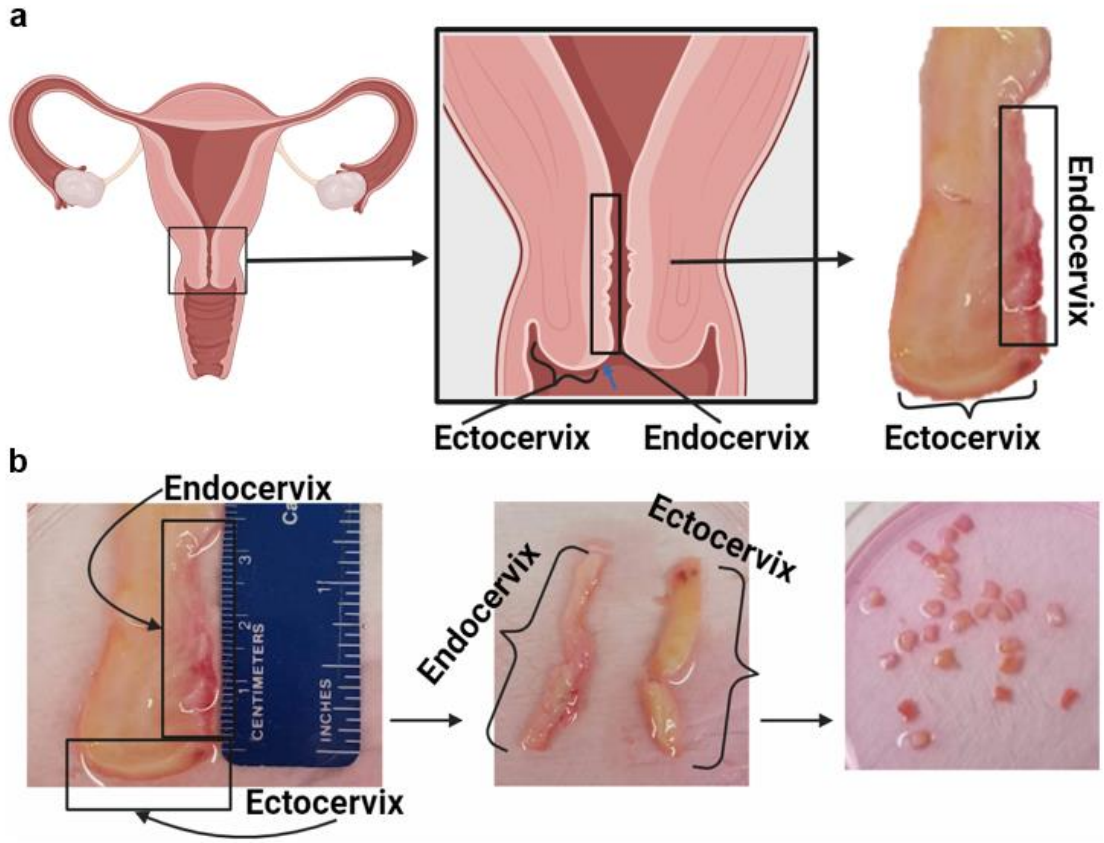

Fig 2. Anatomical origin, features, and dissection of CET specimens.
(**a**) A diagram of the human female reproductive track delineating the position of the cervix (left) with the ecto- and endocervical tissue sites identified (center). The blue arrow indicates the transformation zone at the transition of ectocervix and endocervix. On the right, an excised donor tissue specimen is shown with the ecto- and endocervical tissue sites indicated. (**b**) After assessment and release of a section of the cervix by the surgical pathology laboratory, the remnant tissue should be carefully evaluated, giving particular attention to the overall size and relative amounts and integrity of the ectocervical and endocervical mucosal surfaces (*see* also **Note 1** and **Fig. 6**). The images show a tissue specimen of optimal size (>2cm in length) that was received with discernable regions of endo- and ectocervical mucosae (left), the mucosal surfaces of the endo- and ectocervix after dissection form the submucosal tissue (center), and ~ 2-mm^3 blocks of tissue prepared by further dissection (right). Part of the illustration was created with *biorender.com.*

2. Remove as much of the underlying submucosal tissue as possible and discard (*see* **Note 10**).
3. Place the excised ectocervix and endocervix at opposite ends of the culture dish base. Remove and dispose of the remaining tissue.
4. Position the laminated 2-mm x 2-mm dissection grid under the culture dish.
5. Gripping the excised piece of endocervix or ectocervix with the curve-tip tweezers, cut the tissue in half, then cut those halves in half. Cut away any additional submucosal tissue to leave only the mucosal surface. Using the tissue dissection grid as a reference, continue until the tissue has been dissected into uniform ~ 2-mm^3 blocks. Transfer the blocks from the culture dish base into the tissue culture dish lid.
6. Repeat the dissection steps for the other excised tissue pieces and transfer those blocks into the culture plate lid, keeping the endocervix and ectocervix blocks separated (**Fig. 2**).
7. Count and record the number of tissue blocks for each tissue piece: ectocervix and endocervix. A standard remnant tissue specimen of 2-cm length can yield between 20-40 blocks each of ecto- and endocervix, for a total of 40-80 CET blocks.
8. If necessary, remove excess mucus for the surface of the dissected tissue blocks (*see* **Note 11**).

3.5 Non-polarized CET infection

1. Add 1 ml of CEM to 2 ml screw-cap microtubes. The number of tubes required will depend on the total number of tissue blocks that were obtained by dissection and research-specific experimental parameters, including controls and the number of blocks per infection condition (see below). Use straight-tip tweezers to transfer up to 8

dissected tissue blocks into each microtube. Here too, the number of tissue blocks per tube will depend on the overall experimental design.

2. Thaw the required amount of sNLuc virus stock from -80°C cryostorage. Add a desired amount of virus to the screw-cap microtubes containing tissue blocks (*see* **Note 12**).
3. Because sNLuc is present in the virus inoculum, it may cause relatively high background RLU levels and an appropriate negative control must be included. We suggest including one 2 ml screw-cap microtube containing 1 ml of medium and 2-3 tissue blocks without virus as a negative control, and one inoculated with non-infectious virus stock derived from transfection of 293T cells with *env*-minus sNLuc-IMC virus.
4. Additional controls may include tissue blocks treated with antiretroviral drugs at time points before or after virus inoculation, depending on drug mechanism and experimental design.
5. Securely tighten the cap of each microtube, place the tubes into the paddle attachment of a tube revolver/rotator, and rotate at approximately 10 rpm for 18-24 hours in a 37°C incubator. An overview of the steps described in this section is illustrated in **Fig. 3**.

3.6 CET HIV culture

1. Add 8-10 ml of CEM to a sterile 10 cm tissue culture dish.
2. Cut the gelatin sponge into 1 cm wide strips using sterile dissecting scissors.
3. Use tweezers to gently place the gelatin sponge strips into the CEM, and submerge using the blunt side of the tweezers. The gelatin sponge has sufficiently absorbed CEM when it turns from brittle and white to soft and semi-translucent. This may take up to one hour.

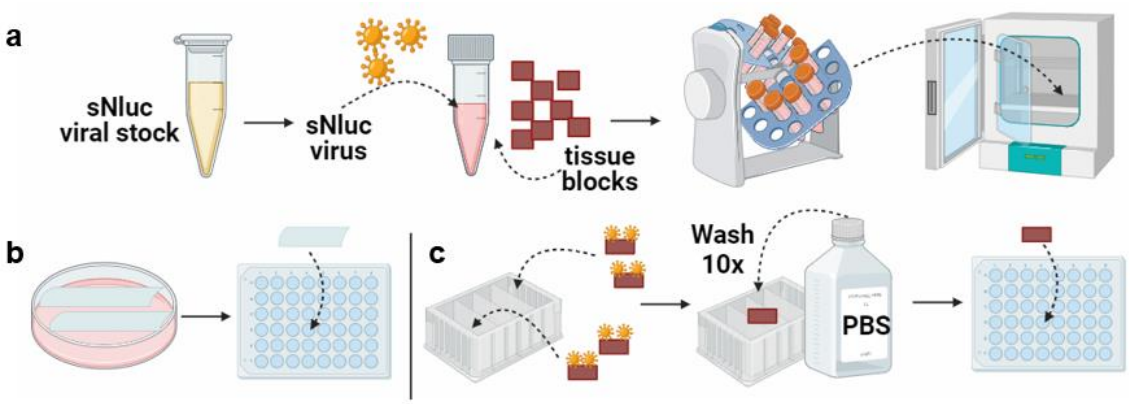

Fig 3. Workflow for virus inoculation and preparation for culture.

(**a**) sNLuc-IMC or sNLuc-Env-IMC reporter virus stocks maintained at -80^{o}C are thawed at room temperature (left). The dissected CET blocks are placed into 2 ml screw-cap tubes, and inoculated with a desired amount of virus (total volume of 1 ml) for 18-24 hours in a 37°C incubator while rotating end-over-end at 10 rpm. (**b**) Gelatin sponge is submerged in CEM until fully saturated, cut into uniform 5-mm x 5-mm squares, and then individually placed into wells of a 48-well plate (left). (**c**) Following the virus inoculation step (a), the tissue blocks are repeatedly washed to minimize sNLuc present in the virus inoculum. Then each CET block is placed into a well of a 48-well plate and gently nestled atop of the gelatin sponge. Illustration created with *biorender.com.*

4. While the gelatin sponge is hydrating, add 2-4 ml of cold PBS to each channel of a 12-channel reagent reservoir.
5. Remove the virus-inoculated tissue blocks from the incubator, and use tweezers to transfer all tissue blocks from one microtube into one channel of the 12-channel reservoir. Label each channel to distinguish the contents from different microtubes.
6. Repeat step 5 for all microtubes, disinfecting the tweezers between microtubes with 70% ethanol. When complete, set the reservoir with tissue blocks aside while performing the next two steps.
7. Using sterile tweezers and dissecting scissors, cut the CEM-saturated gelatin sponge strips into ~0.5-cm x 0.5-cm squares, and for each tissue block place one gelatin sponge square at the bottom of each well of a 48-well plate.
8. Add 400 µl of fresh CEM to each gelatin sponge-containing well.
9. Continue with washing of the tissue blocks by removing the PBS in each reservoir channel and replacing it with ~4 ml of fresh PBS (*see* **Note 13**).
10. After washing, transfer each tissue block atop of the gelatin sponge in a well of the 48-well plate with gentle manipulation so it is positioned securely atop the gelatin sponge (*see* **Note 14**).
11. Place the 48-well plate into a humidified incubator calibrated at 37°C and 5% CO_2.
12. After 24 hours (Day 1), move the plate to the biosafety cabinet, gently remove as much of the CEM as possible from each well, and replenish with 450 µl of pre-warmed, fresh CEM.

13. Perform an 80% medium change anytime the medium color changes from pink/red to yellow or at least every 5 days (*see* **Note 15**). Ensure that the tissue remains submersed and atop the gelatin sponge

3.7 Sample Collection and sNLuc Analysis

1. Move the 48-well culture plate to a Class II biosafety cabinet, collect 20 µl of supernatant immediately adjacent to each tissue block and place into a white 96-well luminometer plate for immediate analysis (*see* **Note 16**).
2. Return the 48-well culture plate to incubator.
3. Prepare the Nano-Glo™ luciferase assay buffer and substrate solution according to the manufacturer's recommendations.
4. Add 20 µl of the luciferase assay solution to each well containing culture supernatant and mix well.
5. Analyze sNLuc relative light units (RLU) using a 96-well microplate luminometer programmed with an integration time of 1 s/well. The sNLuc activity should be analyzed within 10 minutes.
6. Repeat steps 1-6 daily, or as desired, for up to 14 days.
7. Import the raw RLU values into appropriate analytical software for data analysis.

3.7 Representative Performance Characteristics and Data Analysis Considerations

Selected data generated using these methods are presented here to demonstrate expected outcomes and important performance parameters of the sNLuc reporter virus mucosal model, in particular; assay sensitivity, reproducibility, intra- and inter-donor variation, and potential limitations. To augment translation and application of this mucosal model,

example experiments are described below with data that were analyzed and presented to emphasize salient assay performance characteristics.

3.7.1 Detection of productive HIV-1 infection of CET

1. Tissue blocks prepared from CET were inoculated with a sNLuc reporter virus in either the absence or presence of nevirapine to inhibit HIV-1 infection. Over a period of two weeks, supernatant samples from each individual CET block culture were collected and analyzed for sNLuc RLU.
2. Raw RLU values plotted against time are shown in **Fig 4**, demonstrating the following: i) Residual sNLuc RLU from the virus inoculum persists despite extensive washing after virus inoculation (*see* **Note 13**). This is apparent at day 2 by comparing RLU values of samples collected from uninfected versus drug treated controls. ii) Strong evidence of virus infection is shown by a marked increase in RLU values for the non-drug treated CET blocks versus those treated with RT inhibitor. iii) Each of six replica virus-inoculated CET blocks exhibits a similar sNLuc RLU profile of HIV-1 infection and replication.

3.7.2 Profiles of HIV-1 infection and replication in CET

1. Tissue blocks from two different CET donors were prepared and inoculated with sNLuc reporter virus representing two different strains of subtype B virus in either the absence or presence of drug (**Fig. 5**). Over a period of two weeks, supernatant was collected from the CET block cultures and analyzed for sNLuc RLU.
2. The raw RLU values, generated from each CET donor (a and b respectively), are plotted against time (**Fig. 5**), demonstrating the following: i) Similar to Fig. 4a, there is a marked difference in the kinetics of sNLuc expression in CET infected without drug

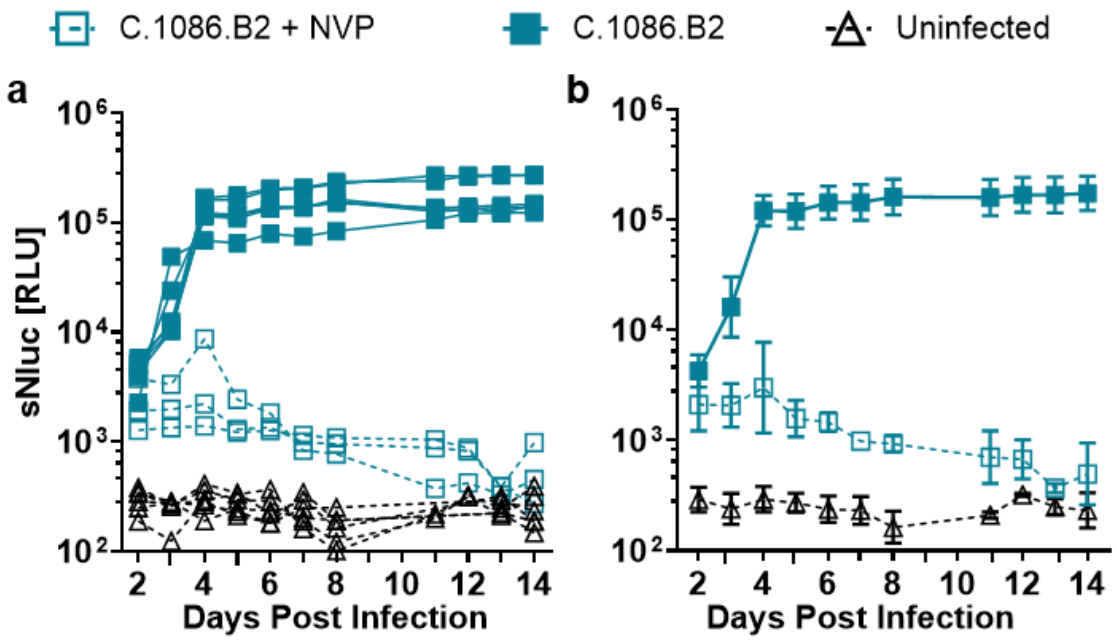

Fig 4. Productive HIV-1 infection of CET and intra-donor reproducibility.
(a) Nine CET blocks prepared by dissection from a single tissue donor were inoculated with sNLuc-Env-IMC reporter virus comprising the C.1086.B2 env. Three of the nine CET blocks were both inoculated and cultured in the presence of 20 ng/ml of nevirapine (NVP) (open squares). Six of the nine CET blocks were not treated with drug (solid squares). Note that the figure clearly distinguishes only three of the non-drug treated CET blocks since the other three had RLU values that were nearly identical to the others. Five additional CET blocks were mock-infected. The CET blocks were washed and then cultured individually in wells of a 48-well plates as described above. Supernatant samples collected from day 2 through day 14 were analyzed to quantify sNLuc RLU. Samples collected from wells with uninfected CET blocks served as a control to help assess residual sNLuc RLU in the samples collected from virus inoculated CET blocks. The raw RLU values (y-axis) were plotted against time (x-axis). (b) The geometric mean RLU values were calculated for each group of replica blocks and plotted with error bars representing geomean standard deviation.

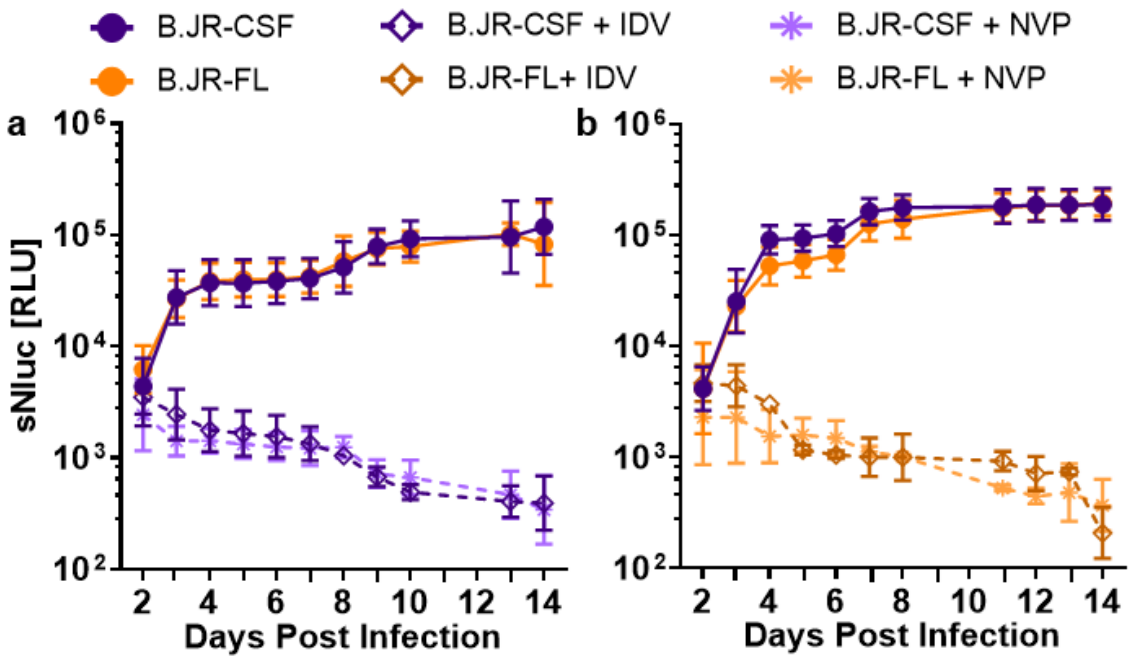

Fig 5. Inter-donor reproducibility of HIV-1 infection and replication profiles in CET.

CET blocks prepared from remnant tissue specimens obtained from two donors were divided into three groups each and inoculated with sNLuc-Env-IMC reporter viruses comprising the B.JR-FL and the B.JR-CSF envs, respectively. Each group included at least five CET blocks that were virus inoculated and subsequently cultured in CEM containing either no inhibitor, 20 μM of NVP, or 2 μM of Indinavir (IDV). Samples collected from day 2 through 14 were analyzed for sNLuc RLU. The sNLuc RLU values in each group are presented as geometric means calculated from replica samples. The data were plotted with error bars representing geomean standard deviation.

3. versus with drug. ii) The RLU kinetic profile of the two different HIV subtype B strains is similar. iii) RLU values from CET treated with protease inhibitor are indistinguishable from CET treated with RT inhibitor. This result has two notable implications for understanding the model system: First, it shows that sNLuc expressed from cells infected in the first round by virus in the inoculum (i.e. prior to secondary infection by *de novo* expressed virus), is not quantifiable over the background RLU; and second, it indicates that the RLU detected subsequent to day 2 represent ongoing HIV replication and spread to secondary target cells in the tissue.

3.8 Concluding remarks

Using the sNLuc-Env-IMC and sNLuc-IMC reporter viruses, we have shown exceptional sensitivity detecting HIV-1 infection in CET. Moreover, the sNLuc enables simple and repeated sampling from culture supernatants and quantitative analysis of virus infection and replication over several days following virus inoculation. Importantly, the viral dynamics exhibited among individual 2-mm^3 CET blocks from a given tissue specimen are highly reproducible. This underpinning enables meaningful comparative analyses of virus infection and replication in the CET model. The methods described herein may be applied to study determinants of viral fitness, to further examine the fitness properties of different HIV-1 subtypes, to test the effectiveness of neutralizing antibodies, or to examine effects of cytokine/chemokine expression. The methods may also be useful for correlative analyses of early virus-host interactions or factors affecting risk of HIV acquisition. Finally, the methods may be adapted for other mucosal tissue studies, including those involving rectal, tonsillar, foreskin, vaginal, or endometrial tissues.

NOTES

1. Access to useful remnant CET is essential, and therefore, considerations of the logistics for effectively accomplishing this routinely are particularly relevant. We highly recommend gaining an understanding of the administrative and practical procedures used by both the tissue procurement service and the surgical pathology lab for postoperative assessment of the tissue. It is imperative to educate the tissue procurement staff of your specific tissue requirement needs. Furthermore, it is critically important to precisely identify and communicate what anatomical features must be retained for your research on the tissue sections released by the surgical pathology lab (i.e., remnant tissue that retains a portion of the endo- and ectocervix mucosae).
2. The experimental needs of any given application determine the specific molecular design of an HIV-1 reporter virus that will be most useful. To give some broader context for the sNLuc reporter viruses used herein, we provide references that will allow the interested reader to gain more in-depth information on the features of the reporter IMCs. Usually, when HIV-1 is modified with reporter genes they are positioned within the 3' end of the genome, including insertion into or adjacent to the *nef* or *env* open reading frames (orfs). The HIV-1 reporter virus approaches developed in our laboratory have found application in various immune-monitoring assays and in other transmission and pathogenesis-related research, including those in mucosal explant tissue and humanized mice [25,31-51]. Our initial design [25] was refined to maintaining Nef protein expression at physiological levels of the parental non-reporter provirus [31] by inserting reporter genes in frame with the *nef* start codon followed by the modified "6ATRi" IRES illustrated in **Fig. 1**. Nef function, including CD4 and MHC

I downregulation, is preserved. This has demonstrated advantages for utilization of reporter IMC encoding *Renilla* luciferase (LucR), sNLuc, NLuc, mouse CD24, or Green Fluorescent Protein (GFP) in several research applications[31,32,37,39,44,52-54]. We have employed the reporter 6ATRi cassette approach both in the context of Env-IMC[31,32,37,44,52-54], as well as IMC, including TF-IMC[37,39,53,54]. The rationale for introducing the *env* ectodomain coding region (spanning from the C1 region of gp120, through the membrane-spanning domain (MSD) of gp41 of heterologous HIV-1 strains of interest, rather than the entire *env* orf, into an isogenic Env-IMC backbone[25,55] is backed by findings that inter-strain and inter-clade recombination sites are also selected for *in vitro* and *in vivo*[56,57]. This approach avoids creating chimeric *tat, rev* and *vpu* genes that can alter the replication properties of Env-IMC, and thus confound *env* comparative analyses. Furthermore, such "Env.ecto"-recombinant Envs maintain the neutralization phenotype of the *env* from which the ectodomain coding region was derived[58]; we consistently found that Env-IMC with full-length and "Env-ecto" heterologous sequences have the same neutralization profile in several different target cell types (Ochsenbauer et al., unpublished). The stable retention of reporter activity is also to be considered since it is critical for experimental applications that require multiple rounds of replication, including tissue explant models. We demonstrated retention of luciferase activity in PBMC using our first- and second-generation HIV-1 reporter virus design[25,31]. Of interest, the work of Roy *et. al* showed that reporter gene retention in, and replication of IMC in humanized mice is improved further by removal of CG dinucleotides in the reporter coding regions[59].

3. Care should be taken when growing bacterial cultures transformed with HIV-1 proviral plasmids. We recommend using STBL2 or STBL3 competent cells and growth temperatures between 30°C and 35°C. This helps with preventing deletions from occurring during culture for DNA miniprep and maxiprep. In our experience, selection pressure for such deletions seems to predominantly come from HIV-1 virus strain specific sequences in the 3' portion of the genome (including *env*). In NL4-3 based Env-IMC without or with reporter gene cassettes, problems with proviral plasmid deletions occur only occasionally, and are *env* stain dependent. For proviral plasmids encoding primary T/F IMC genomes, we observe with higher frequency that parts of the proviral clone become deleted. Therefore, we routinely grow bacteria transformed with such plasmids at 30°C, accepting potentially lower yields of maxiprep DNA in favor of high DNA quality. We occasionally clone TF-IMC genomes into low-copy-number plasmids for increased genetic stability[60].
4. Consideration should be given for the selection of HIV-1 strains. Strains that utilize the CXCR4 coreceptor for cell entry either do not replicate or replicate poorly in the CET model[10,15]. The R5-tropic BaL strain of HIV-1 replicates well[10,12,16,18,20] and is a useful positive control. Biologically relevant HIV-1 strains to consider include those representing T/F viruses. We previously described the generation of sNLuc-Env-IMC, pNL-sNLuc.6ATRi-B.BaL.ecto, that expresses the Env ectodomain of HIV-1_{BaL} within the NL4-3-derived proviral backbone[44]. In addition, we found that proviral clones of sNLuc-Env-IMC comprising *env* sequences derived from several Clade A, B, C, and D T/F HIV strains, and full-length T/F sNLuc-IMCs are infectious and replication competent, and thus well suited for application in the CET model.

5. Certain research studies utilizing the CET model may want to avoid medium that contains phenol-red due to its estrogen-like effect on the mucosa. Phenol-red free DMEM and RPMI are available from various manufacturers. The use of charcoal stripped FBS can be used for the same reason as a substitute for normal FBS.
6. If using the sNLuc gene provided by Promega Inc., users are required to use Promega Nano-Glo reagents, per Promega's Limited Use Label License, available on the company website.
7. While several different methods can be used for DNA transfection, we suggest using the Fugene HD transfection reagent, according to the manufacture's recommendations with 2 µg of proviral plasmid-cloned DNA for each well of a 6-well plate.
8. It is strongly recommended to complete the dissection and infection of the CET as soon as it is received. Since the resected donor tissue will require assessment by surgical pathology it is often not available until relatively late in the day. If the tissue cannot be used the day it is received, place it into ~ 30 ml of fresh CEM at 4°C. Maintaining the CETs at 4°C longer than 24 hours will compromise viability.
9. First, visually evaluate the tissue to assess its general condition and anatomical features. Ideal CET specimens are greater than 2 cm in length and exhibit a healthy tissue appearance and structure, particularly along the mucosal surface of the ecto- and endocervix (**Fig. 2 and 6**). Substandard tissue specimens are small, have non-discernable ecto- and/or endocervix mucosal surfaces, and/or have visible injury. Injury may include "shredding", where the mucosal surface becomes detached or torn from the underlying submucosa, or "burning/charring", where the mucosal surface is

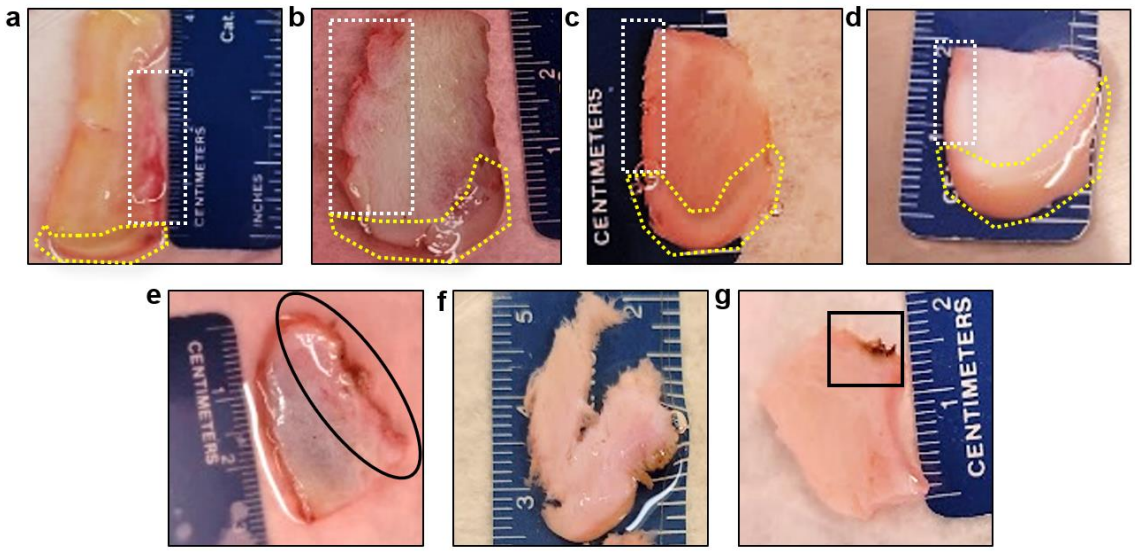

Fig 6. Examples of remnant cervical tissue specimens.
(a–d) Four examples are shown of donor specimens considered at or above standard for preparation of CET blocks. All four specimens are ~2 cm in length or longer, which is considered optimal; they contain undamaged mucosal surfaces, both ecto- and endocervical mucosae are present, and specimens have been cleanly excised from the donor tissue. There are no "burnt" or "charred" areas resulting from cauterization of the donor tissue. (e–g) Three examples of donor specimens considered substandard: The tissue on the left (e) is excessively bloody and the mucosal surface is "shredded". The center tissue (f) is abnormally shaped and lacks the endocervical mucosa. The tissue on the right (g) is missing the ectocervical mucosa, is less than 2 cm in length, and is partially "charred" from cauterization during surgical resection. White and yellow dotted lines delineate endocervical and ectocervical mucosae, respectively. Black outlines draw attention to substandard characteristics in e and g.

blackened from cauterization during surgery (**Fig. 6e-g**). Tissue of poor quality should not be used.

10. It is critical to understand the anatomical features of human cervix, both to identify useful tissue specimens, and to guide the dissection. Ectocervix and endocervix can be distinguished by their physical appearance and relative proximity. Ectocervix is covered by a pink stratified squamous epithelium, consisting of multiple layers of cells and it has a smooth, pearly, opaque appearance. Endocervix comprises columnar epithelium consisting of a single layer of cells that appears reddish in color from the underlying vasculature in the stroma that is visible (**Figs. 2, and 6**). Remove these mucosal surfaces from the underlying tissue by manipulating the scalpel in a guillotine-like motion, with long, unidirectional cuts. Dissection should not use a "sawing" motion as this creates jagged, uneven edges.
11. Endocervix will often continue to secrete mucus after dissection. Excess mucus may by temporally removed using tweezers to gently blot the CET blocks against the surface of the WypAll™ wipe.
12. A virus inoculum of $1x10^6$ IU is generally recommended; however, this may vary depending on the question and experimental design. An inoculum of $1x10^6$ IU should reproducibly result in productive HIV-1 infection of ~ 80% of the virus inoculated tissue blocks.
13. The virus stocks contain an abundance of sNLuc originating from the 293T cells transfected with reporter virus proviral DNA. Therefore, to maximize the detection of sNLuc produced from *de novo* infection of the CET, the tissue blocks must be washed extensively. The tissue blocks should be washed 8-10 times with 2-4 ml of PBS per

wash. Virus stocks prepared by ultracentrifugation will also help reduce RLU background, however, at least two washes are still recommended. Insufficient washing will result in high RLU values, which may obscure the detection of virus infection, particularly at the early time points after inoculation.

14. Surgifoam and similar products are sterile, water-insoluble, malleable, porcine gelatin sponges intended for hemostatic use. The beneficial effects for CET culture include, physical support for the tissue that helps retain tissue cytoarchitecture, slowing the rate of degradation, minimizing cell loss, and facilitating access to culture medium nutrients and oxygen through the sponge capillaries[16].
15. If phenol-red free medium is used to satisfy specific experimental criteria, we recommend to culture one uninfected tissue block on gelatin sponge in phenol-red-containing CEM to help identify when medium changes will be necessary.
16. As an alternative to contemporaneous analysis of sNLuc, samples can be collected and stored at -80°C, in which case it is recommended to collect samples of a larger volume into appropriate tubes or 96-well plates for storage, and to transfer 20 µl into white luminometer plates immediately before analysis. Be aware that volume loss by sampling medium from the wells should be replaced, albeit this is not necessary each time unless an appreciable volume has been removed.

REFERENCES

1. Burgener, A., McGowan, I. & Klatt, N.R. HIV and mucosal barrier interactions: consequences for transmission and pathogenesis. *Curr Opin Immunol* **36**, 22-30 (2015).
2. Global AIDS Update 2016. (UNAIDS, UNAIDS, 2016).
3. Haase, A.T. Early events in sexual transmission of HIV and SIV and opportunities for interventions. *Annu Rev Med* **62**, 127-39 (2011).
4. Keele, B.F. & Estes, J.D. Barriers to mucosal transmission of immunodeficiency viruses. *Blood* **118**, 839-46 (2011).
5. Smedley, J. et al. Tracking the luminal exposure and lymphatic drainage pathways of intravaginal and intrarectal inocula used in nonhuman primate models of HIV transmission. *PLoS One* **9**, e92830 (2014).
6. Stieh, D.J. et al. Vaginal challenge with an SIV-based dual reporter system reveals that infection can occur throughout the upper and lower female reproductive tract. *PLoS Pathog* **10**, e1004440 (2014).
7. Dezzutti, C.S. Animal and human mucosal tissue models to study HIV biomedical interventions: can we predict success? *J Int AIDS Soc* **18**, 20301 (2015).
8. Rollenhagen, C., Lathrop, M.J., Macura, S.L., Doncel, G.F. & Asin, S.N. Herpes simplex virus type-2 stimulates HIV-1 replication in cervical tissues: implications for HIV-1 transmission and efficacy of anti-HIV-1 microbicides. *Mucosal Immunol* **7**, 1165-74 (2014).
9. Grivel, J.-C. & Margolis, L. Use of human tissue explants to study human infectious agents. *Nature Protocols* **4**, 256-269 (2009).
10. Saba, E. et al. HIV-1 sexual transmission: early events of HIV-1 infection of human cervico-vaginal tissue in an optimized ex vivo model. *Mucosal Immunology* **3**, 280-290 (2010).
11. Estes, J.D., Legrand, R. & Petrovas, C. Visualizing the Immune System: Providing Key Insights into HIV/SIV Infections. *Frontiers in Immunology* **9**(2018).
12. Introini, A. et al. Seminal plasma induces inflammation and enhances HIV-1 replication in human cervical tissue explants. *PLoS Pathog* **13**, e1006402 (2017).
13. Merbah, M. et al. Cervico-Vaginal Tissue Ex Vivo as a Model to Study Early Events in HIV-1 Infection. *American Journal of Reproductive Immunology* **65**, 268-278 (2011).
14. Introini, A., Vanpouille, C., Lisco, A., Grivel, J.C. & Margolis, L. Interleukin-7 facilitates HIV-1 transmission to cervico-vaginal tissue ex vivo. *PLoS Pathog* **9**, e1003148 (2013).
15. Abraha, A. et al. CCR5- and CXCR4-tropic subtype C human immunodeficiency virus type 1 isolates have a lower level of pathogenic fitness than other dominant group M subtypes: implications for the epidemic. *J Virol* **83**, 5592-605 (2009).
16. Introini, A., Vanpouille, C., Fitzgerald, W., Broliden, K. & Margolis, L. Ex Vivo Infection of Human Lymphoid Tissue and Female Genital Mucosa with Human Immunodeficiency Virus 1 and Histoculture. *Journal of Visualized Experiments* (2018).

17. Merbah, M. et al. HIV-1 expressing the envelopes of transmitted/founder or control/reference viruses have similar infection patterns of CD4 T-cells in human cervical tissue ex vivo. *PLoS One* **7**, e50839 (2012).
18. Peters, P.J. et al. Infection of ectocervical tissue and universal targeting of T-cells mediated by primary non-macrophage-tropic and highly macrophage-tropic HIV-1 R5 envelopes. *Retrovirology* **12**, 48 (2015).
19. Klein, K. et al. Deep Gene Sequence Cluster Analyses of Multi-Virus-Infected Mucosal Tissue Reveal Enhanced Transmission of Acute HIV-1. *J Virol* **95**(2021).
20. Rohan, L.C. et al. In vitro and ex vivo testing of tenofovir shows it is effective as an HIV-1 microbicide. *PLoS One* **5**, e9310 (2010).
21. Cummins, J.E., Jr. et al. Preclinical testing of candidate topical microbicides for anti-human immunodeficiency virus type 1 activity and tissue toxicity in a human cervical explant culture. *Antimicrob Agents Chemother* **51**, 1770-9 (2007).
22. Buffa, V. et al. Cyanovirin-N potently inhibits human immunodeficiency virus type 1 infection in cellular and cervical explant models. *J Gen Virol* **90**, 234-43 (2009).
23. Fletcher, P. et al. The nonnucleoside reverse transcriptase inhibitor UC-781 inhibits human immunodeficiency virus type 1 infection of human cervical tissue and dissemination by migratory cells. *J Virol* **79**, 11179-86 (2005).
24. Introini, A., Vanpouille, C., Grivel, J.C. & Margolis, L. An ex vivo Model of HIV-1 Infection in Human Lymphoid Tissue and Cervico-vaginal Tissue. *Bio Protoc* **4**(2014).
25. Edmonds, T.G. et al. Replication competent molecular clones of HIV-1 expressing Renilla luciferase facilitate the analysis of antibody inhibition in PBMC. *Virology* **408**, 1-13 (2010).
26. 293T CRL-3216™. in *Human Cells* Vol. 2023 (ATCC).
27. Pear, W.S., Nolan, G.P., Scott, M.L. & Baltimore, D. Production of high-titer helper-free retroviruses by transient transfection. *Proc Natl Acad Sci U S A* **90**, 8392-6 (1993).
28. Wei, X. et al. Emergence of resistant human immunodeficiency virus type 1 in patients receiving fusion inhibitor (T-20) monotherapy. *Antimicrob Agents Chemother* **46**, 1896-905 (2002).
29. Policy, N.O.o.S. NIH GUIDELINES FOR RESEARCH INVOLVING RECOMBINANT OR SYNTHETIC NUCLEIC ACID MOLECULES (NIH GUIDELINES) (ed. Services, D.o.H.a.H.) (National Institutes of Health, https://osp.od.nih.gov/, 2019).
30. Biosafety in Microbiological and Biomedical Laboratories (BMBL) 5th edition 5edn (Centers for Disease Control, 2009).
31. Alberti, M.O. et al. Optimized Replicating Renilla Luciferase Reporter HIV-1 Utilizing Novel Internal Ribosome Entry Site Elements for Native Nef Expression and Function. *AIDS Res Hum Retroviruses* **31**, 1278-96 (2015).
32. Cavrois, M. et al. Mass Cytometric Analysis of HIV Entry, Replication, and Remodeling in Tissue CD4+ T Cells. *Cell Rep* **20**, 984-998 (2017).

33. deCamp, A. et al. Global panel of HIV-1 Env reference strains for standardized assessments of vaccine-elicited neutralizing antibodies. *J Virol* **88**, 2489-507 (2014).
34. Freel, S.A. et al. Phenotypic and functional profile of HIV-inhibitory CD8 T cells elicited by natural infection and heterologous prime/boost vaccination. *J Virol* **84**, 4998-5006 (2010).
35. Naarding, M.A. et al. Development of a luciferase based viral inhibition assay to evaluate vaccine induced CD8 T-cell responses. *J Immunol Methods* **409**, 161-73 (2014).
36. Pollara, J. et al. Association of HIV-1 Envelope-Specific Breast Milk IgA Responses with Reduced Risk of Postnatal Mother-to-Child Transmission of HIV-1. *J Virol* **89**, 9952-61 (2015).
37. Prévost, J. et al. Incomplete Downregulation of CD4 Expression Affects HIV-1 Env Conformation and Antibody-Dependent Cellular Cytotoxicity Responses. *J Virol* **92**(2018).
38. Sarzotti-Kelsoe, M. et al. Optimization and validation of a neutralizing antibody assay for HIV-1 in A3R5 cells. *Journal of Immunological Methods* **409**, 147-160 (2014).
39. Ventura, J.D. et al. Longitudinal bioluminescent imaging of HIV-1 infection during antiretroviral therapy and treatment interruption in humanized mice. *PLOS Pathogens* **15**, e1008161 (2019).
40. Anthony-Gonda, K. et al. Multispecific anti-HIV duoCAR-T cells display broad in vitro antiviral activity and potent in vivo elimination of HIV-infected cells in a humanized mouse model. *Sci Transl Med* **11**(2019).
41. Astronomo, R.D. et al. Rectal tissue and vaginal tissue from intravenous VRC01 recipients show protection against ex vivo HIV-1 challenge. *J Clin Invest* **131**(2021).
42. Astronomo, R.D. et al. Neutralization Takes Precedence Over IgG or IgA Isotype-related Functions in Mucosal HIV-1 Antibody-mediated Protection. *EBioMedicine* **14**, 97-111 (2016).
43. Bardhi, A. et al. Potent In Vivo NK Cell-Mediated Elimination of HIV-1-Infected Cells Mobilized by a gp120-Bispecific and Hexavalent Broadly Neutralizing Fusion Protein. *J Virol* **91**(2017).
44. Gornalusse, G.G. et al. Buprenorphine Increases HIV-1 Infection In Vitro but Does Not Reactivate HIV-1 from Latency. *Viruses* **13**(2021).
45. Mielke, D. et al. Selection of HIV Envelope Strains for Standardized Assessments of Vaccine-Elicited Antibody-Dependent Cellular Cytotoxicity-Mediating Antibodies. *J Virol* **96**, e0164321 (2022).
46. Seay, K. et al. In Vivo Activation of Human NK Cells by Treatment with an Interleukin-15 Superagonist Potently Inhibits Acute In Vivo HIV-1 Infection in Humanized Mice. *J Virol* **89**, 6264-74 (2015).
47. Seay, K. et al. The Vaginal Acquisition and Dissemination of HIV-1 Infection in a Novel Transgenic Mouse Model Is Facilitated by Coinfection with Herpes Simplex Virus 2 and Is Inhibited by Microbicide Treatment. *J Virol* **89**, 9559-70 (2015).

48. Seay, K. et al. Mice transgenic for CD4-specific human CD4, CCR5 and cyclin T1 expression: a new model for investigating HIV-1 transmission and treatment efficacy. *PLoS One* **8**, e63537 (2013).
49. Sung, J.A. et al. Dual-Affinity Re-Targeting proteins direct T cell-mediated cytolysis of latently HIV-infected cells. *J Clin Invest* **125**, 4077-90 (2015).
50. Pollara, J. et al. High-throughput quantitative analysis of HIV-1 and SIV-specific ADCC-mediating antibody responses. *Cytometry A* **79**, 603-12 (2011).
51. Mielke, D. et al. ADCC-mediating non-neutralizing antibodies can exert immune pressure in early HIV-1 infection. *PLoS Pathog* **17**, e1010046 (2021).
52. Neidleman, J.A. et al. Mucosal stromal fibroblasts markedly enhance HIV infection of CD4+ T cells. *PLOS Pathogens* **13**, e1006163 (2017).
53. Fernandez, N. et al. Assessment of a diverse panel of transmitted/founder HIV-1 infectious molecular clones in a luciferase based CD8 T-cell mediated viral inhibition assay. *Front Immunol* **13**, 1029029 (2022).
54. Hayes, P. et al. Breadth of CD8 T-cell mediated inhibition of replication of diverse HIV-1 transmitted-founder isolates correlates with the breadth of recognition within a comprehensive HIV-1 Gag, Nef, Env and Pol potential T-cell epitope (PTE) peptide set. *PLoS One* **16**, e0260118 (2021).
55. Ochsenbauer, C. & Kappes, J.C. New Virologic Reagents for Neutralizing Antibody Assays. Vol. 4 (eds Montefiori, D. & Mascola, J.) 418-425 (Current Opinion in HIV and AIDS, 2009).
56. Simon-Loriere, E. et al. Molecular mechanisms of recombination restriction in the envelope gene of the human immunodeficiency virus. *PLoS Pathog* **5**, e1000418 (2009).
57. Balinda, S.N. et al. Characterization of Near Full-Length Transmitted/Founder HIV-1 Subtype D and A/D Recombinant Genomes in a Heterosexual Ugandan Population (2006-2011). *Viruses* **14**(2022).
58. Binley, J.M. et al. Profiling the specificity of neutralizing antibodies in a large panel of plasmas from patients chronically infected with human immunodeficiency virus type 1 subtypes B and C. *J Virol* **82**, 11651-68 (2008).
59. Roy, C.N., Benitez Moreno, M.A., Kline, C. & Ambrose, Z. CG Dinucleotide Removal in Bioluminescent and Fluorescent Reporters Improves HIV-1 Replication and Reporter Gene Expression for Dual Imaging in Humanized Mice. *J Virol* **95**, e0044921 (2021).
60. Ochsenbauer, C. et al. Generation of Transmitted/Founder HIV-1 Infectious Molecular Clones and Characterization of Their Replication Capacity in CD4 T Lymphocytes and Monocyte-Derived Macrophages. **86**, 2715-2728 (2012).

5. THE HIV-1 ENVELOPE GLYCOPROTEIN OF SUBTYPE A AND D VIRUSES MEDIATE DISTINCT PROPERTIES OF REPLICATION *EX VIVO* IN A CERVICAL MUCOSAL MODEL OF TRANSMISSION

by

DANA F. INDIHAR, FERDINAND AMANOR, JIE ZENG, AUDREY ALEXANDER GARCIA, BOKANI NLEYA, JENNIFER J. JONES, CHRISTINA OCHSENBAUER, AND JOHN C. KAPPES

In preparation for *AIDS Research and Human Retroviruses*

Format adapted for dissertation

ABSTRACT

Previous research suggested viral properties mapping to Env may have significant impact on mucosal HIV-1 transmission. However, whether these properties affect subtype-specific mucosal transmission is unclear. Herein, we investigated whether Env-based properties of different HIV-1 subtypes affect mucosal HIV-1 transmission in a cervical explant tissue (CET) model. We inoculated CETs from 46 donors with HIV-1 infectious molecular clones (IMCs) expressing Env sequences of 10 transmitted/founder (TF) strains representing two genetically distinct subtypes (A and D) with reportedly distinct pathogenic outcomes of infection. Env-IMC were engineered with a secreted nano-luciferase or mouse CD24 reporter gene. The innovative application of this approach enabled exceptionally sensitive and reproducible quantification of HIV-1 replication *ex vivo* within 72 hours following virus exposure by either sampling culture supernatant from individual 2 mm^3 tissue blocks for *de novo* viral gene expression or by flow cytometric identification of infected cells liberated from CETs.

Subtype D Env-IMC replication was significantly greater than that of subtype A Env-IMC over 2 weeks in the CETs. However, no differences were observed between the subtypes in the infection of CD4 T cells liberated from CETs for flow cytometric analysis after 4 days of culture. Replication of subtype A Env-IMC was significantly greater in CETs derived from ectocervix than endocervix. Env amino acids stabilizing inner-outer domain interactions, which affect efficiency of CD4 utilization, are conserved within clades but differ between clade A and D. We hypothesized that introducing "D-like" R429G and/or Q432K mutations into subtype A Env would improve CD4 binding and replication kinetics *ex vivo*. However, the mutations impaired replication in CETs, and

CD4 binding. Of note, subtype A, D, and A-mutant Env-IMC replicated similarly in CD4 T cells from PBMC.

Our findings suggest biologic differences between subtype A and D HIV-1 may manifest at the time of transmission, as modeled *ex vivo*.

INTRODUCTION

Approximately 52% of the ~39 million people infected with HIV-1 globally are women and girls[1,2]. Most women and girls become infected with HIV following heterosexual intercourse[1-6] that may expose the female reproductive tract (FRT) to cell-free virions and productively HIV infected cells[7,8]. HIV-1 can gain access to permissive target cells that reside in the FRT submucosa through micro-lacerations, virion capture by Langerhans cells, epithelial transmigration mechanisms, or a combination of mechanisms[9-11]. However, how clinical HIV-1 infection is established in the FRT following this mucosal exposure remains largely unknown. Viral properties that affect mucosal HIV-1 transmission initiated by productive viral replication in the genital mucosa are poorly understood.

Viral properties reported to affect the efficiency of mucosal HIV transmission *in vivo* include co-receptor tropism[12-14], ability of virus to stimulate early host immune response[15-18], and replicative fitness[14,19,20]. Viral replicative fitness is the capacity of virus to replicate in its host[21] and has been described as a better predictor of disease progression rate than viral load in HIV-infected individuals[16,17,22,23]. It has been shown to correlate with the efficiency of host cell entry both *in vivo* and *ex vivo*[19,24,25], HIV disease progression *in vivo*[19,26], and viral transmission *ex vivo*[25]. In *ex vivo* models of mucosal HIV-1 transmission, viral replicative fitness has been shown to vary based on HIV-1 subtype, with subtype D viruses having greater replicative fitness than those of subtypes A and C[25,27]. It is unknown if these findings are linked to the *in vivo* observation that individuals infected with subtype D experience faster rates of disease progression than those infected with either subtypes A or C[14,15,19,23,28-31].

Klein *et. al* demonstrated that viral replicative fitness within primary CD4+ T cells and macrophages (Mφs) from genital mucosal tissues was largely dictated by the efficiency through which virus gained entry into host cells and was attributable to the viral envelope glycoprotein complex, Env[24]. This finding suggests that properties mapping to HIV-1 Env play a key role in viral transmission, and that Env proteins of different HIV-1 subtypes may impart distinct viral transmission fitness properties. We therefore hypothesized that subtype-specific HIV-1 mucosal transmission and replication phenotypes are affected by Env. To interrogate this hypothesis, we applied our previously described HIV reporter virus technology (originally described in Alberti *et. al*[32]) to an *ex vivo* mucosal tissue model. We designed a panel of infectious molecular clones (IMCs) in which an isogenic proviral backbone was engineered to encode one of two reporter genes (either secreted nano-luciferase [sNLuc] or mouse CD24 [mCD24]) as well as the heterologous Env ectodomain coding regions from a panel of 5 subtype A and 5 subtype D HIV-1 transmitted/founder (TF) virus strains. This design ensured that all the genes of the subtype A and D reporter Env-IMCs were identical except for *env*. Subtypes A and D were selected due to their genetic and pathogenic distinctiveness *in vivo*[14,15,19,23,28-31,33]. The panel of reporter Env-IMC were then used to inoculate remnant human cervical explant tissue (CETs), as previously described[34].

The replication of subtype D reporter Env-IMCs was found to be significantly greater than subtype A reporter Env-IMCs *ex vivo* over 2 weeks following viral inoculation, demonstrating that subtype D was more likely to establish infection and replicate more efficiently in the CETs than subtype A. Further, subtype A Env-IMC were found to replicate more efficiently in CETs derived from ectocervix than those from endocervix.

Interestingly, Env-IMC from both subtypes were found to similarly infect mucosal CD4 T cells in CETs *ex vivo* during the first 4 days post viral exposure and in PBMC-derived CD4 T cells *in vitro*. This suggests that one or more other cell types may contribute to the distinct subtype-specific *ex vivo* replication kinetics after initial infection is established.

We further sought to understand the potential molecular basis for the observed phenotypic difference between subtype A and D replication *ex vivo*. Zhang *et. al* reported that the inner-outer domain interface of Env for subtypes A, B, and C was stabilized through the formation of a salt bridge between a universally conserved aspartic acid at residue 113 and a basic residue at 429 (subtype A) or 432 (subtypes B and C). The formation of the salt bridge was suggested to reduce the flexibility of Env to bind CD4[35], and salt bridge formation may occur more readily with residue 429 than 432. Subtype D has a basic residue at 432 similar to subtypes B and C, and we hypothesized that introducing residues 429 and 432 from subtype D Env into subtype A Env would improve CD4 binding and replication in CETs. However, mutations to subtype A Env residues 429 and 432 significantly impeded viral replication *ex vivo* and CD4 binding *in vitro,* suggesting that the efficiency of CD4 binding may have contributed to the subtype-specific transmission and replication phenotypes observed *ex vivo.*

In summary, we observed that the subtype of HIV-1 Env and efficiency of CD4 binding affected HIV-1 infection and replication in our reporter-based *ex vivo* transmission model. The application of reporter Env-IMCs to CETs offers an approach for modeling mucosal HIV-1 transmission *ex vivo* with unprecedented sensitivity and reproducibility, and use of TF Env sequences in our reporter virus design increased the biological relevance and translatability of our findings. Overall, the identification of Env-based properties of

transmission is crucial for understanding the virologic factors contributing to mucosal HIV-1 acquisition risk in women.

MATERIALS AND METHODS

Ethics statement

All remnant cervical tissue was acquired from the University of Alabama at Birmingham (UAB) Tissue Biorepository (TBR). Tissues were obtained with patient consent and in accordance with pre-approved Institutional Review Board (IRB) and university protocols. All tissues were de-identified except for demographic information regarding age and race.

Generation of reporter IMCs

Our lab has previously designed and implemented a number of HIV-1 reporter virus approaches for *in vitro*, *in vivo*, and *ex vivo* studies pertaining to viral transmission, infection, replication, and pathogenesis[32,36-55]. Herein, we designed a panel of HIV-1 reporter viruses to rigorously interrogate our central hypothesis. The design and cloning process of the reporter viruses was described previously in Alberti *et. al*[32]. Briefly, NL4-3 was used as an isogenic proviral backbone[56] (GenBank ID: M19921) and either the secreted Nano-luciferase (sNLuc)[57] or heat-stable antigen (HSA)/mouse CD24 (mCD24)[39] reporter genes were inserted between *env* and *nef*. The IRES element "6ATRi" was placed downstream of the reporter open reading frame to drive viral gene expression. The **NL4-3 Env signal peptide** with the 4 amino acids following the peptide was incorporated (**ILMICSA**TEKL) at the N-terminus of Env to ensure homogenous Vpu. The ectodomain coding region of NL4-3 was interchanged with the ectodomain coding regions of BaL or

subtype A and D TF viruses. Exchanging just the ectodomain rather than the entire Env sequence avoids the generation of chimeric Rev and Tat since the *rev* and *tat* exons overlap with the gp41 coding region of *env*. The TF subtype A and D Envs used for the IMCs originated from the Uganda Virus Research Institute/Medical Research Council/Welcome Trust HIV high risk cohort[58]. All the subtype A and D viruses we used for these experiments were CCR5 (R5) tropic[58]. As a control, the initiating methionine of D.191882 Env was removed, introducing premature stop codons to generate envelope-defective virus, referred to as "Env Minus".

These isogenic IMCs with differing Env ectodomains are referred to as reporter Env-IMCs hereon. Additional reporter IMCs were generated using the entire TF proviral backbone with sNLuc inserted between *env* and *nef* as described above. These are referred to as reporter TF-IMCs. All reporter Env-IMCs and TF-IMCs are summarized and numbered in Table 1. After cloning the reporter Env-IMCs and TF-IMCs, viral stocks were generated through the transfection of 293T cells with proviral DNA, as described previously[34]. Viral stocks were titered for infectious units per ml (IU/ml) in the β-galactosidase assay using TZM-bl cells, also as described[59].

Infecting PBMC-derived CD4+ T cells with sNLuc and mCD24 IMCs

Frozen stocks of PBMCs from 1 donor (~60 million cells) were thawed in 30 ml of PBMC media [RPMI 1640 media, 20% FBS, 25 mM HEPES, 2 mM L-glutamine, 100 µg/ml streptomycin, 100 U/ml penicillin, and 30 U/ml interleukin-2], placed into a T-75

Table 1. Master Panel of IMCs

#	*Construct Name*	*Lab ID #*	*Env*	*Reporter*
1	NL-HSA.6ATRi-A.R880F.ecto	K5017	A.R880F	mCD24
2	NL-HSA.6ATRi-A.191084.ecto	K5016	A.191084	mCD24
3	NL-HSA.6ATRi-A.191845.ecto	K5018	A.191845	mCD24
4	NL-HSA.6ATRi-D.191859.ecto	K5020	D.191859	mCD24
5	NL-HSA.6ATRi-D.191882.ecto	K5021	D.191882	mCD24
6	NL-HSA.6ATRi-D.191647.ecto	K5019	D.191647	mCD24
7	NL-HSA.6ATRi-D.191882.env-minus	K5321	Δ	mCD24
8	NL-sNLuc.6ATRi-A.R880F.ecto	K5310	A.R880F	sNLuc
9	NL-sNLuc.6ATRi-A.191084.ecto	K5378	A.191084	sNLuc
10	NL-sNLuc.6ATRi-A.191845.ecto	K5820	A.191845	sNLuc
11	NL-sNLuc.6ATRi-A.9004SDM.ecto	K5858	A.9004SDM	sNLuc
12	NL-sNLuc.6ATRi-A.R463F.ecto	K5859	A.R463F	sNLuc
13	NL-sNLuc.6ATRi-D.191859.ecto	K5379	D.191859	sNLuc
14	NL-sNLuc.6ATRi-D.191882.ecto	K5311	D.191882	sNLuc
15	NL-sNLuc.6ATRi-D.191647.ecto	K5821	D.191647	sNLuc
16	NL-sNLuc.6ATRi-D.190049.ecto	K5860	D.190049	sNLuc
17	NL-sNLuc.6ATRi-D.SC191727.ecto	K5861	D.SC191727	sNLuc
18	NL-sNLuc.6ATRi	K5380	NL4-3	sNLuc
19	NL-sNLuc.6ATRi-B.Bal.ecto	K4702	BaL	sNLuc
20	NL-sNLuc.6ATRi-D.191882.env-minus	K5322	Δ	sNLuc
21	A.R880F-sNLuc.6ATRi	K5896	A.R880F	sNLuc
22	A.191845-sNLuc.6ATRi	K5897	A.191845	sNLuc
23	D.191859-sNLuc.6ATRi	K5898	D.191859	sNLuc
24	D.191882-sNLuc.6ATRi	K5899	D.191882	sNLuc
25	NL-sNLuc.6ATRi-A.R880F env.ecto. R429G	K5944	A.R880F	sNLuc
26	NL-sNLuc.6ATRi-A.R880F env.ecto. Q432K.	K5945	A.R880F	sNLuc
27	NL-sNLuc.6ATRi-A.R880Fenv.ecto.R429K+ Q432K	K5946	A.R880F	sNLuc
28	NL-LucR.T2A-Bal26.ecto	K2854	BaL26	LucR

flask, and then rested overnight at 37 °C. The next day, cells and media were pipetted into a 50 ml conical tube and centrifuged at 300 g for 10 minutes. The CD4+ T cells from that pellet were isolated through negative selection via a LS column and the Miltenyi MACS CD4+ T cell isolation kit according to the manufacturer's protocol. The CD4+ T cells were then cultured in PBMC media and stimulated with a CD3-CD28 bispecific antibody (2.6 µg/ml) for 4 days. To inoculate CD4+ T cells with the HIV reporter IMCs, the CD4+ T cells were placed into a 2 ml microtube with 1 ml of PBMC media and one reporter virus. The microtubes were then rotated for 4-6 hours at 37 °C. Following the rotation, cells were washed 2-4x with pre-warmed PBMC media (with centrifugation at each wash occurring at 300 g for 5 minutes). After the final wash, the cell pellets were resuspended in 1 ml of fresh PBMC media then plated in a 24-well plate. For inhibitor-treated conditions, inhibitor was added to the microtube just prior to rotation.

For the sNLuc IMCs (**Table 1, #8-27**): 5E+05 CD4+ T cells were inoculated with virus at a TZM-bl MOI of 0.1. Controls for the CD4+ T cell infection included: cells with media only, Env Minus sNLuc Env-IMC, NL-BaL sNLuc Env-IMC treated with 10 µM of IDV, cells inoculated with either A.R880F-sNLuc.6ATRi or D.191859-sNLuc.6ATRi treated with 10 µM of NVP. Over 2 weeks, 20 µl of supernatant was taken from each well, placed into a white 96-well luminometer plate, combined with 20 µl of the Promega Nano-Glo™ Luciferase Assay System, then analyzed for RLU readout via a Promega GloMax® 96 Microplate Luminometer (rate of 1 second/well). RLU values were recorded for each well over 14 days. Collected data were graphed and visualized using GraphPad Prism.

For the mCD24 Env-IMCs (**Table 1, #1-7**): 3E+05 cells were inoculated with virus at a TZM-bl MOI of 1. An MOI of 1 was used to ensure that a sufficient number of infected

cells would be detectable by flow cytometry after 5 days. Controls included cells without virus, Env Minus mCD24 Env-IMC (**Table 1, #7**), and the mCD24 Env-IMCs were treated with 10 μM of NVP. For the cells inoculated with mCD24 Env-IMCs, at 5 days post infection, cells were stained with a panel of antibodies (**Table 2**) and acquired using a BD FACSymphony™ flow cytometer. Collected data were then analyzed using FlowJo and visualized using GraphPad Prism. Cells were gated on based on the following expression profile: CD3+/CD8-/mCD24+.

Cervical tissue dissection and infection with HIV reporter viruses

We have previously described our tissue dissection and infection methods[34]. Briefly, remnant cervical explant tissue (CET) was acquired from donors who were pre-menopausal, receiving medically necessary hysterectomies, and cancer-free according to pathology reports. CETs were washed and cultured in media containing the following: RPMI 1640 medium, 1X Modified Eagle's medium (MEM) non-essential amino acids solution, 1 mM sodium-pyruvate, 50 μg/ml gentamicin, 15% fetal bovine serum (FBS), 2 mM L-glutamine, 100 U/ml penicillin, 100 ug/ml streptomycin, and 30 U/ml IL-2. The ecto- and endo- cervical mucosal surfaces were excised from the CETs and then further dissected into uniform 2 mm^3 blocks. These CET blocks were incubated with reporter Env-IMC or TF-IMCs overnight, washed, and then cultured on top of a collagen raft in one well of a 48-well plate (one CET block per raft per well). The CETs in this model were not polarized. For inhibitor-treated conditions, inhibitors were added at the time of viral inoculation.

For sNLuc IMCs: Between 6-8 CET blocks of ecto- and/or endo- cervix for each donor were inoculated with one sNLuc Env-IMC. Due to the size of the panel and the small

amount of tissue typically received from one donor, not every donor could be inoculated with the entire sNLuc Env-IMC or TF-IMC panel at once. Details regarding the number of donors inoculated with each sNLuc Env-IMC are described (**Supp. 1**). Over 2 weeks, culture supernatant was sampled daily from each well containing a CET block inoculated with a sNLuc Env-IMC, combined with the Promega Nano-Glo™ Luciferase Assay System, and analyzed for relative light units (RLU) with a luminometer. The raw RLU values were normalized to the RLU values acquired on day 2 to minimize background RLU (**Supp. 2**). Slopes of the normalized RLU data acquired across different time windows from each virally-inoculated individual tissue block were calculated to assess viral replication in each CET block. The application of slope to interpret changes to HIV reporter virus activity over time in human tissues is novel. However, there is precedence for it in the published literature. Slopes have been used to quantify changes to: HIV-1 reverse transcriptase activity and p24 expression over time *in cellulo*[60], HIV-1 viral load over time in humanized mice *in vivo*[61], and GFP expression from a GFP-reporter T cell line over time in the presence of HIV-1[62,63]. For our analyses, the slope represented the change in sNLuc expression over time and was calculated using a semi-log line of fit ($y=10^{(m(\log x)+b)}$). The normalized RLU values ("y"; logarithmic) over time ("x"; linear) were used to calculate slope ("m") for each virally-inoculated CET block. Slopes were calculated for 3 different time windows: (i) early: days 2-4, (ii) late: days 5-14, or (iii) all: days 2-14. The slopes from days 2-14 were then categorized as negative (<0), low (0.0001-0.004999), medium (0.005-0.04999), or high (>0.05) to determine the extent of viral replication as a function of sNLuc expression in the CETs. Slopes were then statistically assessed.

For mCD24 IMCs: 3-4 replica CET blocks were inoculated with the mCD24 Env-IMCs for each donor. Due to limitations in tissue availability, the entire mCD24 Env-IMC panel was not able to be used for every donor, but a minimum of 2 donors were inoculated with each mCD24 Env-IMC. At 4 days post-inoculation, the mCD24-infected tissue blocks were transferred to microtubes containing RPMI 1640, 7.5% FBS (vol/vol), and 5-10 µM of Collagenase IV. The tubes were transferred to a ThermoMixer set to 37 °C and 600 rpm and digested for ~24 hours. A 40 µm sterile cell strainer was secured to a 50 ml conical tube and the contents of the microtube were pipetted through the strainer to filter out individual cells. The strainer was rinsed with 1 ml PBS, and the cells at the bottom of the 50 ml tube were transferred to a FACS tube. Cells were stained with a panel of antibodies (**Table 2**). Compensation controls were established using compensation beads before acquiring flow samples via a BD FACSymphony™ flow cytometer. All flow data were analyzed using the FlowJo Software. Infected CD4 T cells were identified based on their forward/side scatter profile, absence of CD8 expression, and expression of CD3 and mCD24.

Soluble CD4 (sCD4) assay

The sCD4 assay has been described previously[64,65]. Media for this assay included the following: DMEM, 10% FBS, 25 mM HEPES, 2 mM L-glutamine, 100 U/ml of Penicillin-Streptomycin, and 10 µg/ml DEAE-dextran. Soluble CD4 (sCD4) was serially diluted 3-fold eight times (1000 nM starting concentration) and incubated with 10^4 IU/ml of virus for 1 hour at 37° C. TZM-bl cells (10^4) were added to sCD4-virus and incubated for 48 hours at 37° C. The viruses used for this assay are indicated (**Table 1, #8-17 and #25-28**). After 48 hours, cells were lysed using 1x Passive Lysis Buffer and transferred to

Table 2. Flow cytometry antibody panel

Fluorophore	*Marker*	*Description*
AQUA 515	Dead	Dead cell marker
BV711	CD3	T cell marker
PE	CD4	T cell marker
BUV563	CD8	T cell marker
APC	mCD24	Reporter HIV marker

Table 3. Demographic information of the 46 CET donors

Age		*Race*		
Mean	43.2	**Black**	19	41.3% of Total
Median	42.5			
Maximum	62	**White**	27	58.7% of Total
Minimum	24			
Mode	42	**Other**	0	0% of Total

a white 96-well luminometer plate. The contents of the plate were combined with the Promega Luciferase Assay System according to the manufacturer's protocol, and the plate was read using a VICTOR™ X Multilabel Plate Reader. IC50 values of these data were calculated using the ATLAS Science Portal software (SCHARP).

RESULTS

Subtype A and D Env-IMCs infect and replicate similarly in cellulo

Herein, we implemented a reporter virus design based on our work previously published in Alberti *et. al*[32] that would permit the interrogation of Env-based properties of HIV-1 transmission *ex vivo,* in relation to our central hypothesis (**Fig. 1A**). We selected two reporter genes for our reporter virus design that have been used in previous *ex vivo* mucosal studies of HIV-1 transmission (sNLuc[47,48]; mCD24[39,66,67]). The sNLuc reporter permits the sensitive detection of productive HIV-1 infection and replication through culture supernatant. The mCD24 reporter allows for the quantification of *de novo* HIV-infected cells through flow cytometric methods. Our experimental strategy was focused on biological properties mediated by subtype-specific Env glycoprotein and therefore, the Env ectodomain (the extracellular regions of gp120 and gp41) coding region of NL4-3 was exchanged with the ectodomain coding regions of other HIV strains. The design of the reporter Env-IMCs thus ensured that all viral genes were identical except for *env.* We previously reported that the *in vitro* neutralization and cell tropism phenotypes of transmitted/founder (TF) viruses were preserved after transferring their ectodomains into an isogenic proviral reporter backbone[36,68,69]. To assess subtype-specific Env-based properties affecting HIV-1 transmission *ex vivo,* we inserted the ectodomains of TF from two pathogenically and genetically distinct HIV-1 subtypes (A and D) into the reporter

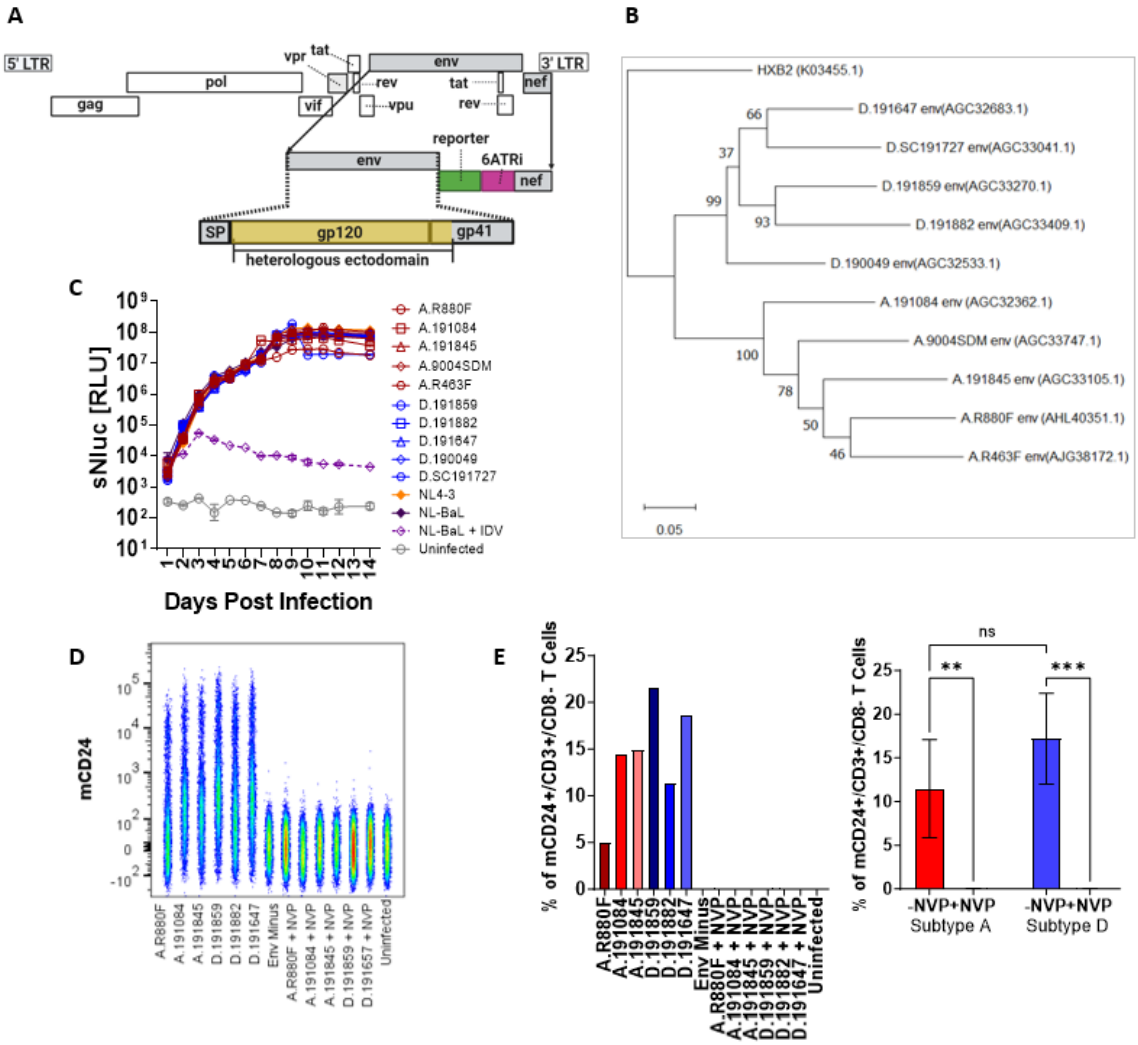

Figure 1. Subtype A and D Env-IMC reporter constructs infect and replicate similarly *in vitro*.

(A) Schematic of reporter Env-IMC.

(B) The evolutionary history of the Subtype A and D *env* sequences was inferred by using the Maximum Likelihood method and JTT matrix-based model. Evolutionary analyses were conducted in MEGA11.

(C) Primary CD4+ T cells from one PBMC donor were infected with a panel of sNluc Env-IMCs at a TZM-bl MOI of 0.1. RLU values were measured over 14 days. Graphed data includes the geometric means of the RLU values with 95% CI.

(D) Raw flow cytometry data showing the number of cells with positive mCD24 expression (y-axis) after 5 days in primary CD3+/CD8- CD4+ T cells infected with mCD24 Env-IMCs and treated with or without 10 μM of NVP (x-axis).

(E) The number of T cells that express mCD24 following inoculation of primary CD4+ T cells with individual mCD24 Env-IMCs (left). Data were then summarized and statistically assessed by viral subtype and inclusion/absence of NVP (right). A Two-way ANOVA was used to determine significance between the two subtypes and between inhibitor treated and untreated conditions.

NL4-3 isogenic backbone described above, then applied the reporter Env-IMCs to CETs (**Fig. 1A**).

Subtypes A and D co-circulate in the same populations in Africa (reviewed in[70]) but have distinct pathogenic outcomes *in vivo*. Subtype D-infected individuals experience more rapid CD4+ T cell decline and disease progression compared to those infected with subtype A, resulting in faster time to AIDS onset[23,28,31,71-77]. Subtype D has also been demonstrated to have greater transmission fitness than subtype A *ex vivo*[25]. Désiré *et. al* reported that subtypes A and D have the largest genetic distance of all group M HIV-1 subtypes[33]. Thus, based on their pathogenic and genetic distinctiveness, we hypothesized that subtypes A and D may have distinguishable mucosal transmission phenotypes in the *ex vivo* CET model. We identified 5 subtype A and 5 subtype D TF viral Envs to use for our studies that had been described previously in Baalwa *et. al*[58]. A Maximum Likelihood phylogenetic tree is shown to illustrate the inferred relationships of the 5 A and 5 D TF Env sequences (**Fig. 1B**)[78-80].

The subtype A and D Env-IMCs were first assessed for their ability to infect and replicate in primary human CD4+ T cells. Primary CD4+ T cells were inoculated at an MOI of 0.1 with either the HIV-1 subtype A and D sNLuc Env-IMCs or control sNLuc Env-IMCs expressing the ectodomains of either NL4-3 or BaL (**Table 1, #8-19**). T cells inoculated with the BaL sNLuc Env-IMC were treated with or without 10 μM of the protease inhibitor Indinavir (IDV) as an additional control. The cell culture supernatants were sampled daily and analyzed for expression of the sNLuc reporter as measured through relative light units (RLUs). Consistent with its mechanism of action, the RLU values of the IDV-treated condition increased until day 3 before declining, indicating replication was

inhibited beyond the first round (**Fig. 1C**). The RLU values for all of the subtype A and D sNLuc Env-IMCs increased with nearly identical kinetics for 8 days before plateauing. The results indicate that the subtype A and D Env-IMCs infect and replicate similarly in primary human CD4+ T cells *in vitro*.

The infection and replication competency of the subtype A and D mCD24 Env-IMCs were evaluated by inoculating PBMC-derived CD4+ T cells at an TZM-bl MOI of 1 and culturing them for 5 days. In parallel cultures, virus-inoculated cells were treated with 10 μM of the reverse transcriptase inhibitor nevirapine (NVP) to inhibit *de novo* infection. As an additional control, T cells were inoculated with Env Minus mCD24 Env-IMC (**Table 1, #1-7**). After 5 days, the cells were stained with a panel of antibodies (**Table 2**) and analyzed by flow cytometry to analyze HIV-1 infection and expression of mCD24 (**Fig. 1D; Supp. 3**). The percent of mCD24-expressing cells was identified for the following: 3 subtype A mCD24 Env-IMCs, 3 subtype D mCD24 Env-IMCs, NVP-treated subtype A and D mCD24 Env-IMCs, the Env Minus mCD24 Env-IMC, and an uninfected control (**Fig. 1D, E**). The flow data were analyzed to determine percent of mCD24+ cells for each experimental condition, and analyzed to assess statistical significance between the A and D subtypes and between NVP treated and non-treated (**Fig. 1E**). The data showed a significant difference in mCD24 expression between NVP-treated and untreated conditions, indicating that the mCD24 Env-IMCs were infectious *in vitro* and that mCD24 expression could be used to distinguish infected cells from uninfected cells. Further, there was no significant difference in the percent of infected T cells (based on mCD24 expression) between the A and D virus groups. These data, coupled with the sNLuc data,

demonstrated that the subtype A and D Env-IMC reporter constructs are similarly infectious and replication-competent *in cellulo.*

The subtype of HIV-1 Env affects virus replication in cervical tissue ex vivo

Subtype D strains of HIV-1 exhibit greater replicative fitness than subtype A *in vitro* and *ex vivo*, which is considered to be analogous to the disease outcomes of subtype D observed *in vivo*[14,25,27,76]. Yet, it is unclear whether there is a difference in how these two subtypes are transmitted across mucosal surfaces. A major obstacle impeding studies of mucosal transmission is that current *ex vivo* models are not sensitive enough to elucidate the earliest viral infection and replication events. *Ex vivo* approaches incorporating CETs have been used previously to model the mucosal transmission and replicative fitness of HIV-1. However, whether these approaches are sensitive enough to interrogate transmission events is unclear since some reported that viral infection/replication was minimally detectable before 6-10 days following virus challenge. We recognized this sensitivity issue and predicted that using sNLuc Env-IMCs to infect CETs would permit the sensitive detection of subtype A and D viral infection/replication earlier than 6 days post-infection (and closer to the time of transmission). We also hypothesized that the sNLuc Env-IMCs could be used to distinguish subtype A and D transmission, infection, and replication phenotypes in explant tissues.

Remnant cervical explant tissue (CET) specimens were obtained with IRB approval and donor consent from 46 non-cancerous patients undergoing medically necessary hysterectomies, 35 of which were used to generate the experimental data shown in Figures 2, 3, and 5 (**Table 3**). The remaining 11 donor tissues were used to generate data for Figures 4 and 6-8. We previously described our methods for processing and infecting CETs with

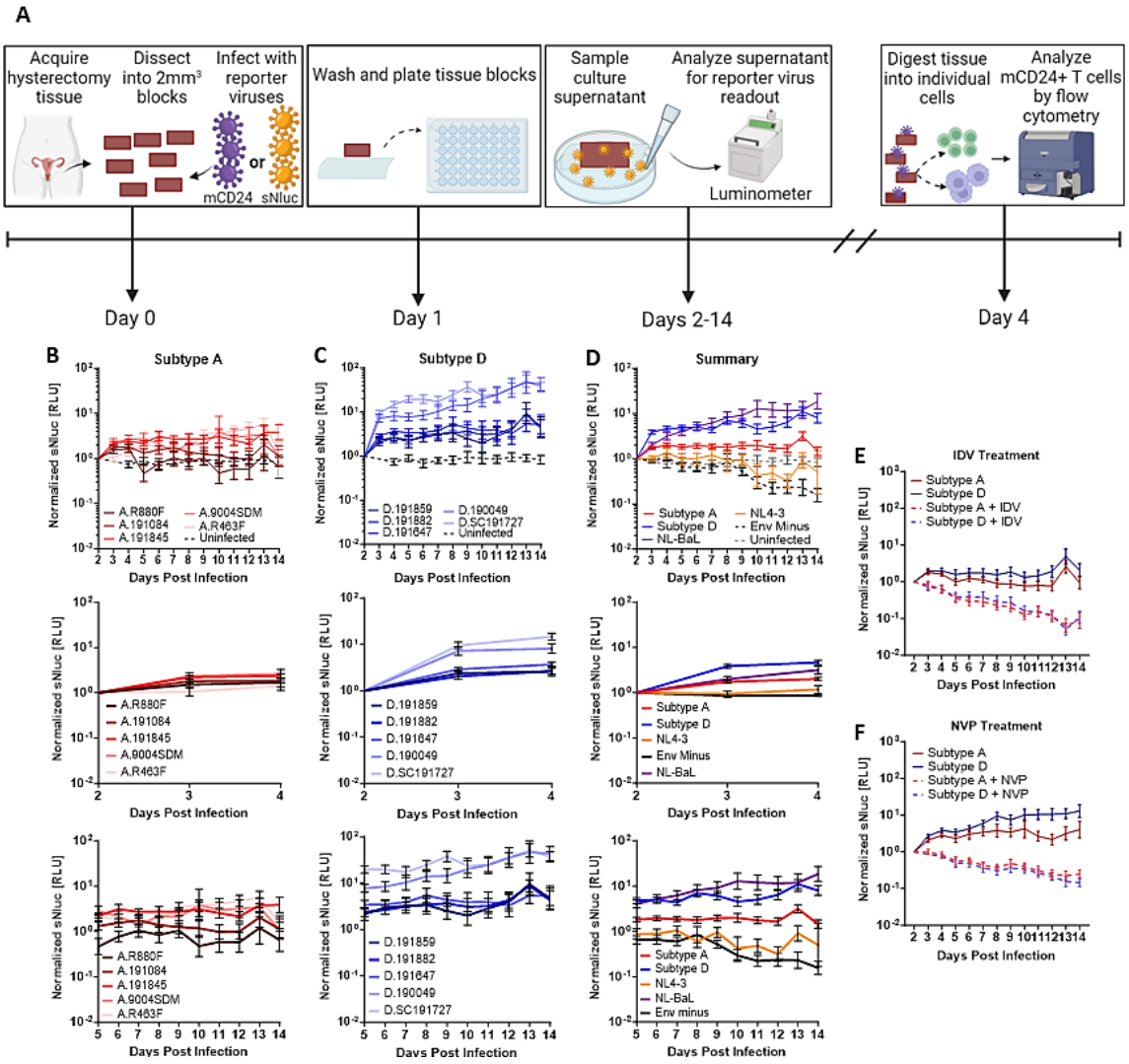

Figure 2. Subtype A and D Env-IMCs have distinct replication kinetic profiles in CETs.

(A) Overview of workflow for CET dissection, infection with reporter Env-IMCs, and primary methods for data acquisition.

(B-D) CET blocks from 35 donors were inoculated with sNLuc Env-IMCs (Table 1, #8-20). The sNLuc activity was measured in relative lights units (RLU), and raw RLU values were normalized to the RLU values from day 2. The geometric means with 95% CI for the normalized RLU values at each time point are shown. The same normalized RLU values are shown at three different time windows: 2-14 days (top), 2-4 days (middle), and 5-14 days (bottom). Data is shown for all 5 individual subtype A sNLuc Env-IMCs (B) and all 5 individual subtype D sNLuc Env-IMCs (C).

(D) The normalized RLU data for all 5 individual subtype A from (B) and all 5 individual subtype D (C) sNLuc Env-IMCs were combined. The geometric means with error bars representing 95% CI of the combined subtype data are shown.

(E-F) CETs from 6 donors were inoculated with 3 subtype A and 3 D sNLuc Env-IMCs. In parallel, CETs were treated with 2 µM of IDV (E) or 20 µM of NVP (F).

reporter Env-IMCs for studies pertaining to mucosal HIV-1[34]. An overview of these methods is shown (**Fig. 2A**). For the experimental data shown in Figures 2, 3, and 5, we inoculated a total of 35 donor tissues with a panel of 5 subtype A, 5 subtype D, and 3 control sNLuc Env-IMCs (**Table 1, #8-20**). Raw RLU values were collected over 2 weeks for each individual tissue block, and the raw values were normalized to the RLU values acquired for that tissue block on day 2 (**Supp. 2**). Normalized RLU values acquired over 2 weeks were then graphed with respect to viral subtype, and the normalized RLU values for all 5 subtype A (**Fig. 2B**) and all 5 subtype 5 sNLuc Env-IMCs (**Fig. 2C**) are shown individually.

Upon visual inspection of the data, the normalized RLU values for the subtype D viruses appeared to increase, suggesting a steady rise in viral gene expression over time, while the normalized RLU values for the subtype A viruses appeared mostly stagnate, making interpretation of the data based on visual inspection alone challenging (**Fig. 2B,C**). However, this visual difference seemed to imply that viral gene expression *ex vivo* differed between the two subtypes. The combined normalized RLU values of all 5 subtype A and 5 subtype D sNLuc Env-IMCs were then graphed and compared to the normalized RLU values of the NL4-3, BaL, and Env Minus sNLuc Env-IMC controls (**Fig. 2D**). The virions derived from transfection of the Env-deficient proviral plasmid were non-infectious, and served as a negative control for sNLuc background in virus inoculum. BaL sNLuc Env-IMC has been used in previous work with CET and is an effective positive control because it efficiently infects and replicates in CETs[81-83]. NL4-3 was included because it utilizes the CXCR4 (X4) co-receptor for cell entry, and it has been shown previously that X4-tropic viruses either do not replicate or replicate poorly in CETs[27,81]. As expected, the normalized

RLU values for BaL sNLuc Env-IMC increased over the 2 weeks, while the values decreased for NL4-3 and Env Minus sNLuc Env-IMCs, suggesting a lack of viral replication in the CETs (**Fig. 2D**). In parallel, 6 of the 35 donors that were inoculated with 3 subtype A (**Table 1, #8-10**) and 3 subtype D (**Table 1, #13-15**) sNLuc Env-IMCs were also treated with either 2 μM of IDV (a protease inhibitor limiting viral replication to a single round) (**Fig. 2E**) or 20 μM of NVP (a reverse transcriptase inhibitor limiting *de novo* viral infection) (**Fig. 2F**). The normalized RLU values of both inhibitor-treated controls declined over the 14 days, suggesting that both the subtype A and the subtype D sNLuc Env-IMCs were infectious and replication-competent *ex vivo.*

The subtype A data were challenging to interpret from visual inspection alone, and we were unsure whether the data indicated that fewer CET blocks became infected or that they became infected at lower rates compared to subtype D-inoculated CETs (**Fig. 2B**). Thus, we devised a mathematical approach to determine whether a CET block was infected and to what extent the block was infected by calculating the slopes of the normalized RLU data acquired across different time windows from each virally-inoculated individual tissue block. For our analyses, the slope represented the change in sNLuc expression over time, where the normalized RLU values ("y"; logarithmic) over time ("x"; linear) were used to calculate slope ("m") for each virally-inoculated CET block using a semi-log line of fit ($y=10^{(m(\log x)+b)}$). Slopes were calculated for 3 different time windows: (i) early: days 2-4, (ii) late: days 5-14, or (iii) all: days 2-14.

Initially, we calculated the early slopes for the IDV- and NVP-treated conditions (**Fig. 3A**) described in (**Fig. 2E,F**) to establish whether initial viral infection and replication of the subtype A and D sNLuc Env-IMCs could be detected by sNLuc reporter readout.

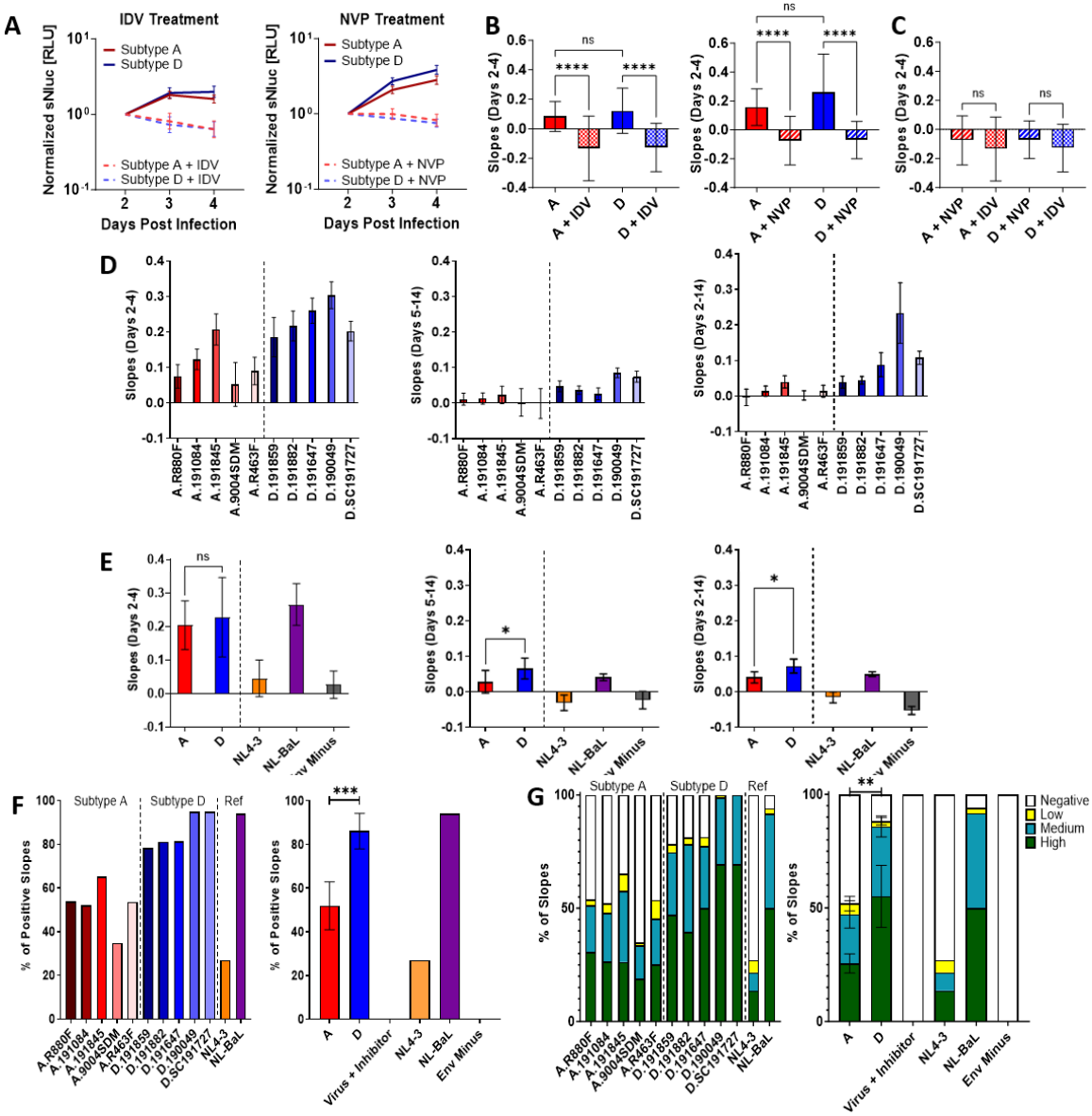

Figure 3. Subtype D Env-IMCs replicate more efficiently *ex vivo* than subtype A Env-IMCs.

(A) The normalized RLU values of the IDV and NVP treated conditions from Fig. 2, limited to the normalized RLU values from the "early" time window.

(B) The slopes of the IDV (left) and NVP (right) conditions from part (A) were assessed using a Kruskal-Wallis test to determine significance between inhibitor-treated and untreated experimental groups. Results of the assessment are shown for the IDV (left; $p<0.0001$) and the NVP (right; $p<0.0001$) data.

(C) The slopes of the IDV and NVP conditions from part (A) were assessed using a Kruskal-Wallis test to determine significance between the NVP and IDV conditions.

(D) Slopes were calculated for every CET inoculated with sNLuc Env-IMCs. Shown is the average with 95% CI of all the slopes for each sNLuc Env-IMC calculated for 3 different time windows, including: days 2-4, days 5-14, and days 2-14.

(E) The slopes for each individual sNLuc Env-IMC described in (D) combined by viral subtype. A Mann-Whitney test was conducted to assess significance between the slopes of the subtype A and D Env-IMCs at each of the three time windows. The analyses for days 2-4 (left; p=ns), days 5-14 (middle; p=0.0159), and days 2-14 (right; p=0.0278) are shown.
(F) The total percent of slopes that were positive from part (D) from days 2-14. Data were divided by individual sNLuc Env-IMC (left) or summarized by viral subtype (right), which shows the average of the percentages with 95% CI. The "Virus + Inhibitor" column includes all tissue blocks that had been inoculated with and A or D sNLuc Env-IMC and treated with IDV or NVP. A Mann-Whitney test was used to determine significance between the subtype A and D viruses (p=0.0007).
(G) The slopes from part (D) days 2-14 were further categorized as Negative (<0), Low (0.0001-0.004999), Medium (0.005-0.04999), or High (>0.05) for each individual sNLuc Env-IMC (left) and then summarized by viral subtype (right). A Mann-Whitney was used to assess the significance of slopes categorized as "High" between the subtype A and D viruses (p=0.0064).

The slopes of the non-inhibitor-treated conditions were significantly greater than the slopes of their inhibitor-treated counterparts, suggesting that initial infection and replication could be detected (**Fig. 3B**). We then compared the early IDV and NVP slopes to each other to determine whether the first round of virus infection could be distinguished from replication by the sNLuc reporter readout and whether there was evidence for virus infection when replication was inhibited (**Fig. 3C**). There was no significant difference in the early slopes between the IDV and NVP inhibitor-treated conditions. This result indicates that RLU values generated by the first round of virus infection were not specifically identifiable, and that at least one additional cycle of virus replication was required before RLU values were distinguishable over background.

To directly address the hypothesis and determine whether subtype A and D had distinct transmission and replication phenotypes *ex vivo*, slopes were calculated at each of the 3 time windows for every individual CET block from the 35 donors inoculated with the

subtype A and D sNLuc Env-IMCs (**Fig. 2B-D**). The average (with 95% CI) of the slopes of the individual 5 subtype A and 5 subtype D sNLuc Env-IMCs are shown for each time window (**Fig. 3D**). The averaged slopes at each time window were then combined based on subtype, and the slopes were statistically assessed for significance between the two subtypes (**Fig. 3E**). Although slopes for each individual virus varied widely (**Fig. 3D**), there was no significant difference in the combined slopes of the CETs inoculated by subtypes A and D for the "early" time window (**Fig. 3E**). This may suggest that subtype A and D Env-IMCs were transmitted similarly *ex* vivo. For the "late" and "all" time windows, however, the combined slopes of the subtype D Env-IMCs were significantly higher than those of the subtype A Env-IMCs, indicating a greater rate of change in subtype D sNLuc expression in the CETs after day 4 compared to subtype A.

To determine whether there was a difference in the ability of the two subtypes to sustain replication in the CETs following transmission, we further examined the slopes calculated from the days 2-14 time window (**Fig. 3D**). Based on the data from the NVP and IDV experiments, we concluded that a negative slope indicated an absence of productive viral infection and replication in the CETs, and that a positive slope in this model, relative to the inhibitor-treated conditions, indicated that a sNLuc Env-IMC was actively replicating in a CET block. Initially, we calculated the percent of slopes that were positive from all CET blocks inoculated with an individual Env-IMC, then averaged those percentages based on the subtype of the individual Env-IMCs (**Fig. 3F**). Significantly more of the subtype D slopes were positive (86.2%) than the subtype A slopes (51.9%), suggesting that subtype D was more likely to sustain replication following transmission to the CETs than subtype A. To further determine the extent of viral replication as a function

of sNLuc expression in the CETs, we categorized the days 2-14 slopes as negative (<0), low (0.0001-0.004999), medium (0.005-0.04999), or high (>0.05). A "high" slope indicated a substantial increase in sNLuc expression over time (**Fig. 3G**). Indeed, significantly more slopes from CETs inoculated with subtype D Env-IMCs were categorized as "high" (55.1%) compared to those inoculated with subtype A Env-IMCs (25.6%), suggesting that subtype D replicated more proficiently *ex vivo* than subtype A.

Since the only difference between the sNLuc Env-IMCs was the Env ectodomain, the data further suggest that the *ex vivo* replication phenotypes observed in Figures 2 and 3 were attributable to Env. Whether host-specific factors interact with Env to precipitate these subtype-specific *ex vivo* transmission and replication phenotypes is not known. Taken together, these data indicate that subtype A and D Env-IMCs may infect and replicate in CETs similarly within the first 72-96 hours of infection, but that subtype D is significantly more likely to sustain higher levels of replication *ex vivo* after 96 hours than subtype A. In summary, the subtype of HIV-1 Env affected the efficiency of viral transmission and replication *ex vivo*.

Subtype A and D Env sNLuc reporter viruses replicate similarly in CET compared to their full-length TF counterparts

The Envs used in this work to generate the subtype A and D Env-IMCs had been characterized previously in Baalwa *et. al*. Baalwa and colleagues generated full-length infectious and replication-competent IMCs of the 5 subtype A and 5 subtype D viruses (TF-IMCs) and used them to infect PBMC-derived CD4+ T cells from 3 different donors[58]. After quantifying p24 antigen concentrations over 16 days, they observed that the full-length subtype D IMCs had greater replication kinetics *in vitro* than subtype A. When we

tested our subtype A and D Env-IMCs *in vitro*, however, we observed no differences between their replication kinetics, or even their ability to infect and spread through culture (**Fig. 1C-E**). Based on the findings from Baalwa *et. al*, we sought to understand whether there was a difference in the replication kinetics between the sNLuc Env-IMCs and their sNLuc TF IMC counterparts *ex vivo.* We generated reporter TF IMCs using the entire proviral backbone of 2 subtype A (A.R880F and A.191845) and 2 subtype D TF viruses (D.191859 and D.191882) with the sNLuc reporter sequence inserted between *env* and *nef* (TF IMCs), as described above[32] (**Table 1, #21-24**). These 2 A and 2 D TF viruses were selected because they had diverse replication kinetics *ex vivo.* The infection and replication competency of the sNLuc TF IMCs was verified through the use of primary CD4+ T cells isolated by negative selection from PBMCs, as described above (data not shown).

CETs from 6 donors (6-12 CET blocks per donor) were inoculated as described above (**Fig. 2A**) with the 4 sNLuc TF IMCs (**Table 1, #27-30**) and the cognate sNLuc Env-IMCs (**Table 1, #14, #16, #19, and #20**), with or without inhibitors. Culture supernatant samples were collected over 10 days, analyzed for RLU, and the RLU values were normalized. Results represent the combined analysis of all 6 donors. The replication kinetics of the reporter IMCs and their Env-IMC counterparts for both subtype A (**Fig. 4A**) and subtype D (**Fig. 4B**) are shown. Slopes from days 2-4 and days 2-10 were calculated for the sNLuc TF-IMCs and the Env-IMCs. When comparing the slopes from those two time windows, there was no significant difference in the slopes between the sNLuc TF-IMCs and Env-IMCs for either subtype (**Fig. 4C**). This suggests that replication between the reporter TF IMCs and their Env-IMC counterparts were similar in the CETs at both time windows. The percentage of positive slopes from days 2-10 was identified for both

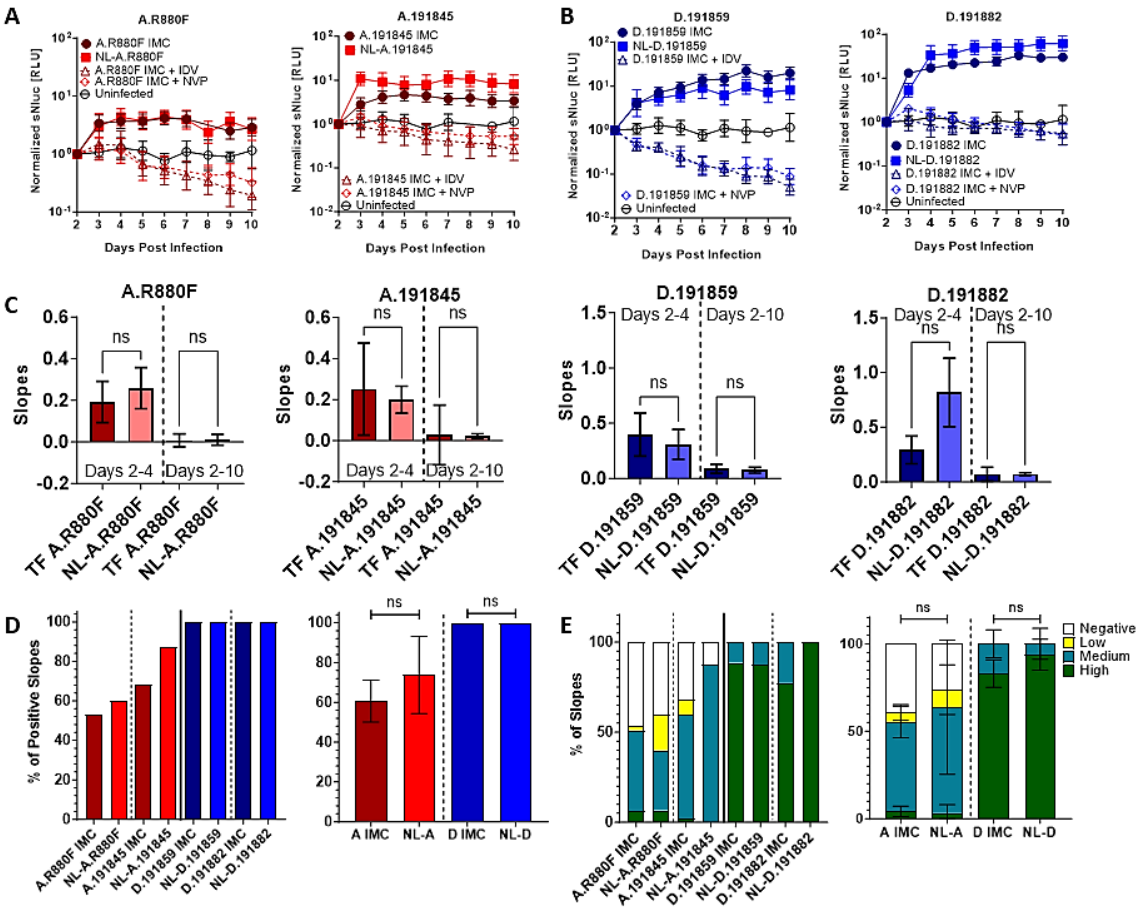

Figure 4. Subtype A and D sNLuc TF-IMCs infect and replicate similarly to their Env-IMC counterparts.

(A-B) CETs from 6 donors were infected with subtype A and D TF-IMC sNLuc reporters (indicated as "IMC) and their respective sNLuc Env-IMC counterparts (indicated as "NL-"): (A) A.R880F (left) and A.191845 (right); (B) D.191859 (left) and D.191882 (right). TF-IMC-infected tissue was also treated with 2 µM of IDV or 20 µM of NVP. The graphed data represent the geometric means with 95% CI for the normalized RLU values at each time point.

(C) Slopes of the RLU values from days 2-4 and days 2-10 were calculated as described above. Mann-Whitney t-tests comparing the slopes of all tissue blocks inoculated with a full-length IMC sNLuc reporter to tissue blocks inoculated with the Env-IMC counterpart. Two separate t-tests were conducted; one for the slopes from days 2-4 and one for the slopes from days 2-10.

(D) The percent of tissue blocks with positive slopes inoculated with the 4 TF-IMCs compared to their Env-IMC counterparts (left). Data were then summarized by subtype and whether the virus was a TF-IMC (indicated as "A IMC" or "D IMC") or an Env-IMC (indicated as "NL-A" or "NL-D") (right). A two-way ANOVA was used to determine significance between the TF IMC and Env-IMC groups.

(E) Slopes were categorized as Negative, Low, Medium, or High. The categorized slopes of the 4 TF IMCs were compared to their Env-IMC counterparts (left). Data were then summarized by subtype and whether the virus was a TF IMC or an Env-IMC (right). A Mann-Whitney t-test was used to determine significance for the percent of "High" slopes between the Env-IMC and TF-IMC groups.

the reporter TF IMCs and the Env-IMCs. Following the combined analysis of the 2 viruses representing each of the subtypes, there was no significant difference in the percentage of positive slopes between the TF IMCs and Env-IMCs for either subtype (**Fig. 4D**). When the days 2-10 slopes were further categorized as negative, low, medium, or high, there was no difference in the "High" category between the reporter TF IMCs and Env-IMCs for either subtype (**Fig. 4E**). Overall, the sNLuc Env-IMCs replicated in the CETs similarly to their reporter TF-IMC counterparts, indicating that placement of the Env ectodomain into an isogenic proviral reporter backbone did not significantly affect the *ex vivo* subtype-specific replication of the A.R880F, A.191845, D.191859, and D.191882 sNLuc Env-IMCs. Importantly, the subtype-specific replication kinetics of the sNLuc Env-IMCs observed in Figures 2 and 3 were also observed with the TF-IMCs.

Subtype A viruses are more infectious and replicate more efficiently in ectocervix compared to endocervix

Previous studies have shown that human cervical tissues differ in regards to HIV-1 target cell populations and vulnerability to HIV infection, and that abundance of target cell populations can vary before and after sexual intercourse[84-87]. Of all the cervical mucosal surfaces, the transformation zone (TZ) contains the highest numbers of HIV-1 target cells, including CD4+ T cells and Mφs[86]. Trifonova *et. al* reported that ectocervix contains more CD4+ T cells, CD8+ T cells, and B cells than endocervix, and that ectocervix has higher

concentrations of HIV-susceptible CD4+ T cells than endocervix. Despite this, using an agarose-embedded polarized explant model with 6 donor cervixes, they observed that endocervix supported the replication of HIV_{BaL} slightly better than ectocervix[84]. We are unaware of any studies that have compared the transmission or replication properties of subtype A and D TF viruses between the endo- and ecto- cervix tissues. Thus, we hypothesized that the subtype A and D sNLuc Env-IMCs would have distinct transmission and replication profiles in different types of cervical tissues.

To investigate this hypothesis, we separated the sNLuc data described in Figures 2 and 3 based on whether the CET blocks originated from ectocervix or endocervix. The 35 donor cervical tissues we received were cut in such a way that preserved much of the ecto- and endo- mucosal surfaces, but not enough of the TZ was preserved for sufficient experimentation (**Fig. 5A**). Thus, our analysis focused only on ectocervix and endocervix and excluded the TZ. The normalized slopes values calculated from each of the ecto- and endo- CET blocks inoculated with the subtype A and D sNLuc Env-IMCs were statistically analyzed, both with regards to tissue type and viral subtype. The results revealed that the days 2-4 slopes were significantly different between ectocervix and endocervix CET blocks inoculated with subtype A virus group, but there was no difference observed for with the subtype D viruses (**Fig. 5B**). This suggests that subtype A viruses may be transmitted to and/or replicate in ectocervix differently from endocervix *ex vivo* within the first 96 hours following viral inoculation. When comparing the days 2-14 slopes data, the difference between the subtype A-inoculated ectocervix and endocervix CET blocks remained significant, while there was no difference between subtype D-inoculated blocks (**Fig. 5C**). The percent of positive slopes from days 2-14 were then assessed to determine if there was

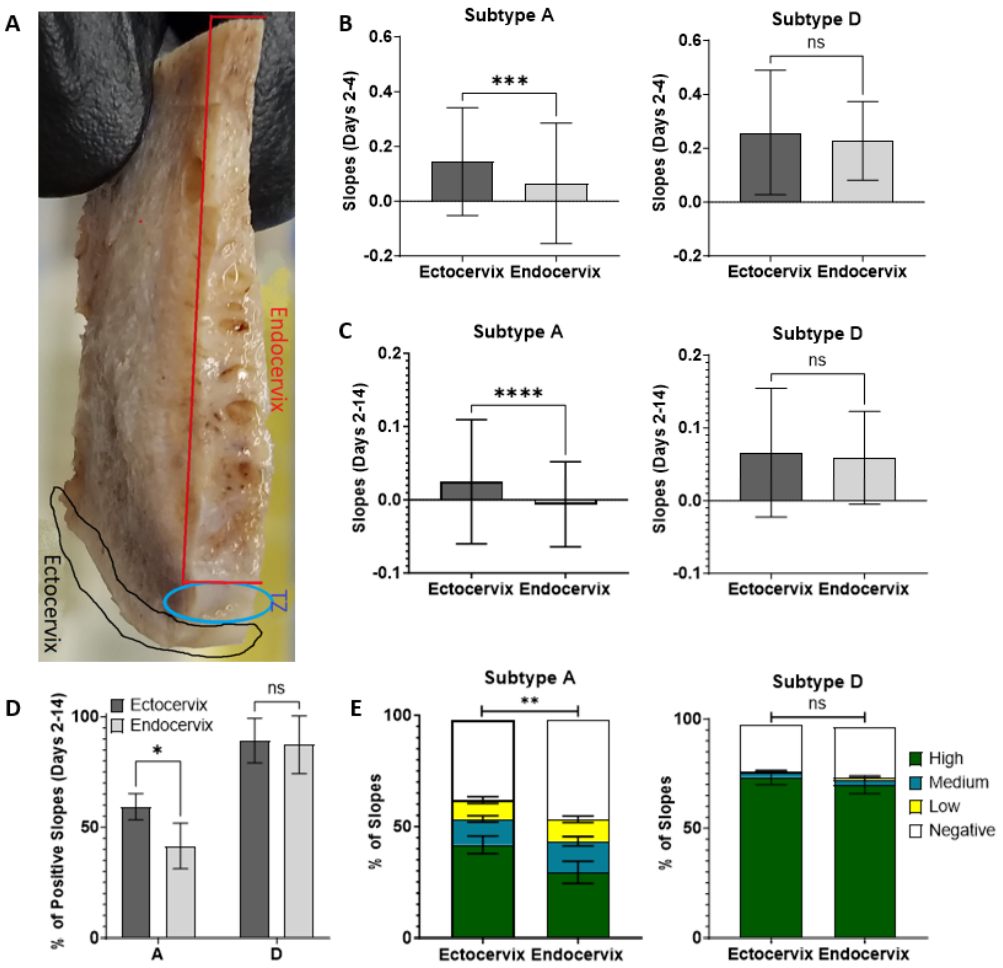

Figure 5. Subtype A Env-IMCs replicate differently in ectocervix compared to endocervix.

(A) Formalin-fixed CET. The transformation zone (TZ) is circled in blue, the ectocervix is circled in black, and the endocervix is underlined in red.

(B-E) The slopes data acquired in Figures 2 and 3 were separated by whether the CET blocks originated from ectocervix or endocervix. These data were then statistically assessed with regards to viral subtype and tissue type.

(B) The average with SD of the slopes from days 2-4 of all ectocervix and endocervix tissue blocks infected with either subtype A (left) or subtype D (right). A Mann-Whitney test was used to determine significance (Subtype A, p=0.0004; Subtype D, p=ns).

(C) The average with SD of the slopes from days 2-14 of all ectocervix and endocervix tissue blocks infected with either subtype A (left) or subtype D (right). A Mann-Whitney test was used to determine significance (Subtype A, p<0.0001; Subtype D, p=ns).

(D) The percent of positive slopes from days 2-14 for ecto- and endo- cervix infected with either subtype A or D sNLuc Env-IMCs. A Two-Way ANOVA was used to determine significance between the tissue types for subtype A (p=0.0279) and subtype D (p=ns).

(E) The positive slopes from part (D) were further categorized as Negative (<0), Low (0.0001-0.004999), Medium (0.005-0.04999), or High (>0.05). A Two-Way ANOVA was used to determine significance of slopes categorized as "High" between ectocervix and endocervix for both viral subtypes (Subtype A, p=0.0047; Subtype D, p=ns).

a difference between the two tissue types to sustain viral replication. Ectocervical tissues inoculated with subtype A were significantly more likely to have a positive slope than endocervix (**Fig. 5D**). The slope values were further analyzed by categorization as negative, low, medium, or high for the ectocervix and endocervix CET blocks inoculated by subtype A or D sNLuc Env-IMCs (**Fig. 5E**). Significantly more slopes were considered "High" in ectocervix inoculated by subtype A than endocervix, indicating that subtype A sNLuc expression over time was greater in ectocervix. There was no difference in the "High" slopes between ectocervix and endocervix inoculated with subtype D virus. Taken together, these data indicate that ectocervix is more likely to support subtype A viral transmission and replication than endocervix *ex vivo*, while subtype D transmission and replication are similarly supported by the two mucosal tissues.

Mucosal CD4 T cells are similarly infected ex vivo by subtype A and D Env-IMCs

Previous CET models have demonstrated that productive explant infection by R5-tropic viruses preferentially occurs through activated CD4+ T cells, which are key targets of early mucosal HIV-1 infection[81,88,89]. However, whether infection of CD4+ T cells contributes to the subtype-specific transmission and replication phenotypes observed *ex vivo* is unclear. From the sNLuc data, we observed no significant difference between the subtype A and D virus replication kinetics from the days 2-4 "early" time window, but a significant difference was observed between the subtypes from days 5-14 (**Fig. 3E**). Based on these data, we sought to interrogate the CD4+ T cell populations at day 4 to: (i)

determine if there was a difference between early subtype A and D infection of tissue resident CD4+ T cell populations and (ii) assess whether infection of the CD4+ T cells may have contributed to the subtype-specific *ex vivo* transmission and replication phenotypes. We hypothesized that more CD4+ T cells would be infected by subtype D virus by day 4 days compared with subtype A virus.

CET blocks were prepared from 5 different donor tissues as described above (**Fig. 2A**) and then inoculated with 3 subtype A and 3 subtype D mCD24 Env-IMC viruses and the Env Minus mCD24 Env-IMC control virus (**Table 1, #1-7**). In parallel, virus-inoculated tissue blocks were treated with 20 μM NVP. A limitation in tissue availability meant that infection in ecto- and endo- CET blocks was not able to assessed separately, and these blocks were combined for flow analysis. After 4 days in culture, individual cells were isolated from the CET blocks as described in the Methods section. Cells were stained using the panel of flow cytometry antibodies listed in **Table 2**. The number of mCD24+/CD3+/CD8- CD4 T cells for each experimental condition was determined (**Fig. 6A; Supp. 4**). The data were then statistically assessed to determine if there was a difference in the infection of the T cells by subtypes A and D mCD24 Env-IMC and whether infection was distinguishable from inhibitor-treated controls (**Fig. 4B**). Based on the results from the 5 donors, we determined that there was no statistically significant difference in the percentage of infected (CD3+/CD8-/mCD24+) T cells between subtypes A and D. Inhibitor-treated conditions were significantly different from non-treated conditions. Thus, while CD4 T cells may still be key to establishing productive infection in CETs, CD4 T cell infection likely did not contribute to the subtype-specific *ex vivo* mucosal transmission and replication phenotypes observed *ex vivo*. It is possible that one

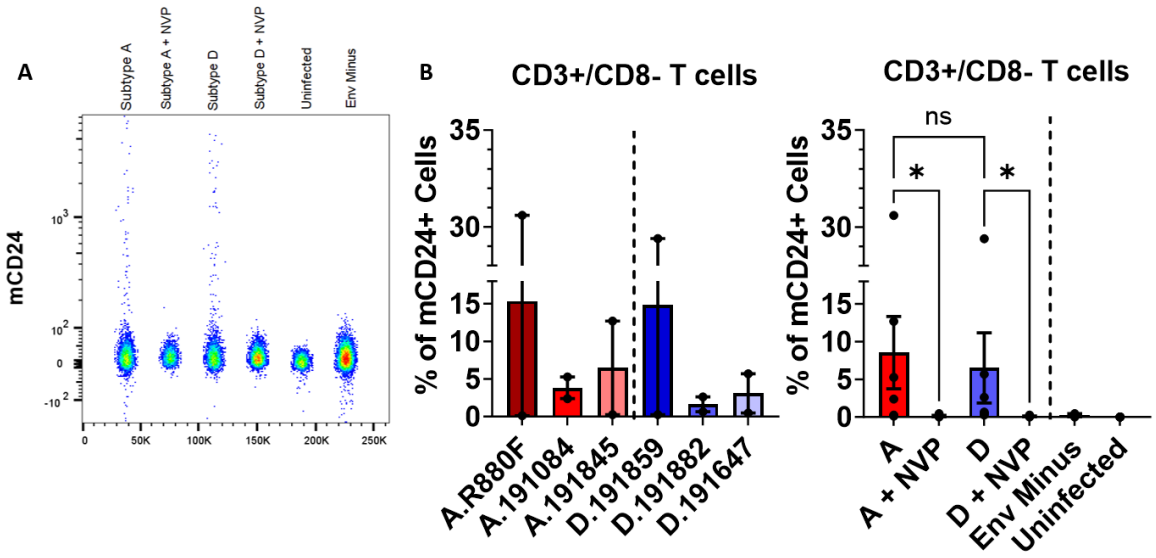

Figure 6. Subtype A and D Env-IMCs similarly infect CD4 T cells derived from CETs at early timepoints.

(A) Raw flow data showing the number of mCD24+ CD4 T cells derived from 3-4 digested CETs that had been inoculated with one subtype A or one subtype D mCD24 Env-IMC with or without NVP treatment, in parallel with uninfected and Env Minus controls. The CD4 T cells were assessed for mCD24 expression, the gating strategy for which is shown in Supp. 4.

(B) CETs from 5 donors were inoculated with a panel of mCD24 Env-IMCs (**Table 1, #1-7**), digested at 4 days post-inoculation, and the percent of mCD24+/CD3+/CD8- cells was identified for each mCD24 Env-IMC. Individual subtype A and D mCD24 Env-IMCs were used to inoculate 2 donors (left), and these data were further combined by subtype (right). The combined data show the average with SEM. A Kruskal-Wallis test was used to assess significance among groups, including subtype and NVP treatment.

or more other cell types may have contributed to the subtype-specific replication kinetics observed in the CETs.

Mutations to HIV Env at residues 429 and 432 affect subtype-specific transmission and replication kinetics ex vivo

Compared to subtype A, subtype D Envs are rich in AU-biased sequences, which have been shown to strongly induce early host interferon synthesis and response *in vitro*[90]. This may affect subtype D pathogenesis *in vivo* as it may lead to greater immune activation during early infection[15,90-92]. Additionally, host cell entry efficiency of subtype D is greater than that of subtype A[76], and this entry efficiency has been associated with faster CD4+ T cell decline following infection[16]. The efficient cell entry of subtype D compared to subtype A may be linked to differences in the binding of the Env glycoprotein to CD4. Zhang *et. al* reported subtype A Env contains a basic residue at 429 (that is almost exclusively arginine) that interacts with a highly conserved aspartic acid at residue 113 to form a salt bridge. The salt bridge locks the inner and outer domains of subtype A Env trimer into a pre-fusion configuration, stabilizing it in a closed conformation that limits its transition to more open conformations (i.e., State 2 and 3), thus reducing the flexibility and exposure of the CD4 binding site[35]. Notably, subtype D Envs primarily have a glycine or glutamic acid residue at the 429 position but instead has a basic residue at 432 (**Fig. 7A**), which is reported to still form a salt bridge with residue 113[35]. Although we are currently unaware of any published structures of subtype D Env, we suspect that the glycine/glutamic acid at residue 429 in subtype D Env may be more destabilizing at this position than a basic residue, potentially increasing the flexibility of the gp120 inner and outer domains and exposure of the CD4 Phe-43 binding site.

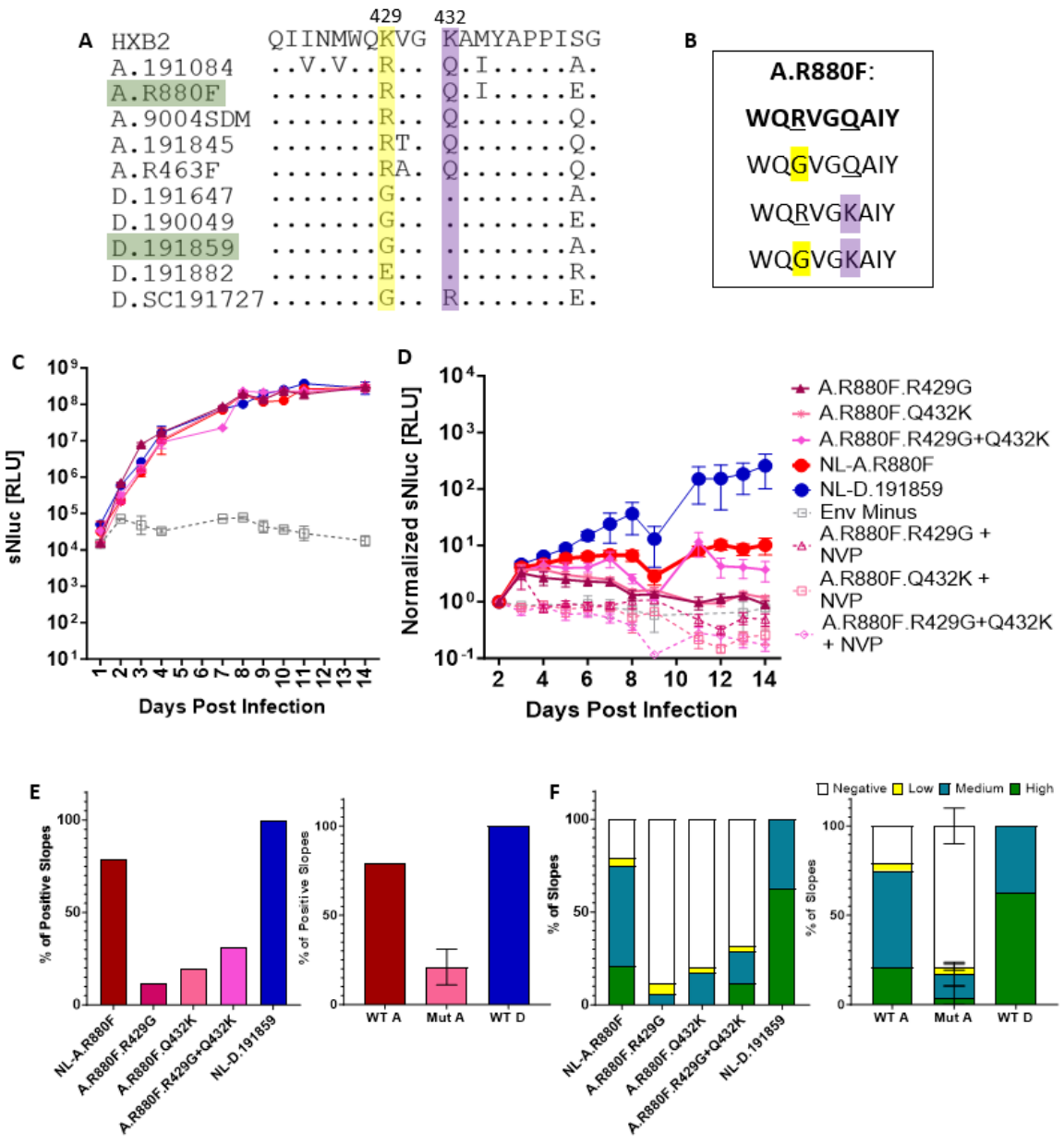

Figure 7. Mutations to HIV Env at residues 429 and 432 affect subtype-specific replication kinetics.

(A) Alignment of 5 subtype A and 5 subtype Env sequences to HXB2 Env. Residue 429 is highlighted in yellow, and residue 432 is highlighted in purple.

(B) The region of A.R880F Env spanning residues 427 to 435 (bold). Mutations introduced to residue 429 are highlighted in yellow and mutations to residue 432 are highlighted in purple.

(C) CD4+ T cells inoculated with the 3 subtype A mutant constructs in parallel to their wildtype counterparts, the D.191859 Env-IMC, and the Env Minus sNLuc Env-IMC.

(D) CETs from 5 donors were infected with the 3 mutant A Env-IMCs, their subtype A wildtype counterpart, NVP-treated A Env-IMCs, D.191859 Env-IMC, and Env minus. RLU values were collected over 14 days and then normalized to the RLU values collected on day 2. Drop in RLU values on day 9 due to 80% culture media change.
(E) The total percent of tissue blocks that had positive slopes from days 2-14 for each individual mCD24 Env-IMC (left) and then summarized by viral subtype ("WT A" or "WT D") or whether the virus was a mutant ("Mut A") (right).
(F) The slopes from days 2-14 were further categorized as Negative (<0), Low (0.0001-0.004999), Medium (0.005-0.04999), or High (>0.05) for each mCD24 Env-IMC (left) and then summarized by viral subtype and mutant status (right).

Thus, we hypothesized that residues R429 and Q432 contributed to the *ex vivo* phenotypes exhibited by subtype A viruses in the reporter-CET model, and that subtype A transmission/replication could be improved if destabilizing mutations replaced residue 429 and/or 432 of Env. To test this hypothesis, we generated mutant subtype A sNLuc Env-IMCs by introducing the following mutations into one subtype A Env (A.R880F): (i) R429G, (ii) Q432K, and (iii) a double mutant with R429G and Q432K (**Table 1, #25-27**). In short, subtype A Env was mutated to resemble subtype D Env at residues 429 and 432 (**Fig. 7B**). Double and single mutants were introduced to test whether modifications to both residues 429 and 432 were necessary to improve the *ex vivo* phenotypes or if only one modification was needed. We then inoculated PBMC-derived CD4+ T cells with the 3 mutant A sNLuc Env-IMCs in parallel to their wildtype (WT) counterpart (**Table 1, #8**) to assess whether the mutant Env-IMCs were infectious and replication-competent. A subtype D sNLuc Env-IMC (D.191859) and Env Minus sNLuc Env-IMC were included as controls (**Table 1, #13 and #20**, respectively). Supernatant samples were taken from the culture supernatant and measured for sNLuc activity over 14 days. The RLU values for all Env-IMCs increased with similar kinetics, with the exception of the Env Minus Env-IMC (**Fig.**

7C). This result shows that all 3 mutant subtype A Env-IMCs replicated in primary CD4 T cells with kinetics similar to that of the subtype A WT parental virus.

Next, we inoculated CETs from 5 donors with the mutant subtype A sNLuc Env-IMCs either in the presence or absence of 20 μM of NVP, the subtype D WT counterpart, the D.191859 sNLuc Env-IMC, and Env minus sNLuc Env-IMCs (**Table 1, #8, #13, #20, #25-27**). We predicted that the replacement of the arginine with a glycine at residue 429 would improve subtype A replication kinetics, resulting in a replication phenotype that would resemble subtype D. However, mutations to subtype A Env at residues 429 and 432 appeared to severely and negatively impact *ex vivo* replication kinetics, regardless of whether it was a single or double mutation (**Fig. 7D**). Slopes were calculated from the normalized RLU values of the virally-inoculated CET blocks from the 5 donors. The percentage of slopes that were positive from days 2-14 for the mutant and WT viruses was calculated (**Fig. 7E**). Only 21% of the mutant A viruses on average had positive slopes, while around 79% of the WT A slopes were positive. The slopes were then categorized as negative, low, medium, or high (**Fig. 7F**). Almost none of the mutant A virus slopes could be classified as "high" (only 3.81% on average), in contrast to the WT A slopes (20.8% of slopes could be classified as "high"). These results suggest that the transmission and replication of all three mutant A viruses may be poorly supported by the CETs in comparison to WT. Importantly, the slopes of the CET blocks inoculated with the three mutant A viruses were also analyzed by whether the data were generated with ectocervix or endocervix. There was no significant difference in the slopes between ectocervix and endocervix inoculated with any of the three mutant A viruses (data not shown).

We further statistically assessed the slopes of the mutant and WT viruses described in Figure 7 at the "early", "late", and "all" time windows. Interestingly, there was no significant difference in the "early" slopes (days 2-4) between the mutant and WT conditions, suggesting either that the Env-IMCs were similarly transmitted *ex vivo*, that the replication kinetics of the mutant and WT Env-IMCs were similar immediately following *ex vivo* transmission, or both (**Fig. 8A**). When comparing the slopes at the "late" and "all" time windows, however, both the WT subtype A and D Env-IMCs had significantly greater slopes compared to the slopes of all three of the mutant A viruses (**Fig. 8B,C**). Compared to the single mutants, the slopes of the double mutant were the most similar to WT, but the slopes of the WT A virus were still significantly greater than the slopes of the double mutant. Thus, the poor transmission and replication kinetics observed with all three mutant viruses indicated that the efficiency of subtype A transmission and replication was not improved by the introduction of destabilizing mutations. Instead, these data indicate that both residues of 429 and 432 are critical for subtype A transmission and replication *ex vivo*.

CD4 binding by HIV Env affects subtype-specific ex vivo mucosal transmission and replication

After analyzing the *ex vivo* data from the mutant A Env-IMCs, we suspected that the mutations to Env residues 429 and 432 negatively impacted the ability of the virions to bind CD4, contributing to the replication kinetics for the mutant viruses observed *ex vivo*. Host cell entry by subtype A has been demonstrated to be less efficient than subtype D *in vitro*[76], which may reflect a difference in the two subtypes to bind CD4. Unlike subtype A, subtype D is Mφ-tropic *in vitro*[30,93], and Mφ-tropic strains are able to use lower densities of surface CD4 for cell entry[94,95]. The arginine at residue 429 of subtype A Env stabilizes

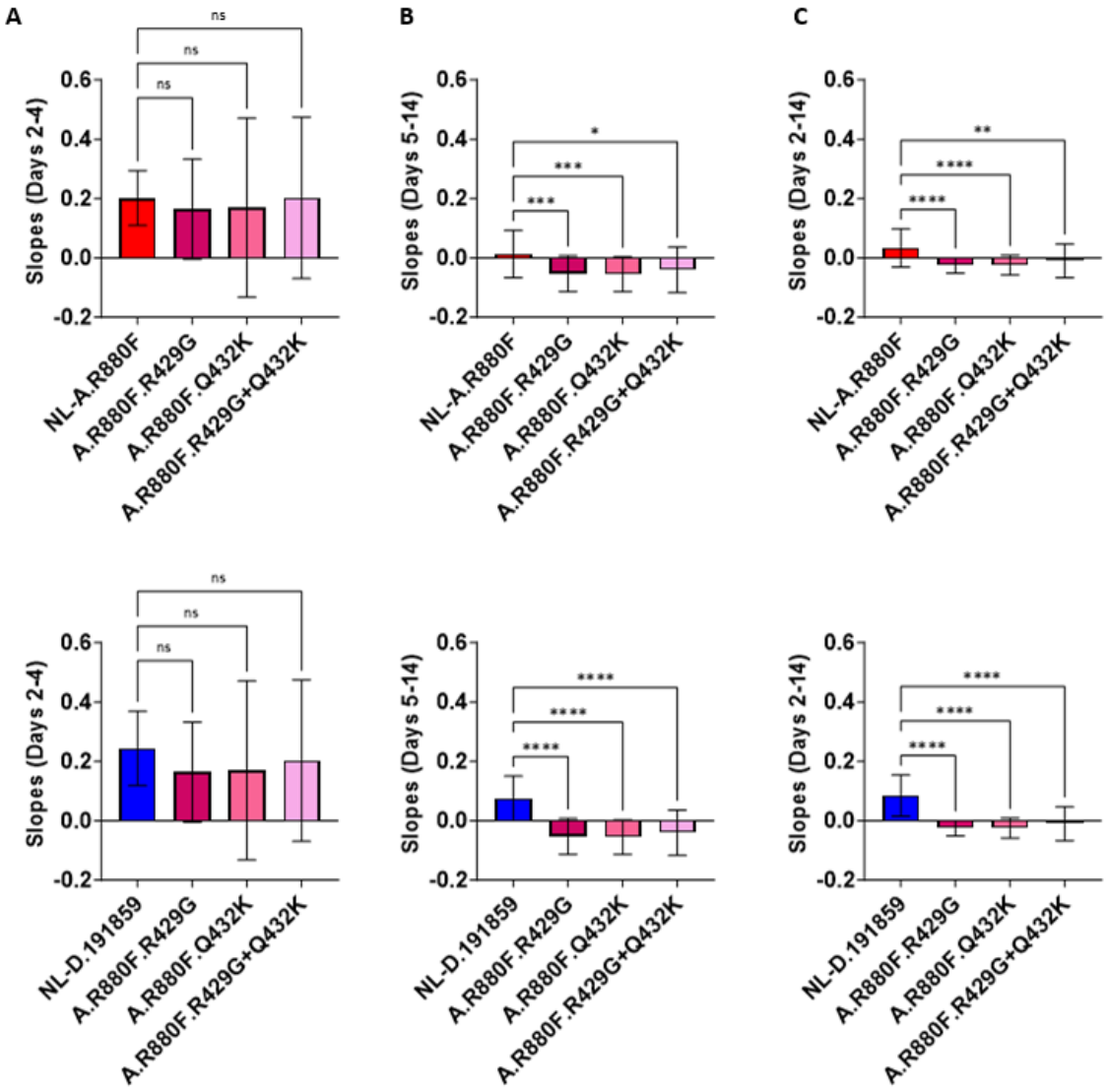

Figure 8. Mutations to subtype D Env at residues 429 and 432 induce a replication phenotype similar to wildtype subtype A virus.

(A) A Kruskal-Wallis test was conducted to assess significance of the slopes described in Figure 7 from days 2-4 between wildtype A and mutant A (top) and wildtype D and mutant A (bottom).

(B) A Kruskal-Wallis test was conducted to assess significance of the slopes described in Figure 7 from days 5-14 between wildtype A and mutant A (top) and wildtype D and mutant A (bottom).

(C) A Kruskal-Wallis test was conducted to assess significance of the slopes described in Figure 7 from days 2-14 between wildtype A and mutant A (top) and wildtype D and mutant A (bottom).

Env, and stabilized Env has been shown to minimally bind CD4 with crystallized protein structure models[35]. From the findings of Zhang *et. al*, we would expect that replacing the arginine at residue 429 in the subtype A Env with glycine would result in a more flexible Env, possibly enhancing gp120 interaction with CD4. However, based on our results presented in Figure 7, we hypothesize that subtype A Env binding to CD4 is less efficient when destabilizing mutations are introduced to residues 429 and 432.

To interrogate our hypothesis, we employed a soluble CD4 (sCD4) neutralization assay, as described previously[64,65]. This is a competition assay where sCD4 binds competitively to the gp120 region of Env, inhibiting viral entry into CD4+ cells because viral recognition of cellular CD4 is blocked by the sCD4. If viral entry is inhibited by lower concentrations of sCD4, it may indicate that the virus is more efficient at binding CD4, which may reflect the ability of the virus to utilize lower levels of surface CD4 for cell entry. We initially analyzed the panel of 5 subtype A and 5 subtype D Env-IMCs in parallel to BaL26 Env-IMC, which served as a positive control (**Table 1, #28**). Three of the five subtype A Env-IMCs did not achieve an IC50 in the sCD4 neutralization assay, indicating these Envs were largely refractory to competitive inhibition. An IC50 was achieved with each of the subtype D Envs, which ranged from about 20 to 400 nM (**Fig. 9A**). This result demonstrated the IC50 values of the subtype D Env-IMCs were significantly less than those of the subtype A Env-IMCs. The percent of inhibition at the highest concentration of sCD4 (1000 nM) used in the assay (maximum percent inhibition, MPI) for each Env-IMC was then calculated. The subtype D viruses were inhibited at a level of 89%, while the subtype A group was inhibited at a level of 41% (**Fig. 9B**). In sum, these data suggest that subtype D can bind CD4 more efficiently than subtype A.

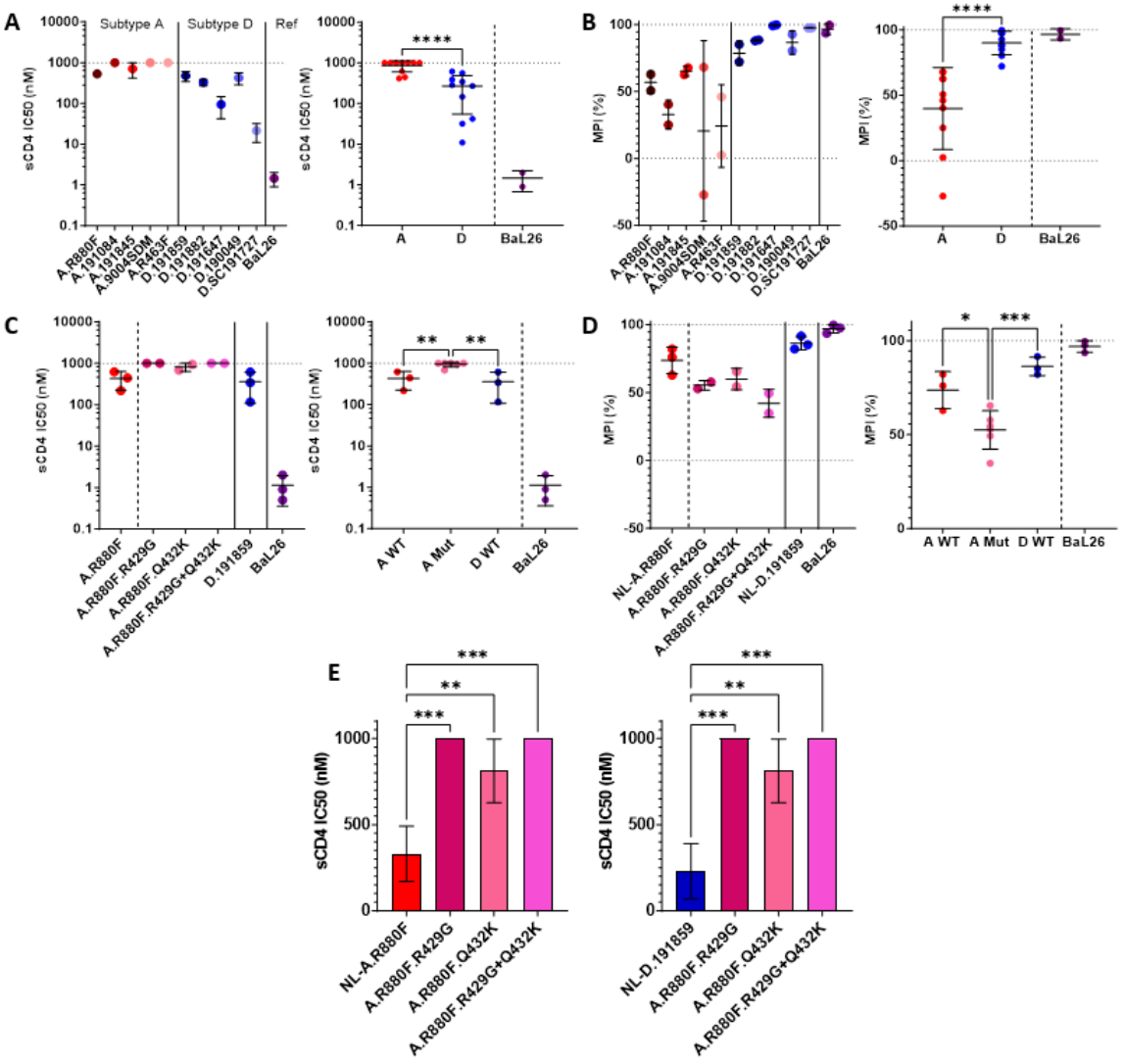

Figure 9. Mutations to HIV Env at residues 429 and 432 affect Env sensitivity to soluble CD4.

(A) The sCD4 IC50 values of all 5 subtype A and all 5 subtype D viruses starting at 1000 nM of sCD4 (left). Data were then summarized by viral subtype and a Welch's t test was used to determine significance ($p<0.0001$) (right). This experiment was repeated twice, resulting in 2 data points for each virus and a total of 10 data points per subtype. Bal26 was included as a positive control.

(B) The maximum percent inhibition (MPI) of all 5 subtype A and all 5 subtype D viruses (left), that were then combined by subtype and statistically assessed for significance using a Mann-Whitney test ($p<0.0001$).

(C) The sCD4 IC50 values of the mutant A Env-IMCs in parallel to their wildtype counterpart and the D.191859 Env-IMC starting at 1000 nM of sCD4 (left). This experiment was repeated twice, resulting in 2 data points for the mutant viruses, but the WT and BaL26 conditions were repeated three times, resulting in 3 data points for those viruses. Data were then summarized by subtype ("A WT" or "D WT") and mutant status ("A Mut") (right), and a one-way ANOVA was used to determine significance across groups.
(D) The MPI of the mutant A viruses, their WT counterparts, and the D.191859 Env-IMC (right). Data were then combined based on subtype or mutant status then statistically assessed for significance using a one-way ANOVA.
(E) A one-way ANOVA was conducted to assess significance between wildtype and mutant virus sCD4 IC50 values. These are the same data shown in (C), but with the statistical analysis performed between the WT A virus (left) or WT D virus (right) and each individual mutant A virus.

The 3 mutant A Env-IMCs, their WT counterpart, the D.191859 sNLuc Env-IMC, and the BaL26 Env-IMC control (**Table 1, #8, #13, #25-28**) were then analyzed for sCD4 inhibition. The IC50 values of all 3 mutant A viruses were significantly higher than the IC50 values of the WT A and D viruses (**Fig. 9C,E**). Further, the average MPI of the 3 mutant A Env-IMCs was significantly less (53%) than the parental WT A virus (76%) or WT D (86%) (**Fig. 9D**). Together, these data indicate that mutations to residues 429 and 432 of subtype A Env resulted in reduced CD4 binding, which may be reflected in the replication phenotypes of the mutant A viruses observed *ex vivo*. These data may also suggest that efficient CD4 binding by HIV Env is crucial for efficient mucosal transmission and replication *ex vivo*.

DISCUSSION

Understanding the virologic properties affecting the efficiency of mucosal transmission may elucidate key biological and molecular factors leading to the acquisition of productive clinical HIV infection in women. The identification of these properties may further inform the development of new HIV prevention modalities that target these

properties. Herein, we sought to investigate Env-based properties affecting mucosal HIV transmission by infecting human cervical tissue with HIV Env-IMCs expressing reporter genes. The design of these Env-IMCs ensured that the infection/replication phenotypes observed *ex vivo* were attributable solely to Env (**Fig. 1A**) and maintained WT replication phenotypes (**Fig. 4**). Using this approach, we demonstrated that the subtype of HIV Env and the efficiency of CD4 binding by HIV Env impacted viral transmission and replication *ex vivo*.

Previously described strategies to HIV transmission *ex vivo* are limited in their sensitivity and reproducibility to measure HIV infection and/or replication at early time points, which has been an enduring issue with explant models. Current explant models often rely on non-reporter viral proteins (such as Gag p24) secreted into the culture media to determine infection. Such proteins are often difficult to distinguish before 4-6 days, require a high concentration for detection, or involve time-intensive analyses of samples. To overcome sensitivity issues, some laboratories digest the explants and isolate cell populations of interest prior to infection. Although this *in vitro* format is useful for some applications, it removes the cells from the context of their *ex vivo* microenvironment, reducing the translational applicability of the cell-cell and virus-cell dynamics observed. Issues with donor variability have also been noted with these CET models, limiting data reproducibility.

To interrogate our hypothesis, we recognized a need to identify and optimize a highly sensitive approach for detecting and quantifying HIV transmission *ex vivo.* We inoculated CETs with sNLuc and mCD24 reporter Env-IMCs to enable the sensitive detection and quantification of replicating virus. Inoculation with the sNLuc reporter

permitted rapid quantification of virus activity from culture supernatant and did not require the digestion of tissues to determine productive infection/replication. Through the sNLuc reporter data, we demonstrated in 35 distinct CET donors that subtype D replicated more efficiently than subtype A, and we were able to distinguish differences between subtype A and D replication within 4 days following viral inoculation. Quantification of viral replication kinetics via changes to reporter activity was possible through calculation of slope. Although slopes have not been used to assess changes to HIV reporter-infected CETs previously, this mathematical approach is a logical method for quantifying changes to "y" (RLU values) with respect to "x" (time).

Importantly, our sNLuc reporter approach preserved the transmission and replication of R5-tropic and not X4-tropic virus strains, which has been observed with previous *ex vivo* cervical tissue studies[27,81]. The mucosal transmission of primarily R5-tropic TF strains is also observed *in vivo* with HIV-infected patients[96,97]. The mCD24 reporter allowed us to quantify *de novo* HIV-infected cells from digested CETs as early as 4 days post-inoculation. Using viral proteins like p24 to determine infection (as with previous explant models) can be problematic because p24 is not always indicative of *de novo* infection. It can come from other sources, including infected cells that have been phagocytized by antigen presenting cells[98]. The mCD24 Env-IMCs produce mCD24 that becomes anchored to the cell surface through glycosylphosphatidylinositol (GPI) following infection by the reporter virus, and is thus an exogenously expressed product of *de novo* viral infection[39].

Both the sNLuc and the mCD24 reporter approaches had limitations, however. During transfection with proviral DNA containing the sNLuc reporter sequence, sNLuc

was produced and transferred to virus stock. This background sNLuc was not able to be removed completely by centrifugation or ultracentrifugation. Thus, if the CETs were not thoroughly washed following inoculation by sNLuc virus, the resulting background sNLuc would result in artificially high RLU values (i.e. 10^6 RLU or more), which made accurate calculations of slope nearly impossible. However, thorough washing does not remove all background RLU, which is why we normalized raw RLU values to day 2. Further, the inclusion of the IDV and NVP inhibitors ensured that the RLU values acquired between days 2-4 were indeed attributable to productively replicating virus and not background sNLuc that was trapped and then released by the CETs. For the mCD24 reporter, the number of detectable mCD24+ cells represented less than 1% of the total amount of cells isolated from digested tissue. Thus, due to the rarity of the mCD24+ cell populations, it was challenging to detect sufficient numbers of mCD24+ cells from a single tissue block. Hence, the percentage of mCD24+ cells was unable to be evaluated within individual tissue blocks; instead, cells from 3 or more tissue blocks had to be combined and digested together to ensure a detectable mCD24+ population. We considered using beads to isolate and enrich the mCD24+ cell populations, but we were concerned about losing too many of the rare mCD24+ cells during the separation process.

Our first major finding was that the subtype of the HIV Env affected HIV transmission efficiency. We designed our mCD24 and sNLuc reporter viruses with NL4-3 as an isogenic proviral backbone, exchanging the NL4-3 ectodomain sequence for either a subtype A or D ectodomain. This preserved homogenous Vpu, Rev, and Tat and ensured that any differences in transmission, infection, and/or replication mapped to Env. We first inoculated PBMC-derived CD4+ T cells with the subtype A and D Env-IMCs and

determined that their ability to infect, replicate in, and spread to these cells was similar *in vitro* (**Fig. 1**). When CETs were inoculated with the same constructs, the replication kinetics of the subtype A and D Env-IMCs were only similar from days 2-4. These results indicated that either the two subtypes were similarly transmitted or the two subtypes replicated similarly immediately following transmission *ex vivo*. After 4 days, however, the replication kinetics of the subtype A and D Env-IMCs diverged, and we determined that the transmission and replication efficiencies of the subtype D Env-IMCs were greater than those of subtype A (**Figs. 2-3**). We suspect that one or more factors present in the tissue interacted with HIV Env in a subtype-dependent manner (through a currently unknown mechanism), where interactions with subtype A Env limited mucosal replication after 4 days while interactions with subtype D Env either maintained or enhanced viral replication *ex vivo*.

One major advantage of our reporter Env-IMC approach is the use of TF Envs, which enhances the biological and clinical relevance of our findings. In clinical settings, subtype D viruses demonstrate greater resistance to anti-retroviral therapies (ARTs)[14,28,99] and cause faster CD4+ T cell loss[23,28,29,31,75-77] compared to subtype A, leading to greater pathogenesis and faster progression to AIDS in subtype D-infected individuals. Interestingly, the prevalence of subtype D is declining[70,100,101], and it is hypothesized that the high degree of pathogenicity observed with subtype D infection reduces opportunity for transmission events to occur[100]. Throughout sub-Saharan Africa (SSA) are several genetically diverse HIV-1 subtypes— including subtypes A and D— and circulating recombinant forms (CRFs) of those subtypes endemic to the region (reviewed in[70]). The prevalence of CRFs across SSA has increased over the past decades as a consequence of

the high rate of transmission and co-circulation of multiple HIV subtypes in that region, increasing opportunity for recombination when individuals are co-infected by multiple strains ([102], reviewed in[103-105]). A/D recombinants are just one type of CRF. For these A/D CRFs, Env is a "hotspot" for recombination[106,107], and it has been reported that the gp120 region of Env is often derived from subtype A while the gp41 region of Env is usually derived from subtype D[58,106]. The reason(s) why gp120 primarily comes from subtype A and gp41 comes from subtype D so commonly in these A/D CRFs are poorly understood, but it may impact the pathogenicity of the CRF within the host. Individuals infected with A/D CRFs do not progress to AIDS as fast as those infected with subtype D, but they still progress to AIDS faster than those infected with subtype A[108]. Thus, identifying the HIV subtype(s) from which the CRF Env is derived may be useful for predicting mucosal transmission and replication phenotypes of CRFs.

One factor contributing to the subtype-specific replication phenotypes *ex vivo* may be the distinct abilities of the two subtypes to bind CD4. Using a sCD4 neutralization assay, we demonstrated that subtype D bound sCD4 more efficiently than subtype A (**Fig. 9A**). This finding is supported by a recent study that used a CD4 mimetic compound (YIR-821) to inhibit cellular entry, and it was determined that subtype D cellular entry was significantly more inhibited by YIR-821 than subtype A entry[109]. Interestingly, this difference in CD4 sensitivity may not be reflected in the ability of the two subtypes to enter and infect CD4+ T cells, as we demonstrated both *in vitro* and *ex vivo* that the two subtypes similarly infected and replicated in these cells (**Figs. 1 and 4**). Based on our data, it was unlikely that CD4+ T cells were the reason for the difference in the *ex vivo* replication kinetics between subtypes A and D. However, another cell type, such as Mφs, could have

contributed to the difference in replication kinetics. Subtype D, and not subtype A, displays a tropism for Mφs *in vitro*[30,93]. Since Mφs express lower densities of surface CD4 than T cells, HIV strains that are Mφ tropic are able to utilize lower levels of surface CD4 for cell entry[94,95] and are inhibited by lower concentrations of sCD4[69,95]. Whether subtype D can infect Mφs within CETs is not well-defined, but elucidation of this topic may enhance our understanding of virologic factors contributing to subtype D transmission and replication *ex vivo*.

Another finding of note was the difference in viral transmission and replication between ectocervix and endocervix. Ectocervix may be more vulnerable to HIV transmission because of its susceptibility to physical trauma that can damage the mucosal surface following intercourse and its high prevalence of intraepithelial CD4+ T cells, while the endocervix may be more vulnerable because it is comprised of a single, fragile epithelial layer (discussed in[10,11,84]). Using both human cervical explants and an *in vivo* rhesus macaque vaginal transmission model, Carias *et. al* demonstrated that while HIV-1 can penetrate both ecto- and endo- cervix to interact with target cells, the presence of mucus significantly reduced the ability of virus to penetrate endocervix[110]. Using explant tissues, Asin *et. al* reported that HIV-1 transcription was significantly higher in ectocervical tissue compared to endometrial tissue[111], which neighbors endocervical tissue in human uteri. We demonstrated that ectocervix supported the transmission and replication of subtype A significantly better than endocervix, while there was no difference in the transmission/replication of subtype D (**Fig. 5**). This may suggest that transmission efficiency to different types of cervical tissue surfaces— or the ability to overcome host-immune factors like mucus to establish infection— is subtype-dependent. This statement

aligns with the findings of Klein *et. al*, who suggested that successful HIV transmission may depend on the ability of the virus to overcome the mucosal lectin trap found within mucosal tissues[24]. Ectocervix may also be more susceptible to subtype A infection than endocervix due to the higher number of target cells like CD4+ T cells in the ectocervix compared endocervix, even though Trifonova *et. al* reported greater replication of HIV_{BaL} in endocervix compared to ectocervix[84]. We may have observed different outcomes from Trifonova *et. al* because we used: a non-polarized model of infection instead of a polarized one, sNLuc instead of p24 to monitor viral replication over time, a greater number of donors, and TF viruses instead of a reference strain alone to infect our CETs.

We initially hypothesized that mutating residue 429 of subtype A Env from an arginine to a glycine would improve the replication kinetics of subtype A because we predicted that the glycine would destabilize Env trimer. This rationale was based on the work of Zhang *et. al*, who used crystallized protein models to demonstrate that the arginine in subtype A Env has stabilizing effects on trimer, negatively affecting its ability to bind CD4[35]. However, those crystallized protein models may not be reflective of HIV Env in a dynamic *ex vivo* environment. When destabilizing mutations were introduced into residues 429 and 432 of subtype A Env, both mutations negatively impacted viral replication kinetics in CETs and CD4 binding (**Figs. 7-9**). These results may indicate that both Env residues 429 and 432 are critical to CD4 binding and *ex vivo* transmission and replication phenotypes. Residues 429 and 432 are highly conserved in both subtype A and D Env. In a sample of 226 subtype A Envs, nearly 100% had an arginine at 429 and ~75% had a glutamine at 432, while in a sample of 108 subtype D Envs, residue 429 was almost always

either a glycine or glutamic acid and 100% had a basic residue at residue 432[35]. The highly conserved nature of these two residues may thus underpin their importance to Env function.

Miller and Shattock suggested that the results gained from "normal", non-inflamed FRT explant tissues used in Western explant models may not be applicable to women worldwide because an estimated 30-70% of women in developing countries have underlying inflammation in their reproductive tracts[112]. The 46 donor tissues we received were from individuals undergoing medically necessary hysterectomies to alleviate non-cancerous histopathological conditions, including: fibroids, benign cysts, acute/chronic cervicitis, uterovaginal prolapse, and more. Many of these conditions can lead to inflammatory states within the FRT[113]. Thus, it could be hypothesized that low levels of inflammation in the FRT are "normal" in Western explant models. We are unsure if the potential inflammatory states caused by the histopathological conditions affected the transmission and replication of the viruses we applied *ex vivo*. Though beyond the scope of this work, future studies will examine the presence of pro- and anti- inflammatory cytokines and chemokines present in the CETs before and after viral inoculation to determine their effects on HIV transmission and replication *ex vivo*.

In conclusion, the subtype of HIV Env, CD4 binding, and the highly conserved residues at 429 and 432 were Env-based properties that affected the efficiency of mucosal HIV transmission. The efficiency of viral transmission and replication *ex vivo* was linked to viral subtype and CD4 binding ability. Our CET model described herein, coupled with extensive and rigorous statistical assessment, permitted the sensitive and reproducible study of reporter HIV transmission and replication *ex vivo*. Although *ex vivo* transmission and replication may not completely represent the HIV transmission and replication events

observed *in vivo*, we are confident that the data and observations generated from our work herein provide important insights into Env-based properties affecting the efficiency of mucosal HIV transmission.

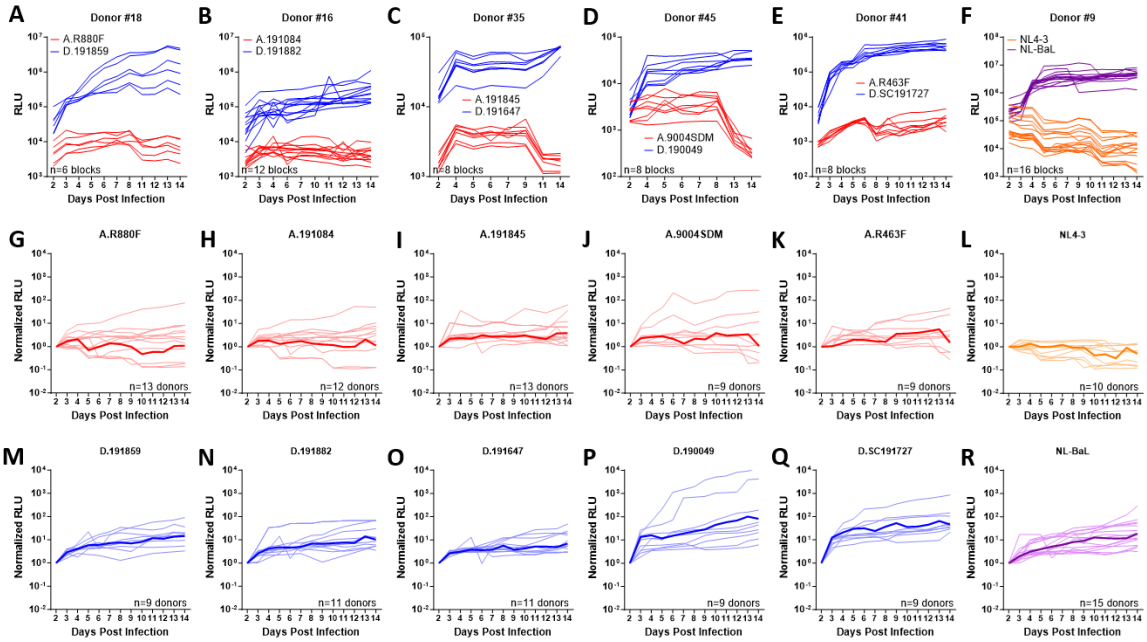

Supplementary Figure 1.

(A-F) Representative donors from the 35 donors inoculated with the Subtype A (red) and Subtype D (blue) sNLuc Env-IMCs. A representative donor infected by NL4-3 (orange) and NL-BaL (purple) sNLuc Env-IMCs is also included. Each line represents one tissue block, and the number of tissue blocks inoculated with each virus in each donor is indicated. Between 6-8 CET blocks of ecto- and /or endo- cervix from each donor were inoculated.

(G-R) The normalized RLU data from each donor infected with an indicated sNLuc Env-IMC. Each lightly colored line indicates the geometric mean of the RLU values from one donor, while the darkly colored lines indicate the geometric mean of all the donors infected by the indicated sNluc virus. Total number of donors infected by each virus is indicated.

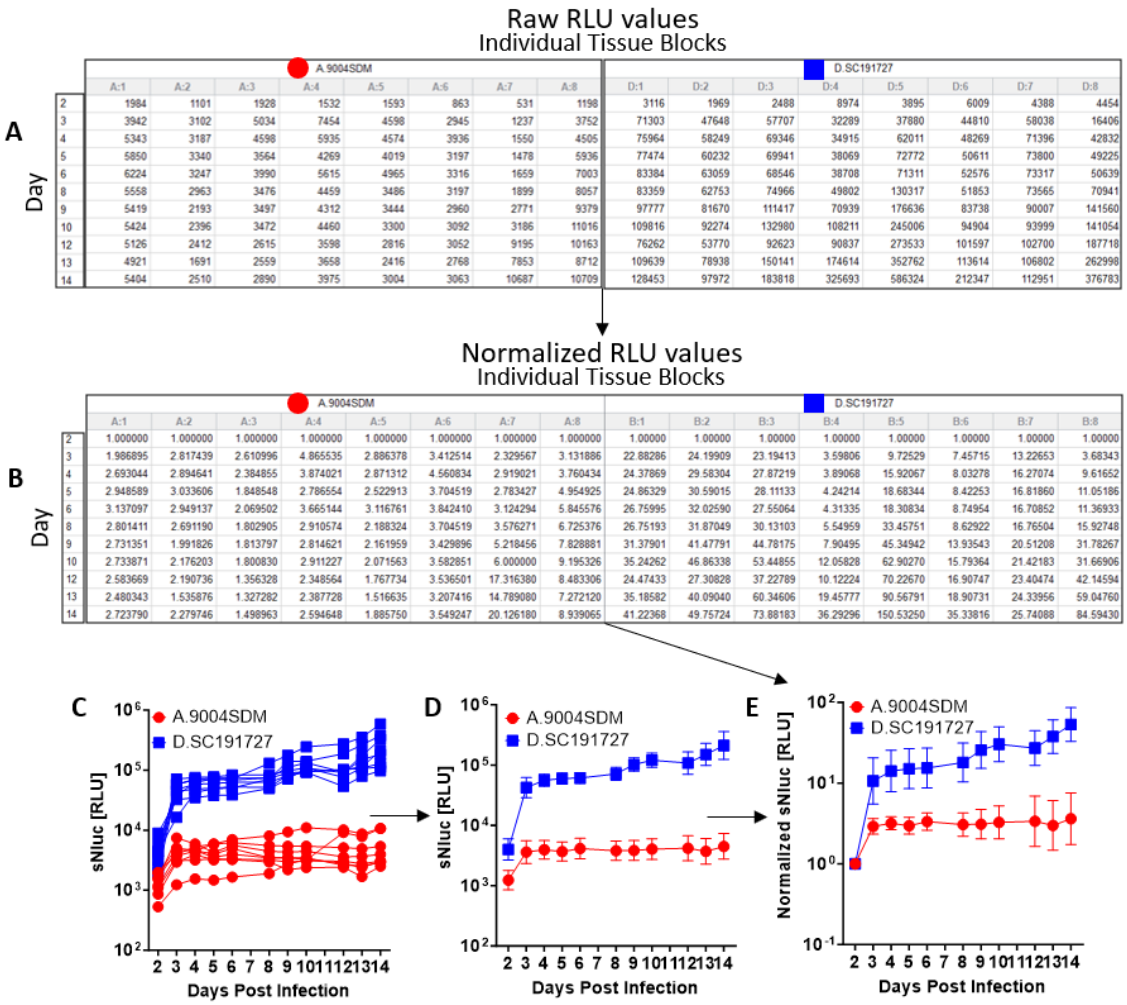

Supplementary Figure 2.

(A) Raw RLU values as acquired from luminometer. Eight replica CET tissue blocks were inoculated with either one subtype A or one subtype D sNLuc Env-IMC. After RLU values were acquired on days 6 and 10, an 80% tissue culture media change was done. Because of this, RLU values were not acquired on days 7 and 11.

(B) Raw RLU values from part (A) normalized to the RLU values acquired on day 2.

(C) The raw RLU values of each individual tissue block from part (A) graphed.

(D) The geometric mean with 95% CI of the raw RLU values of all tissue blocks inoculated with either the subtype A or D sNLuc Env-IMC from part (C) graphed.

(E) The geometric mean with 95% CI of the normalized RLU values of all tissue blocks inoculated with either the subtype A or D sNLuc Env-IMC from part (B).

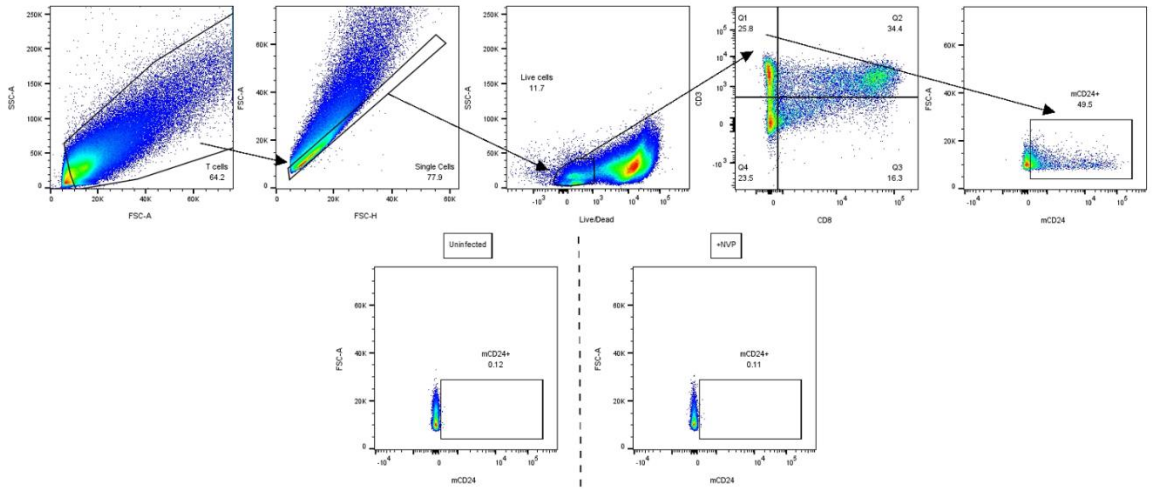

Supplementary Figure 3. Gating strategy to identify mCD24+ CD4 T cells derived from PBMCs.

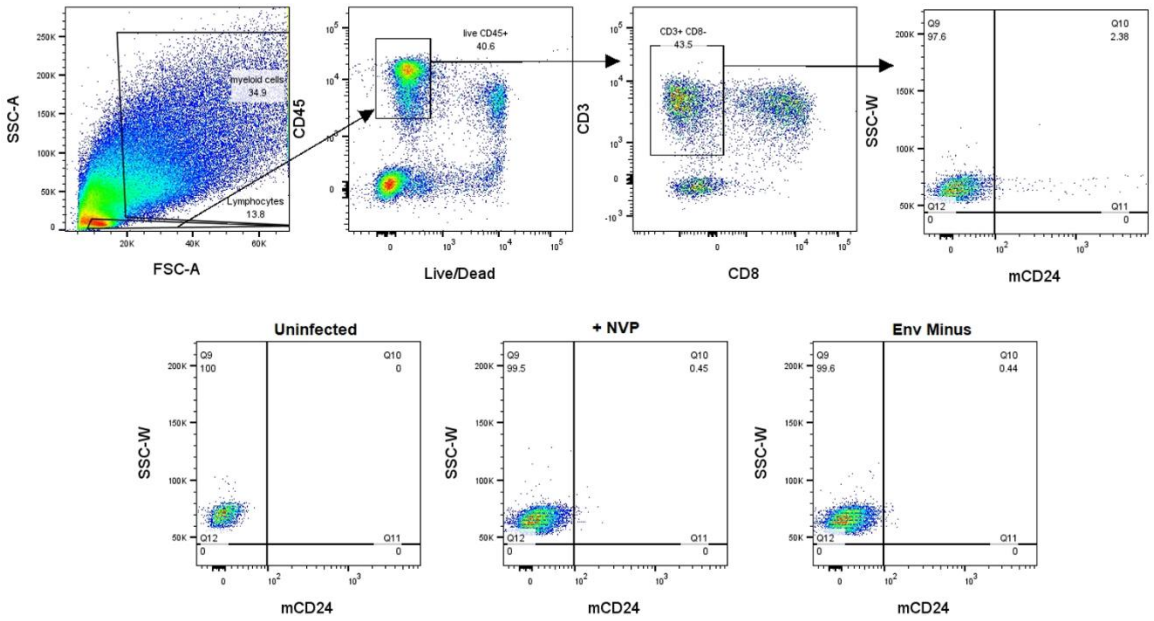

Supplementary Figure 4. Gating strategy to identify mCD24+ CD4 T cells from digested tissue.

REFERENCES

1. HIV Basics. Vol. 2020 (Centers for Disease Control and Prevention, 2020).
2. UNAIDS. UNAIDS 2017. (2017).
3. HIV in the Southern United States. (Centers for Disease Control, 2019).
4. UNAIDS. In Danger: UNAIDS Global AIDS Update 2022. (Geneva: Joint United Nations Programme on HIV/AIDS, 2022).
5. UNAIDS. UNAIDS 2020. 2 edn (2020).
6. UNAIDS. Global AIDS Response Progress Reporting 2015. (World Health Organization and UNAIDS 2015, UNAIDS.org, 2015).
7. Saba, I. et al. Immunocompetent Human 3D Organ-Specific Hormone-Responding Vaginal Mucosa Model of HIV-1 Infection. *Tissue Eng Part C Methods* **27**, 152-166 (2021).
8. Bernard-Stoecklin, S. et al. Semen CD4+ T Cells and Macrophages Are Productively Infected at All Stages of SIV infection in Macaques. *PLoS Pathogens* **9**, e1003810 (2013).
9. Nijmeijer, B.M. et al. HIV-1 subverts the complement system in semen to enhance viral transmission. *Mucosal Immunology* **14**, 743-750 (2021).
10. Gonzalez, S.M., Aguilar-Jimenez, W., Su, R.-C. & Rugeles, M.T. Mucosa: Key Interactions Determining Sexual Transmission of the HIV Infection. *Frontiers in Immunology* **10**(2019).
11. Shacklett, B.L. Mucosal Immunity in HIV/SIV Infection: T Cells, B Cells and Beyond. *Curr Immunol Rev* **15**, 63-75 (2019).
12. Kaleebu, P. et al. Relation between chemokine receptor use, disease stage, and HIV-1 subtypes A and D: results from a rural Ugandan cohort. *J Acquir Immune Defic Syndr* **45**, 28-33 (2007).
13. Huang, W. et al. Coreceptor Tropism in Human Immunodeficiency Virus Type 1 Subtype D: High Prevalence of CXCR4 Tropism and Heterogeneous Composition of Viral Populations. *Journal of Virology* **81**, 7885-7893 (2007).
14. Kyeyune, F. et al. Treatment failure and drug resistance is more frequent in HIV-1 subtype D versus subtype A-infected Ugandans over a 10-year study period. *Aids* **27**, 1899-909 (2013).
15. Kapaata, A. et al. Infection with HIV-1 subtype D among acutely infected Ugandans is associated with higher median concentration of cytokines compared to subtype A. *IJID Regions* **3**, 89-95 (2022).
16. Claiborne, D.T. et al. Replicative fitness of transmitted HIV-1 drives acute immune activation, proviral load in memory CD4+ T cells, and disease progression. *Proceedings of the National Academy of Sciences* **112**, E1480-E1489 (2015).
17. Deeks, S.G. et al. Immune activation set point during early HIV infection predicts subsequent CD4+ T-cell changes independent of viral load. *Blood* **104**, 942-7 (2004).
18. Ganesan, A. et al. Immunologic and virologic events in early HIV infection predict subsequent rate of progression. *J Infect Dis* **201**, 272-84 (2010).
19. Venner, C.M. et al. Infecting HIV-1 Subtype Predicts Disease Progression in Women of Sub-Saharan Africa. *EBioMedicine* **13**, 305-314 (2016).

20. Troyer, R.M. et al. Changes in human immunodeficiency virus type 1 fitness and genetic diversity during disease progression. *J Virol* **79**, 9006-18 (2005).
21. Barbour, J.D. & Grant, R.M. The clinical implications of reduced viral fitness. *Current Infectious Disease Reports* **6**, 151-158 (2004).
22. Giorgi, J.V. et al. Shorter survival in advanced human immunodeficiency virus type 1 infection is more closely associated with T lymphocyte activation than with plasma virus burden or virus chemokine coreceptor usage. *J Infect Dis* **179**, 859-70 (1999).
23. Baeten, J.M. et al. HIV-1 Subtype D Infection Is Associated with Faster Disease Progression than Subtype A in Spite of Similar Plasma HIV-1 Loads. *The Journal of Infectious Diseases* **195**, 1177-1180 (2007).
24. Klein, K. et al. Deep Gene Sequence Cluster Analyses of Multi-Virus-Infected Mucosal Tissue Reveal Enhanced Transmission of Acute HIV-1. *J Virol* **95**(2021).
25. Ariën, K.K. et al. The replicative fitness of primary human immunodeficiency virus type 1 (HIV-1) group M, HIV-1 group O, and HIV-2 isolates. *J Virol* **79**, 8979-90 (2005).
26. Kyeyune, F. et al. Treatment failure and drug resistance is more frequent in HIV-1 subtype D versus subtype A-infected Ugandans over a 10-year study period. *AIDS* **27**, 1899-1909 (2013).
27. Abraha, A. et al. CCR5- and CXCR4-tropic subtype C human immunodeficiency virus type 1 isolates have a lower level of pathogenic fitness than other dominant group M subtypes: implications for the epidemic. *J Virol* **83**, 5592-605 (2009).
28. Kaleebu, P. et al. Effect of human immunodeficiency virus (HIV) type 1 envelope subtypes A and D on disease progression in a large cohort of HIV-1-positive persons in Uganda. *J Infect Dis* **185**, 1244-50 (2002).
29. Parczewski, M. et al. Infection with HIV-1 subtype D adversely affects the live expectancy independently of antiretroviral drug use. *Infection, Genetics and Evolution* **90**, 104754 (2021).
30. Vasan, A. et al. Different rates of disease progression of HIV type 1 infection in Tanzania based on infecting subtype. *Clin Infect Dis* **42**, 843-52 (2006).
31. Easterbrook, P.J. et al. Impact of HIV-1 viral subtype on disease progression and response to antiretroviral therapy. *J Int AIDS Soc* **13**, 4 (2010).
32. Alberti, M.O. et al. Optimized Replicating Renilla Luciferase Reporter HIV-1 Utilizing Novel Internal Ribosome Entry Site Elements for Native Nef Expression and Function. *AIDS Res Hum Retroviruses* **31**, 1278-96 (2015).
33. Désiré, N. et al. Characterization update of HIV-1 M subtypes diversity and proposal for subtypes A and D sub-subtypes reclassification. *Retrovirology* **15**, 80 (2018).
34. Dana F. Indihar, J.J.J., Christina Ochsenbauer, and John C. Kappes. Highly Sensitive Analysis of Cervical Mucosal HIV-1 Infection using Reporter Viruses Expressing Secreted Nanoluciferase. in *HIV Protocols* (ed. Vinayaka Prasad, G.K.) (Humana New York, NY, 2024).
35. Zhang, P. et al. Interdomain Stabilization Impairs CD4 Binding and Improves Immunogenicity of the HIV-1 Envelope Trimer. *Cell Host Microbe* **23**, 832-844.e6 (2018).

36. Edmonds, T.G. et al. Replication competent molecular clones of HIV-1 expressing Renilla luciferase facilitate the analysis of antibody inhibition in PBMC. *Virology* **408**, 1-13 (2010).
37. Sarzotti-Kelsoe, M. et al. Optimization and validation of a neutralizing antibody assay for HIV-1 in A3R5 cells. *Journal of Immunological Methods* **409**, 147-160 (2014).
38. deCamp, A. et al. Global panel of HIV-1 Env reference strains for standardized assessments of vaccine-elicited neutralizing antibodies. *J Virol* **88**, 2489-507 (2014).
39. Cavrois, M. et al. Mass Cytometric Analysis of HIV Entry, Replication, and Remodeling in Tissue CD4+ T Cells. *Cell Rep* **20**, 984-998 (2017).
40. Prévost, J. et al. Incomplete Downregulation of CD4 Expression Affects HIV-1 Env Conformation and Antibody-Dependent Cellular Cytotoxicity Responses. *J Virol* **92**(2018).
41. Ventura, J.D. et al. Longitudinal bioluminescent imaging of HIV-1 infection during antiretroviral therapy and treatment interruption in humanized mice. *PLOS Pathogens* **15**, e1008161 (2019).
42. Freel, S.A. et al. Phenotypic and functional profile of HIV-inhibitory CD8 T cells elicited by natural infection and heterologous prime/boost vaccination. *J Virol* **84**, 4998-5006 (2010).
43. Naarding, M.A. et al. Development of a luciferase based viral inhibition assay to evaluate vaccine induced CD8 T-cell responses. *J Immunol Methods* **409**, 161-73 (2014).
44. Pollara, J. et al. High-throughput quantitative analysis of HIV-1 and SIV-specific ADCC-mediating antibody responses. *Cytometry A* **79**, 603-12 (2011).
45. Pollara, J. et al. Association of HIV-1 Envelope-Specific Breast Milk IgA Responses with Reduced Risk of Postnatal Mother-to-Child Transmission of HIV-1. *J Virol* **89**, 9952-61 (2015).
46. Sung, J.A. et al. Dual-Affinity Re-Targeting proteins direct T cell-mediated cytolysis of latently HIV-infected cells. *J Clin Invest* **125**, 4077-90 (2015).
47. Astronomo, R.D. et al. Neutralization Takes Precedence Over IgG or IgA Isotype-related Functions in Mucosal HIV-1 Antibody-mediated Protection. *EBioMedicine* **14**, 97-111 (2016).
48. Astronomo, R.D. et al. Rectal tissue and vaginal tissue from intravenous VRC01 recipients show protection against ex vivo HIV-1 challenge. *J Clin Invest* **131**(2021).
49. Gornalusse, G.G. et al. Buprenorphine Increases HIV-1 Infection In Vitro but Does Not Reactivate HIV-1 from Latency. *Viruses* **13**(2021).
50. Mielke, D. et al. ADCC-mediating non-neutralizing antibodies can exert immune pressure in early HIV-1 infection. *PLoS Pathog* **17**, e1010046 (2021).
51. Mielke, D. et al. Selection of HIV Envelope Strains for Standardized Assessments of Vaccine-Elicited Antibody-Dependent Cellular Cytotoxicity-Mediating Antibodies. *J Virol* **96**, e0164321 (2022).
52. Seay, K. et al. Mice transgenic for CD4-specific human CD4, CCR5 and cyclin T1 expression: a new model for investigating HIV-1 transmission and treatment efficacy. *PLoS One* **8**, e63537 (2013).

53. Seay, K. et al. In Vivo Activation of Human NK Cells by Treatment with an Interleukin-15 Superagonist Potently Inhibits Acute In Vivo HIV-1 Infection in Humanized Mice. *J Virol* **89**, 6264-74 (2015).
54. Bardhi, A. et al. Potent In Vivo NK Cell-Mediated Elimination of HIV-1-Infected Cells Mobilized by a gp120-Bispecific and Hexavalent Broadly Neutralizing Fusion Protein. *J Virol* **91**(2017).
55. Anthony-Gonda, K. et al. Multispecific anti-HIV duoCAR-T cells display broad in vitro antiviral activity and potent in vivo elimination of HIV-infected cells in a humanized mouse model. *Sci Transl Med* **11**(2019).
56. Adachi, A. et al. Production of acquired immunodeficiency syndrome-associated retrovirus in human and nonhuman cells transfected with an infectious molecular clone. *J Virol* **59**, 284-91 (1986).
57. Li, J. et al. Optimized application of the secreted Nano-luciferase reporter system using an affinity purification strategy. *PLoS One* **13**, e0196617 (2018).
58. Baalwa, J. et al. Molecular identification, cloning and characterization of transmitted/founder HIV-1 subtype A, D and A/D infectious molecular clones. *Virology* **436**, 33-48 (2013).
59. Smale, S.T. Beta-galactosidase assay. *Cold Spring Harb Protoc* **2010**, pdb.prot5423 (2010).
60. Martinez-Picado, J. & Martínez, M.A. HIV-1 reverse transcriptase inhibitor resistance mutations and fitness: A view from the clinic and ex vivo. *Virus Research* **134**, 104-123 (2008).
61. Wang, P. et al. Quantifying the contribution of Fc-mediated effector functions to the antiviral activity of anti–HIV-1 IgG1 antibodies in vivo. *Proceedings of the National Academy of Sciences* **117**, 18002-18009 (2020).
62. Capel, E., Parera, M., Clotet, B. & Martínez, M.A. Significant changes in integrase-associated HIV-1 replication capacity between early and late isolates. *Virology* **444**, 274-281 (2013).
63. Brockman, M.A., Tanzi, G.O., Walker, B.D. & Allen, T.M. Use of a novel GFP reporter cell line to examine replication capacity of CXCR4- and CCR5-tropic HIV-1 by flow cytometry. *Journal of Virological Methods* **131**, 134-142 (2006).
64. Salazar-Gonzalez, J.F. et al. Genetic identity, biological phenotype, and evolutionary pathways of transmitted/founder viruses in acute and early HIV-1 infection. *Journal of Experimental Medicine* **206**, 1273-1289 (2009).
65. Keele, B.F. et al. Identification and characterization of transmitted and early founder virus envelopes in primary HIV-1 infection. *Proc Natl Acad Sci U S A* **105**, 7552-7 (2008).
66. Lewis, M.J. et al. HIV-1 Nef sequence and functional compartmentalization in the gut is not due to differential cytotoxic T lymphocyte selective pressure. *PLoS One* **8**, e75620 (2013).
67. Ma, T. et al. HIV efficiently infects T cells from the endometrium and remodels them to promote systemic viral spread. *Elife* **9**(2020).
68. Binley, J.M. et al. Comprehensive cross-clade neutralization analysis of a panel of anti-human immunodeficiency virus type 1 monoclonal antibodies. *J Virol* **78**, 13232-52 (2004).

69. Ochsenbauer, C. et al. Generation of Transmitted/Founder HIV-1 Infectious Molecular Clones and Characterization of Their Replication Capacity in CD4 T Lymphocytes and Monocyte-Derived Macrophages. **86**, 2715-2728 (2012).
70. Bbosa, N., Kaleebu, P. & Ssemwanga, D. HIV subtype diversity worldwide. *Current Opinion in HIV and AIDS* **14**, 153-160 (2019).
71. Parczewski, M. et al. Infection with HIV-1 subtype D adversely affects the live expectancy independently of antiretroviral drug use. *Infect Genet Evol* **90**, 104754 (2021).
72. Kiwanuka, N. et al. HIV-1 viral subtype differences in the rate of CD4+ T-cell decline among HIV seroincident antiretroviral naive persons in Rakai district, Uganda. *J Acquir Immune Defic Syndr* **54**, 180-4 (2010).
73. Kiwanuka, N. et al. Effect of human immunodeficiency virus Type 1 (HIV-1) subtype on disease progression in persons from Rakai, Uganda, with incident HIV-1 infection. *J Infect Dis* **197**, 707-13 (2008).
74. Kanki, P.J. et al. Human Immunodeficiency Virus Type 1 Subtypes Differ in Disease Progression. *The Journal of Infectious Diseases* **179**, 68-73 (1999).
75. Longosz, A.F. et al. Comparison of antibody responses to HIV infection in Ugandan women infected with HIV subtypes A and D. *AIDS Res Hum Retroviruses* **31**, 421-7 (2015).
76. Venner, C.M. et al. Infecting HIV-1 Subtype Predicts Disease Progression in Women of Sub-Saharan Africa. *EBioMedicine* **13**, 305-314 (2016).
77. Bousheri, S. et al. Infection with different hiv subtypes is associated with CD4 activation-associated dysfunction and apoptosis. *J Acquir Immune Defic Syndr* **52**, 548-52 (2009).
78. Jones D.T., T.W.R., and Thornton J.M. The rapid generation of mutation data matrices from protein sequences. *Computer Applications in the Biosciences* **8**, 275-282 (1992).
79. J, F. Confidence limits on phylogenies: An approach using the bootstrap. *Evolution* **39**, 783-791 (1985).
80. Tamura K., S.G., and Kumar S. . MEGA 11: Molecular Evolutionary Genetics Analysis Version 11. (Molecular Biology and Evolution, https://doi.org/10.1093/molbev/msab120, 2021).
81. Saba, E. et al. HIV-1 sexual transmission: early events of HIV-1 infection of human cervico-vaginal tissue in an optimized ex vivo model. *Mucosal Immunology* **3**, 280-290 (2010).
82. Peters, P.J. et al. Infection of ectocervical tissue and universal targeting of T-cells mediated by primary non-macrophage-tropic and highly macrophage-tropic HIV-1 R5 envelopes. *Retrovirology* **12**, 48 (2015).
83. Introini, A., Vanpouille, C., Fitzgerald, W., Broliden, K. & Margolis, L. Ex Vivo Infection of Human Lymphoid Tissue and Female Genital Mucosa with Human Immunodeficiency Virus 1 and Histoculture. *Journal of Visualized Experiments* (2018).
84. Trifonova, R.T., Lieberman, J. & Van Baarle, D. Distribution of Immune Cells in the Human Cervix and Implications for HIV Transmission. *American Journal of Reproductive Immunology* **71**, 252-264 (2014).

85. Woodward Davis, A.S. et al. The human memory T cell compartment changes across tissues of the female reproductive tract. *Mucosal Immunology* (2021).
86. Pudney, J., Quayle, A.J. & Anderson, D.J. Immunological Microenvironments in the Human Vagina and Cervix: Mediators of Cellular Immunity Are Concentrated in the Cervical Transformation Zone. *Biology of Reproduction* **73**, 1253-1263 (2005).
87. Prakash, M., Patterson, S., Gotch, F. & Kapembwa, M.S. Recruitment of CD4+ T lymphocytes and macrophages into the cervical epithelium of women after coitus. *American Journal of Obstetrics and Gynecology* **188**, 376-381 (2003).
88. Shen, R. et al. Macrophages in Vaginal but Not Intestinal Mucosa Are Monocyte-Like and Permissive to Human Immunodeficiency Virus Type 1 Infection. *Journal of Virology* **83**, 3258-3267 (2009).
89. Merbah, M. et al. Cervico-Vaginal Tissue Ex Vivo as a Model to Study Early Events in HIV-1 Infection. *American Journal of Reproductive Immunology* **65**, 268-278 (2011).
90. Vabret, N. et al. The biased nucleotide composition of HIV-1 triggers type I interferon response and correlates with subtype D increased pathogenicity. *PLoS One* **7**, e33502 (2012).
91. Keating, S.M. et al. Magnitude and Quality of Cytokine and Chemokine Storm during Acute Infection Distinguish Nonprogressive and Progressive Simian Immunodeficiency Virus Infections of Nonhuman Primates. *Journal of Virology* **90**, 10339-10350 (2016).
92. Lei, J., Yin, X., Shang, H. & Jiang, Y. IP-10 is highly involved in HIV infection. *Cytokine* **115**, 97-103 (2019).
93. von Briesen, H. et al. Infection of monocytes/macrophages by HIV in vitro. *Research in Virology* **141**, 225-231 (1990).
94. Swanstrom, R. & Coffin, J. HIV-1 pathogenesis: the virus. *Cold Spring Harb Perspect Med* **2**, a007443 (2012).
95. Arrildt, K.T. et al. Phenotypic Correlates of HIV-1 Macrophage Tropism. *Journal of Virology* **89**, 11294-11311 (2015).
96. Margolis, L. & Shattock, R. Selective transmission of CCR5-utilizing HIV-1: the 'gatekeeper' problem resolved? *Nature Reviews Microbiology* **4**, 312-317 (2006).
97. Grivel, J.-C., Shattock, R.J. & Margolis, L.B. Selective transmission of R5 HIV-1 variants: where is the gatekeeper? *Journal of Translational Medicine* **9**, S6 (2010).
98. Schüpbach, J. Viral RNA and p24 antigen as markers of HIV disease and antiretroviral treatment success. *International archives of allergy and immunology* **132**, 196-209 (2003).
99. Eshleman, S.H. et al. Characterization of Nevirapine Resistance Mutations in Women With Subtype A Vs. D HIV-1 6–8 Weeks After Single-Dose Nevirapine (HIVNET 012). *JAIDS Journal of Acquired Immune Deficiency Syndromes* **35**, 126-130 (2004).
100. Grant, H.E. et al. A large population sample of African HIV genomes from the 1980s reveals a reduction in subtype D over time associated with propensity for CXCR4 tropism. *Retrovirology* **19**, 28 (2022).

101. Gounder, K. et al. Complex Subtype Diversity of HIV-1 Among Drug Users in Major Kenyan Cities. *AIDS Res Hum Retroviruses* **33**, 500-510 (2017).
102. Billings, E. et al. New Subtype B Containing HIV-1 Circulating Recombinant of sub-Saharan Africa Origin in Nigerian Men Who Have Sex With Men. *J Acquir Immune Defic Syndr* **81**, 578-584 (2019).
103. Giovanetti, M., Ciccozzi, M., Parolin, C. & Borsetti, A. Molecular Epidemiology of HIV-1 in African Countries: A Comprehensive Overview. *Pathogens* **9**(2020).
104. McCutchan, F.E. Global epidemiology of HIV. *J Med Virol* **78 Suppl 1**, S7-s12 (2006).
105. Buonaguro, L., Tornesello, M.L. & Buonaguro, F.M. Human immunodeficiency virus type 1 subtype distribution in the worldwide epidemic: pathogenetic and therapeutic implications. *J Virol* **81**, 10209-19 (2007).
106. Balinda, S.N. et al. Characterization of Near Full-Length Transmitted/Founder HIV-1 Subtype D and A/D Recombinant Genomes in a Heterosexual Ugandan Population (2006-2011). *Viruses* **14**(2022).
107. Bagaya, B.S. et al. Functional bottlenecks for generation of HIV-1 intersubtype Env recombinants. *Retrovirology* **12**, 44 (2015).
108. Ssemwanga, D. et al. Effect of HIV-1 Subtypes on Disease Progression in Rural Uganda: A Prospective Clinical Cohort Study. *PLOS ONE* **8**, e71768 (2013).
109. Matsumoto, K. et al. Characterization of a Novel CD4 Mimetic Compound YIR-821 against HIV-1 Clinical Isolates. *J Virol* **97**, e0163822 (2023).
110. Carias, A.M. et al. Defining the Interaction of HIV-1 with the Mucosal Barriers of the Female Reproductive Tract. *Journal of Virology* **87**, 11388-11400 (2013).
111. Asin, S.N., Eszterhas, S.K., Rollenhagen, C., Heimberg, A.M. & Howell, A.L. HIV Type 1 Infection in Women: Increased Transcription of HIV Type 1 in Ectocervical Tissue Explants. *The Journal of Infectious Diseases* **200**, 965-972 (2009).
112. Miller, C.J. & Shattock, R.J. Target cells in vaginal HIV transmission. *Microbes Infect* **5**, 59-67 (2003).
113. Jessica L. Gleason, M.E.T., Naomi Zukerman Willinger, and Edmond D. Shenassa. Endometriosis and Uterine Fibroids and Their Associations with Elevated C-Reactive Protein and Leukocyte Telomere Length Among a Representative Sample of U.S. Women: Data from the National Health and Nutrition Examination Survey, 1999–2002. *Journal of Women's Health* **31**, 1020-1028 (2022).

CONCLUSION

Summary of Key Findings

Our work presented herein focused on studies of HIV-1 transmission in an *ex vivo* mucosal cervical explant tissue (CET) model of infection and replication that were facilitated by the optimization and utilization of innovative HIV-1 infectious molecular clone (IMC) reporter virus technologies.

As described in Chapter 1, we initially sought to engineer novel HIV-1 reporter IMCs that would enable the sensitive detection of HIV-1 infection *in cellulo* and *ex vivo*, avoid interference with *nef*, and maintain wildtype expression and function of viral proteins. Prior findings indicated that the HIV-1 accessory protein Vif, when truncated by the C-terminal 19 amino acids (Vif.TR), retained its function. In the new HIV-1 reporter IMC, we appended the luminescent peptide, HiBiT, via a linker toVif.TR. The resulting Vif.HB-IMCs were replication-competent in cells non-permissive for *vif*-defective HIV-1, preserved stable HiBiT reporter activity over multiple rounds of viral replication, and maintained native levels of Nef expression upon infection of primary cells. Our finding that replication competence was retained by Vif.TR- and Vif.HB-IMCs indicated that the C-terminus of Vif was dispensable and could be modified without disrupting Vif function. This was further evidenced by the ability of the Vif.HB proteins from 3 distinct HIV-1 strains to mediate host APOBEC3G degradation similarly to wildtype Vif. We envision that the new Vif.HB-IMC reporter approach will have utility in experimental

applications requiring fully-functional Vif and Nef, stable reporter activity over multiple rounds of replication, and/or the highly sensitive detection of infected cells *in vitro*, *in vivo*, and *ex vivo*.

We hypothesized that viral properties mapping to HIV-1 Env affected mucosal transmission in the FRT. However, testing this hypothesis with previously described *ex vivo* CET model approaches presented significant challenges because these models were limited in their sensitivity for detecting early viral infection and replication events and the number of experimental conditions that could be tested at once. Recognizing a need for improved experimental approaches to interrogate our hypothesis, we devised and optimized a new approach that applied reporter Env-IMCs and TF-IMCs to CETs. This innovative methodology, described in detail in Chapter 4, enabled the highly sensitive and reproducible detection of viral infection and replication *ex vivo*, and reduced intra- and inter- donor tissue variability. Chapter 5 describes our findings from employing the reporter-HIV CET methodology to investigate whether Env strains representing two HIV-1 clades (A and D) mediated distinct phenotypes of viral infection of and replication in mucosal tissue *ex vivo* as a model for efficiency of mucosal transmission. We infected CETs from a total of 46 donors with reporter (sNLuc or mCD24) Env-IMCs that were isogenic except for heterologous *env* sequences representing subtype A and D TF HIV-1 strains Any findings of distinct phenotypes would thus be attributable to Env.

Following inoculation by the sNLuc Env-IMCs, we found significant subtype-specific differences in transmission and replication in the CETs over 14 days. Flow cytometric analyses for mCD24+ CD4 T cells liberated from CETs inoculated by the mCD24 Env-IMCs at 4 days after viral inoculation revealed no subtype-specific differ-

ence in the infection of the CD4+ T cells. This suggested that the subtype-specific differences in replication kinetics observed *ex vivo* were due to the contribution of one or more other cell types in the tissue after 4 days. According to published protein crystal structures, residues R429 and Q432 in subtype A Env contribute to the conformational stability of Env, which was proposed to affect its flexibility to bind and interact with CD4. Thus, we hypothesized that CD4 binding efficiency differed between subtypes A and D, contributing to the diverging replication phenotypes observed *ex vivo.* To test this hypothesis, we introduced R429G and Q432K mutations alone and in combination into one of the subtype A sNLuc Env-IMCs to determine whether the mutations would improve the CD4 binding and *ex vivo* replication kinetics of subtype A. We observed significantly reduced binding to sCD4 and impaired replication kinetics *ex vivo* with all three mutants compared to the parental subtype A-Env-IMC. We concluded that the subtype of HIV-1 Env and possibly CD4 binding efficiency were properties affecting mucosal HIV-1 transmission *ex vivo*.

The reporter-HIV CET model approach we developed improves on previously published approaches because it enables the sensitive, reproducible detection of *de novo* viral gene expression from tissue culture supernatant or infected cells isolated from digested CETs within 72-96 hours following virus exposure. Further, the reporter Env-IMCs and TF IMCs used to inoculate the CETs are replication-competent *ex vivo*, preserve the orfs of all virus genes, and incorporate TF viral strains, all of which enhance the biological relevance and translatability of our approach. We anticipate that this reporter-HIV CET model will have a diverse array of applications to address gaps in knowledge in the HIV field, with some examples described below.

Future Directions

Many questions remain regarding how clinical HIV-1 infection is established in the mucosal tissues of women. With the innovative tools and approaches described herein, these questions can be addressed effectively since the reporter technologies will offer sensitive, quantifiable, and reproducible analyses of virus-cell interactions and host response to virus.

One open question is how the spatiotemporal interaction between HIV-1 and host immune cells contribute to mucosal transmission and the establishment of clinical HIV-1 infection in women. Although we focused on CD4+ T cell infection by HIV-1 herein, we plan to investigate the interactions between virus and other host immune cells including Mφs, Langerhans cells, and dendritic cells with the Env-IMC and TF-IMC reporter technologies. These immune cells have been shown to become infected by HIV-1, or to capture and transfer virus to CD4+ T cells through synapse formation, which facilitates virus transfer between infected and uninfected cells both *in vitro* and *in vivo*. Yet, the potential involvement, e.g. as "potentiators" of initial CD4+ T cell infection, of these immune cell populations in establishing clinical HIV-1 infection in women is unclear. Combining reporter technologies with microscopy, single-cell, or multi-omics approaches will further enable the study of the spatiotemporal relationships between virus and host cells. Learning which immune cells become infected or transfer virus, and the timing behind that infection or transference following initial viral exposure, will be valuable for informing potential immunological mechanisms or risk factors that contribute to mucosal HIV-1 acquisition.

It is also unclear whether host immune responses— including cytokines, chemokines, or interferon— are elicited differently by distinct HIV-1 subtypes, and whether the early elicitation of these immune factors affects mucosal transmission. With the global rise in CRFs, understanding the extent to which distinct subtypes and their recombinants elicit host immune responses potentially operative during early infection is critical for informing interventions aimed at early infection mechanisms. The Env-IMC and TF-IMC reporter technologies applied *ex vivo* could be used to evaluate host immune responses to genetically diverse HIV-1 strains, and whether the induction of these responses offers transmission advantages or disadvantages to some strains.

Efficiency of HIV-1 transmission may also be affected by the mucosal tissue type. It is currently unknown whether different mucosal tissues favor the transmission of one subtype over another. For example, subtype B is more common among MSM while subtype A is more common among heterosexual populations. Whether this is because the sexual activities of homosexual and heterosexual populations have limited overlap (causing the HIV-1 epidemic to evolve separately in the two populations) or because of tissue-specific factors that limit the transmission of some subtypes is not known. To sensitively and reproducibly address these questions, reporter technologies can be applied to rectal, penile, and cervicovaginal tissue models.

Overall, pursuing answers to these open questions will deepen our understanding of the early mechanisms and determinants of HIV-1 transmission, informing the design of targeted prevention strategies and potentially also advancing the field towards an effective HIV-1 vaccine for women.

Impact

More than half of the approximately 39 million individuals infected with HIV-1 are women and girls, the majority of whom become infected following heterosexual intercourse. Women face unique biological risk factors for HIV-1 acquisition, and the mechanisms that establish clinical infection in the mucosal tissues of women are poorly understood. Therefore, research that facilitates the identification of key viral or host determinants/properties that may affect HIV-1 transmission to women is urgently needed. The IMCs expressing reporter genes described herein have transformed our ability to model and study the effects of different viral properties on the transmission efficiency of HIV-1, permitting the quantifiable and real-time visualizations of viral dynamics both *in cellulo* and *ex vivo*. The reporter-HIV CET model permits the sensitive observation and quantification of viral transmission, infection, and replication in a clinically relevant system, which can be further optimized to assess the efficacy of anti-HIV microbicides, virally-induced host responses, etc. This research will be advantageous for guiding the development of targeted prevention strategies for women worldwide at high risk of HIV-1 acquisition.

GENERAL LIST OF REFERENCES

1. Lu, K., Heng, X. & Summers, M.F. Structural determinants and mechanism of HIV-1 genome packaging. *J Mol Biol* **410**, 609-33 (2011).
2. International Committee on Taxonomy of Viruses: ICTV. (2022).
3. Coffin JM, H.S., Varmus HE. The Place of Retroviruses in Biology. in *Retroviruses* (Cold Spring Harbor Laboratory Press, Cold Spring Harbor, NY, 1997).
4. Zhang, J. & Crumpacker, C. HIV UTR, LTR, and Epigenetic Immunity. *Viruses* **14**(2022).
5. Nilson, K.A. & Price, D.H. The Role of RNA Polymerase II Elongation Control in HIV-1 Gene Expression, Replication, and Latency. *Genet Res Int* **2011**, 726901 (2011).
6. van Heuvel, Y., Schatz, S., Rosengarten, J.F. & Stitz, J. Infectious RNA: Human Immunodeficiency Virus (HIV) Biology, Therapeutic Intervention, and the Quest for a Vaccine. *Toxins (Basel)* **14**(2022).
7. Emery, A. & Swanstrom, R. HIV-1: To Splice or Not to Splice, That Is the Question. *Viruses* **13**(2021).
8. Tazi, J. et al. Alternative splicing: regulation of HIV-1 multiplication as a target for therapeutic action. *The FEBS Journal* **277**, 867-876 (2010).
9. Sertznig, H., Hillebrand, F., Erkelenz, S., Schaal, H. & Widera, M. Behind the scenes of HIV-1 replication: Alternative splicing as the dependency factor on the quiet. *Virology* **516**, 176-188 (2018).
10. Ganser-Pornillos, B.K., Yeager, M. & Pornillos, O. Assembly and architecture of HIV. *Adv Exp Med Biol* **726**, 441-65 (2012).
11. Stano, A. et al. Dense Array of Spikes on HIV-1 Virion Particles. *J Virol* **91**(2017).
12. Sundquist, W.I. & Kräusslich, H.G. HIV-1 assembly, budding, and maturation. *Cold Spring Harb Perspect Med* **2**, a006924 (2012).
13. Jiao, Y. et al. Profile of HIV-1 infected patients from an AIDS clinic in Beijing from 2007-2008. *Current HIV research* **8**, 515-20 (2010).
14. HIV Basics. Vol. 2020 (Centers for Disease Control and Prevention, 2020).
15. Wawer, M.J. et al. Rates of HIV-1 transmission per coital act, by stage of HIV-1 infection, in Rakai, Uganda. *J Infect Dis* **191**, 1403-9 (2005).
16. Gonzalez, S.M., Aguilar-Jimenez, W., Su, R.-C. & Rugeles, M.T. Mucosa: Key Interactions Determining Sexual Transmission of the HIV Infection. *Frontiers in Immunology* **10**(2019).
17. Pudney, J., Quayle, A.J. & Anderson, D.J. Immunological Microenvironments in the Human Vagina and Cervix: Mediators of Cellular Immunity Are Concentrated in the Cervical Transformation Zone. *Biology of Reproduction* **73**, 1253-1263 (2005).

18. Cohen, M.S., Shaw, G.M., McMichael, A.J. & Haynes, B.F. Acute HIV-1 Infection. *N Engl J Med* **364**, 1943-54 (2011).
19. Peters, P.J. et al. Infection of ectocervical tissue and universal targeting of T-cells mediated by primary non-macrophage-tropic and highly macrophage-tropic HIV-1 R5 envelopes. *Retrovirology* **12**, 48 (2015).
20. Klein, K. et al. Deep Gene Sequence Cluster Analyses of Multi-Virus-Infected Mucosal Tissue Reveal Enhanced Transmission of Acute HIV-1. *J Virol* **95**(2021).
21. Baxter, A. et al. Macrophage Infection via Selective Capture of HIV-1-Infected CD4+ T Cells. *Cell Host & Microbe* **16**, 711-721 (2014).
22. Cassol, E., Cassetta, L., Alfano, M. & Poli, G. Macrophage polarization and HIV-1 infection. *J Leukoc Biol* **87**, 599-608 (2010).
23. Ochsenbauer, C. et al. Generation of Transmitted/Founder HIV-1 Infectious Molecular Clones and Characterization of Their Replication Capacity in CD4 T Lymphocytes and Monocyte-Derived Macrophages. **86**, 2715-2728 (2012).
24. Rodriguez-Garcia, M. et al. Estradiol reduces susceptibility of CD4+ T cells and macrophages to HIV-infection. *PLoS One* **8**, e62069 (2013).
25. Shen, R. et al. Macrophages in Vaginal but Not Intestinal Mucosa Are Monocyte-Like and Permissive to Human Immunodeficiency Virus Type 1 Infection. *Journal of Virology* **83**, 3258-3267 (2009).
26. Tuttle, D.L., Harrison, J.K., Anders, C., Sleasman, J.W. & Goodenow, M.M. Expression of CCR5 increases during monocyte differentiation and directly mediates macrophage susceptibility to infection by human immunodeficiency virus type 1. *J Virol* **72**, 4962-9 (1998).
27. Kruize, Z. & Kootstra, N.A. The Role of Macrophages in HIV-1 Persistence and Pathogenesis. *Frontiers in Microbiology* **10**(2019).
28. Stieh, D. et al. Th17 Cells Are Preferentially Infected Very Early after Vaginal Transmission of SIV in Macaques. *Cell Host & Microbe* **19**, 529-540 (2016).
29. Woodham, A.W. et al. Human Immunodeficiency Virus Immune Cell Receptors, Coreceptors, and Cofactors: Implications for Prevention and Treatment. *AIDS Patient Care STDS* **30**, 291-306 (2016).
30. Yi, Y. et al. Role of CXCR4 in cell-cell fusion and infection of monocyte-derived macrophages by primary human immunodeficiency virus type 1 (HIV-1) strains: two distinct mechanisms of HIV-1 dual tropism. *J Virol* **73**, 7117-25 (1999).
31. Ward, A.B. & Wilson, I.A. Insights into the trimeric HIV-1 envelope glycoprotein structure. *Trends Biochem Sci* **40**, 101-7 (2015).
32. Wilen, C.B., Tilton, J.C. & Doms, R.W. HIV: cell binding and entry. *Cold Spring Harb Perspect Med* **2**(2012).
33. Rathore, U. et al. Glycosylation of the core of the HIV-1 envelope subunit protein gp120 is not required for native trimer formation or viral infectivity. *J Biol Chem* **292**, 10197-10219 (2017).
34. Pancera, M. et al. Structure of HIV-1 gp120 with gp41-interactive region reveals layered envelope architecture and basis of conformational mobility. *Proc Natl Acad Sci U S A* **107**, 1166-71 (2010).

35. Prabakaran, P., Dimitrov, A.S., Fouts, T.R. & Dimitrov, D.S. Structure and function of the HIV envelope glycoprotein as entry mediator, vaccine immunogen, and target for inhibitors. *Adv Pharmacol* **55**, 33-97 (2007).
36. Zhao, C., Li, H., Swartz, T.H. & Chen, B.K. The HIV Env Glycoprotein Conformational States on Cells and Viruses. *mBio* **13**, e01825-21 (2022).
37. Zhang, S. et al. Dual Pathways of Human Immunodeficiency Virus Type 1 Envelope Glycoprotein Trafficking Modulate the Selective Exclusion of Uncleaved Oligomers from Virions. *Journal of Virology* **95**, 10.1128/jvi.01369-20 (2021).
38. Claeys, E. & Vermeire, K. The CD4 Receptor: An Indispensable Protein in T Cell Activation and A Promising Target for Immunosuppression. *Archives of Microbiology & Immunology* **3**, 133-150 (2019).
39. Shaik, M.M. et al. Structural basis of coreceptor recognition by HIV-1 envelope spike. *Nature* **565**, 318-323 (2019).
40. Hu, W.S. & Hughes, S.H. HIV-1 reverse transcription. *Cold Spring Harb Perspect Med* **2**(2012).
41. Chauhan, A. & Khandkar, M. Endocytosis of human immunodeficiency virus 1 (HIV-1) in astrocytes: a fiery path to its destination. *Microb Pathog* **78**, 1-6 (2015).
42. Aiken, C. & Rousso, I. The HIV-1 capsid and reverse transcription. *Retrovirology* **18**, 29 (2021).
43. Müller, T.G., Zila, V., Müller, B. & Kräusslich, H.-G. Nuclear Capsid Uncoating and Reverse Transcription of HIV-1. *Annual Review of Virology* **9**, 261-284 (2022).
44. Hill, M., Tachedjian, G. & Mak, J. The packaging and maturation of the HIV-1 Pol proteins. *Curr HIV Res* **3**, 73-85 (2005).
45. Corona, A. et al. Ribonuclease H/DNA Polymerase HIV-1 Reverse Transcriptase Dual Inhibitor: Mechanistic Studies on the Allosteric Mode of Action of Isatin-Based Compound RMNC6. *PLOS ONE* **11**, e0147225 (2016).
46. Overview of Reverse Transcription. in *Retroviruses* (ed. Coffin JM, H.S., Varmus HE) (Cold Spring Harbor Laboratory Press, Cold Spring Harbor, NY, 1997).
47. Engelman, A.N. & Singh, P.K. Cellular and molecular mechanisms of HIV-1 integration targeting. *Cell Mol Life Sci* **75**, 2491-2507 (2018).
48. Ohlmann, T., Mengardi, C. & López-Lastra, M. Translation initiation of the HIV-1 mRNA. *Translation (Austin)* **2**, e960242 (2014).
49. Karn, J. & Stoltzfus, C.M. Transcriptional and posttranscriptional regulation of HIV-1 gene expression. *Cold Spring Harb Perspect Med* **2**, a006916 (2012).
50. Richter, S.N., Frasson, I. & Palù, G. Strategies for inhibiting function of HIV-1 accessory proteins: a necessary route to AIDS therapy? *Curr Med Chem* **16**, 267-86 (2009).
51. Das, A.T., Klaver, B. & Berkhout, B. The 5' and 3' TAR elements of human immunodeficiency virus exert effects at several points in the virus life cycle. *J Virol* **72**, 9217-23 (1998).
52. Buffalo, C.Z., Iwamoto, Y., Hurley, J.H. & Ren, X. How HIV Nef Proteins Hijack Membrane Traffic To Promote Infection. *J Virol* **93**(2019).

53. Foster, J.L. & Garcia, J.V. HIV-1 Nef: at the crossroads. *Retrovirology* **5**, 84 (2008).
54. Magadán, J.G. et al. Multilayered Mechanism of CD4 Downregulation by HIV-1 Vpu Involving Distinct ER Retention and ERAD Targeting Steps. *PLOS Pathogens* **6**, e1000869 (2010).
55. Brakier-Gingras, L., Charbonneau, J. & Butcher, S.E. Targeting frameshifting in the human immunodeficiency virus. *Expert Opin Ther Targets* **16**, 249-58 (2012).
56. Freed, E.O. HIV-1 assembly, release and maturation. *Nature Reviews Microbiology* **13**, 484-496 (2015).
57. Mouzakis, K.D., Lang, A.L., Vander Meulen, K.A., Easterday, P.D. & Butcher, S.E. HIV-1 frameshift efficiency is primarily determined by the stability of base pairs positioned at the mRNA entrance channel of the ribosome. *Nucleic Acids Res* **41**, 1901-13 (2013).
58. Guerrero, S. et al. HIV-1 replication and the cellular eukaryotic translation apparatus. *Viruses* **7**, 199-218 (2015).
59. Khan, N. & Geiger, J.D. Role of Viral Protein U (Vpu) in HIV-1 Infection and Pathogenesis. *Viruses* **13**(2021).
60. Sheehy, A.M., Gaddis, N.C., Choi, J.D. & Malim, M.H. Isolation of a human gene that inhibits HIV-1 infection and is suppressed by the viral Vif protein. *Nature* **418**, 646-650 (2002).
61. Sheehy, A.M., Gaddis, N.C. & Malim, M.H. The antiretroviral enzyme APOBEC3G is degraded by the proteasome in response to HIV-1 Vif. *Nature medicine* **9**, 1404-1407 (2003).
62. Marin, M., Rose, K.M., Kozak, S.L. & Kabat, D. HIV-1 Vif protein binds the editing enzyme APOBEC3G and induces its degradation. *Nature medicine* **9**, 1398-1403 (2003).
63. Stopak, K., de Noronha, C., Yonemoto, W. & Greene, W.C. HIV-1 Vif blocks the antiviral activity of APOBEC3G by impairing both its translation and intracellular stability. *Mol Cell* **12**, 591-601 (2003).
64. Wiegand, H.L., Doehle, B.P., Bogerd, H.P. & Cullen, B.R. A second human antiretroviral factor, APOBEC3F, is suppressed by the HIV-1 and HIV-2 Vif proteins. *EMBO J* **23**, 2451-8 (2004).
65. Hu, Y. et al. Structural basis of antagonism of human APOBEC3F by HIV-1 Vif. *Nature Structural & Molecular Biology* **26**, 1176-1183 (2019).
66. Emerman, M. HIV-1, Vpr and the cell cycle. *Current Biology* **6**, 1096-1103 (1996).
67. González, M.E. The HIV-1 Vpr Protein: A Multifaceted Target for Therapeutic Intervention. *International Journal of Molecular Sciences* **18**, 126 (2017).
68. Nodder, S.B. & Gummuluru, S. Illuminating the Role of Vpr in HIV Infection of Myeloid Cells. *Frontiers in Immunology* **10**(2019).
69. Yandrapalli, N. et al. Self assembly of HIV-1 Gag protein on lipid membranes generates PI(4,5)P(2)/Cholesterol nanoclusters. *Sci Rep* **6**, 39332 (2016).
70. Waheed, A.A., Ono, A. & Freed, E.O. Methods for the study of HIV-1 assembly. *Methods Mol Biol* **485**, 163-84 (2009).
71. Rossi, E., Meuser, M.E., Cunanan, C.J. & Cocklin, S. Structure, Function, and Interactions of the HIV-1 Capsid Protein. *Life (Basel)* **11**(2021).

72. Samal, A.B., Green, T.J. & Saad, J.S. Atomic view of the HIV-1 matrix lattice; implications on virus assembly and envelope incorporation. *Proceedings of the National Academy of Sciences* **119**, e2200794119 (2022).
73. Ghanam, R.H., Samal, A.B., Fernandez, T.F. & Saad, J.S. Role of the HIV-1 Matrix Protein in Gag Intracellular Trafficking and Targeting to the Plasma Membrane for Virus Assembly. *Front Microbiol* **3**, 55 (2012).
74. Weiss, E.R. & Göttlinger, H. The role of cellular factors in promoting HIV budding. *J Mol Biol* **410**, 525-33 (2011).
75. London, R.E. Structural Maturation of HIV-1 Reverse Transcriptase-A Metamorphic Solution to Genomic Instability. *Viruses* **8**(2016).
76. Agniswamy, J., Sayer, J.M., Weber, I.T. & Louis, J.M. Terminal interface conformations modulate dimer stability prior to amino terminal autoprocessing of HIV-1 protease. *Biochemistry* **51**, 1041-50 (2012).
77. Harrison, J. et al. Cryo-EM structure of the HIV-1 Pol polyprotein provides insights into virion maturation. *Sci Adv* **8**, eabn9874 (2022).
78. Weber, I.T., Wang, Y.F. & Harrison, R.W. HIV Protease: Historical Perspective and Current Research. *Viruses* **13**(2021).
79. Schmidt, T., Schwieters, C.D. & Clore, G.M. Spatial domain organization in the HIV-1 reverse transcriptase p66 homodimer precursor probed by double electron-electron resonance EPR. *Proceedings of the National Academy of Sciences* **116**, 17809-17816 (2019).
80. Kleinpeter, A.B. & Freed, E.O. HIV-1 Maturation: Lessons Learned from Inhibitors. *Viruses* **12**, 940 (2020).
81. Doitsh, G. & Greene, W.C. Dissecting How CD4 T Cells Are Lost During HIV Infection. *Cell Host Microbe* **19**, 280-91 (2016).
82. Chen, Q. et al. HIV associated cell death: Peptide-induced apoptosis restricts viral transmission. *Front Immunol* **14**, 1096759 (2023).
83. Coffin, J.M. & Hughes, S.H. Clonal Expansion of Infected CD4+ T Cells in People Living with HIV. *Viruses* **13**(2021).
84. Siliciano, R.F. & Greene, W.C. HIV latency. *Cold Spring Harb Perspect Med* **1**, a007096 (2011).
85. Vanhamel, J., Bruggemans, A. & Debyser, Z. Establishment of latent HIV-1 reservoirs: what do we really know? *J Virus Erad* **5**, 3-9 (2019).
86. UNAIDS. In Danger: UNAIDS Global AIDS Update 2022. (Geneva: Joint United Nations Programme on HIV/AIDS, 2022).
87. Baral, S. et al. Burden of HIV among female sex workers in low-income and middle-income countries: a systematic review and meta-analysis. *Lancet Infect Dis* **12**, 538-49 (2012).
88. Jewkes, R.K., Dunkle, K., Nduna, M. & Shai, N. Intimate partner violence, relationship power inequity, and incidence of HIV infection in young women in South Africa: a cohort study. *Lancet* **376**, 41-8 (2010).
89. Violence against women prevalence estimates, 2018: global, regional and national prevalence estimates for intimate partner violence against women, and global and regional prevalence estimates for non-partner sexual violence against women. (Geneva, 2021).

90. Lincoln, C., Perera, R., Jacobs, I. & Ward, A. Macroscopically detected female genital injury after consensual and non-consensual vaginal penetration: A prospective comparison study. *Journal of Forensic and Legal Medicine* **20**, 884-901 (2013).
91. Gilliam, B.L., Riedel, D.J. & Redfield, R.R. Clinical use of CCR5 inhibitors in HIV and beyond. *Journal of Translational Medicine* **9**, S9 (2011).
92. Ramana, L.N., Anand, A.R., Sethuraman, S. & Krishnan, U.M. Targeting strategies for delivery of anti-HIV drugs. *J Control Release* **192**, 271-83 (2014).
93. Lalezari, J.P. et al. A phase II clinical study of the long-term safety and antiviral activity of enfuvirtide-based antiretroviral therapy. *AIDS* **17**, 691-698 (2003).
94. Jamjian, M.C. & McNicholl, I.R. Enfuvirtide: first fusion inhibitor for treatment of HIV infection. *American Journal of Health-System Pharmacy* **61**, 1242-1247 (2004).
95. Matsumoto, K. et al. Characterization of a Novel CD4 Mimetic Compound YIR-821 against HIV-1 Clinical Isolates. *J Virol* **97**, e0163822 (2023).
96. Umotoy, J.C. & de Taeye, S.W. Antibody Conjugates for Targeted Therapy Against HIV-1 as an Emerging Tool for HIV-1 Cure. *Front Immunol* **12**, 708806 (2021).
97. Holec, A.D., Mandal, S., Prathipati, P.K. & Destache, C.J. Nucleotide Reverse Transcriptase Inhibitors: A Thorough Review, Present Status and Future Perspective as HIV Therapeutics. *Curr HIV Res* **15**, 411-421 (2017).
98. Jayne, J. Drug Resistance and Pre-exposure Prophylaxis (PrEP) Breakthrough Infections Threaten Goals to End the HIV/AIDS Epidemic. (American Society for Microbiology, Online, 2020).
99. Namasivayam, V. et al. The Journey of HIV-1 Non-Nucleoside Reverse Transcriptase Inhibitors (NNRTIs) from Lab to Clinic. *Journal of Medicinal Chemistry* **62**, 4851-4883 (2019).
100. Zhao, A.V. et al. A clinical review of HIV integrase strand transfer inhibitors (INSTIs) for the prevention and treatment of HIV-1 infection. *Retrovirology* **19**, 22 (2022).
101. Biswas, P., Jiang, X., Pacchia, A.L., Dougherty, J.P. & Peltz, S.W. The human immunodeficiency virus type 1 ribosomal frameshifting site is an invariant sequence determinant and an important target for antiviral therapy. *J Virol* **78**, 2082-7 (2004).
102. Anokhina, V.S. & Miller, B.L. Targeting Ribosomal Frameshifting as an Antiviral Strategy: From HIV-1 to SARS-CoV-2. *Accounts of Chemical Research* **54**, 3349-3361 (2021).
103. Thenin-Houssier, S. & Valente, S.T. HIV-1 Capsid Inhibitors as Antiretroviral Agents. *Curr HIV Res* **14**, 270-82 (2016).
104. Carnes, S.K., Sheehan, J.H. & Aiken, C. Inhibitors of the HIV-1 capsid, a target of opportunity. *Curr Opin HIV AIDS* **13**, 359-365 (2018).
105. McFadden, W.M. et al. Rotten to the core: antivirals targeting the HIV-1 capsid core. *Retrovirology* **18**, 41 (2021).
106. Diseases, N.I.o.D.a.D.a.K. LiverTox: Clinical and Research Information on Drug-Induced Liver Injury. in *Protease Inhibitors (HIV)* (Bethesda, MD, 2012).

107. Lv, Z., Chu, Y. & Wang, Y. HIV protease inhibitors: a review of molecular selectivity and toxicity. *HIV AIDS (Auckl)* **7**, 95-104 (2015).
108. Taylor, B.S., Sobieszczyk, M.E., McCutchan, F.E. & Hammer, S.M. The challenge of HIV-1 subtype diversity. *N Engl J Med* **358**, 1590-602 (2008).
109. Sharp, P.M. et al. The origins of acquired immune deficiency syndrome viruses: where and when? *Philos Trans R Soc Lond B Biol Sci* **356**, 867-76 (2001).
110. Hahn, B.H., Shaw, G.M., De Cock, K.M. & Sharp, P.M. AIDS as a zoonosis: scientific and public health implications. *Science* **287**, 607-14 (2000).
111. Sharp, P.M. & Hahn, B.H. The evolution of HIV-1 and the origin of AIDS. *Philos Trans R Soc Lond B Biol Sci* **365**, 2487-94 (2010).
112. Sharp, P.M. & Hahn, B.H. Origins of HIV and the AIDS pandemic. *Cold Spring Harb Perspect Med* **1**, a006841 (2011).
113. Rupp, S., Ambata, P., Narat, V. & Giles-Vernick, T. Beyond the Cut Hunter: A Historical Epidemiology of HIV Beginnings in Central Africa. *Ecohealth* **13**, 661-671 (2016).
114. Wertheim, J.O. & Worobey, M. Dating the age of the SIV lineages that gave rise to HIV-1 and HIV-2. *PLoS Comput Biol* **5**, e1000377 (2009).
115. Salemi, M. et al. Dating the common ancestor of SIVcpz and HIV-1 group M and the origin of HIV-1 subtypes using a new method to uncover clock-like molecular evolution. *Faseb j* **15**, 276-8 (2001).
116. Faria, N.R. et al. HIV epidemiology. The early spread and epidemic ignition of HIV-1 in human populations. *Science* **346**, 56-61 (2014).
117. Chitnis, A., Rawls, D. & Moore, J. Origin of HIV type 1 in colonial French Equatorial Africa? *AIDS Res Hum Retroviruses* **16**, 5-8 (2000).
118. Vidal, N. et al. Unprecedented degree of human immunodeficiency virus type 1 (HIV-1) group M genetic diversity in the Democratic Republic of Congo suggests that the HIV-1 pandemic originated in Central Africa. *J Virol* **74**, 10498-507 (2000).
119. Worobey, M. et al. Direct evidence of extensive diversity of HIV-1 in Kinshasa by 1960. *Nature* **455**, 661-664 (2008).
120. Gilbert, M.T. et al. The emergence of HIV/AIDS in the Americas and beyond. *Proc Natl Acad Sci U S A* **104**, 18566-70 (2007).
121. Kaleebu, P. et al. Relation between chemokine receptor use, disease stage, and HIV-1 subtypes A and D: results from a rural Ugandan cohort. *J Acquir Immune Defic Syndr* **45**, 28-33 (2007).
122. Robertson, D.L. et al. HIV-1 nomenclature proposal. *Science* **288**, 55-6 (2000).
123. Kessler, H.H. et al. Determination of human immunodeficiency virus type 1 subtypes by a rapid method useful for the routine diagnostic laboratory. *Clin Diagn Lab Immunol* **8**, 1018-20 (2001).
124. Fonjungo, P.N. et al. Human immunodeficiency virus type 1 group m protease in cameroon: genetic diversity and protease inhibitor mutational features. *J Clin Microbiol* **40**, 837-45 (2002).
125. Mendes Da Silva, R.K., Monteiro de Pina, A., II, Venegas Maciera, K., Gonçalves Morgado, M. & Lindenmeyer Guimarães, M. Genetic Characterization of a New HIV-1 Sub-Subtype A in Cabo Verde, Denominated A8. *Viruses* **13**(2021).

126. Hemelaar, J., Gouws, E., Ghys, P.D. & Osmanov, S. Global trends in molecular epidemiology of HIV-1 during 2000-2007. *Aids* **25**, 679-89 (2011).
127. Williams, A. et al. Geographic and Population Distributions of Human Immunodeficiency Virus (HIV)–1 and HIV-2 Circulating Subtypes: A Systematic Literature Review and Meta-analysis (2010–2021). *The Journal of Infectious Diseases* **228**, 1583-1591 (2023).
128. Gartner, M.J., Roche, M., Churchill, M.J., Gorry, P.R. & Flynn, J.K. Understanding the mechanisms driving the spread of subtype C HIV-1. *eBioMedicine* **53**(2020).
129. Bbosa, N., Kaleebu, P. & Ssemwanga, D. HIV subtype diversity worldwide. *Current Opinion in HIV and AIDS* **14**, 153-160 (2019).
130. Vidal, N., Bazepeo, S.E., Mulanga, C., Delaporte, E. & Peeters, M. Genetic characterization of eight full-length HIV type 1 genomes from the Democratic Republic of Congo (DRC) reveal a new subsubtype, A5, in the A radiation that predominates in the recombinant structure of CRF26_A5U. *AIDS Res Hum Retroviruses* **25**, 823-32 (2009).
131. Abidi, S.H. et al. Origin and evolution of HIV-1 subtype A6. *PLoS One* **16**, e0260604 (2021).
132. Grant, H.E. et al. A large population sample of African HIV genomes from the 1980s reveals a reduction in subtype D over time associated with propensity for CXCR4 tropism. *Retrovirology* **19**, 28 (2022).
133. Gounder, K. et al. Complex Subtype Diversity of HIV-1 Among Drug Users in Major Kenyan Cities. *AIDS Res Hum Retroviruses* **33**, 500-510 (2017).
134. Désiré, N. et al. Characterization update of HIV-1 M subtypes diversity and proposal for subtypes A and D sub-subtypes reclassification. *Retrovirology* **15**, 80 (2018).
135. Avila, M.M. et al. Two HIV-1 epidemics in Argentina: different genetic subtypes associated with different risk groups. *J Acquir Immune Defic Syndr* **29**, 422-6 (2002).
136. Tongo, M. et al. Phylogenetics of HIV-1 subtype G env: Greater complexity and older origins than previously reported. *Infection, Genetics and Evolution* **35**, 9-18 (2015).
137. Faria, N.R. et al. Distinct rates and patterns of spread of the major HIV-1 subtypes in Central and East Africa. *PLOS Pathogens* **15**, e1007976 (2019).
138. Triques, K. et al. Near-full-length genome sequencing of divergent African HIV type 1 subtype F viruses leads to the identification of a new HIV type 1 subtype designated K. *AIDS Res Hum Retroviruses* **16**, 139-51 (2000).
139. Yamaguchi, J. et al. Brief Report: Complete Genome Sequence of CG-0018a-01 Establishes HIV-1 Subtype L. *J Acquir Immune Defic Syndr* **83**, 319-322 (2020).
140. Li, X. et al. Tracing the epidemic history of HIV-1 CRF01_AE clusters using near-complete genome sequences. *Scientific Reports* **7**, 4024 (2017).
141. Alexiev, I. et al. Molecular Epidemiological Analysis of the Origin and Transmission Dynamics of the HIV-1 CRF01_AE Sub-Epidemic in Bulgaria. *Viruses* **13**(2021).

142. Kostaki, E.-G. et al. Spatiotemporal Characteristics of the Largest HIV-1 CRF02_AG Outbreak in Spain: Evidence for Onward Transmissions. *Frontiers in Microbiology* **10**(2019).
143. Rolland, M. & Modjarrad, K. Multiple co-circulating HIV-1 subtypes in the Middle East and North Africa. *Aids* **29**, 1417-9 (2015).
144. Shaw, G.M. & Hunter, E. HIV transmission. *Cold Spring Harb Perspect Med* **2**(2012).
145. Kariuki, S.M., Selhorst, P., Ariën, K.K. & Dorfman, J.R. The HIV-1 transmission bottleneck. *Retrovirology* **14**, 22 (2017).
146. Bagaya, B.S. et al. Functional bottlenecks for generation of HIV-1 intersubtype Env recombinants. *Retrovirology* **12**, 44 (2015).
147. Grivel, J.-C., Shattock, R.J. & Margolis, L.B. Selective transmission of R5 HIV-1 variants: where is the gatekeeper? *Journal of Translational Medicine* **9**, S6 (2010).
148. Margolis, L. & Shattock, R. Selective transmission of CCR5-utilizing HIV-1: the 'gatekeeper' problem resolved? *Nature Reviews Microbiology* **4**, 312-317 (2006).
149. Keele, B.F. et al. Identification and characterization of transmitted and early founder virus envelopes in primary HIV-1 infection. *Proc Natl Acad Sci U S A* **105**, 7552-7 (2008).
150. Parrish, N.F. et al. Phenotypic properties of transmitted founder HIV-1. *Proceedings of the National Academy of Sciences* **110**, 6626-6633 (2013).
151. Samson, M. et al. Resistance to HIV-1 infection in caucasian individuals bearing mutant alleles of the CCR-5 chemokine receptor gene. *Nature* **382**, 722-5 (1996).
152. Lopalco, L. CCR5: From Natural Resistance to a New Anti-HIV Strategy. *Viruses* **2**, 574-600 (2010).
153. Abecasis, A.B. et al. HIV-1 subtype distribution and its demographic determinants in newly diagnosed patients in Europe suggest highly compartmentalized epidemics. *Retrovirology* **10**, 7 (2013).
154. Buonaguro, L., Tornesello, M.L. & Buonaguro, F.M. Human immunodeficiency virus type 1 subtype distribution in the worldwide epidemic: pathogenetic and therapeutic implications. *J Virol* **81**, 10209-19 (2007).
155. van Harmelen, J. et al. An association between HIV-1 subtypes and mode of transmission in Cape Town, South Africa. *Aids* **11**, 81-7 (1997).
156. Ball, S.C. et al. Comparing the ex vivo fitness of CCR5-tropic human immunodeficiency virus type 1 isolates of subtypes B and C. *J Virol* **77**, 1021-38 (2003).
157. Junqueira, D.M. & Almeida, S.E.d.M. HIV-1 subtype B: Traces of a pandemic. *Virology* **495**, 173-184 (2016).
158. Pernas, B. et al. High prevalence of subtype F in newly diagnosed HIV-1 persons in northwest Spain and evidence for impaired treatment response. *Aids* **28**, 1837-40 (2014).
159. James, A. & Dixit, N.M. Transmitted HIV-1 is more virulent in heterosexual individuals than men-who-have-sex-with-men. *PLOS Pathogens* **18**, e1010319 (2022).
160. Patel, P. et al. Estimating per-act HIV transmission risk: a systematic review. *AIDS* **28**, 1509-1519 (2014).

161. Baeten, J.M. et al. HIV-1 Subtype D Infection Is Associated with Faster Disease Progression than Subtype A in Spite of Similar Plasma HIV-1 Loads. *The Journal of Infectious Diseases* **195**, 1177-1180 (2007).
162. Easterbrook, P.J. et al. Impact of HIV-1 viral subtype on disease progression and response to antiretroviral therapy. *J Int AIDS Soc* **13**, 4 (2010).
163. Eshleman, S.H. et al. Characterization of nevirapine resistance mutations in women with subtype A vs. D HIV-1 6-8 weeks after single-dose nevirapine (HIVNET 012). *J Acquir Immune Defic Syndr* **35**, 126-30 (2004).
164. Huang, W. et al. Coreceptor Tropism in Human Immunodeficiency Virus Type 1 Subtype D: High Prevalence of CXCR4 Tropism and Heterogeneous Composition of Viral Populations. *Journal of Virology* **81**, 7885-7893 (2007).
165. Kaleebu, P. et al. Effect of human immunodeficiency virus (HIV) type 1 envelope subtypes A and D on disease progression in a large cohort of HIV-1-positive persons in Uganda. *J Infect Dis* **185**, 1244-50 (2002).
166. Kapaata, A. et al. Infection with HIV-1 subtype D among acutely infected Ugandans is associated with higher median concentration of cytokines compared to subtype A. *IJID Regions* **3**, 89-95 (2022).
167. Kiwanuka, N. et al. HIV-1 viral subtype differences in the rate of CD4+ T-cell decline among HIV seroincident antiretroviral naive persons in Rakai district, Uganda. *J Acquir Immune Defic Syndr* **54**, 180-4 (2010).
168. Kyeyune, F. et al. Treatment failure and drug resistance is more frequent in HIV-1 subtype D versus subtype A-infected Ugandans over a 10-year study period. *AIDS* **27**, 1899-1909 (2013).
169. Parczewski, M. et al. Infection with HIV-1 subtype D adversely affects the live expectancy independently of antiretroviral drug use. *Infection, Genetics and Evolution* **90**, 104754 (2021).
170. Venner, C.M. et al. Infecting HIV-1 Subtype Predicts Disease Progression in Women of Sub-Saharan Africa. *EBioMedicine* **13**, 305-314 (2016).
171. Balinda, S.N. et al. Characterization of Near Full-Length Transmitted/Founder HIV-1 Subtype D and A/D Recombinant Genomes in a Heterosexual Ugandan Population (2006-2011). *Viruses* **14**(2022).
172. Ssemwanga, D. et al. Effect of HIV-1 Subtypes on Disease Progression in Rural Uganda: A Prospective Clinical Cohort Study. *PLOS ONE* **8**, e71768 (2013).
173. Panos, G. & Nelson, M. HIV-1 tropism. *Biomarkers in Medicine* **1**, 473-481 (2007).
174. Abraha, A. et al. CCR5- and CXCR4-tropic subtype C human immunodeficiency virus type 1 isolates have a lower level of pathogenic fitness than other dominant group M subtypes: implications for the epidemic. *J Virol* **83**, 5592-605 (2009).
175. Ringel, O. et al. The Hard Way towards an Antibody-Based HIV-1 Env Vaccine: Lessons from Other Viruses. *Viruses* **10**(2018).
176. Kim, D., Elizaga, M. & Duerr, A. HIV vaccine efficacy trials: towards the future of HIV prevention. *Infect Dis Clin North Am* **21**, 201-17, x (2007).
177. Ng'uni, T., Chasara, C. & Ndhlovu, Z.M. Major Scientific Hurdles in HIV Vaccine Development: Historical Perspective and Future Directions. *Front Immunol* **11**, 590780 (2020).

178. Borgo, G.M. & Rutishauser, R.L. Generating and measuring effective vaccine-elicited HIV-specific CD8 + T cell responses. *Curr Opin HIV AIDS* **18**, 331-341 (2023).
179. Global HIV & AIDS statistics — Fact sheet. (UNAIDS, 2023).
180. HIV.gov. The Global HIV and AIDS Epidemic. in *Data & Trends* Vol. 2024 (ed. HIV.gov) (HIV.gov, 2023).
181. UNAIDS. UNAIDS 2017. (2017).
182. HIV.gov. Impact on Racial and Ethnic Minorities. in *Data & Trends* Vol. 2024 (ed. HIV.gov) (HIV.gov, 2023).
183. HIV.gov. US Statistics. in *Data and Trends* Vol. 2024 (HIV.gov, Online, 2021).
184. HIV in the Southern United States. (Centers for Disease Control, 2019).
185. Li, S. et al. Overview of the reporter genes and reporter mouse models. *Animal Model Exp Med* **1**, 29-35 (2018).
186. Ghim, C.M., Lee, S.K., Takayama, S. & Mitchell, R.J. The art of reporter proteins in science: past, present and future applications. *BMB Rep* **43**, 451-60 (2010).
187. Consortium, U. Q9U6Y8 · RFP_DISSP. (ed. UniProt) (UniProt, 2024).
188. Gorman, C.M., Merlino, G.T., Willingham, M.C., Pastan, I. & Howard, B.H. The Rous sarcoma virus long terminal repeat is a strong promoter when introduced into a variety of eukaryotic cells by DNA-mediated transfection. *Proceedings of the National Academy of Sciences* **79**, 6777-6781 (1982).
189. Smale, S.T. Chloramphenicol acetyltransferase assay. *Cold Spring Harb Protoc* **2010**, pdb.prot5422 (2010).
190. Gendelman, H.E. et al. Trans-activation of the human immunodeficiency virus long terminal repeat sequence by DNA viruses. *Proc Natl Acad Sci U S A* **83**, 9759-63 (1986).
191. Ben-Artzi, H., Zeelon, E., Gorecki, M. & Panet, A. Double-stranded RNA-dependent RNase activity associated with human immunodeficiency virus type 1 reverse transcriptase. *Proc Natl Acad Sci U S A* **89**, 927-31 (1992).
192. Serganova, I. & Blasberg, R.G. Molecular Imaging with Reporter Genes: Has Its Promise Been Delivered? *Journal of Nuclear Medicine* **60**, 1665-1681 (2019).
193. Jefferson, R.A., Kavanagh, T.A. & Bevan, M.W. GUS fusions: beta-glucuronidase as a sensitive and versatile gene fusion marker in higher plants. *Embo j* **6**, 3901-7 (1987).
194. Lis, J.T., Simon, J.A. & Sutton, C.A. New heat shock puffs and beta-galactosidase activity resulting from transformation of Drosophila with an hsp70-lacZ hybrid gene. *Cell* **35**, 403-10 (1983).
195. Wei, X. et al. Emergence of resistant human immunodeficiency virus type 1 in patients receiving fusion inhibitor (T-20) monotherapy. *Antimicrob Agents Chemother* **46**, 1896-905 (2002).
196. Platt, E.J., Wehrly, K., Kuhmann, S.E., Chesebro, B. & Kabat, D. Effects of CCR5 and CD4 cell surface concentrations on infections by macrophagetropic isolates of human immunodeficiency virus type 1. *J Virol* **72**, 2855-64 (1998).
197. Sarzotti-Kelsoe, M. et al. Optimization and validation of the TZM-bl assay for standardized assessments of neutralizing antibodies against HIV-1. *J Immunol Methods* **409**, 131-46 (2014).

198. England, C.G., Ehlerding, E.B. & Cai, W. NanoLuc: A Small Luciferase Is Brightening Up the Field of Bioluminescence. *Bioconjug Chem* **27**, 1175-1187 (2016).
199. de Wet, J.R., Wood, K.V., Helinski, D.R. & DeLuca, M. Cloning of firefly luciferase cDNA and the expression of active luciferase in Escherichia coli. *Proc Natl Acad Sci U S A* **82**, 7870-3 (1985).
200. Tannous, B.A., Kim, D.E., Fernandez, J.L., Weissleder, R. & Breakefield, X.O. Codon-optimized Gaussia luciferase cDNA for mammalian gene expression in culture and in vivo. *Mol Ther* **11**, 435-43 (2005).
201. Suree, N., Koizumi, N., Sahakyan, A., Shimizu, S. & An, D.S. A novel HIV-1 reporter virus with a membrane-bound Gaussia princeps luciferase. *J Virol Methods* **183**, 49-56 (2012).
202. Maguire, C.A. et al. Gaussia luciferase variant for high-throughput functional screening applications. *Anal Chem* **81**, 7102-6 (2009).
203. Hall, M.P. et al. Engineered luciferase reporter from a deep sea shrimp utilizing a novel imidazopyrazinone substrate. *ACS Chem Biol* **7**, 1848-57 (2012).
204. Terwilliger, E.F., Godin, B., Sodroski, J.G. & Haseltine, W.A. Construction and use of a replication-competent human immunodeficiency virus (HIV-1) that expresses the chloramphenicol acetyltransferase enzyme. *Proc Natl Acad Sci U S A* **86**, 3857-61 (1989).
205. Chen, B.K., Saksela, K., Andino, R. & Baltimore, D. Distinct modes of human immunodeficiency virus type 1 proviral latency revealed by superinfection of nonproductively infected cell lines with recombinant luciferase-encoding viruses. *J Virol* **68**, 654-60 (1994).
206. KATHLEEN A. PAGE, T.L., and MARK B. FEINBERG. Use of a Green Fluorescent Protein as a Marker for Human Immunodeficiency Virus Type 1 Infection. *AIDS Research and Human Retroviruses* **13**, 1077-1081 (1997).
207. Jamieson, B.D. & Zack, J.A. In Vivo Pathogenesis of a Human Immunodeficiency Virus Type 1 Reporter Virus. *Journal of Virology* **72**, 6520-6526 (1998).
208. Levy, D.N., Aldrovandi, G.M., Kutsch, O. & Shaw, G.M. Dynamics of HIV-1 recombination in its natural target cells. *Proc Natl Acad Sci U S A* **101**, 4204-9 (2004).
209. Edmonds, T.G. et al. Replication competent molecular clones of HIV-1 expressing Renilla luciferase facilitate the analysis of antibody inhibition in PBMC. *Virology* **408**, 1-13 (2010).
210. Brown, A., Gartner, S., Kawano, T., Benoit, N. & Cheng-Mayer, C. HLA-A2 down-regulation on primary human macrophages infected with an M-tropic EGFP-tagged HIV-1 reporter virus. *J Leukoc Biol* **78**, 675-85 (2005).
211. Müller, B. et al. Construction and characterization of a fluorescently labeled infectious human immunodeficiency virus type 1 derivative. *J Virol* **78**, 10803-13 (2004).
212. Kirui, J. & Freed, E.O. Generation and validation of a highly sensitive bioluminescent HIV-1 reporter vector that simplifies measurement of virus release. *Retrovirology* **17**(2020).

213. Hübner, W. et al. Sequence of Human Immunodeficiency Virus Type 1 (HIV-1) Gag Localization and Oligomerization Monitored with Live Confocal Imaging of a Replication-Competent, Fluorescently Tagged HIV-1. *Journal of Virology* **81**, 12596-12607 (2007).
214. Donnelly, M.L.L. et al. Analysis of the aphthovirus 2A/2B polyprotein 'cleavage' mechanism indicates not a proteolytic reaction, but a novel translational effect: a putative ribosomal 'skip'. *J Gen Virol* **82**, 1013-1025 (2001).
215. Alberti, M.O. et al. Optimized Replicating Renilla Luciferase Reporter HIV-1 Utilizing Novel Internal Ribosome Entry Site Elements for Native Nef Expression and Function. *AIDS Res Hum Retroviruses* **31**, 1278-96 (2015).
216. Prévost, J. et al. Incomplete Downregulation of CD4 Expression Affects HIV-1 Env Conformation and Antibody-Dependent Cellular Cytotoxicity Responses. *J Virol* **92**(2018).
217. deCamp, A. et al. Global panel of HIV-1 Env reference strains for standardized assessments of vaccine-elicited neutralizing antibodies. *J Virol* **88**, 2489-507 (2014).
218. Simon-Loriere, E. et al. Molecular mechanisms of recombination restriction in the envelope gene of the human immunodeficiency virus. *PLoS Pathog* **5**, e1000418 (2009).
219. Binley, J.M. et al. Comprehensive cross-clade neutralization analysis of a panel of anti-human immunodeficiency virus type 1 monoclonal antibodies. *J Virol* **78**, 13232-52 (2004).
220. Salazar-Gonzalez, J.F. et al. Genetic identity, biological phenotype, and evolutionary pathways of transmitted/founder viruses in acute and early HIV-1 infection. *Journal of Experimental Medicine* **206**, 1273-1289 (2009).
221. Cavrois, M. et al. Mass Cytometric Analysis of HIV Entry, Replication, and Remodeling in Tissue CD4+ T Cells. *Cell Rep* **20**, 984-998 (2017).
222. Ventura, J.D. et al. Longitudinal bioluminescent imaging of HIV-1 infection during antiretroviral therapy and treatment interruption in humanized mice. *PLOS Pathogens* **15**, e1008161 (2019).
223. Freel, S.A. et al. Phenotypic and functional profile of HIV-inhibitory CD8 T cells elicited by natural infection and heterologous prime/boost vaccination. *J Virol* **84**, 4998-5006 (2010).
224. Pollara, J. et al. Association of HIV-1 Envelope-Specific Breast Milk IgA Responses with Reduced Risk of Postnatal Mother-to-Child Transmission of HIV-1. *J Virol* **89**, 9952-61 (2015).
225. Sung, J.A. et al. Dual-Affinity Re-Targeting proteins direct T cell-mediated cytolysis of latently HIV-infected cells. *J Clin Invest* **125**, 4077-90 (2015).
226. Astronomo, R.D. et al. Neutralization Takes Precedence Over IgG or IgA Isotype-related Functions in Mucosal HIV-1 Antibody-mediated Protection. *EBioMedicine* **14**, 97-111 (2016).
227. Astronomo, R.D. et al. Rectal tissue and vaginal tissue from intravenous VRC01 recipients show protection against ex vivo HIV-1 challenge. *J Clin Invest* **131**(2021).
228. Gornalusse, G.G. et al. Buprenorphine Increases HIV-1 Infection In Vitro but Does Not Reactivate HIV-1 from Latency. *Viruses* **13**(2021).

229. Seay, K. et al. In Vivo Activation of Human NK Cells by Treatment with an Interleukin-15 Superagonist Potently Inhibits Acute In Vivo HIV-1 Infection in Humanized Mice. *J Virol* **89**, 6264-74 (2015).
230. Seay, K. et al. The Vaginal Acquisition and Dissemination of HIV-1 Infection in a Novel Transgenic Mouse Model Is Facilitated by Coinfection with Herpes Simplex Virus 2 and Is Inhibited by Microbicide Treatment. *J Virol* **89**, 9559-70 (2015).
231. Bardhi, A. et al. Potent In Vivo NK Cell-Mediated Elimination of HIV-1-Infected Cells Mobilized by a gp120-Bispecific and Hexavalent Broadly Neutralizing Fusion Protein. *J Virol* **91**(2017).
232. Anthony-Gonda, K. et al. Multispecific anti-HIV duoCAR-T cells display broad in vitro antiviral activity and potent in vivo elimination of HIV-infected cells in a humanized mouse model. *Sci Transl Med* **11**(2019).
233. George, A.F. et al. Female Genital Fibroblasts Diminish the In Vitro Efficacy of PrEP against HIV. *Viruses* **14**, 1723 (2022).
234. Ma, T. et al. HIV efficiently infects T cells from the endometrium and remodels them to promote systemic viral spread. *Elife* **9**(2020).
235. Fernandez, N. et al. Assessment of a diverse panel of transmitted/founder HIV-1 infectious molecular clones in a luciferase based CD8 T-cell mediated viral inhibition assay. *Frontiers in Immunology* **13**(2022).
236. Hayes, P. et al. Breadth of CD8 T-cell mediated inhibition of replication of diverse HIV-1 transmitted-founder isolates correlates with the breadth of recognition within a comprehensive HIV-1 Gag, Nef, Env and Pol potential T-cell epitope (PTE) peptide set. *PLOS ONE* **16**, e0260118 (2021).
237. Richardson, S.I. et al. HIV Broadly Neutralizing Antibodies Expressed as IgG3 Preserve Neutralization Potency and Show Improved Fc Effector Function. *Frontiers in Immunology* **12**(2021).
238. Xie, G. et al. Characterization of HIV-induced remodeling reveals differences in infection susceptibility of memory CD4(+) T cell subsets in vivo. *Cell Rep* **35**, 109038 (2021).
239. Fujiwara, S. Humanized mice: A brief overview on their diverse applications in biomedical research. *J Cell Physiol* **233**, 2889-2901 (2018).
240. Council, N.R. Genetically Altered Mice: A Revolutionary Research Resource. in *Sharing Laboratory Resources: Genetically Altered Mice: Summary of a Workshop Held at the National Academy of Sciences, March 23-24, 1993* (National Academies Press, Washington DC, 1994).
241. Seay, K. et al. The Vaginal Acquisition and Dissemination of HIV-1 Infection in a Novel Transgenic Mouse Model Is Facilitated by Coinfection with Herpes Simplex Virus 2 and Is Inhibited by Microbicide Treatment. *Journal of Virology* **89**, 9559-9570 (2015).
242. Seay, K. et al. Mice transgenic for CD4-specific human CD4, CCR5 and cyclin T1 expression: a new model for investigating HIV-1 transmission and treatment efficacy. *PLoS One* **8**, e63537 (2013).
243. Anthony-Gonda, K. et al. In vivo killing of primary HIV-infected cells by peripheral-injected early memory-enriched anti-HIV duoCAR T cells. *JCI Insight* **7**(2022).

244. Mielke, D. et al. ADCC-mediating non-neutralizing antibodies can exert immune pressure in early HIV-1 infection. *PLOS Pathogens* **17**, e1010046 (2021).
245. Fouda, G.G. et al. Postnatally-transmitted HIV-1 Envelope variants have similar neutralization-sensitivity and function to that of nontransmitted breast milk variants. *Retrovirology* **10**, 3 (2013).
246. Grenningloh, R. et al. Ets-1 Maintains IL-7 Receptor Expression in Peripheral T Cells. *The Journal of Immunology* **186**, 969-976 (2011).
247. Freel, S.A. et al. Initial HIV-1 Antigen-Specific CD8⁺ T Cells in Acute HIV-1 Infection Inhibit Transmitted/Founder Virus Replication. *Journal of Virology* **86**, 6835-6846 (2012).
248. Naarding, M.A. et al. Development of a luciferase based viral inhibition assay to evaluate vaccine induced CD8 T-cell responses. *J Immunol Methods* **409**, 161-73 (2014).
249. Sok, D., Moldt, B. & Burton, D.R. SnapShot: broadly neutralizing antibodies. *Cell* **155**, 728-728.e1 (2013).
250. Haynes, B.F. et al. Strategies for HIV-1 vaccines that induce broadly neutralizing antibodies. *Nat Rev Immunol* **23**, 142-158 (2023).
251. Gilbert, P.B. et al. Neutralization titer biomarker for antibody-mediated prevention of HIV-1 acquisition. *Nature Medicine* **28**, 1924-1932 (2022).
252. Pollara, J. et al. High-throughput quantitative analysis of HIV-1 and SIV-specific ADCC-mediating antibody responses. *Cytometry Part A* **79A**, 603-612 (2011).
253. Mielke, D. et al. Selection of HIV Envelope Strains for Standardized Assessments of Vaccine-Elicited Antibody-Dependent Cellular Cytotoxicity-Mediating Antibodies. *Journal of Virology* **96**, e01643-21 (2022).
254. Deniskin, R. & Satter, L.F. Natural Kills Cells. in *Encyclopedia of Infection and Immunity* (ed. Rezaei, N.) 118-129 (Elsevier, Oxford, 2022).
255. Ganesan, A. et al. Immunologic and virologic events in early HIV infection predict subsequent rate of progression. *J Infect Dis* **201**, 272-84 (2010).
256. Claiborne, D.T. et al. Replicative fitness of transmitted HIV-1 drives acute immune activation, proviral load in memory CD4+ T cells, and disease progression. *Proceedings of the National Academy of Sciences* **112**, E1480-E1489 (2015).
257. Quiñones-Mateu, M.E. et al. A dual infection/competition assay shows a correlation between ex vivo human immunodeficiency virus type 1 fitness and disease progression. *J Virol* **74**, 9222-33 (2000).
258. Ariën, K.K. et al. The replicative fitness of primary human immunodeficiency virus type 1 (HIV-1) group M, HIV-1 group O, and HIV-2 isolates. *J Virol* **79**, 8979-90 (2005).
259. Calantone, N. et al. Tissue myeloid cells in SIV-infected primates acquire viral DNA through phagocytosis of infected T cells. *Immunity* **41**, 493-502 (2014).
260. Carias, A.M. et al. Defining the Interaction of HIV-1 with the Mucosal Barriers of the Female Reproductive Tract. *Journal of Virology* **87**, 11388-11400 (2013).
261. Hsu, M. et al. Increased Mucosal Transmission but Not Enhanced Pathogenicity of the CCR5-Tropic, Simian AIDS-Inducing Simian/Human Immunodeficiency Virus SHIV_{SF162P3} Maps to Envelope gp120. *Journal of Virology* **77**, 989-998 (2003).

262. Wessels, J.M. et al. Depot medroxyprogesterone acetate (DMPA) enhances susceptibility and increases the window of vulnerability to HIV-1 in humanized mice. *Scientific Reports* **11**, 3894 (2021).
263. Trifonova, R.T., Lieberman, J. & Van Baarle, D. Distribution of Immune Cells in the Human Cervix and Implications for HIV Transmission. *American Journal of Reproductive Immunology* **71**, 252-264 (2014).
264. Saba, I. et al. Immunocompetent Human 3D Organ-Specific Hormone-Responding Vaginal Mucosa Model of HIV-1 Infection. *Tissue Eng Part C Methods* **27**, 152-166 (2021).
265. Garcia-Tellez, T. et al. Non-human primates in HIV research: Achievements, limits and alternatives. *Infect Genet Evol* **46**, 324-332 (2016).
266. Grivel, J.-C. & Margolis, L. Use of human tissue explants to study human infectious agents. *Nature Protocols* **4**, 256-269 (2009).
267. Saba, E. et al. HIV-1 sexual transmission: early events of HIV-1 infection of human cervico-vaginal tissue in an optimized ex vivo model. *Mucosal Immunology* **3**, 280-290 (2010).
268. Estes, J.D., Legrand, R. & Petrovas, C. Visualizing the Immune System: Providing Key Insights into HIV/SIV Infections. *Frontiers in Immunology* **9**(2018).
269. Asin, S.N., Eszterhas, S.K., Rollenhagen, C., Heimberg, A.M. & Howell, A.L. HIV Type 1 Infection in Women: Increased Transcription of HIV Type 1 in Ectocervical Tissue Explants. *The Journal of Infectious Diseases* **200**, 965-972 (2009).
270. Buffa, V. et al. Cyanovirin-N potently inhibits human immunodeficiency virus type 1 infection in cellular and cervical explant models. *J Gen Virol* **90**, 234-43 (2009).
271. Rohan, L.C. et al. In vitro and ex vivo testing of tenofovir shows it is effective as an HIV-1 microbicide. *PLoS One* **5**, e9310 (2010).
272. Merbah, M. et al. Cervico-vaginal tissue ex vivo as a model to study early events in HIV-1 infection. *Am J Reprod Immunol* **65**, 268-78 (2011).
273. Rollenhagen, C. & Asin, S.N. Enhanced HIV-1 replication in ex vivo ectocervical tissues from post-menopausal women correlates with increased inflammatory responses. *Mucosal Immunology* **4**, 671-681 (2011).
274. Introini, A., Vanpouille, C., Lisco, A., Grivel, J.-C. & Margolis, L. Interleukin-7 Facilitates HIV-1 Transmission to Cervico-Vaginal Tissue ex vivo. *PLOS Pathogens* **9**, e1003148 (2013).
275. Scott, Y.M., Park, S.Y. & Dezzutti, C.S. Broadly Neutralizing Anti-HIV Antibodies Prevent HIV Infection of Mucosal Tissue Ex Vivo. *Antimicrobial Agents and Chemotherapy* **60**, 904-912 (2016).
276. Introini, A., Vanpouille, C., Fitzgerald, W., Broliden, K. & Margolis, L. Ex Vivo Infection of Human Lymphoid Tissue and Female Genital Mucosa with Human Immunodeficiency Virus 1 and Histoculture. *Journal of Visualized Experiments* (2018).
277. Perez-Zsolt, D. et al. Dendritic Cells From the Cervical Mucosa Capture and Transfer HIV-1 via Siglec-1. *Frontiers in Immunology* **10**(2019).

278. Nijmeijer, B.M. et al. HIV-1 subverts the complement system in semen to enhance viral transmission. *Mucosal Immunology* **14**, 743-750 (2021).
279. Fletcher, P. et al. The nonnucleoside reverse transcriptase inhibitor UC-781 inhibits human immunodeficiency virus type 1 infection of human cervical tissue and dissemination by migratory cells. *J Virol* **79**, 11179-86 (2005).
280. Maher, D., Wu, X., Schacker, T., Horbul, J. & Southern, P. HIV binding, penetration, and primary infection in human cervicovaginal tissue. *Proceedings of the National Academy of Sciences* **102**, 11504-11509 (2005).
281. Cummins, J.E., Jr. et al. Preclinical testing of candidate topical microbicides for anti-human immunodeficiency virus type 1 activity and tissue toxicity in a human cervical explant culture. *Antimicrob Agents Chemother* **51**, 1770-9 (2007).
282. Wheeler, L.A. et al. Inhibition of HIV transmission in human cervicovaginal explants and humanized mice using CD4 aptamer-siRNA chimeras. *J Clin Invest* **121**, 2401-12 (2011).
283. Palacio, J. et al. In vitro HIV1 infection of human cervical tissue. *Res Virol* **145**, 155-61 (1994).
284. Gupta, P. et al. Memory CD4(+) T cells are the earliest detectable human immunodeficiency virus type 1 (HIV-1)-infected cells in the female genital mucosal tissue during HIV-1 transmission in an organ culture system. *J Virol* **76**, 9868-76 (2002).
285. Patterson, B.K. et al. Susceptibility to human immunodeficiency virus-1 infection of human foreskin and cervical tissue grown in explant culture. *Am J Pathol* **161**, 867-73 (2002).
286. Zussman, A., Lara, L., Lara, H.H., Bentwich, Z. & Borkow, G. Blocking of cell-free and cell-associated HIV-1 transmission through human cervix organ culture with UC781. *AIDS* **17**, 653-661 (2003).